Distribution Agreement

In presenting this thesis or dissertation as a partial fulfillment of the requirements for an advanced degree from Emory University, I hereby grant to Emory University and its agents the non-exclusive license to archive, make accessible, and display my thesis or dissertation in whole or in part in all forms of media, now or hereafter known, including display on the world wide web. I understand that I may select some access restrictions as part of the online submission of this thesis or dissertation. I retain all ownership rights to the copyright of the thesis or dissertation. I also retain the right to use in future works (such as articles or books) all or part of this thesis or dissertation.

Signature:

_____ _____

Robert Esterberg Date

Molecular Events Surrounding Embryonic Patterning During Late Gastrulation in *Danio rerio*

By
Robert Michael Esterberg
Doctor of Philosophy

Graduate Division of Biological and Biomedical Science
Genetics and Molecular Biology

_____
Andreas Fritz, Ph.D.
Advisor

_____
Ping Chen, Ph.D.
Committee Member

_____
Steven L'Hernault, Ph.D.
Committee Member

_____
Winfield Sale, Ph.D.
Committee Member

_____
Iain Shepherd
Committee Member

Accepted:

_____
Lisa A. Tedesco, Ph.D. Dean of the Graduate School

_____
Date

Molecular Events Surrounding Embryonic Patterning During Late Gastrulation in *Danio rerio*

By

Robert Michael Esterberg
B.S., University of West Florida, 2002

Advisor: Andreas Fritz, Ph.D.

An abstract of
A dissertation submitted to the Faculty of the Graduate School of Emory University
in partial fulfillment of the requirements for the degree of Doctor of Philosophy
in
Graduate Division of Biological and Biomedical Science
Genetics and Molecular Biology
2008

Abstract
Molecular Events Surrounding Embryonic Patterning During Late Gastrulation
in *Danio rerio*
By Robert Michael Esterberg

Cell signaling events are essential throughout development, playing inductive roles in axis establishment, embryonic patterning, and tissue specification. How a relatively small number of distinct signaling pathways are integrated to reliably pattern an embryo is still largely unknown. As perturbation of even a single signaling pathway often disrupts many aspect of embryogenesis, it can be difficult to examine signaling requirements in a particular spatial-temporal context. Further complicating this matter is mounting evidence that suggests that signaling activity gradients vary dramatically as development proceeds.

In this work, we have begun to address the spatial-temporal requirements for signaling activity during events that occur during late gastrulation and early somitogenesis in zebrafish. We focus particular attention on two tissues, chordamesoderm and the pre-placodal region, both of which require local modulation of BMP activity, particularly Bmp4, for proper development. In these tissues, we demonstrate the mechanisms through which appropriate levels of BMP activity are maintained. Chordamesoderm achieves this regulation through the secretion of two genes structurally related to Follistatin, a classical BMP antagonist. Appropriate levels of BMP activity are attained in the pre-placodal region through the regulation of a multifunctional BMP modulator, Crossveinless 2, which is necessary for lowering BMP activity within the pre-placodal region while likely promoting it in adjacent domains. Our results demonstrate the different approaches that tissues utilize to regulate signaling activity levels during development.

Molecular Events Surrounding Embryonic Patterning During Late Gastrulation in *Danio rerio*

By

Robert Michael Esterberg
B.S., University of West Florida, 2002

Advisor: Andreas Fritz, Ph.D.
Department of Biology

A dissertation submitted to the Faculty of the Graduate School of Emory University
in partial fulfillment of the requirements for the degree of Doctor of Philosophy
in
Graduate Division of Biological and Biomedical Science
Genetics and Molecular Biology
2008

Table of Contents

Figures and Tables

CHAPTER 1

General Introduction

One of the most fundamental questions in developmental biology is how a single-celled zygote becomes a complex multicellular organism, containing cells that differ in morphology and gene expression profiles. Embryonic development results from a succession of cell-cell inductions in which groups of cells, or signaling centers, signal the differentiation of their neighbors. In general, the developing embryo is initially divided into broad regions. Subsequently, cell fate is gradually refined and the primordia for different tissues begin to emerge. This involves communication within and between groups of cells as well as changes in gene expression that instruct a cell to adopt characteristics common to a particular fate.

Classical embryological experiments revealed that embryonic regions possess equivalent developmental potential, or morphogenetic fields, and these utilize self-regulatory properties to re-form after experimental perturbations (Huxley and de Beer, 1934; Driesch, 1892; Driesch, 1893; Harrison, 1918; Roux, 1888; Spemann, 1903; Spemann, 1938). In one early example, Hans Spemann divided *Xenopus* embryos at the four-cell stage and monitored the ability of the halves to generate a complete body plan (Spemann, 1903; in English in Spemann, 1938). One half developed containing only ventral tissue, while the other developed into a well-proportioned embryo containing both dorsal and ventral structures. His results demonstrated that the dorsal half was capable of compensating for the missing ventral half. Inherent to the idea of a regulative process are interactions between embryonic cells, interactions that specify cell fate.

Further insight into the embryo's self-regulative capabilities came about from landmark experiments performed by Hans Spemann and Hilde Mangold in 1924 (De Robertis, 2006; Spemann and Mangold, 1924; in English in Spemann and Mangold,

1964). Their results demonstrated that the embryonic axes are determined by the inductive properties of organizing centers. Transplantation of a small fragment of dorsal mesoderm, termed the Spemann organizer in *Xenopus* (hereafter referred to as the dorsal organizer, which encompasses equivalent structures in all vertebrates), into the ventral mesoderm of a salamander gastrula generated a fully formed twinned embryo complete with a normal dorsoventral (DV) axis. The transplanted cells altered the cell fate of neighboring ventral tissue in the host, instructing these cells to instead become dorsal tissue, or dorsalized. Thus, the embryonic axes are patterned according to inductive interactions from signaling centers that arise from within the axes themselves. Recent advances have begun to address the issue of self-regulation, and the communication between groups of cells that must occur to compensate when signaling is perturbed. How signals emanating over distant points can confer upon cells when to differentiate, proliferate, or die is key to understanding how embryos, tissues and organs are patterned.

Cell fate specification during gastrulation

Nowhere is cell signaling more important than during gastrulation, when a complex series of morphological movements establish the foundation of the body plan from a seemingly random assortment of cells. Although some aspects are unique to particular vertebrates, general themes emerge (Beetschen, 2001; Heisenberg and Tada, 2002; Schier and Talbot, 2005; Zernicka-Goetz, 2002). During this time, the three germ layers – endoderm, mesoderm, and ectoderm – migrate to positions where they will develop into structures of the adult body. This involves the transformation of a three-dimensional embryo from a sheet of cells, with the germ layers arranged in their correct

positions in relation to each other. In order for this to occur, ectodermal cells migrate to cover the outer surface of the embryo while presumptive endo- and mesoderm migrate beneath the ectoderm at the site of the dorsal organizer. Endo- and mesodermal cells then follow differing morphogenetic movements, allowing endoderm to form the gut tube along the anteroposterior (AP) axis and mesoderm to migrate along both axes to give rise to varying mesodermal derivatives. As a consequence of cell migration, the DV and AP axes also become evident.

Cell labeling during early embryogenesis with a traceable dye allows the identification of that cell's contribution to the embryo later in development. This type of fate mapping has been performed on a global scale in several vertebrate species, and has revealed that by early gastrulation cell fate has largely been assigned (Kimmel et al., 1990; Kozlowski et al., 1997; Warga and Nusslein-Volhard, 1999). However, genes that define presumptive territories within the embryo do not possess discreet borders; rather, expression boundaries share extensive overlap between adjacent markers (Wardle and Smith, 2004). These observations have led to the conclusion that although general tissue domains are apparent, the cells within them are still plastic- they can contribute to other tissues in the correct inductive environment (Kimelman, 2006; Schier and Talbot, 2005). Thus, segregation of cells in the establishment of the vertebrate triploblastic lineage and their later fate refinement as well as patterning the embryonic axes requires multiple signaling centers to regulate fate assignment.

Gastrulation occurs over a period of several hours during which cells are subject to complex movements as the germ layers and axes are established. One would therefore expect cells to be exposed to widely varying concentrations of signaling ligands and their

antagonists during this process. However, widely accepted models of axis and tissue patterning posit that signaling activity levels remain static during gastrulation (De Robertis, 2006; De Robertis and Kuroda, 2004; De Robertis et al., 1991; Kimelman, 2006; Niehrs et al., 1994; Schier and Talbot, 2005; Smith, 1997; Wessely and De Robertis, 2002). These models assume that cumulative signaling activity, rather than its timing or duration, establishes cell identity. Recent evidence from studies examining BMP, FGF, and Nodal signaling have begun to amend these models (Ben-Zvi et al., 2008; Hagos and Dougan, 2007; Kicheva and Gonzalez-Gaitan, 2008; Kornberg and Guha, 2007; Plouhinec and De Robertis, 2007; Reversade and De Robertis, 2005; Sander et al., 2007; Tucker et al., 2008), revealing a more dynamic requirement for signaling activity during gastrulation that accounts for the migration of cells towards or away from signaling centers.

Signaling affecting embryonic patterning during gastrulation

Signaling gradients are important throughout gastrulation, acting together as a positioning system in the early embryo. These signaling gradients provide coordinates for the body plan that determine where subsequent self-regulating organ morphogenetic fields for parts such as sensory organs, neural tissue, structural elements, and limbs are placed at later stages of development. Signaling from BMP, FGF, Nodal, and WNT family members generate positional information that leads to the restricted expression of transcription factors that, in a combinatorial fashion, control cell type specification. Furthermore, increasing evidence suggests that signaling systems are integrated on several levels (Eivers et al., 2008; Fuentealba et al., 2007; Knockaert et al., 2006; Pera et

al., 2003; Sapkota et al., 2007; Sapkota et al., 2006; Seoane et al., 2004). Through this integration, complex positive and negative feedback mechanisms have evolved than can buffer both minor and major signaling perturbations. These mechanisms facilitate the reproducible formation of the embryonic body plan even in the presence of intrinsic and extrinsic differences.

In this introduction, I will illustrate the roles of the four major families of signaling molecules: FGFs, Nodal, WNTs, and focus particular attention on BMPs. The best-studied integration of cell communication and fate specification involve the all-or-none requirement of BMP signaling in the inhibition of dorsal mesoderm and neural ectoderm (Eivers et al., 2008; Fuentealba et al., 2007; Kretzschmar et al., 1997; Massague, 2003; Pera et al., 2003; Sapkota et al., 2007; Sapkota et al., 2006; Seoane et al., 2004). On some, albeit varying, levels all aforementioned signaling molecules act to regulate the duration and intensity of BMP signaling so that gradients of low to moderate BMP activity are present in the embryo that can influence fate specification contrary to those specified by high levels of BMP signaling. How these signaling molecules are integrated in the processing of these decisions will be discussed, but is still largely unknown.

BMP signaling in axis patterning and cell fate specification

The roles and functions of BMPs in embryogenesis, from insects to mammals, mostly during the early stages, have attracted the interest of many scientists. Embryological studies involving BMP signaling have gravitated towards *Xenopus* and zebrafish, mainly due to the ease of experimental manipulation. Large-scale mutagenesis

screens in zebrafish have allowed identification of genes involved in early development (Hammerschmidt et al., 1996a; Hammerschmidt et al., 1996b; Mullins et al., 1996). Much knowledge, mostly about the function of genes and the relationships among them, is being accumulated. Many of the components of the BMP signaling cascade have been isolated, but their precise requirements in embryological development are still unknown.

Members of the TGF-β superfamily of signaling molecules play extensive roles in early embryonic patterning. Members include BMPs (Bone Morphogenetic Proteins) as well as Nodal ligands, which will be discussed later. The DV axis is established in large part through the actions of BMP signaling (De Robertis, 2006; De Robertis and Kuroda, 2004; Schier and Talbot, 2005). Interestingly, this role in DV patterning is conserved throughout the animal kingdom, implying an ancient origin for the role of this conserved pathway in development. Inverted relative to vertebrates, the same mechanisms of BMP signaling in DV establishment have been characterized in *Drosophila* (Carroll, 2001; De Robertis and Kuroda, 2004). In vertebrates, various levels of BMP signaling subdivide ectoderm and mesoderm into dorsal and ventral territories. Specification of ventral fate involves BMP signaling and the activation of downstream transcription factors such as SMAD1/5/8, *vent1*, and *vox* (Kimelman, 2006; Schier and Talbot, 2005). Direct examination of BMP signaling using antibodies specific to the active form of SMAD1/5/8 indicate that BMP activity is highest on the ventral side of early gastrulas and decreases dorsally (Tucker et al., 2008). SMAD1/5/8 activity on the presumptive ventral side of the blastula activates the expression of ventral genes, while *vent1*, *ved*, and *vox* repress the expression of genes that confer dorsal identity (Imai et al., 2001; Melby et

al., 2000). Thus, the division of dorsal and ventral fate regulates initial tissue differentiation of the vertebrate embryo.

An elaborate system of extracellular protein–protein interactions refine the gradient of BMP signaling that is initially established on the presumptive ventral side of the embryo. Increasing evidence gathered from studies of vertebrate and invertebrates shows that in the context of DV patterning, extracellular modulators perform vital roles in the formation of differential BMP signaling levels that activate different programs of gene expression in a dose-dependent manner, thus specifying distinct cell fates across large fields of cells. This is mediated through two major interactions. The first is amongst BMP antagonists, which are secreted from or around the dorsal organizer and include Chordin, Noggin, and Follistatin (Bauer et al., 1998; Dal-Pra et al., 2006; Fainsod et al., 1997; Fürthauer et al., 1999; Harland, 1994; Khokha et al., 2005). These antagonists bind BMP ligands and prevent their interaction with the appropriate receptor, and offer an explanation for the dorsalization of mesoderm observed in Spemann's transplantation experiments. The second group of BMP signaling modulators includes serine proteases such as Tolloid. Through the facilitation of proteolytic processing, these modulators serve to inhibit BMP antagonists (Blader et al., 1997; Connors et al., 1999; Connors et al., 2006; Hopkins et al., 2007; Oelgeschlager et al., 2000; Piccolo et al., 1997; Wardle et al., 1999). These proteases act to inhibit the action of BMP antagonists by facilitating their cleavage, thus preventing interactions with BMP ligands. The interaction between extracellular BMP ligands and antagonists is thought to establish a BMP activity gradient (Lee et al., 2006), where the concentrations of secreted BMP ligands and antagonists between opposing ventral and dorsal signaling centers provide

further basis for DV patterning (Kimelman, 2006; Nguyen et al., 1998; Schier and Talbot, 2005; Tribulo et al., 2003). According to this model, high levels of BMP activity specify ventral and epidermal fates, intermediate levels specify lateral and neural crest fates, and low levels specify dorsal and neural fates in mesoderm and ectoderm, respectively.

Examination of BMP signaling pathways has begun to shed light on the self-regulative nature of the embryo first observed when Hans Spemann bisected *Xenopus* embryos. In addition to the well-known BMP signaling center on the ventral side of the embryo, it was recently demonstrated that a novel BMP signaling center existed on the dorsal side of the embryo – within the dorsal organizer itself (Reversade and De Robertis, 2005). As observed by Spemann, in the absence of a ventral signaling center the embryo would be expected to become dorsalized. However, when this organizer is removed the embryo forms an intact DV axis. Only when the dorsal BMP signaling center is also depleted does the embryo become dorsalized. Thus, complex positive and negative feedback mechanisms between these ventral and dorsal BMP signaling centers maintain homeostatic levels of BMP signaling (Reversade and De Robertis, 2005; Sander et al., 2007) and offer an insight into the molecular mechanisms of self-regulation of morphogenetic fields.

Complex models of BMP activity gradients and signaling integration pose the question: why is there such complexity in the regulation of BMP signaling? Given that differential levels of BMP activity in the gastrula specify distinct tissue types, clearly it is crucial to have tight regulation of BMP signaling across the DV and even AP axes. Importantly, the complex interactions between BMP agonists and antagonists allow an embryo to convert a relatively simple BMP ligand gradient into a differential BMP

activity gradient such that some tissues would be exposed to higher BMP activity, while the adjacent tissues could receive relatively little BMP activity. The elucidation of how this process operates in a combinatorial, temporal, and spatial manner as cells proceed through the morphogenetic movements of gastrulation remains a challenge. In Chapters 2 and 3, I present evidence suggesting that BMP signaling requirements change over time, and that different tissues utilize uniqe strategies to modulate BMP activity to levels appropriate for further development.

FGF signaling and dorsoanterior patterning

Members of the FGF family (Fibroblast Growth Factor) play perhaps the most diverse role in embryonic development, where they have been implicated in mesoderm formation as well as both DV and AP patterning (Bottcher and Niehrs, 2005; Itoh and Ornitz, 2004; Itoh and Ornitz, 2008; Thisse and Thisse, 2005). The expression patterns of downstream targets of FGF signaling have revealed that the pathway is first active at the region of the dorsal organizer (Fürthauer et al., 2001; Raible and Brand, 2001). The cooperation of FGF signaling and BMP antagonists, which will be discussed in more detail later, act to confer dorsal fate onto mesoderm within proximity to the dorsal organizer.

The main signaling activated through the stimulation of FGF receptors (FGFRs) is the Ras/MAPK (Mitogen Activated Protein Kinase) pathway (Bottcher and Niehrs, 2005). Activation of FGFRs leads to the binding and localization of several small adaptor molecules and the subsequent activation of the GTP-binding protein Ras. Ras activation results in the phosphorylation and activation of downstream Raf, MEK, and

MAPK, the last of which translocates into the nucleus and phosphorylates target transcription factors. This in turn activates transcription of target genes.

FGF inhibition of BMP signaling

Of all the signaling families known to play roles in early embryonic patterning, FGF signaling has been most widely characterized in opposing the actions of BMP signaling. Data in *Xenopus* and zebrafish mainly suggest an early role for FGF signaling by establishing the DV axis through the repression of BMP signaling. During early gastrulation, these signaling molecules and their downstream target genes often share complementary patterns of expression. Misexpression of FGF ligands can inhibit expression of *bmp2b*/*7* and lead to the dorsalization of the embryo (Fürthauer et al., 2002; Fürthauer et al., 2001; Fürthauer et al., 1997; Fürthauer et al., 2004). Interestingly, blocking FGF activity during early gastrulation does not result in a ventralized embryo. However, a synergism is observed when hypomorphic mutations in BMP antagonists such as *chordin* and FGF family members such as *fgf8* are combined. These results suggest that BMP antagonists and FGF signaling contribute to blocking BMP activity along the dorsal side of the gastrula. Conversely, hyperactivation of FGF signaling results in the repression of BMP ligand expression and the expansion of dorsal derivatives at the expense of ventral tissue (Fürthauer et al., 1997; Fürthauer et al., 2004). Taken together, these results establish the early role of FGF activity in restricting BMP expression and activity. Exactly how FGF signaling inhibits BMP expression is currently unknown.

In addition to the transcriptional repression of BMP ligands and their targets, FGF signaling also directly interferes with the intracellular BMP signaling cascade. Smad1 contains canonical MAPK phosphorylation sites in its linker region, which connects DNA binding domains of the SMAD proteins. Phosphorylation of the linker region by activated MAPK inhibits the activating phosphorylation of SMAD1 in response to BMP signaling, and thus prevents its translocation into the nucleus (Kretzschmar et al., 1997; Pera et al., 2003; Sapkota et al., 2007). Evidence for this comes from studies in *Xenopus*, where overexpression of phosphorylation resistant mutants of SMAD1 increased ventral tissue at the expense of dorsal tissue (Pera et al., 2003). Thus, the activity of the BMP pathway can be tempered by activated MAPKs downstream of FGF signaling. These studies demonstrate that *in vivo* MAPK plays a key role in the regulation of BMP signal transduction. Interestingly, MAPK phosphorylation sites are conserved in all BMP-activated SMADs, and present in every vertebrate examined (Eivers et al., 2008).

The reciprocal regulation of FGF activity by BMP signaling also appears to occur during embryogenesis. In murine limb bud development, BMP activity inhibits FGF signaling by downregulating *Fgf4* expression in the apical ectodermal ridge (Ganan et al., 1996; Pizette and Niswander, 1999; Zuniga et al., 1999). In Chapter 3, I demonstrate that tight regulation of BMP activity is critical in the maintenance of FGF activity; Inappropriate increases in BMP activity are capable of modulating FGF activity through regulation of FGF receptor expression.

Nodal signaling and mesoderm induction

Members of the Nodal family of signaling molecules, a second class of the TGF-ß superfamily, have been demonstrated to play central roles in the formation of the DV and AP axes as well as mesoderm induction (Schier, 2003; Shen, 2007; Tian and Meng, 2006; Weng and Stemple, 2003). In contrast to other signaling systems, Nodal genes have not been found in *Drosophila* or *C. elegans*. This suggests that that the evolution of Nodal signaling has been coupled to developmental processes that are distinct to chordates, such as mesoderm induction.

Gene expression and fate map analyses in *Xenopus* and zebrafish have revealed that Nodal signaling acts before and during gastrulation to specify endo- and mesodermal cell fate. This occurs in a dose-dependent manner; a Nodal signaling gradient exists along the DV and animal-vegetal axes where the highest levels of Nodal activity received by cells closest to the dorsal organizer become endoderm, while cells surrounding the dorsal organizer receive slightly lower levels of Nodal activity and are fated to become mesendoderm and mesoderm (Birsoy et al., 2006; Dale et al., 1992; Gritsman et al., 2000; Kelly et al., 1995; Kimelman and Kirschner, 1987; Koster et al., 1991; Slack et al., 1987; Smith, 1987; Szeto and Kimelman, 2004). Loss of function analyses have revealed that reduced levels of Nodal activity result in the transfating of endoderm into mesoderm (Gritsman et al., 2000). The levels of Nodal activity that mesodermal cells receive also serve to specify their position along the AP axis; cells exposed to higher levels of Nodal activity adopt positions more anterior than those exposed to lower levels (Erter et al., 1998).

Through the use of small molecule inhibitors of Nodal signaling, Hagos and Dougan (2007) have demonstrated that timing of Nodal signaling is critical in both axis

patterning as well as the timing of cell specification. Nodal levels control a developmental program that determines the fate of responding cells and controls when these fates are specified. Inhibition or hyperactivation of Nodal signaling is capable of delaying or expediting, respectively, the adoption of particular endo- and mesodermal characteristics while the length of exposure to Nodal signaling determines whether the competent cell becomes endoderm or mesoderm. Thus, cells responsive to particular molecules acquire their fate based upon the cumulative dose of signaling received. This is a function of both the competence of the receiving cells as well as the strength of the signal.

Initiation of the Nodal signaling cascade involves binding to Nodal transmembrane receptors and an EGF-CFC co-receptor (Bamford et al., 2000; Shen and Schier, 2000). This binding facilitates phosphorylation of SMAD2/3, where a complex of PSMAD2/3 and a DNA binding cofactor mediate transcription of Nodal target genes (Kumar et al., 2001; Lee et al., 2001; Yeo and Whitman, 2001). Despite the importance of these intracellular regulators of Nodal signaling, little is known about how they integrate signaling duration and intensity into regulation of Nodal target genes.

Nodal inhibition of BMP signaling

As with FGF-mediated inhibition of BMP signaling, there is evidence to suggest that components of Nodal signaling also inhibit BMP activity. In addition to activating SMAD2/3, Nodal ligands can also antagonize the activation of the BMP signaling cascade. This happens, at least in part because some Nodal ligands can form signaling-inactive heterodimers with BMP ligands (Yeo and Whitman, 2001). *Xenopus* Xnr3, a

Nodal family member, lacks the ability to initiate Nodal signaling cascades within the cell but is capable of binding BMP2/4, preventing them from interacting with their appropriate receptors (Wessely et al., 2001). Similarly, the secreted molecule Follistatin acts as a multifunctional antagonist of both BMP and Nodal ligands (Nakamura et al., 1991).

In addition to direct interference with BMP ligands, Nodal signaling appears capable of indirectly inhibiting the activation of SMAD1/5/8. Cell culture studies have indicated that Nodal co-receptor EGF-CFC proteins activate non- TGF-ß signaling pathways. For example, activation of MAPK by Cripto, one such Nodal co-receptor, has been observed in mouse and human cell culture (Adamson et al., 2002). In *Xenopus,* the EGF-CFC protein FLR-1 has been shown to inhibit BMP activity by activating MAPK (Kinoshita et al., 1995; Yabe et al., 2003).

Taken together, these studies indicate that different levels of Nodal signaling activity in a cell can induce different fates. This raises the question of how Nodal signaling is differentially modulated *in vivo*. While the interaction of the Nodal pathway with other pathways is clear, the extent of these interactions is unknown. It is interesting to note that through both direct and indirect means, Nodal signaling inhibits BMP signaling. What is the rationale for this interaction? Do Nodal and BMP activity play opposing roles in fate specification, or do the pathway-specific SMADs compete for the common SMAD4? It remains possible that the specification of some mesodermal cell types require the input of both Nodal and BMP signaling, although this has not been examined. Conversely, it is also possible that the two signaling pathways act to directly oppose each other. There is some evidence to suggest this interpretation from loss of

function studies involving the BMP signaling pathway. In embryos lacking functional BMP signaling components, some cell types specified by Nodal signaling are expanded.

WNT signaling and AP patterning

As with other families of signaling molecules, WNT signals are pleiotropic, with effects that include mitogenic stimulation, cell fate specification, and differentiation. The WNT family of signaling proteins has been implicated in multiple developmental events during embryogenesis, most notably in establishing the dorsal side of the embryo in *Xenopus* and zebrafish. The nuclear translocation of maternally deposited ß-catenin is the mechanism through which WNT signaling provides the earliest molecular DV asymmetry, and is critical in the establishment of the dorsal organizer (Dougan et al., 2003; Logan and Nusse, 2004; Schneider et al., 1996). In the absence of this maternally derived factor, the dorsal organizer does not form, and the embryo is ventralized (Kelly et al., 2000; Nojima et al., 2004).

In addition, WNT signaling patterns the AP axis in a manner that is conserved amongst vertebrates (Logan and Nusse, 2004; Schier and Talbot, 2005). Studies involving WNT signaling members suggest that WNT activity promotes posterior cell fate, where loss of function analyses involving WNT pathway members result in an expansion of anterior tissue at the expense of posterior domains (Dorsky et al., 2003; Erter et al., 2001; Heisenberg et al., 2001; Kim et al., 2000; Lekven et al., 2001; Shimizu et al., 2005; Woo and Fraser, 1997). Conversely, overexpression of WNT ligands in *Xenopus* and zebrafish posteriorize the embryo, repressing anterior gene expression and promoting the anterior misexpression of posterior genes (Lekven et al., 2001).

Information from these studies have led to a WNT activity model, where high levels of WNT signaling specify the presumptive posterior domain of the embryo, with decreasing levels of WNT activity specifying progressively more anterior fate.

A hallmark of WNT pathway activation is the elevation of cytoplasmic β-catenin protein levels. WNT signaling through a Frizzled-Lrp (Low-density Lipoprotein Receptor) receptor complex and a number of cytoplasmic proteins act to stabilize β-catenin within the cell. In the absence of WNT signaling, β-catenin is phosphorylated by the GSK3 kinase (Amit et al., 2002; Liu et al., 2002; Yanagawa et al., 2002; Yost et al., 1996). The interaction between these kinases and β-catenin is facilitated by the scaffolding proteins Axin and APC (Hart et al., 1998; Kishida et al., 1998; Sakamoto et al., 2000). Together, these proteins form a β-catenin degradation complex that allows phosphorylated β-catenin to be targeted for ubiquitination and degradation (Aberle et al., 1997; Latres et al., 1999; Liu et al., 1999). Activation of WNT signaling inhibits β-catenin phosphorylation and hence its degradation. Elevation of β-catenin levels leads to its nuclear accumulation (Cox et al., 1999; Miller and Moon, 1997; Tolwinski and Wieschaus, 2004) and complex formation with LEF/TCF transcription factors (Behrens et al., 1996; Molenaar et al., 1996; van de Wetering et al., 1997). β-catenin mutant forms that lack the phosphorylation sites required for its degradation are WNT unresponsive and can activate WNT target genes constitutively (Munemitsu et al., 1996; Yost et al., 1996). The increased stability of β-catenin following WNT signaling leads to the transcriptional activation of target genes mediated by β-catenin interactions with the TCF/LEF DNA-binding proteins. Conversely, in the absence of WNT signaling, TCF

acts as a repressor of WNT target genes (Behrens et al., 1996; Brannon et al., 1997; Cavallo et al., 1998; Molenaar et al., 1996; van de Wetering et al., 1997).

WNT and BMP signaling integration

Another layer of complexity to BMP signaling has recently been uncovered by examining interactions between WNT and BMP signaling. In the specification of the embryonic axes, it has been noticed that WNT and BMP signaling cooperate in the promotion of similar yet sometimes distinct embryonic domains (De Robertis and Kuroda, 2004; Eivers et al., 2008; Schier, 2003; Schier and Talbot, 2005). For example, the BMP target genes *vent* and *vox* are also target genes of WNT signaling, and the combined action of WNT and BMP signaling are thought to define the size of the dorsal organizer (Imai et al., 2001; Kelly et al., 2000; Kimelman, 2006; Melby et al., 2000; Ramel et al., 2005; Schier, 2003; Schier and Talbot, 2005). It is not surprising, then, that the molecules secreted from the dorsal organizer act to inhibit WNT signaling. Some of these inhibitors, such as Cerberus, are multifunctional antagonists of WNT and BMP signaling (Piccolo et al., 1999). Others, such as Sizzled, bear structural resemblance to the sFRP family of WNT antagonists yet act solely as BMP antagonists (Lee et al., 2006).

Recently, a novel branch of the WNT signaling cascade was revealed through the discovery that in addition to MAPK, GSK3 also serves to phosphorylate SMAD1 at a region in its linker domain (Fuentealba et al., 2007). This phosphorylation targets SMAD1 for ubiquitination and degradation. As GSK3 is inhibited by WNT signaling, a mechanism for the integration of WNT and BMP signaling has emerged where the promotion of venteroposterior cell fate involves cross talk between WNT and BMP signaling cascades. Through this model, it has been proposed that WNT signaling acts to

prolong the effects of BMP signaling by preventing SMAD1 linker phosphorylation by GSK3 (Eivers et al., 2008).

Additive effects of signaling integration on cell fate

Individual signaling pathways have been extensively characterized, from the levels of the ligand to the signaling cascade that is activated and the target gene that is expressed as a result. However, rarely do signaling events occur in isolation within the embryo. The next challenge to understand signaling requirements during embryogenesis is to understand how signaling systems influence each other, and how multiple signals create a unique output in terms of cell fate. This is essential to understand how one ligand can induce the adoption of many different fates. Signaling integration has been most extensively characterized in the process of neural induction, with further implications projected onto DV and AP patterning and cell fate specification in general.

Neural induction

It has long been known that inhibition of BMP and WNT activity promotes neural fate in ectoderm (De Robertis and Kuroda, 2004; Weinstein and Hemmati-Brivanlou, 1999). Many secreted molecules involved in head formation are multifunction antagonists of both signaling pathways. Overexpression of these antagonists or dominant negative components of the BMP or WNT signaling cascades expand the domain of neural tissue (Aubert et al., 2002; Glinka et al., 1997; Hurtado and De Robertis, 2007; Lemaire et al., 2002; Piccolo et al., 1999; Reversade et al., 2005). Similarly, explants of naïve ectoderm can be induced to adopt neural characteristics when exposed to BMP

antagonists (Wilson and Hemmati-Brivanlou, 1995). High levels of FGF activity have the same effect as inhibition of BMP and WNT activity (Hurtado and De Robertis, 2007; Kuroda et al., 2005; Pera et al., 2003), leading to the hypothesis that the neuralizing effect of BMP and WNT inhibition is somehow tied to FGF signaling.

The identification that SMAD1 is a downstream target of WNT and FGF signaling (Fuentealba et al., 2007; Kretzschmar et al., 1997; Massague, 2003; Pera et al., 2003; Sapkota et al., 2007) has demonstrated that signaling integration occurs in the most fundamental of processes. A model has been proposed that following the activating phosphorylation of SMAD1 through BMP signaling, two sequential phosphorylation events limit the duration of the intracellular BMP signaling cascade (Eivers et al., 2008). In this model, the fate of cells receiving high levels of BMP is tempered through inhibitory phosphorylations brought about by FGF signaling and GSK3 (where there are low levels of WNT activity). Thus, in regions where there are high levels of BMP and WNT activity, BMP signaling regulates the intensity of the signal, while WNT and FGF signaling regulate the duration of activated PSMAD1 received by the nucleus. The two qualities regulated by this integration – intensity and duration – likely affect transcriptional regulation differently. Although the reason behind this additional level of signaling regulation and integration is not fully understood, it likely provides a more robust mechanism of patterning precision.

Integrating DV and AP patterning through SMAD1

During development the dorsal and ventral sides of the embryo must be able to talk to each other over the distance of many cell lengths. The regulation of SMAD1 by

BMP, FGF, and WNT signaling may provide a common mechanism through which the embryonic axes are patterned. The establishment of the DV axis occurs through opposing actions mediated by BMP and FGF signaling, with high levels of BMP and FGF activity specifying ventral and dorsal identity, respectively. Although it has not been examined, attenuation of the BMP signaling cascade on the presumptive dorsal side of the embryo likely involves inhibitory SMAD1 phosphorylation by MAPK. In a similar manner, BMP and WNT signaling may converge in the patterning of the AP axis. The WNT activity gradient specifies cell identity along the AP axis, where high levels of WNT signaling promote posterior cell fate. Inhibition of GSK3 by high levels of WNT activity along the posterior end of the embryo likely prolong the duration of the BMP signal, while this duration shortens anteriorly due to lower levels of the WNT activity gradient and thus higher levels of intracellular GSK3. Some evidence for the integration comes from studies in *Xenopus* and zebrafish, where hyperactivation of the WNT signaling pathway expands the expression of ventral markers at the expense of dorsal ones (Erter et al., 2001; Kelly et al., 1995; Lekven et al., 2001; Ramel et al., 2005; Shimizu et al., 2005). Conversely, inactivation of WNT pathway members produces a severe loss of ventroposterior structures, with a concomitant expansion of dorsal fates. Although DV and AP patterning at the level of SMAD1 integration has yet to be demonstrated, the aforementioned signal integration in neural induction offers compelling evidence for this model.

A recent study addressing the link between DV and AP patterning has demonstrated the temporal importance of BMP activity during gastrulation. By inactivating BMP signaling at specific points, Tucker and colleagues demonstrated that

BMP activity establishes DV fate in an anterior to posterior wave, concomitant with the progression of gastrulation (Tucker et al., 2008). Through the generation of inducible BMP transgenes, Tucker demonstrated that dorsalization defects of BMP mutants in progressively decreasing regions of posterior structures could be rescued as gastrulation proceeds, but anterior structures specified before induction of the transgene remained dorsalized. The finding suggests that differentiation along the AP axis is controlled by distinct temporal intervals of BMP signaling, with an early specification of anterior DV polarity followed by a later specification of more posterior DV fate. Their results suggest that requirements for signaling activity changes as gastrulation proceeds, and may provide an interesting temporal dimension to the proposed mechanisms of integrating the DV and AP axes by SMAD1 phosphorylation.

Signaling integration in tissue induction and patterning

Although the broad specification of embryonic axes and tissue type has been relatively well characterized, many nuances involving the refinement of cell communication between signaling centers and competent cells are still unknown. As mentioned above, only recently has evidence emerged suggesting that signaling activity gradients are not static during gastrulation but rather change over time in response to tissue specification. Even less is understood about the synergy occurring between signaling interactions at the intracellular level, raising the distinct possibility that embryonic cells do not respond to simply one ligand during fate specification. Evidence suggesting an intracellular link between DV and AP patterning demonstrate that the integration between multiple signaling activities exert a far greater influence over cell

fate than their sum totals would suggest. Furthermore, it is unclear how transcriptional targets of signaling molecules respond to this signaling integration, especially in the establishment of positive or negative feedback loops that promote or inhibit signaling to surrounding territories.

Most of what is known surrounding signaling interactions focuses on early embryonic events. Mutagenesis screens performed in zebrafish have identified a number of loci involved in signaling during early embryogenesis. Often these genes are required prior to the end of gastrulation. During these stages, morphological defects brought about by signaling perturbations are easy to identify. However, these signaling pathways continue to be utilized during later stages of embryogenesis, as well as in adult homeostasis and tissue repair. Many oncogenes are components of signaling pathways (Bottcher and Niehrs, 2005; Eivers et al., 2008; Logan and Nusse, 2004; Thisse and Thisse, 2005). Thus, understanding interactions that occur during cell communication is critical for understanding multiple biological processes.

I will discuss stage specific requirements of signaling activities in the establishment of two seemingly different tissues: the otic placode and the notochord. Although the otic placode and notochord arise from ecto- and mesoderm, respectively, they both require input from multiple signaling molecules. Through local interactions with signaling antagonists, activity gradients are established that define the eventual fate of these cells. How these gradients specify cell fate is key to understanding embryogenesis.

Signaling events surrounding the formation of the inner ear

The vertebrate inner ear is a complex sensory structure responsible for the detection of sound, gravity, and acceleration. Comprised of a series of communicating chambers and multiple cell types, it is complex in both structure and function (Ohyama et al., 2007; Schneider-Maunoury and Pujades, 2007; Streit, 2007). This complexity arises from a simple thickening of epithelium, the otic placode, which lies adjacent to the neural plate. The otic placode undergoes complex morphological rearrangements to form the otic vesicle, which will eventually give rise to the inner ear. Well before the otic placode is morphologically distinct, signaling events emanating from neural as well as non-neural ectoderm act to induce and pattern otic cell fate. These events make otic precursor cells distinct from other cells in the region that will contribute to other cranial sensory placodes.

Classical embryological manipulations as well as recent molecular techniques have provided evidence that otic induction is a multi-step process, requiring multiple inductive events in otic placode formation (Bhattacharyya et al., 2004; Jacobson, 1963; Kozlowski et al., 1997; Martin and Groves, 2006; Noramly and Grainger, 2002; Ohyama et al., 2007; Schlosser, 2006; Streit, 2007). Cells must first acquire an identity common to all cranial sensory organs; cells possessing this identity occupy the preplacodal region (PPR). Secondly, a pre-otic field must be established within the PPR. Finally, further inductive events are necessary to refine this domain into the otic placode.

Positioning the PPR

Like neural and epidermal precursors, placodal cells are ectodermal derivatives. Fate-mapping studies in *Xenous*, zebrafish, and chick have demonstrated that during early

to mid gastrulation, ectoderm is largely divided into neural and non-neural ectoderm with a region demarcating the two that shares characteristics of both types termed the border region (Bhattacharyya et al., 2004; Jacobson, 1963; Kozlowski et al., 1997). This segregation of fates is reflected by the expression of transcription factors that define neural, non-neural, and border ectoderm. In the border region, members of the *Dlx*, *Fox*, and *Msx* families of transcription factors are expressed in response to BMP activity and appear to be critical in specifying this domain (Akimenko et al., 1994; Feledy et al., 1999; Liu et al., 2003; Luo et al., 2001; Matsuo-Takasaki et al., 2005; Nguyen et al., 1998; Ohyama and Groves, 2004; Papalopulu and Kintner, 1993; Pera et al., 1999; Phillips et al., 2006; Solomon et al., 2003; Suzuki et al., 1997). As the definitive neural plate forms during late gastrulation, the expression of these genes in border ectoderm is progressively upregulated and confined to a stripe bordering the neural plate. Fate-mapping studies in *Xenopus*, zebrafish, and chick have shown that cells expressing these transcription factors contribute to sensory placodes and neural crest (Bhattacharyya et al., 2004; Kozlowski et al., 1997).

Shortly thereafter, PPR cells begin to express genes belonging to the *Six/Eya/Dach* transcriptional network, and these cells migrate to the lateral border regions (Ahrens and Schlosser, 2005; Bessarab et al., 2004; Kobayashi et al., 2000; Litsiou et al., 2005; McLarren et al., 2003; Pandur and Moody, 2000; Schlosser and Ahrens, 2004). Ultimately, cells expressing members of this transcriptional network migrate and coalesce at positions around the neural plate corresponding with the future location of cranial sensory placodes (Bhattacharyya et al., 2004; Kozlowski et al., 1997; Streit, 2002). Thus, the segregation of non-neural ectoderm during gastrulation is a critical

process in the establishment of the PPR. In order to adopt a PPR specific fate, non-neural cells must first adopt border identity.

Signaling integration in PPR induction

Once the neural border is established, inductive signals from adjacent neural and epidermal ectoderm as well as underlying head endo- and mesoderm are critical in subdividing border ectoderm into neural crest and PPR (Schlosser and Ahrens, 2004; Streit, 2007). These molecules include signals from BMP, WNT, and FGF family members. Unlike BMPs and FGFs, WNT molecules likely play no direct role in PPR specification. Although they seem to cooperate with BMP signaling in neural crest specification (see below), their major role seems to be in establishing the posterior boundary of the PPR (Litsiou et al., 2005; Streit, 2007).

Evidence from *Xenopus* and chick suggest that BMP activity plays dual functions in this subdivision (Ahrens and Schlosser, 2005; Brugmann et al., 2004; Litsiou et al., 2005; McLarren et al., 2003). Lowering BMP activity through local and global application of BMP antagonists can expand the PPR at the expense of neural crest. Conversely, local application of BMP ligands in the border region inhibits formation of the PPR. Of the family of BMP ligands, Bmp4 is most likely involved in the subdivision of border ectoderm; it has been implicated in both neural crest specification as well as PPR inhibition (Ahrens and Schlosser, 2005; Glavic et al., 2004; Rossi et al., 2008; Tribulo et al., 2003).

Although low levels of BMP activity can expand the size of the PPR and induce expression of some PPR genes in misexpression studies, modulation of BMP activity

alone cannot confer PPR fate onto a group of cells (Ahrens and Schlosser, 2005; Litsiou et al., 2005). FGF signaling seems to also be required in this process., although it is also not sufficient for this process. The inhibition of BMP activity along with FGF activity, however, does appear to be able to induce the full range of PPR markers in *Xenopus* and chick (Ahrens and Schlosser, 2005; Brugmann et al., 2004; Litsiou et al., 2005). PPR markers that cannot be induced with ectopic FGF activity alone can be induced when BMP activity is additionally inhibited. Together, these studies demonstrate that signaling requirements change during PPR specification. BMP signaling is initially required to specify border ectoderm, where it later must be attenuated laterally to subdivide neural crest and PPR domains. The added requirement of FGF signaling in PPR specification may act to further depress BMP activity within PPR cells as has been demonstrated in neural induction, although this has yet to be examined. In Chapter 3, I present evidence addressing the strategies of the PPR in modulating BMP activity to appropriate levels for further development. When the PPR is incapable of maintaining appropriate low levels of BMP activity, FGF activity is depressed within the otic placode and adjacent hindbrain, demonstrating that these signaling pathways are mutually antagonistic during PPR formation.

Specification of otic fate

As development proceeds, become fated to contribute to specific placodes. A number of signaling molecules have been implicated in the specification of various placodal fates. Recent work suggests that the default state of pre-placodal cells is to

adopt lens identity, with subsequent signals responsible for conferring additional identities to PPR cells and restricting lens identity to only a small region in the PPR (Bailey et al., 2006).

In *Xenopus*, zebrafish, chick, and mouse, FGF signaling has been shown to play a critical role in instructing PPR cells to adopt an otic identity. In zebrafish and chick, treatment of zebrafish embryos with the FGF signaling inhibitor SU5402 results in the complete loss of otic vesicles as well as loss of otic markers (Leger and Brand, 2002; Maroon et al., 2002). Similar results are observed in chick, where treatment of presumptive otic explants with SU5402 also inhibits otic marker expression (Martin and Groves, 2006). Furthermore, FGF signaling appears to be required to maintain otic gene expression; SU5402 application in zebrafish at any developmental time point results in a rapid loss of otic marker expression (Leger and Brand, 2002).

In zebrafish, chick, and mouse, the FGF ligands responsible for otic placode induction have been identified. In zebrafish, mutagenesis screens and morpholino analyses have revealed the Fgf3 and Fgf8 mediate otic fate decisions (Leger and Brand, 2002; Maroon et al., 2002; Phillips et al., 2001; Reifers et al., 1998). Loss of either Fgf3 or Fgf8 results in reduced otic vesicle size as well as decreased domain of otic marker expression. In chick, signaling by Fgf3 and Fgf19 ligands are required for otic placode induction (Ladher et al., 2005), displaying otic phenotypes similar to those of zebrafish *fgf3* or *fgf8* mutants when either FGF is inactivated. In mouse, Fgf3 and Fgf10 are considered otic inducers, and as in zebrafish, embryos containing mutations in both genes fail to form otic vesicles and express otic markers (Alvarez et al., 2003; Wright and Mansour, 2003).

Gain and loss of function studies have provided clear evidence that the hindbrain and underlying mesoderm, which secrete FGF ligands necessary for otic development, act as FGF signaling centers in otic induction. Disruption of mesoderm induction and patterning through inactivation of Nodal signaling in zebrafish results in a much smaller otic vesicle (Gritsman et al., 2000; Leger and Brand, 2002). In quail, replacement of cranial mesoderm underlying the otic placode with mesoderm occupying a different position along the AP axis prevents otic placode induction (Kil et al., 2005). Similarly, zebrafish and mice mutants that do not form properly segmented hindbrains for otic vesicles that are reduced in size and abnormally patterned (Dolle et al., 1993; Giudicelli et al., 2003; Helmbacher et al., 1998; Kwak et al., 2002; Lecaudey et al., 2007; McKay et al., 1994; Moens et al., 1998; Prince et al., 1998; Wiellette and Sive, 2003). In summary, both mesoderm and the presumptive hindbrain likely act as signaling centers that generate levels of FGF activity necessary for otic placode induction.

Unlike in PPR specification, FGF signaling is sufficient to induce otic fate. Ectopic Fgf3 in *Xenopus*, zebrafish, and chick is capable of inducing ectopic otic vesicles (Adamska et al., 2001; Lombardo et al., 1998; Lombardo and Slack, 1998; Solomon et al., 2004). Although these experiments have demonstrated the inductive properties of FGF signaling, they have not addressed whether this information is conferred directly upon PPR cells. It is possible that FGF signaling induces the expression of other otic inducing molecules in FGF-competent tissues. Evidence from chick has addressed this issue through local exposure of PPR cells to ectopic FGF signaling. In these embryos, otic markers expression was initiated near FGF-soaked beads within a short time after exposure (Martin and Groves, 2006). This suggests that FGF signaling directly confers

otic identity to PPR cells. It is unclear which FGF receptors are responsible for mediating FGF signals involved in otic induction. In Chapter 4, I examine the requirements of known FGF receptors in this process.

Although FGF activity plays a significant role in otic placode induction, the effects of other signaling gradients on this process are less clear. A simple gradient composed of only FGF ligands emanating from the hindbrain and mesoderm is unlikely, as several BMP ligands are expressed in the otic placode of zebrafish, chick, and mouse shortly after its induction (Groves and Bronner-Fraser, 2000; Mowbray et al., 2001). FGF activity may play dual roles in otic placode induction by both specifying otic fate as well as inhibiting cellular responses to BMP activity. Furthermore, BMP ligand expression in otic cells is unaffected by SU5402 treatment (Leger and Brand, 2002; Martin and Groves, 2006), suggesting a complex interaction between FGF and BMP signaling in otic induction and later stages of patterning. The effects of BMP signaling in this process have yet to be resolved.

Maintenance of otic fate

As previously mentioned, prolonged FGF activity during otogenesis is key to maintaining the expression of otic markers as well as proper patterning of the inner ear. In addition to FGFs, WNT signaling is likely involved in maintenance of otic determination among placodal cells after induction by FGF activity. Transgenic mice driving WNT reporter constructs have revealed that canonical WNT activity is present in the otic field following placode induction (Ohyama et al., 2006). When β-catenin is artificially stabilized, mice generate enlarged otic placodes at the expense of epidermis. Conversely, when WNT signaling is disrupted in these mice, epidermis expanded at the

expense of the otic placode. Furthermore, inhibition of WNT activity in zebrafish reduces otic vesicle size, although it is unclear if any otic cells adopt a similar epidermal fate (Ohyama et al., 2006). Taken together, these results suggest that in addition to FGF signaling, WNT activity is required to maintain cells in an otic state of determination. In Chapter 5, we present preliminary evidence suggesting that two transcription factors expressed within the otic placode, Tbx2a/b, are critical in regulating otic competence to WNT signaling.

Integrating multiple signals over distinct stages of otic development

From these data, a model emerges where signaling integration is critical for the specification of specific cranial placodes. Otic induction and patterning requires multiple levels of BMP, FGF, and WNT activity in distinct phases beginning at mid gastrulation and lasting throughout neurulation. Initially, specification of border ectoderm requires high levels of BMP activity adjacent to the neural plate, which must then be attenuated to generate a placodal ground state that has the potential to contribute to all cranial sensory organs. Specific cranial placodes are then specified through differential signaling activities that are generated through the PPR cell's proximity to a signaling center. Although general requirements for the specification of placodal identity have been identified, much remains to be understood about how signaling centers and their antagonists surrounding the establish activity gradients responsible for this acquisition. Further studies are required to determine the relationship between signaling molecules in PPR and sensory placode induction.

Signaling events surrounding the formation of the notochord

The notochord is an embryonic midline structure common to members of the phylum Chordata, and has at least two major functions (Stemple, 2005). First, the notochord is positioned centrally in the embryo with respect to both the DV and left-right axes. Here, it acts as a signaling center, where through the secretion of various inducing factors, acts to pattern axial structures. Signaling from the notochord is responsible for providing position and fate information to surrounding cells. In this regard the notochord is important for specifying ventral fates in the neural tube, controlling aspects of left-right asymmetry, and specifying a variety of cell types in nascent somites (Christ et al., 2004; Danos and Yost, 1995; Lohr et al., 1997; Pourquie et al., 1993; Scaal and Christ, 2004; Yamada et al., 1993). Second, the notochord plays an important structural role. As a tissue the notochord is most closely related to cartilage. Accordingly, the notochord serves as the axial skeleton of the embryo until other elements, such as the vertebrae, form. In some vertebrates, such as lampreys and primitive fish, the notochord persists throughout life. In higher vertebrates, however, the notochord becomes ossified in regions of developing vertebrae and contributes to the intervertebral discs (Linsenmayer et al., 1986; Smits and Lefebvre, 2003; Swiderski and Solursh, 1992). Although much is known about the roles of the notochord as a signaling center and structural support, relatively little is known about the signaling interactions required to define notochord fate. In Chapter 2, I provide evidence suggesting that although initially excluded from notochord cells, BMP activity is critical in regulating both the proliferative state of the notochord as well as the timing of its differentiation.

Establishment of the dorsal organizer

In vertebrates, the notochord arises from the dorsal organizer (Kimmel et al., 1990; Saude et al., 2000). At the beginning of gastrulation, the ventral BMP signaling center positioned 180° from the dorsal organizer. Because of proximity and secretion of BMP antagonists from the dorsal organizer and surrounding tissues, cells in this region receive relatively little BMP activity. This gradient is critical in establishing the size of the dorsal organizer; loss of function analyzes have demonstrated that BMP activity antagonizes the formation of these dorsal-most structures. For example, when BMP activity is elevated in the dorsal gastrula the dorsal organizer fails to form and resulting embryos lack a notochord (Fekany et al., 1999; Lele et al., 2001; Saude et al., 2000; Shih and Fraser, 1996; Willot et al., 2002).

Induction of chordamesoderm

The first inductive event that must occur in notochord development is the transition of some cells comprising the dorsal organizer into axial mesoderm. This is largely specified through Nodal signaling, where differential gradients of Nodal activity specify cell fate within the dorsal organizer. Embryos containing mutations in Nodal pathway members fail to form prechordal plate, where instead this tissue transfates to become chordamesoderm. Thus, high levels of Nodal, received by cells deep within the organizer, specify cells to become prechordal plate (Gritsman et al., 2000; Saude et al., 2000). Low levels of Nodal activity found in the superficial organizer specify cells to become chordamesoderm, the antecedent of the notochord (Gritsman et al., 2000; Saude et al., 2000). Furthermore, notochord specification appears to be controlled locally by

molecules secreted by the superficial organizer. When this tissue is transplanted anywhere into an equivalently staged host, a second notochord is generated from the donor cells (Saude et al., 2000).

Notochord elongation and outgrowth

The origin of axial mesoderm from within the dorsal organizer suggests that it initially receives low levels of BMP activity. As gastrulation proceeds, however, the ventral BMP signaling center and the dorsal organizer migrate within close apposition of each other to form the tailbud, a composite structure comprised of both signaling centers (Agathon et al., 2003; Gont et al., 1993; Kanki and Ho, 1997; Tucker and Slack, 1995). Ectopic expression of the factors secreted from each signaling center has revealed that structures of the tail originate from a particular signaling center. For example, axial mesoderm arises from the dorsal organizer (Gont et al., 1993; Pyati et al., 2005) while paraxial and lateral mesoderm arise from the ventral signaling center (Agathon et al., 2003). Given the proximity of each signaling center, it is likely that axial mesoderm formed during tail outgrowth receives some level of BMP activity. How secreted molecules from each signaling center interact to generate a functional tail comprised of axial, paraxial, and lateral mesoderm is poorly understood, and may be key to understanding cell fate decisions within tailbud precursors.

Chordamesodermal transition into notochord

Little is understood regarding the transition from chordamesoderm into mature notochord, although it is known that this transition is critical in regulating the type and

duration of signals emanating from the notochord (Stemple, 2005; Stemple et al., 1996). For example, signaling ligands expressed in chordamesoderm are extinguished as the tissue matures. These include *sonic* and *indian hedgehog* homologues, which are responsible for specifying myofiber cell type within paraxial mesoderm as well as motor neuron identity in the ventral neural tube (Currie and Ingham, 1996; Krauss et al., 1993; Pollard et al., 2006; Stemple et al., 1996; Yan et al., 1995). Prolonging the maintenance of chordamesodermal tissue can elevate Hedgehog signaling emanating from this tissue, resulting in a depletion of fast muscle cells and abnormal motor neuron patterning (Pagnon-Minot et al., 2008). Thus, chordamesoderm acts as a signaling center along the midline of the embryo (Stemple, 2005). Timing of notochord maturation is critical in proper specification of surrounding cell types. The nature of the signal responsible for promoting notochord development has yet to be defined.

Concluding remarks – combining signals to build an embryo

From studies centering on signaling during axis development, four general themes have emerged. First, morphogenetic signaling centers are generated locally that can influence the development of overlapping and neighboring cells, even those at a distance from the signaling center. Second, differential signaling activity can induce different cell fates. Third, positive and negative regulatory loops determine the activity of signaling in a given cell. Fourth, the requirements for a particular signaling molecule in cell fate specification is not all-or-none. Multiple signaling pathways converge, integrating the intensity and duration of a particular signal and thus regulating the transcriptional output of the target cell.

Although we can describe a particular process as being largely influenced by one signaling family, recent evidence suggests that this may be an oversimplification. In several experimental models, multiple signaling families act redundantly or even in a synergistic manner in the promotion of cell and tissue fate. Recent studies have begun to reveal that cell identity is not governed solely by the absolute state of a particular ligand, but rather that timing, duration, and intensity of signaling are critical in determining cell fate. Thus, the steps involving specification of a particular fate are highly dynamic throughout embryonic development. Furthermore, while all of the signaling families that are important in patterning the gastrula have likely been identified, individual factors in these processes remain to be characterized. How these factors interact with one another in the generation of an embryonic body plan is far from being understood. Investigation of the mechanisms underlying tissue induction and development can provide a deeper understanding of how signaling systems interact during embryogenesis.

In the following chapters, I provide evidence for the molecular strategies that embryos utilize to integrate and modulate signaling inputs, with the effects these inputs have on tissue patterning. In Chapter 2, I demonstrate that BMP signaling is required to regulate cell division as well as tissue maturation of chordamesoderm, a structure that initially requires very low levels of BMP activity in its specification. In Chapter 3, I demonstrate that the regulation of a BMP modulator within the PPR is critical in further steps of PPR, and later otic, development. In the absence of proper BMP regulation within this tissue, FGF activity is disrupted. In Chapter 4, I examine the requirements of four known FGF receptors in otic induction. Finally, in Chapter 5, I present evidence

suggesting that factors intrinsic to pre-otic cells are critical in regulating competence to respond to WNT signaling, after initial requirements for FGF activity in otic induction.

CHAPTER 2

Tailbud-derived Bmp4 drives proliferation and inhibits maturation of zebrafish chordamesoderm

(Esterberg, Delalande, and Fritz, *Development*, in press)

Abstract

In zebrafish, BMP signaling establishes cell identity along the dorsoventral (DV) axis during gastrulation. Due to the early requirements of BMP activity in DV patterning, it has been difficult to assign later roles in cell fate specification to specific BMP ligands. In this study, we have taken advantage of two *follistatin-like* genes (*fstl1* and *fstl2*), as well as a transgenic zebrafish line carrying an inducible truncated form of the BMP-type I receptor to study the role of Bmp4 outside of the context of DV specification. Characterization of *fstl1/2* suggests that they exert a redundant role as BMP antagonists during late gastrulation, regulating BMP activity in axial mesoderm. Maintenance of appropriate levels of BMP signaling is critical for the proper development of chordamesoderm, a subset of axial mesoderm that gives rise to the notochord, but not prechordal mesoderm, which gives rise to the prechordal plate. Bmp4 activity in particular is required during a critical window beginning at late gastrulation and lasting through early somitogenesis to promote chordamesoderm proliferation. In the absence of Bmp4, the notochord precursor pool is depleted, and the notochord differentiates prematurely. Our results illustrate a role for Bmp4 in the proliferation and timely differentiation of axial tissue after DV axis specification.

In zebrafish, BMP signaling acts progressively during gastrulation to establish mesodermal cell identity. Mesoderm is specified early in gastrulation and contributes to tissues that can be roughly categorized as dorsal or ventral in nature. The specification of ventral fate involves Bmp2b/7 signaling and activation of downstream transcription factors such as SMAD1/5/8, *vent1*, *ved*, and *vox* (Kimelman, 2006; Schier and Talbot, 2005; Yamamoto and Oelgeschlager, 2004). SMAD1/5/8 activity on the presumptive ventral side of the blastula activates the expression of ventral genes, while *vent1*, *ved*, and *vox* repress the expression of genes that confer dorsal identity such as the BMP antagonist *chordin* (Imai et al., 2001; Kawahara et al., 2000; Melby et al., 2000). Establishment of the DV axis is followed by a second phase of BMP signaling during mid to late gastrulation when the interaction of BMP antagonists and agonists is thought to establish a BMP activity gradient (Kimelman, 2006; Schier and Talbot, 2005). According to this model, high, intermediate, and low levels of BMP activity in the mesoderm specify ventral, intermediate, and dorsal fate, respectively.

Low levels of BMP activity direct cells surrounding the dorsal organizer to become axial mesoderm, while their positions within this tissue influence their exposure to other activity gradients (Schier and Talbot, 2005; Stemple, 2005). For example, Nodal activity is critical for the process of further specification of axial mesoderm. High levels of Nodal, received by cells deep in the organizer, specify cells to become prechordal plate (Gritsman et al., 2000; Saude et al., 2000). Low levels of Nodal activity found in the superficial organizer specify cells to become chordamesoderm, the antecedent of the notochord (Gritsman et al., 2000; Saude et al., 2000).

The molecular events surrounding the transition of chordamesoderm into mature notochord are not fully understood, although there are several defining features of the process (Stemple, 2005). Differentiated notochord cells acquire large vacuoles that allow the tissue to provide structural support to the embryo. Coupled to this, genes expressed in chordamesoderm are extinguished as the tissue matures. These include the *sonic* and *indian hedgehog* homologues, *shha* and *ihhb*, respectively, as well as the extracellular matrix (ECM) gene *collagen 2a* (*col2a1a*) (Currie and Ingham, 1996; Krauss et al., 1993; Yan et al., 1995). Mutagenesis screens and studies examining ECM members have begun to elucidate the chordamesodermal transition into mature notochord. Embryos lacking Laminin 1 subunits (*bashful*, *grumpy*, and *sleepy*; Parsons et al., 2002), Laminin α4/5 (Pollard et al., 2006), and Collagen15a1 (Pagnon-Minot et al., 2008) continue to express chordamesodermal markers after expression has been extinguished in wild-type embryos, suggesting that notochord differentiation is impaired. However, given their nature, these proteins are unlikely to play instructive roles in notochord differentiation. The signal responsible for promoting notochord development has yet to be defined.

While it is clear that initial specification of chordamesoderm is reliant upon the absence of BMP from the dorsal organizer, subsequent proliferation and differentiation of this tissue may depend upon it. Posterior to the notochord lies the chordoneural hinge (CNH), a stem cell pool that contributes to notochord, floor plate, and tailbud mesoderm (Cambray and Wilson, 2002; Cambray and Wilson, 2007; Charrier et al., 1999; Davis and Kirschner, 2000; Kanki and Ho, 1997). Several agonists of BMP activity, including the BMP ligand ADMP, are expressed in axial territories during gastrulation and in the CNH during segmentation stages (Dickmeis et al., 2001; Lele et al., 2001). Thus, BMP

signaling may play an important role in the development of axial mesoderm after specification of the DV axis. However, the role of BMPs in DV establishment masks their later functions. For example, manipulation of ADMP levels within the embryo causes DV patterning phenotypes that are difficult to resolve from tissue specific defects (Lele et al., 2001; Willot et al., 2002).

In contrast to the known role of BMP activity in DV establishment, prior studies have not addressed the role of the BMP activity gradient as it pertains to axial mesoderm. In this study, we have identified both a requirement for BMP activity in the development of this tissue, as well as the signaling molecule responsible for notochord differentiation. We have been able to address these issues through the inactivation of two BMP antagonists, *fstl1* and *fstl2* (Dal-Pra et al., 2006), that act redundantly to inhibit BMP activity beginning at late gastrulation. Inactivation of these genes, as well as Bmp4 and BMP signaling, reveals that Bmp4 promotes the proliferative capacity of notochord and CNH cells. In the absence of Bmp4, chordamesoderm fails to proliferate and the notochord differentiates prematurely. Our results illustrate the requirement of *fstl1* and *fstl2* in late gastrulation to maintain proper BMP activity levels, which are necessary for the development and timely differentiation of dorsal structures.

Experimental Procedures

Heat-shock conditions

Tg(hsp70l:dnBmpr-GFP)^{w30} (*tBR*) transgenic zebrafish were obtained from the Kimelman lab (University of Washington, Seattle). This transgenic line contains a truncated Type I BMP receptor containing GFP in place of the kinase domain under the control of a heat shock promoter (Pyati et al., 2005). *tBR* embryos were heat-shocked at

37°C for one hour at the time indicated according to Pyati et al. (2005). Where appropriate, wild-type embryos were heat-shocked under the same conditions to serve as controls.

In situ hybridization

The following probes were used: *admp* (Lele et al., 2001), *bmp4* (Nikaido et al., 1997), *col2a1a* (Yan et al., 1995), *eve1* (Joly et al., 1993), *flh* (Talbot et al., 1995), *fstl1* (Dal-Pra et al., 2006), *fstl2* (Dal-Pra et al., 2006), *gsc* (Schulte-Merker et al., 1994), *ihhb* (Currie and Ingham, 1996), *ntl* (Schulte-Merker et al., 1992), *shha* (Krauss et al., 1993), and *spt* (Griffin et al., 1998).

mRNA synthesis

Full length *fstl1/2* cDNA was cloned into pCS2+. Capped mRNAs were transcribed using RNA polymerase in vitro transcription kits (mMESSAGE mMACHINE; Ambion). Approximately 100pg of *fstl1* or *fstl2* mRNA was injected into one- and two-cell stage embryos.

Morpholino injection

Translation-blocking morpholinos are overlap with 22nt at the 5' end of the previously published MO sequence (Dal-Pra et al., 2006). *fstl1* and *fstl2* translation-blocking MOs were as follows: *fstl1* 5'- GCAGCTGCATGGACAGAGTGAAAAC -3'; *fstl2* 5'- CACGGGTAAACACCGAAACATCATT -3'. *fstl* splice-blocking morpholinos were as follows: *fstl1* 5'- CAGACTTACCTTCACATTGTCCGTC -3'; *fstl2* 5'-

AAATTAAAGCTCACCATCACAAGTC -3'. To ensure MO function, RNA was isolated from injected embryos and RT-PCR was performed using primers designed around intron-exon boundaries. Those sequences are as follows: *fstl1* 5'-TAATCATCCAGTCTGTGGCAGTAAT -3' and 5'- CTTGGGCTGTTGATGAT -3'; *fstl2* 5'- GGTCTGCACCGCCATGACTTGT -3' and 5'-ACACGGCGGGTCCACTCCTC -3'. For single morpholino injections, 8ng of MO were injected into one- and two-cell stage embryos. For double morpholino injections, approximately 6ng of each MO was injected. The control morpholino sequence used was 5'-CCTCTTACCTCAGTTACAATTTATA -3'. Where appropriate, control MO was injected into embryos that were subsequently heat-shocked at 37°C for one hour. The *bmp4* splice-blocking morpholino used has been previously characterized (Chocron et al., 2007).

Antibody staining

Labeling with PSMAD1/5/8 was as previously described (Rentzsch et al., 2006). Labeling with Myf5 and F59 were as previously described (Hammond et al., 2007; Topczewska et al., 2001). The primary antibodies were against Myf5 (anti-Myf5 recognizes MyoD in zebrafish; Santa Cruz, C-20) at 1:50, F59 (anti-MyHC; University of Iowa Developmental Studies Hybridoma Bank) at 1:10, 4D9 (anti-Engrailed; University of Iowa Developmental Studies Hybridoma Bank) at 1:20, Prox1 (Angiobio Inc.) at 1:500, and P-SMAD1/5/8 (Chemicon International) at 1:100. Alexa-conjugated Phalloidin (Molecular Probes) was used at a 1:50 dilution to label F-actin. Appropriate Alexa Fluor (Molecular Probes) secondary antibodies were used.

Western blots

Protein extracts were prepared by standard procedures (Westerfield, 1994). Anti-P SMAD1/5/8 and Anti-P SMAD2 (Cell Signaling Technology) were used at a concentration of 1:1000.

BrdU labeling

12-somite embryos were incubated with a solution of 425µl BrdU labeling reagent (Roche Applied Science) and 75µl DMSO for 45 minutes at 6°C. They were then washed in embryo medium for 30 minutes at 28.5°C and fixed with 4% PFA in PBS. BrdU incorporated cells were detected using Alexa Fluor 594 goat anti-mouse IgG at 1:500.

Cell transplantation and margin extripation

Surgical transplantation and extirpation experiments were performed as described (Saude et al., 2000). For ventral margin extirpation, approximately 100 cells were removed by suction from the ventral margin of 80% epiboly embryos. For cell transplantation, donor embryos were injected with a 5% solution of fluorescein dextran (10K MW; Molecular Probes) at one- and two-cell stage embryos. Approximately 30 ventral margin cells taken from shield-stage donors were transplanted into the dorsal organizer of an equivalently staged host. *tBR* embryos were obtained from an incross of homozygous *tBR* parents. Both donor and host embryo were then heat-shocked after

transplantation to maximize BMP signaling inhibition according to previous transplantation protocols (Pyati et al., 2005).

Cell cycle inhibition

Published protocols were followed with slight modifications (Stern et al., 2005). Embryos were treated with a combination of 150μM aphidicolin and 20mM hydroxyurea in 4% DMSO between 80% epiboly and bud stage. Cell proliferation was assayed through BrdU incorporation at stages during and after application.

Bead implantation

Human Bmp2/7 and zebrafish Bmp4 protein-coated beads (R&D Systems) were prepared by overnight incubation of 45μm polystyrene beads (Polysciences) in a 500μg/ml solution of recombinant Bmp2/7 or Bmp4 protein (R&D Systems) in PBS. Before implantation, beads were rinsed three times for 10 minutes in PBS. Control beads were loaded with 500μg/ml BSA.

Cell counting

DAPI-positive cells were quantified and compared by one-way ANOVA, followed by a two-tailed, equal variance *t*-test.

Results

Two BMP antagonists redundantly antagonize BMP activity after DV axis specification

To explore the significance of BMP activity after the onset of gastrulation, we further characterized the roles of two previously identified *follistatin-like* genes (*fstl1* and *fstl2*) (Dal-Pra et al., 2006). These genes are structurally and functionally related to Follistatin (Fst), a known inhibitor of Bmp4 and ADMP (Dal-Pra et al., 2006; Dosch and Niehrs, 2000; Fainsod et al., 1997; Iemura et al., 1998). While *fstl2* mRNA can be detected in cleavage stage embryos, *fstl1* expression is initiated during late gastrulation in dorsal structures. Unlike *fst*, which is expressed only in anterior paraxial mesoderm (Bauer et al., 1998), *fstl1/2* share largely overlapping expression patterns throughout axial and paraxial mesoderm during late gastrulation and segmentation stages (Figure 2.1; Dal-Pra et al., 2006). Fstl2 plays a minor role in BMP antagonism during DV axis specification, as depletion of Fstl2 in a Chordin/Noggin1 deficient embryo slightly increases the severity of the ventralization phenotype observed in Chordin/Noggin1 double morphants. Loss of Fstl2 in either Chordin or Noggin1 single morphant embryos does not enhance the ventralization phenotype (Dal-Pra et al., 2006). As shown by these authors, we observed no DV patterning defects when either Fstl protein was reduced by itself or in combination. The most pronounced morphological defect observed in Fstl1/2 morphants was an enlarged, undulating notochord that became less prominent as somitogenesis continued (see Figures 2.3, 2.4, and 2.10). In addition, we found an increase in molecular markers indicative of an increase in BMP activity (Figures 2.2, 2.3, 2.4).

The domain of the tailbud, which is dependant on BMP activity (Holley, 2006; Szeto and Kimelman, 2006), was increased in Fstl morphant embryos and enlarged to a greater degree when Fstl1/2 were knocked down in concert. The expression domain of

spadetail (*spt*), a T-box domain transcription factor required for trunk segmental identity (Griffin et al., 1998), was increased in Fstl1/2 morphant embryos (Figure 2.2A,B, Figure 2.3). The domain of expression of BMP agonists, which are positively regulated in response to BMP activity, was expanded in the tailbud in a similar fashion (Yamamoto and Oelgeschlager, 2004). This included the expression domains of *bmp4* and the transcriptional target of BMP activity, *eve1* (Figure 2.2E,F,M,N, Figure 2.3; Pyati et al., 2005), as well as *admp* in the posterior notochord (Figure 2.2Q,R). We also observed an increase in phosphorylated (P) SMAD 1/5/8 in the tailbud, which is activated in response to BMP signaling (Fig. 1I,J; Yamamoto and Oelgeschlager, 2004). Western blots against PSMAD1/5/8 indicated that BMP activity is increased in Fstl1/2 morphants beginning at late gastrulation. Prior to 80% epiboly, we observed no change in PSMAD1/5/8 levels (not shown). At the end of gastrulation, we observed an increase in BMP activity that was present at every stage assayed, through 18-somites (Figure 2.2U). Follistatin also binds Activin ligands with high affinity, which initiates intracellular Nodal cascades (Harrington et al., 2006; Nakamura et al., 1991). We observed no change in PSMAD2 levels, a target of Nodal signaling (reviewed in Kitisin et al., 2007), in Fstl1/2 morphants at any stage assayed (Figure 2.2U).

To assess morpholino specificity, we compared the phenotypes generated using non-overlapping translation- and splice- blocking morpholino sequences. The tailbud and notochord phenotypes observed using translation-blocking morpholinos were indistinguishable from those observed using splice-blocking morpholinos (Figure 2.3). In general, morphant phenotypes were reliable and were observed in greater than 90% of embryos (n>500). Furthermore, we attempted to rescue the tailbud phenotype observed

in Fstl1/2 morphants. Injection of either *fstl1* or *fstl2* mRNA caused a reduction in the tailbud domain, consistent with a decrease in BMP activity and a role for Fstl1/2 as BMP antagonists (Figure 2.2C,G,K,O,S; not shown). Coinjection of either *fstl1* or *fstl2* mRNA and *fstl1/2* morpholinos was sufficient to rescue the Fstl1/2 double morphant phenotype, demonstrating the specificity of our morpholinos and a functional redundancy between Fstl1 and Fstl2 (Figure 2.2D,H,L,P,T; not shown). As all of the morphant phenotypes were comparable to each other, the Fstl1/2 morphant phenotypes illustrated here are of embryos injected with *fstl1/2* splice-blocking morpholinos.

Bmp4 activity during late gastrulation is required for chordamesoderm patterning

The expression of *fstl1/2* along the dorsal midline and the notochord defects observed in *fstl1/2* morphants suggest a function in axial development. We observed no changes in the expression of axial markers in Fstl1/2 morphants until late gastrulation, consistent with the temporal rise in PSMAD1/5/8 levels. At 70% epiboly, *goosecoid* (*gsc*) expression in prechordal mesoderm (Schulte-Merker et al., 1994) and *floating head* (*flh*), *no tail* (*ntl*), and *admp* expression in chordamesoderm (Dickmeis et al., 2001; Schulte-Merker et al., 1992; Talbot et al., 1995) of Fstl1/2 morphants were comparable to controls (Figure 2.4A,B,H,I,O,P,V,W). At 90% epiboly, the domain of prechordal mesoderm was unchanged in Fstl1/2 morphant embryos (Figure 2.4C,D), but the domain of chordamesoderm was expanded anteriorly (Figure 2.4J,K,Q,R,X,Y).

Since changes in chordamesodermal gene expression in Fstl1/2 morphants appeared to be a result of increased BMP activity, we wished to determine the effects of

lowering BMP activity on this tissue. We were able to conditionally inactivate BMP activity through the use of a transgenic zebrafish line carrying a truncated BMP-type I receptor fused to GFP under the control of a heat shock promoter (abbreviated *tBR*; Pyati et al., 2005). Heat-shocking these embryos for one hour at 37°C blocks BMP effector expression for at least two hours and is capable of inducing severe dorsalization phenotypes depending on the timing of heat shock (Pyati et al., 2005). To determine the temporal effectiveness of this transgene, *tBR* embryos were heat-shocked during late gastrulation in hourly intervals and stained with PSMAD1/5/8 antibodies (Figure 2.5). Between one and three hours post heatshock, PSMAD1/5/8-positive cells were not detectable in *tBR* embryos, suggesting that heatshock attenuates BMP activity over this time range during early somitogenesis.

As we observed an expanse in chordamesoderm and an increase in PSMAD1/5/8 levels during late gastrulation in Fstl1/2 morphants, we heat-shocked *tBR* embryos at 80% epiboly to examine the consequence of blocking BMP activity on chordamesoderm. In these embryos, the domain of prechordal mesoderm was unchanged relative to heat-shocked controls (Figure 2.4E), while chordamesoderm was absent anteriorly (Figure 2.4L,S,Z). Knockdown of Bmp4 also resulted in a reduction of chordamesoderm (Figure 2.4M,T,AA), but not of prechordal mesoderm (Figure 2.4F). The reduced domain of chordamesoderm observed when Fstl1/2 and Bmp4 were knocked down together resembled that of Bmp4 morphant embryos (Figure 2.4N,U,BB).

A critical window of Bmp4 activity establishes the proliferative state and size of the CNH and notochord

Using riboprobes against *shha* and *ntl* we examined the effect of manipulating BMP activity on the size of the notochord and CNH. The size of the CNH in Fstl1/2 morphant embryos was expanded when compared to controls (Figure 2.6A,B,K,L). Sections through the trunk between somites 5-10 revealed that the diameter of the notochord was also increased in these embryos; the mean number of cells populating the notochord was increased by 63% when compared to controls (Figure 2.6F,G; 4.1 cells vs. 6.5 cells, n=10; $p<0.001$).

In contrast to the expansion of the notochord and CNH observed in Fstl1/2 morphant embryos, attenuation of Bmp4 activity caused a reduction in both the diameter of the notochord as well as the size of the CNH. The axial phenotype observed when Bmp4 was knocked down largely resembled that of *tBR* embryos that were heat-shocked at 80% epiboly (Figure 2.6C,E,M,O), with the mean number of cells populating the notochord decreased by approximately 41% (Figure 2.6H,J; 4.1 cells vs. 2.4 cells and 2.9 cells, n=10; $p<0.001$). The difference in notochord cells of *tBR* embryos and Bmp4 morphants was not significant from one another ($p>0.05$). In both *tBR* embryos heat-shocked at 80% epiboly and Bmp4 morphants, we observed the formation of ectopic tail structures. These observations are consistent with roles assigned to BMP activity in patterning ventroposterior tissues during late gastrulation (Pyati et al., 2005; Stickney et al., 2007).

To determine the temporal requirements of axial cells for BMP activity, we heat-shocked *tBR* embryos at hourly intervals beginning at 80% gastrulation, corresponding to the time at which increased PSMAD1/5/8 levels were observed in Fstl1/2 morphants. The size of the notochord and CNH in embryos heat-shocked at bud stage was

comparable to those of embryos heat-shocked at 80% epiboly (not shown). Embryos heat-shocked at the 3-somite stage yielded a notochord diameter and CNH domain that were indistinguishable from heat-shocked controls (Figure 2.6D,I,N; 4.1 cells vs. 4.3 cells, n=10; $p>0.05$).

We wished to address the underlying cause of the increase in chordamesoderm. Because chordamesoderm transfates to paraxial mesoderm in *flh* mutants (Halpern et al., 1995), we reasoned that an expanse in chordamesoderm may occur at the expense of paraxial mesoderm. However, the analysis of *deltaC* (*dlC*), *myoD*, and *paraxial protocadherin* (*papc*) expression revealed no changes in paraxial territory of Fstl1/2 morphants or in *tBR* embryos heat-shocked at 80% epiboly (see Figure 2.14).

Because our results did not suggest that fate assignment was disrupted in Fstl1/2 morphants, we addressed whether the increase in chordamesoderm was due to increased cell proliferation by assaying BrdU incorporation. In 14-somite controls, we observed PSMAD1/5/8 and BrdU antibodies co-labelling notochord cells (Figure 2.7A-A''). In addition to labeling these cells in Fstl1/2 morphants, cells of the CNH were positive for PSMAD1/5/8 and BrdU, and axial cells that were BrdU-positive were also positive for PSMAD1/5/8 (Figure 2.7B-B''). Axial cells of Fstl1/2 morphants that were BrdU-positive were also found in positions more anterior than in controls (not shown). In contrast, heat-shocking *tBR* embryos at 80% epiboly or bud stage resulted in loss of BrdU incorporation in both endogenous and ectopic axial structures (Figure 2.7C-C''; not shown). We observed no changes in cell proliferation when we heat-shocked *tBR* embryos at 3-somites (not shown). The presence of PSMAD1/5/8-positive axial cells in Bmp4 morphants (Figure 2.7D-D'') indicates that axial cells receive signaling from

multiple BMP ligands, and also that loss of Bmp4 does not affect signaling of other BMPs, consistent with previous reports (Stickney et al., 2007). Nevertheless, reduction of Bmp4 levels was sufficient to inhibit axial proliferation; cell proliferation in Bmp4 morphants resembled that of *tBR* embryos heat-shocked at 80% epiboly. This suggests that BMP activity, particularly Bmp4, acts prior to 3-somites to promote chordamesodermal proliferation.

Ventral margin as the source of axially required BMP ligands

The ventral margin acts as the major secreting center of BMPs during gastrulation (Agathon et al., 2003; Schier and Talbot, 2005; Yamamoto and Oelgeschlager, 2004) and is in close proximity to dorsal cells at the end of gastrulation. However, because BMP signaling initiates positive feedback mechanisms in target cells (Yamamoto and Oelgeschlager, 2004), an alternate source of BMP ligands might initiate from PSMAD1/5/8-positive chordamesoderm. To demonstrate that BMP signals originate from the ventral margin, we removed approximately 100 cells from the ventral side of the embryo at 80% epiboly and examined the effects on chordamesoderm. Embryos lacking most of their ventral margin resembled Bmp4 morphants; the sizes of ventral fin and ventral somitic mesoderm were reduced (Figure 2.8). Both the domain of chordamesoderm as well as cell proliferation in this tissue was reduced, resembling that of Bmp4 morphants and *tBR* embryos heat-shocked at 80% epiboly (Figure 2.8B-E’’). This suggests that chordamesoderm possesses a requirement for ventrally-derived BMP ligands during late gastrulation.

BMP activity levels influence the temporal state of the notochord

In addition to notochord size, we wished to determine if alteration of BMP activity affects the timing of notochord differentiation. In both *tBR* embryos heat-shocked at 80% epiboly and Bmp4 morphants, the expression of markers indicative of chordamesoderm was shifted such that they resembled expression patterns seen in more mature notochord. Expression of *ihhb* at 9-somites, which can be detected throughout the entire notochord in control embryos, was maintained only in the caudal notochord of embryos lacking Bmp4 (Figure 2.9A-C). Likewise, *shha* expression was lost from the notochord but maintained in floor plate and the diencephalon in 24hpf *tBR* embryos, Bmp4 morphants, and embryos lacking ventral margin (Figure 2.9E-G, I-K, Figure 2.8G). These results were confirmed by loss of *ptc1* expression from the trunk and tail, where the expression pattern of 24hpf embryos lacking Bmp4 resembled 36hpf controls (Figure 2.9M-O,DD, Figure 2.8H). *col2a1a* expression was absent from the floor plate of 36hpf *tBR* embryos heat-shocked at 80% epiboly and Bmp4 morphants, more closely resembling the expression observed in 48hpf controls (Figure 2.9Q-S,GG).

Conversely, in Fstl1/2 morphants chordamesodermal gene expression was prolonged when compared to controls, resembling that of embryos at younger developmental stages. Expression of *ihhb*, which is restricted to the caudal notochord in 18-somite embryos, was maintained in the rostral notochord of Fstl1/2 morphant embryos (Figure 2.9U,V). We also observed *shha* expression in vacuolated notochord cells and *ptc1* expression in axial and paraxial tissues of the trunk of 36hpf Fstl1/2 morphants, where they are not expressed in controls (Figure 2.9X,Y,AA,BB,DD,EE). *col2a1a* expression was maintained in the notochord of 48hpf Fstl1/2 morphants (Figure

2.9GG,HH), resembling expression of 24hpf controls (Yan et al., 1995). The gene expression patterns observed in Fstl1/2 morphants are consistent with a delay in transitioning into differentiated notochord, as is observed in embryos lacking Col15a1 (Pagnon-Minot et al., 2008) and Laminin1/4/5 (Parsons et al., 2002; Pollard et al., 2006).

As cells populating the notochord become vacuolated during differentiation, we examined the morphology of the notochord in embryos with altered BMP activity. In 24hpf controls, notochord cells swell and become vacuolated in an anterior to posterior fashion (Figure 2.10A,C,D). While we did not observe any changes in anterior cell morphology at the level of the hind yolk extension in Fstl1/2 morphants, cells of the caudal notochord at the level of the cloaca were smaller than those observed in control embryos (Figure 2.10B,E,F). Conversely, *tBR* embryos heat-shocked at 80% epiboly and Bmp4 morphants exhibited caudal notochord cells at the level of the cloaca that became vacuolated well before those observed in control embryos (Figure 2.10G-J). Precocious vacuolation of notochord cells was also observed in embryos lacking ventral margin (Figure 2.8F). This suggests that prolonged BMP activity delays the chordamesodermal transition into mature notochord. In the absence of Bmp4, the notochord differentiates prematurely.

The proliferative state of chordamesoderm establishes the timing of notochord maturation

Alterations in BMP activity levels influence both the proliferative properties of chordamesoderm as well as the timing of its differentiation. To determine whether the proliferative capacity of chordamesoderm influences the timing of its maturation, we

used small molecule inhibitors of the cell cycle (Stern et al., 2005) to block cell proliferation during the window in which BMP activity influences the proliferative capacity of chordamesoderm. We found that treating embryos from 80% epiboly to bud stage with a combination of hydroxyurea and aphidicolin effectively blocked cell proliferation during late gastrulation (Figure 2.11A,B; not shown). Removing the inhibitors at bud stage allowed proliferation to resume two hours after washing, although BrdU incorporating cells were not observed in chordamesoderm (Figure 2.11C-C''). The chordamesoderm defects observed in embryos treated with cell cycle inhibitors during late gastrulation resembled the defects observed in embryos lacking Bmp4. Expression of the chordamesodermal markers *ihhb*, *shha*, and *col2a1a* resembled expression in Bmp4 morphants (Figure 2.9D,H,L,P,T), and notochord cells at the level of the cloaca became vacuolated before those of controls (Figure 2.10K,L).

In contrast to embryos with reduced BMP activity, chordamesoderm proliferation is increased and transition into mature notochord is delayed in Fstl1/2 morphants. By treating Fstl1/2 morphants with hydroxyurea and aphidicolin from 80% epiboly to bud stage, we were able to rescue the prolonged expression of chordamesoderm markers. Expression of *ihhb* and *shha* was restricted to caudal notochord in these embryos, resembling comparably staged controls (Figure 2.9W,Z,CC). Similarly, *col2a1a* expression was lost from the notochord and floor plate of 48hpf Fstl1/2 morphants treated with cell cycle inhibitors, also resembling controls (Figure 2.9I). This suggests that the proliferative state of chordamesoderm, which is established during late gastrulation, determines the timing of the chordamesoderm transition into mature notochord.

A direct role for BMP signaling in notochord development

The presence of PSMAD1/5/8-positive cells (Figure 2.7) suggests that chordamesoderm is directly influenced by BMP activity. To demonstrate that this tissue autonomously responds to BMP signaling, we removed approximately 30 cells from the ventral margin of shield stage embryos and transplanted them into the dorsal organizer of an equivalently staged host (Figure 2.10O). Upon placing wild-type cells into a wild-type host, these cells reliably populated the notochord, consistent with previous fate mapping and transplantation studies (Gritsman et al., 2000; Saude et al., 2000). Transplantation of ventral wild-type cells into *tBR* embryos heat-shocked after transplantation resulted in donor cell morphology resembling that of control embryos (94/132; Figure 2.10P,Q). Surprisingly, we found that these cells populated the entire notochord at the exclusion of endogenous *tBR* cells. Following the transplantation of ventral *tBR* cells into wild-type embryos, the *tBR* cells consistently failed to populate the notochord (0/151; Figure 2.10R,S). They did, however, populate adjacent paraxial mesoderm, contributing to myofibers and somitic cells. Thus, BMP activity biases cells in proximity of the dorsal organizer to become chordamesoderm.

To further explore the effects of Bmp4 activity on notochord fate, recombinant zebrafish Bmp4-soaked beads were implanted near the organizer of shield stage embryos (Figure 2.12A). This way, involuting cells would be exposed to Bmp4. Embryos exposed to ectopic Bmp4 exhibited an expanse of chordamesoderm at late gastrulation stages and an increase in notochord and CNH size in segmentation stage embryos when compared to embryos exposed to BSA-soaked beads (Figure 2.12B,C,J,K). At 24hpf, the notochord of these embryos was composed of a bilayer of cells rather than a monolayer

observed in controls, and development of the floor plate was delayed (Figure 2.12D,F,G,I). By 48hpf, the floor plate became visible in Bmp4-treated embryos, although notochord cell morphology remained irregular (Figure 2.12M,N). These cells did not fully vacuolate, and some cells remained arranged in a bilayer. *tBR* embryos exposed to Bmp4-soaked beads and heat-shocked at 80% epiboly did not exhibit enlarged notochords (Figure 2.12E,H).

Because we observed that axial cells remained PSMAD1/5/8-positive when Bmp4 was knocked down, we wished to examine the effects of other BMPs on notochord development (Figure 2.13). Implantation of beads soaked with recombinant human Bmp2/7 did not noticeably alter the domain of chordamesoderm or notochord morphology when compared to controls.

The timing of notochord maturation influences myotome patterning

Because delays in notochord maturation disrupt myotome patterning (Pagnon-Minot et al., 2008), we examined slow and medial fast muscle specification in Fstl1/2 morphant embryos. During early somitogenesis stages, Hedgehog (Hh) activity maintains *myoD* expression in slow and medial fast muscle precursors (Barresi et al., 2000; Linker et al., 2003; Wolff et al., 2003). In embryos lacking Fstl1/2, *myoD* expression was upregulated in the presumptive slow and medial fast territories of the somite (Figure 2.14A,B). Immunostaining with antibodies against MyoD confirmed a significant increase in MyoD-positive cells when compared to controls (Figure 2.14; 74.6 vs. 120.4, n=5; $p<0.001$). Fstl1/2 morphant embryos also displayed an increase in horizontal myoseptum size, as evidenced by immunostaining with F59 antibodies that

recognize mainly slow muscle (Figure 2.14G,H; Devoto et al., 1996). Likewise, the number of Engrailed-positive cells, which are induced in response to Hh activity (Wolff et al., 2003), was increased in Fstl1/2 morphants (Figure 2.14J,K,M,N).

Attenuation of BMP activity at 80% epiboly had the converse effect on myofiber specification. While *myoD* expression was maintained in presumptive slow muscle cells in *tBR* embryos, a significantly smaller number of MyoD-positive cells were found in the presumptive medial fast muscle domain (Figure 2.14C,F; 57.2 vs. 74.6, n=5; $p<0.001$). Embryos failed to form an organized horizontal myoseptum, and exhibited a reduction in Engrailed-positive muscle pioneers and medial fast muscle fibers (Figure 2.14I,L,O). The disruptions in myofiber specification suggest that the timing of notochord maturation influences Hh activity levels in adjacent paraxial mesoderm.

Discussion

Members of the BMP family of signaling molecules are typically assigned roles in specification of ventral cell fate. Here we describe a previously unappreciated function for BMP signaling in the promotion of dorsal fate. We demonstrate that Bmp4 patterns axial tissue by promoting chordamesoderm proliferation, ultimately influencing the size of the notochord and CNH. Two BMP antagonists, Fstl1/2, modulate BMP activity to appropriate levels in chordamesoderm. In their absence the chordamesoderm domain is expanded, and these cells do not transition into mature notochord in a timely manner. Conversely, in the absence of Bmp4 the chordamesodermal domain shrinks and notochord cells differentiate prematurely. As such, we demonstrate a requirement for BMP activity in the timing of notochord differentiation.

Axial requirements for BMP activity change as gastrulation proceeds

Models addressing BMP activity in embryogenesis have established the ventralizing role of BMP signaling in specifying DV fate (Kimelman, 2006; Schier and Talbot, 2005). Surprisingly, our study demonstrates a dynamic requirement of axial tissue for BMP activity during gastrulation. Following establishment of the DV axis, axial cells require tightly regulated levels of BMP activity for proper patterning of chordamesoderm and its precursor pool. Changes in axial requirements for BMP activity is consistent with two recent studies in zebrafish examining BMP and Nodal activity during zebrafish gastrulation. Tucker and colleagues (2008) demonstrated that BMP patterning of the DV axis occurs progressively in an anterior to posterior fashion as gastrulation proceeds. Hagos and Dougan (2007) demonstrated that cells responsive to Nodal signaling acquire their fate based upon the cumulative dose of Nodal signals the cell receives. This is a function of both the competence of the receiving cells as well as the strength of the signal. These studies suggest that cells possess different requirements for activity gradients as gastrulation proceeds. This is in agreement with the characteristic migration of two margins into proximity with the other during gastrulation- the ventral margin secreting BMP ligands and the dorsal organizer secreting BMP antagonists (Agathon et al., 2003). As the circumference of the margins decrease during epiboly, cells populating ventral and dorsal margins receive increasing amounts of factors secreted from the other margin. The question is, at what point does distance between the two margins influence the BMP activity gradient on the dorsal side of the gastrula?

Our results demonstrate that the ventral margin does indeed influence cells arising from the dorsal margin, beginning during the transition from mid- to late-gastrulation.

Attenuation of total BMP activity at any developmental stage between 80% epiboly and 3-somites arrests chordamesodermal proliferation, culminating in a reduction in the size of the notochord and CNH. Because attenuation of BMP activity after the 3-somite stage has no apparent effect on axial structures, we propose that BMP ligands emanating from the ventral organizer during late gastrulation signal presumptive axial cells in the dorsal margin.

It is possible, although unlikely, that axial cells require BMP activity prior to late gastrulation. Labeling embryos with PSMAD1/5/8 antibodies at hourly intervals has revealed that PSMAD1/5/8-positive cells are not observed in the dorsal gastrula until late gastrulation (Tucker et al., 2008). Therefore, the rise of PSMAD1/5/8 levels after 80% epiboly in Fstl1/2 morphants is consistent with a role in mediating BMP activity in axial tissue.

Selective requirement of BMP activity in the chordamesoderm

Nodal activity is critical for both the induction of mesoderm and the specification of axial cell fate (Kimelman, 2006; Schier and Talbot, 2005; Stemple, 2005). The location of cells within the dorsal organizer dictates the level of Nodal activity that axial mesoderm receives. High levels of Nodal signaling specify deep *gsc*-expressing prechordal plate, while lower levels specify more superficial *flh*-expressing chordamesoderm (Gritsman et al., 2000; Saude et al., 2000). Since Follistatin binds Activin ligands (Harrington et al., 2006; Nakamura et al., 1991), one possibility for the notochord phenotype observed in Fstl1/2 morphants is an alteration in Nodal activity. If this activity were significantly altered, one would expect a transfating between types of

axial mesoderm, as has been observed in mutants lacking zygotic contribution of the Nodal co-receptor Oep (Gritsman et al., 2000). However, we observe no changes in the prechordal domain of Fstl1/2 morphants as assayed by the expression of the Nodal-responsive gene *gsc* and PSMAD2 levels. Furthermore, the phenotypes observed in chordamesoderm and notochord of embryos with reduced BMP activity are complementary to those observed in Fstl1/2 morphants. Thus, the main role of Fstl1/2 is to modulate BMP activity.

Two models can explain the inability of prechordal cells to respond to BMP signaling: the location of these cells during gastrulation, or their competence to respond to Bmp4. As gastrulation proceeds, prechordal plate cells rapidly increase their distance from the ventral margin, distancing themselves from BMP-secreting cells. If prechordal cells were competent to respond to Bmp4, *gsc* expression would be altered in embryos receiving Bmp4-soaked beads. Therefore, a more plausible model is that prechordal plate cells are not competent to respond to Bmp4 during mid- to late-gastrulation, which would make them distinct from chordamesoderm precursors in the dorsal organizer.

A balance between proliferation of the CNH and differentiation of chordamesoderm

Our results indicate that during late gastrulation through early somitogenesis, BMP signaling regulates the size of the chordamesodermal domain by establishing its proliferative state. In the absence of Bmp4, chordamesodermal cells prematurely transition into differentiated notochord. Conversely, chordamesodermal proliferation is increased in Fstl1/2 morphants and maturation of the notochord is delayed. BMP

signaling may play a dual, independent role to control the proliferative status of the CNH and chordamesoderm and to regulate the timely differentiation of notochord precursors. By inhibiting cell proliferation over the same window at which BMP activity influences the proliferative state of chordamesoderm, we were able to mimic the notochord phenotype observed in *tBR* embryos and Bmp4 morphants. Additionally, blocking cell proliferation inhibits the prolonged maintenance of chordamesodermal character observed in Fstl1/2 morphants. Since heat-shocking *tBR* embryos after 3-somites has no apparent effect on indicators of notochord differentiation, it is likely that BMP activity does not directly delay chordamesoderm maturation. Rather, the evidence presented suggests a single role for BMP signaling in controlling proliferation and favors a causal link between CNH proliferation and notochord maturation. We propose a model where the size of the axial precursor pool, established by Bmp4 and tightly controlled by two Fstl proteins, ultimately determines the maturation schedule of the notochord. While we demonstrate the requirement of Fstl1/2 in this process, both *chordin* (*chd*) and *noggin1/2* (*nog1/2*) are also chordamesodermally expressed, with *nog1/2* expression persisting in the CNH through notochord maturation (Fürthauer et al., 1999; Miller-Bertoglio et al., 1997). Although their requirement in DV specification prevents simple morpholino-mediated inactivation (Dal-Pra et al., 2006; Hammerschmidt et al., 1996a; Hammerschmidt et al., 1996b; Schulte-Merker et al., 1997), we cannot rule out that either *chd* or *nog1/2* might act synergistically with *fstl1/2* in chordamesoderm development as they do in early DV patterning. Similar models for a role of Bmp4 signaling in balancing proliferation and differentiation have been proposed in other contexts. The influence Bmp4 exerts over hematopoietic stem cell (HSC) proliferation (Zhang and Li, 2005)

draws parallels with the effect of losing Bmp4 on the CNH. Bmp4 promotes the proliferative state of HSCs while delaying differentiation (Zhang et al., 2003). In the absence of Bmp4, HSCs exit the cell cycle and differentiate prematurely (Bhatia et al., 1999).

In addition to notochord contributions, cells from the CNH give rise to floor plate and tailbud mesoderm (Cambray and Wilson, 2002; Charrier et al., 1999; Davis and Kirschner, 2000). Our transplantation experiments suggest a particular requirement for BMP responsiveness in chordamesoderm: BMP-responsive cells preferentially populate the notochord, while cells unresponsive to BMP signaling contribute to paraxial and tailbud mesoderm. In addition to its role in proliferation and differentiation, differential levels of BMP activity appear to be critical in relegating CNH cells to a particular fate.

Experiments by Agathon and colleagues (2003) have shown that the BMP-rich ventral margin in zebrafish posses tail organizer activity that contributes to non-axial derivatives in the tail, while the CNH, derived from the dorsal organizer, contributes to axial components. Their data, along with other studies (Beck et al., 2001; Gont et al., 1993; Pyati et al., 2005; Tucker and Slack, 1995) suggest that axial and non-axial tissues of the tailbud can develop independently under certain experimental conditions. However, as these two organizing centers move into close proximity at the end of gastrulation, they likely need to interact with each other to promote the coordinated growth, patterning, and differentiation of the tailbud. Our studies have revealed a requirement for BMP signaling from the ventral margin on the dorsal organizer, providing a mechanism by which such coordination can be achieved and demonstrating

previously unappreciated roles of BMP activity in the patterning and maturation of axial structures.

Acknowledgements

We would like to thank M. Halpern for comments and criticisms on the manuscript, D. Kimelman and U. Pyati for the *Tg(hsp70l:dnBmpr-GFP)*^{w30} zebrafish line, M. Esterberg for assistance with statistics. The F59 and 4D9 antibodies developed by F. Stockdale and C. Goodman, respectively, were obtained from the Developmental Studies Hybridoma Bank developed under the auspices of the NICHD and maintained by The University of Iowa, Department of Biology, Iowa City, IA 52242. This work was supported by an NIH grant to A.F. (DC004701).

Figure 2.1: Expression of *follistatin-like* genes *1* and *2*.

(A) Lateral view, animal pole at the top. (C,D) Lateral views, ventral to the left. (E-H) Dorsal views, with anterior to the top. (I,J) Transverse sections through the trunk of 6-somite embryos. (K,L) Lateral views, with anterior to the left. (M,N) Transverse sections of 24hpf embryos at the level of somites 10-15.

Figure 2.1

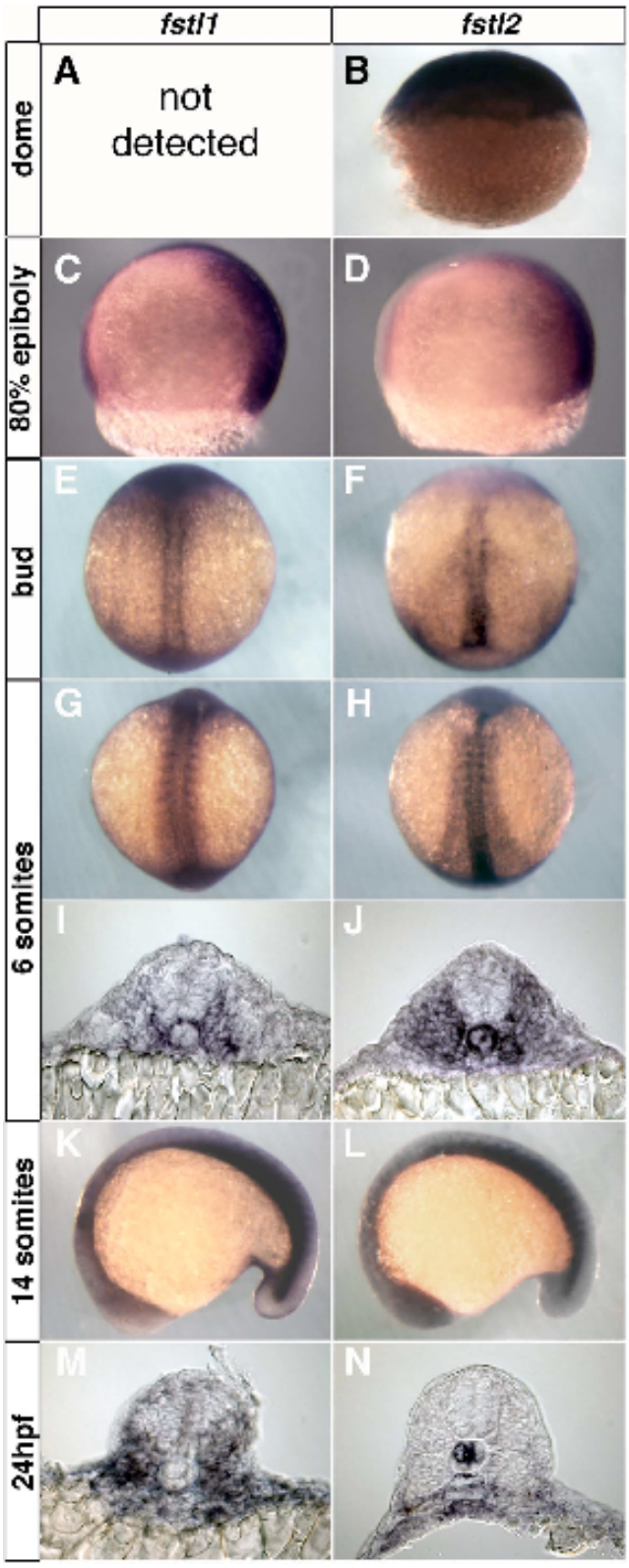
fstl1
fstl2
dome
80% epiboly
bud
6 somites
14 somites
24hpf
A
not
detected
B
C
D
E
F
G
H
I
J
K
L
M
N

Figure 2.2: Expansion of the tailbud in Fstl1/2 morphant embryos.

Expression of the tailbud markers *spt* (A-D), *bmp4* (E-H), PSMAD1/5/8 (I-L), *eve1* (M-P), and the posterior axial marker *admp* (Q-T) in 6-somite embryos. (U) Levels of PSMAD1/5/8, but not PSMAD2, are increased in Fstl1/2 morphants beginning at late gastrulation. All views except (E-L) are dorsal views, with anterior to the top. (E-L) are lateral views, with anterior to the left. Brackets illustrate the expression domain observed in control embryos.

Figure 2.2

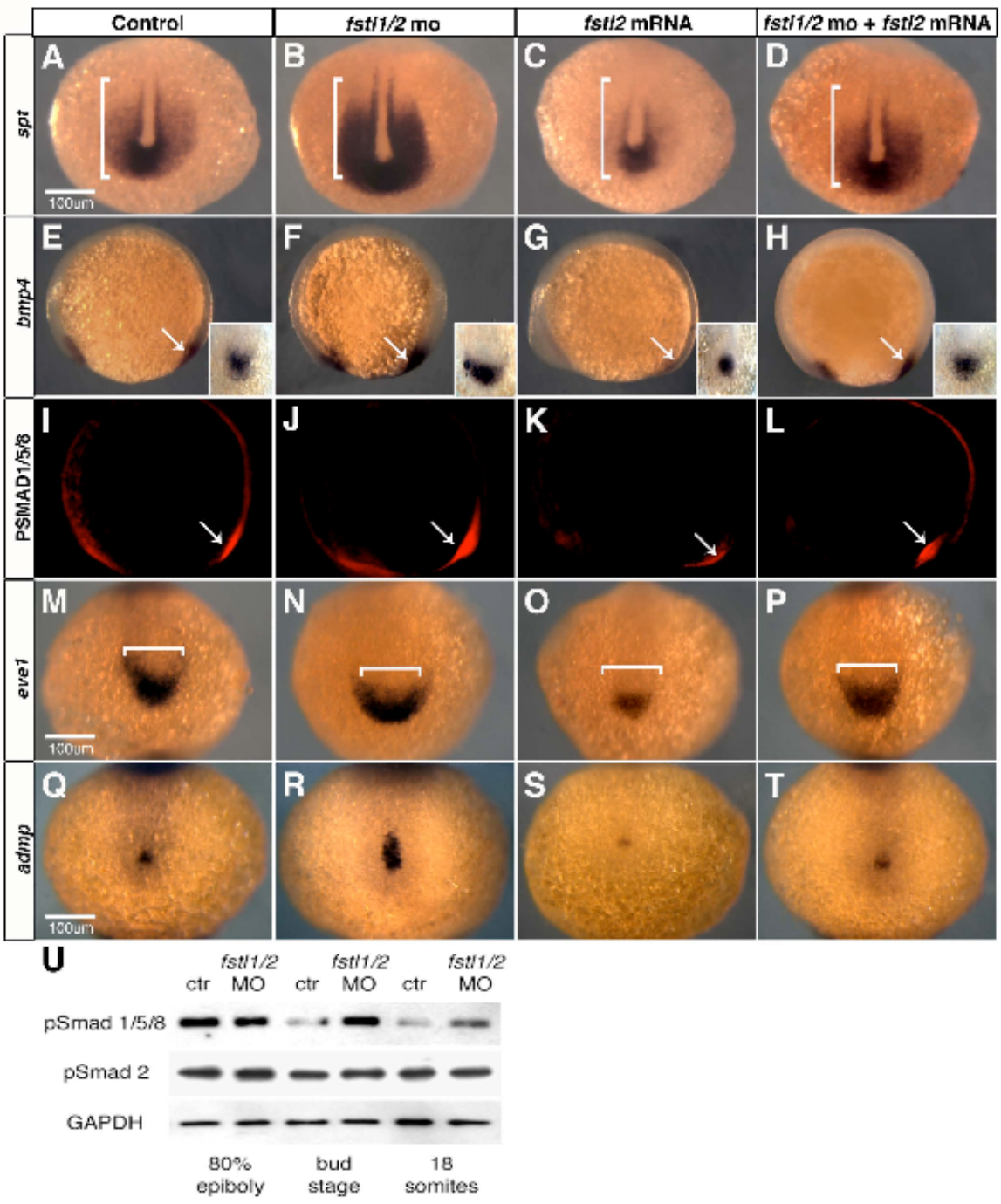
Control
fstl1/2 mo
fstl2 mRNA
fstl1/2 mo + fstl2 mRNA
spt
bmp4
PSMAD1/5/8
eve1
admp
A
B
C
D
E
F
G
H
I
J
K
L
M
N
O
P
Q
R
S
T
100um
U
fstl1/2
ctr MO ctr MO ctr MO
pSmad 1/5/8
pSmad 2
GAPDH
80% epiboly
bud stage
18 somites

Figure 2.3: Phenotype of translation-blocking *fstl1/2* morpholinos.

The size of the notochord and tailbud are increased in embryos injected with a single *fstl* morpholino, and to a greater extent when *fstl1/2* morpholinos are injected in combination. Brackets illustrate the domain observed in control embryos.

Figure 2.3

Figure 2.4: Bmp4 is required in the establishment of chordamesoderm during late gastrulation.

(A,B,H,I,O,P,V,W) Morpholino knockdown of Fstl1/2 has no effect on the development of axial structures prior to 70% epiboly. (C-F,J-M,Q-T,X-AA) At 90% epiboly, alteration of BMP signaling reveals a requirement for BMP activity in patterning of chordamesoderm. *gsc* (C-G) expression in prechordal plate, and *flh* (J-N), *ntl* (Q-U), and *admp* (X-BB) expression in chordamesoderm. (A-G,O,P) Views are lateral, with ventral to the left. Insets in (A-G) are dorsal views of the prechordal plate domain. Insets in (O,P) are dorsal views of chordamesodermal domain. All other views are dorsal views, with anterior to the top. Scale bar in (A) is for all panels.

Figure 2.4

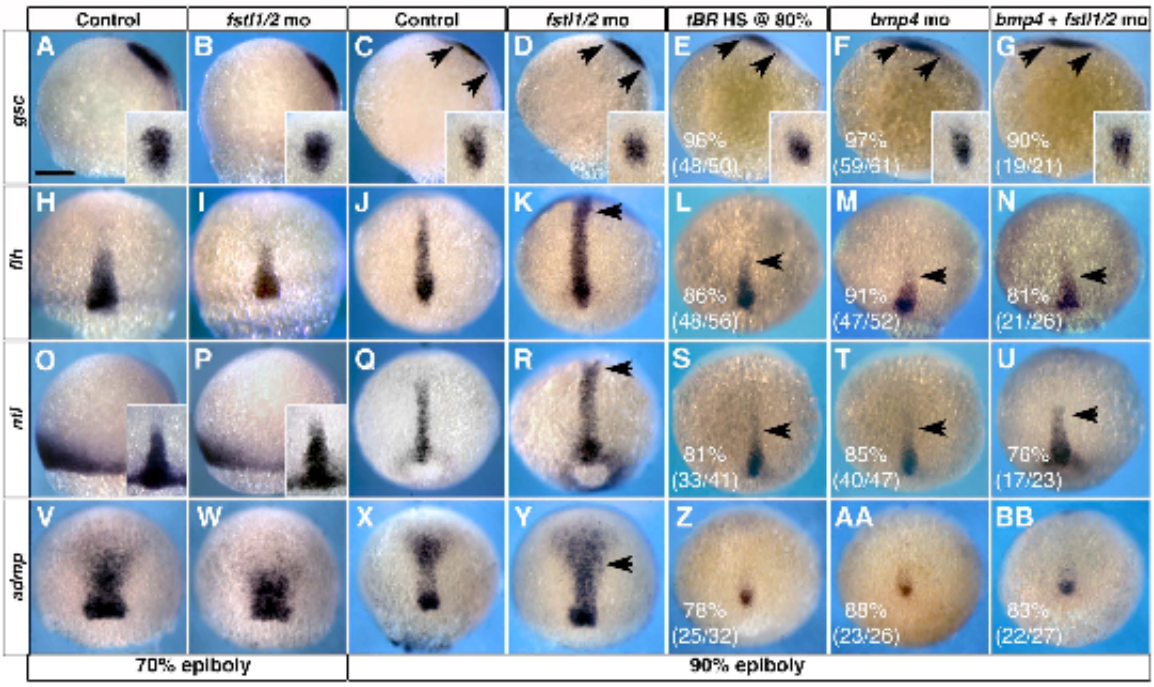
Control
fstl1/2 mo
Control
fstl1/2 mo
tBR HS @ 80%
bmp4 mo
bmp4 + fstl1/2 mo
gsc
flh
ntl
admp
A
B
C
D
E
F
G
96%
(48/50)
97%
(59/61)
90%
(19/21)
H
I
J
K
L
M
N
86%
(48/56)
91%
(47/52)
81%
(21/26)
O
P
Q
R
S
T
U
81%
(33/41)
85%
(40/47)
76%
(17/23)
V
W
X
Y
Z
AA
BB
78%
(25/32)
88%
(23/26)
85%
(22/27)
70% epiboly
90% epiboly

Figure 2.5: BMP attenuation in *tBR* embryos heat-shocked during late gastrulation. Wild-type and *tBR* embryos were heat-shocked during late gastrulation and fixed at 30 minute intervals. Antibodies against PSMAD1/5/8 (red) labels cells responding to BMP activity at the times and backgrounds indicated.

Figure 2.5

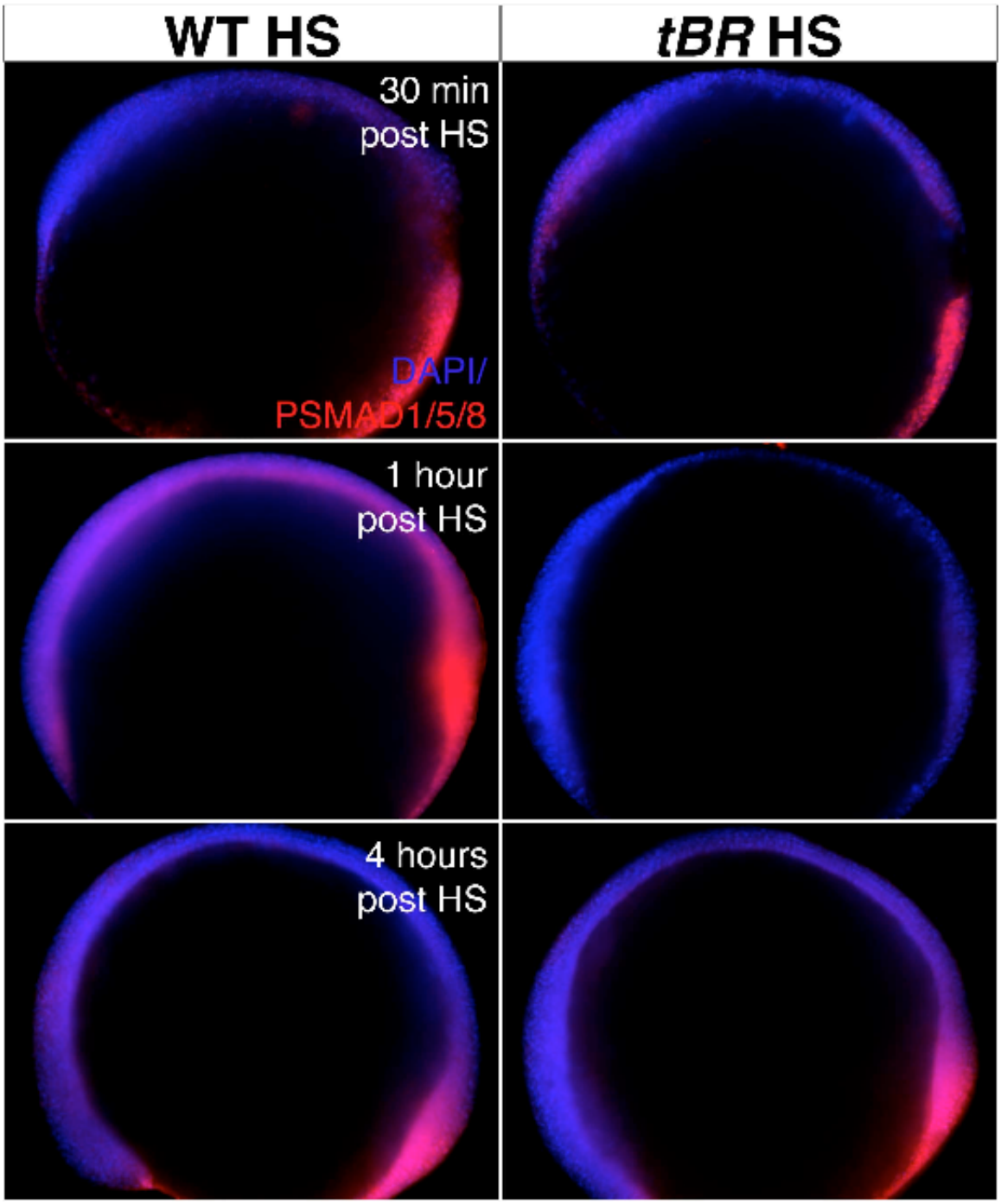
WT HS
tBR HS
30 min
post HS
DAPI/
PSMAD1/5/8
1 hour
post HS
4 hours
post HS

Figure 2.6: Sizes of the notochord and chordoneural hinge (CNH) are influenced by Bmp4 activity during late gastrulation.

(A-E) *shha* expression in 14-somite embryos. Insets are lateral views of the CNH. (K-O) *shha* expression in sections through somites 5-10 of 18-somite embryos. Insets are cropped images of the same section stained with DAPI. The mean number of DAPI-stained cells from 10 experimental embryos was subjected to one-way ANOVA, followed by a two-tailed, equal variance *t*-test. Asterisks denote significance ($p<0.001$). (U-Y) *ntl* expression in 24hpf embryos. CNH domains are denoted with arrowheads, arrows point to ectopic tail formation. (A-E) Dorsal views, with anterior to the left. (U-Y) Lateral views, with anterior to the left.

Figure 2.6

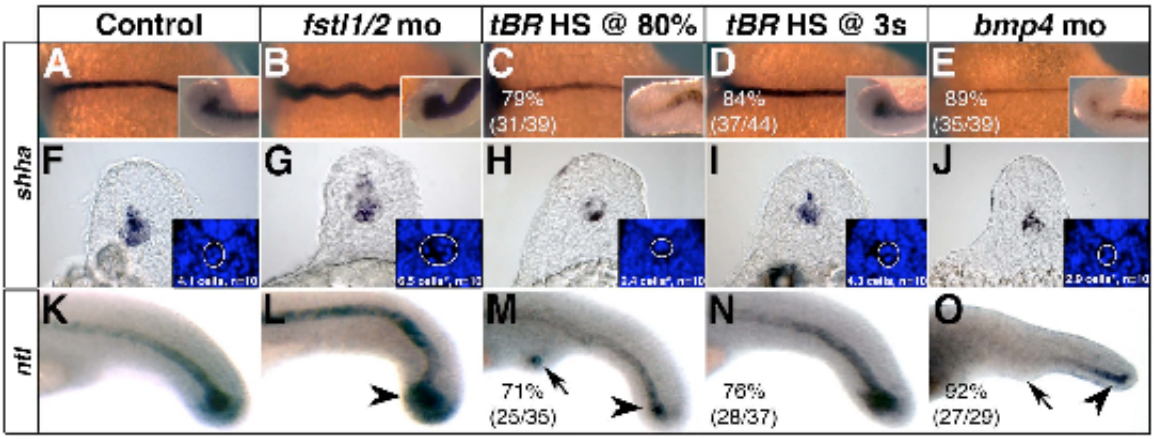
Control
fstl1/2 mo
tBR HS @ 80%
tBR HS @ 3s
bmp4 mo
shha
ntl
A
B
C
79%
(31/39)
D
84%
(37/44)
E
89%
(35/39)
F
G
H
I
J
K
L
M
71%
(25/35)
N
76%
(28/37)
O
92%
(27/29)

Figure 2.7: BMP activity establishes proliferation in axial mesoderm.

Longitudinal sections through the tailbud of 14-somite embryos exposed to PSMAD1/5/8 (red) and BrdU (green) antibodies reveal that axial cells undergoing proliferation are responding to BMP activity. Cell proliferation is increased in axial tissue of Fstl1/2 morphants (B-B''), and reduced in *tBR* embryos heat-shocked at 80% epiboly (C-C'') and Bmp4 morphants (E-E''). Arrowheads denote the CNH. Anterior is to the left in all views.

Figure 2.7

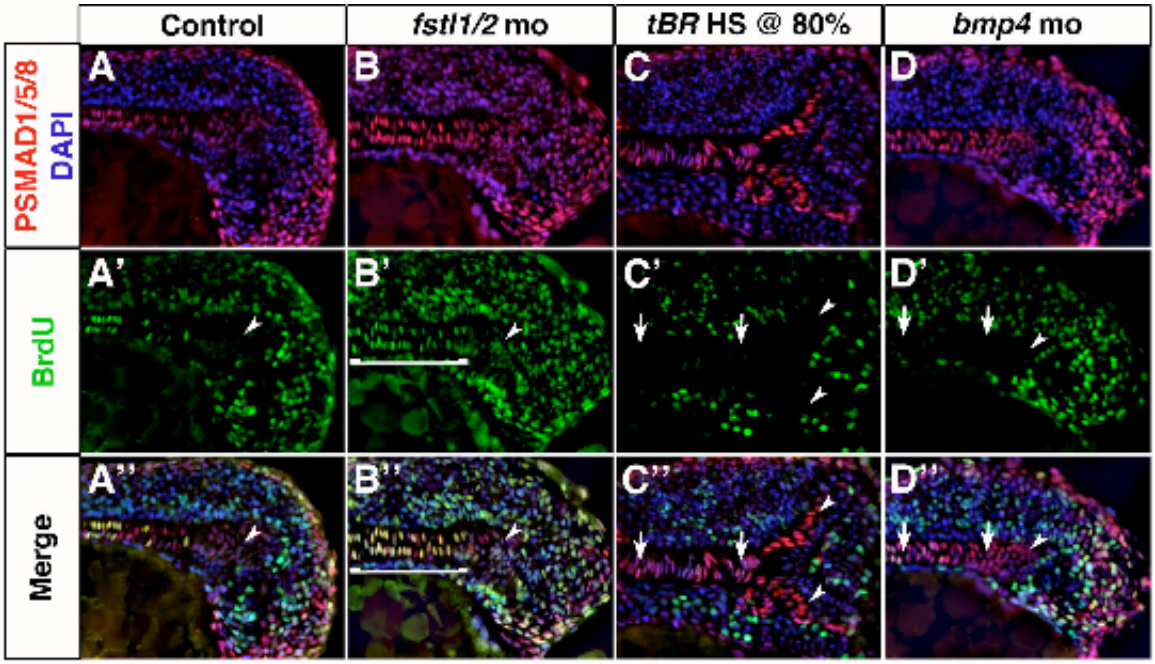
Control
fstl1/2 mo
tBR HS @ 80%
bmp4 mo
PSMAD1/5/8
DAPI
BrdU
Merge
A
B
C
D
A'
B'
C'
D'
A''
B''
C''
D''

Figure 2.8: The ventral margin as the source of Bmp4.

(A) Model of ventral margin extirpation. Approximately 100 cells were removed from the ventral margin (red) of 80% epiboly embryos. All images shown are of embryos with their ventral margins removed. (B-D) *flh* (B), *ntl* (C), and *admp* (D) expression in embryos at 90% epiboly. (E-E'') Antibodies against PSMAD1/5/8 (red) and BrdU (green) in longitudinal sections of the tail of 14-somite embryos. (F) High magnification view of notochord cells of 24hpf embryos at the level of the cloaca. (G,H) *shha* and *ptc1* expression in 24hpf.

Figure 2.8

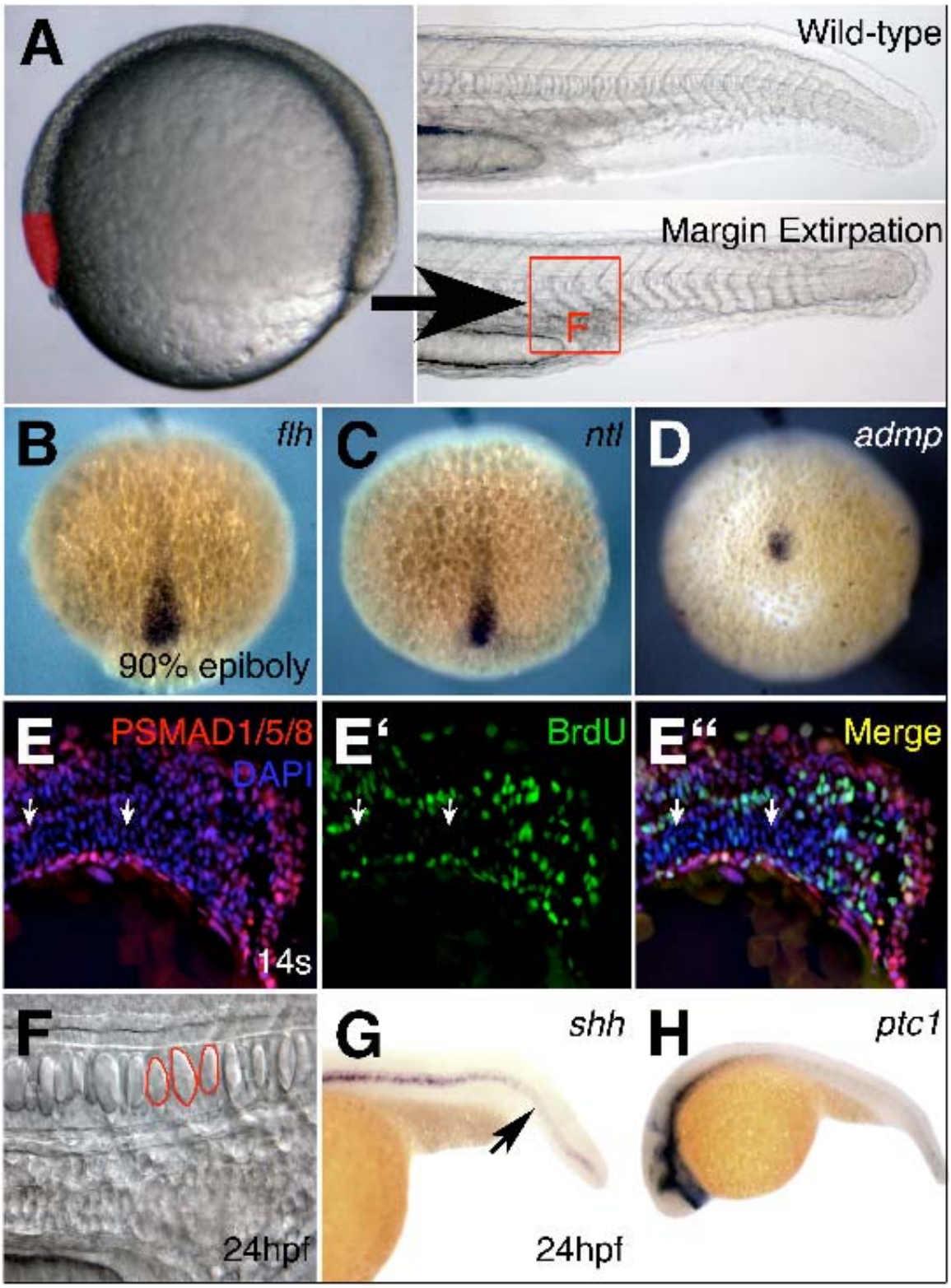
A
Wild-type
Margin Extirpation
F
B
flh
90% epiboly
C
ntl
D
admp
E
PSMAD1/5/8
DAPI
14s
E'
BrdU
E''
Merge
F
24hpf
G
shh
H
ptc1
24hpf

Figure 2.9: The temporal state of the notochord changes with the alteration of BMP activity.

The expression of chordamesoderm markers in embryos with reduced BMP activity is strongly reduced, resembling older embryos. Fstl1/2 morphant embryos maintain expression of these genes well past equivalently staged controls, resembling the expression patterns observed in younger embryos. (A-D, U-W) *ihhb* expression in 9-somite (A-D) or 18-somite (U-W) embryos. (E-L, X-CC) *shha* expression in 24 hpf (E-L) and 36hpf (X-CC) embryos. (I-L, AA-CC) High magnification view of the trunk. (M-P, DD-FF) *ptc1* expression in 24hpf (M-P) and 36hpf (DD-FF) embryos. (Q-T, GG-II) *col2a1a* expression in 36hpf (Q-T) and 48hpf (GG-II) embryos; arrows in (R-T) indicate absence of floorplate expression; nc, notochord. All views are lateral, with anterior to the left. Insets in (A-D) are flat-mount dorsal views. (Q-T, GG-II) are lateral views of the trunk.

Figure 2.9

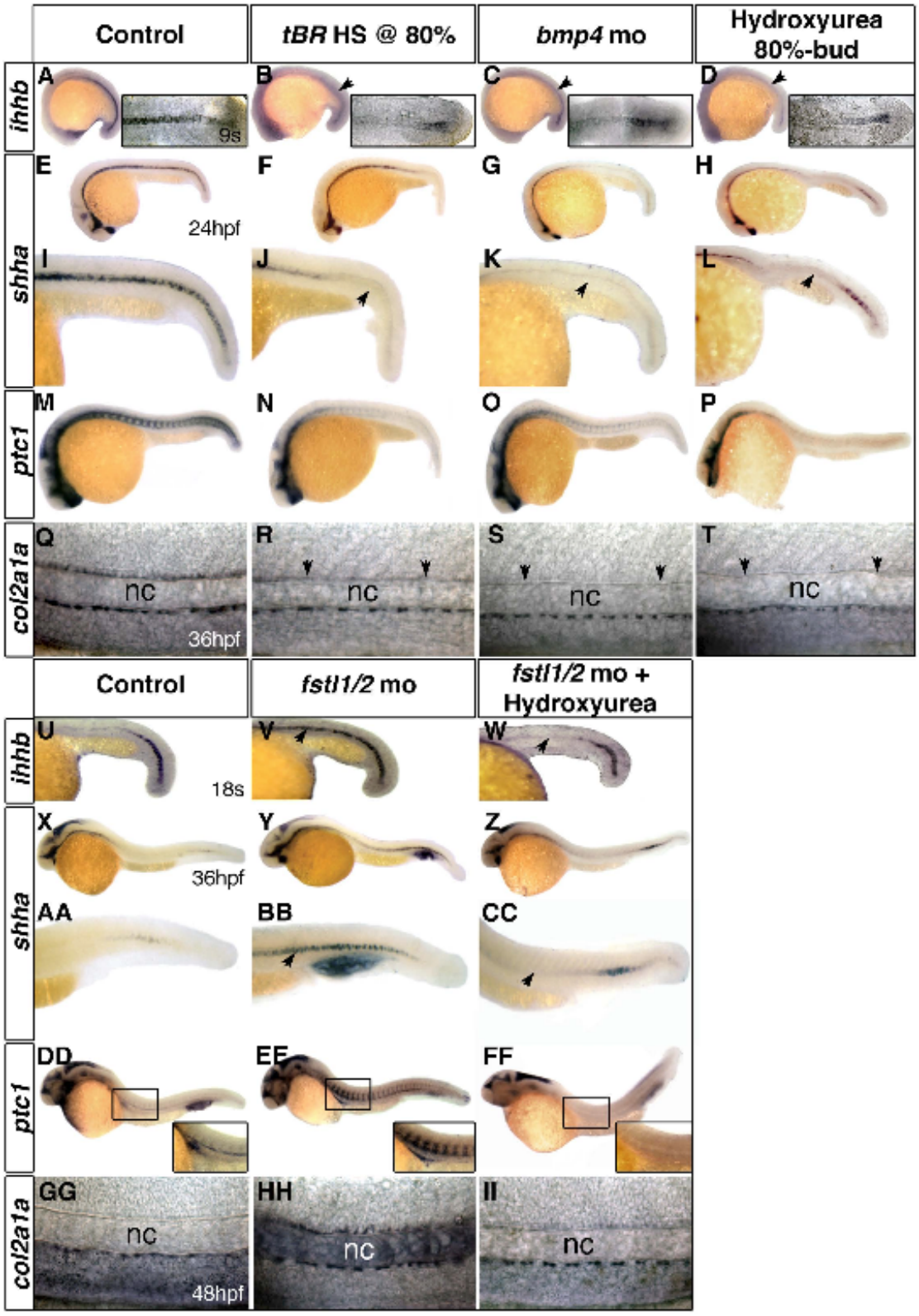
Control
tBR HS @ 80%
bmp4 mo
Hydroxyurea 80%-bud
ihhb
shha
ptc1
col2a1a
A
B
C
D
9s
E
F
G
H
24hpf
I
J
K
L
M
N
O
P
Q
R
S
T
nc
36hpf
Control
fstl1/2 mo
fstl1/2 mo + Hydroxyurea
U
V
W
18s
X
Y
Z
36hpf
AA
BB
CC
DD
EE
FF
GG
HH
II
48hpf

Figure 2.10: Disruption of the temporal state of the notochord can be observed through notochord cell morphology.

(A,C,D) 24hpf control embryos, notochord cells differentiate in an anterior to posterior manner. High magnification view of notochord cells at the level of the hind yolk extension (C) and at the level of the cloaca (D). (B,E,F) 24hpf Fstl1/2 morphants. High magnification view of notochord cells at the level of the hind yolk extension (E) and at the level of the cloaca (F). (G-L) 24hpf *tBR* embryos heat-shocked at 80% epiboly (G,H) and Bmp4 morphants (I,J). (K-N) Application of cell cycle inhibitors in wild-type (K,L) and Fstl1/2 morphants (M,N). (O) Cell transplantation procedure. See text for details. (P,Q) Wild-type donor cells (green) populating the notochord of *tBR* embryos do not enlarge and vacuolate prematurely (Q). (R,S) *tBR* donor cells (green) consistently fail to populate the notochord of wild-type hosts; instead they contribute to tissues in paraxial mesoderm. All views except (R) are lateral views of 24hpf embryos with anterior to the left. (R) is a dorsal view, with anterior to the left.

Figure 2.10

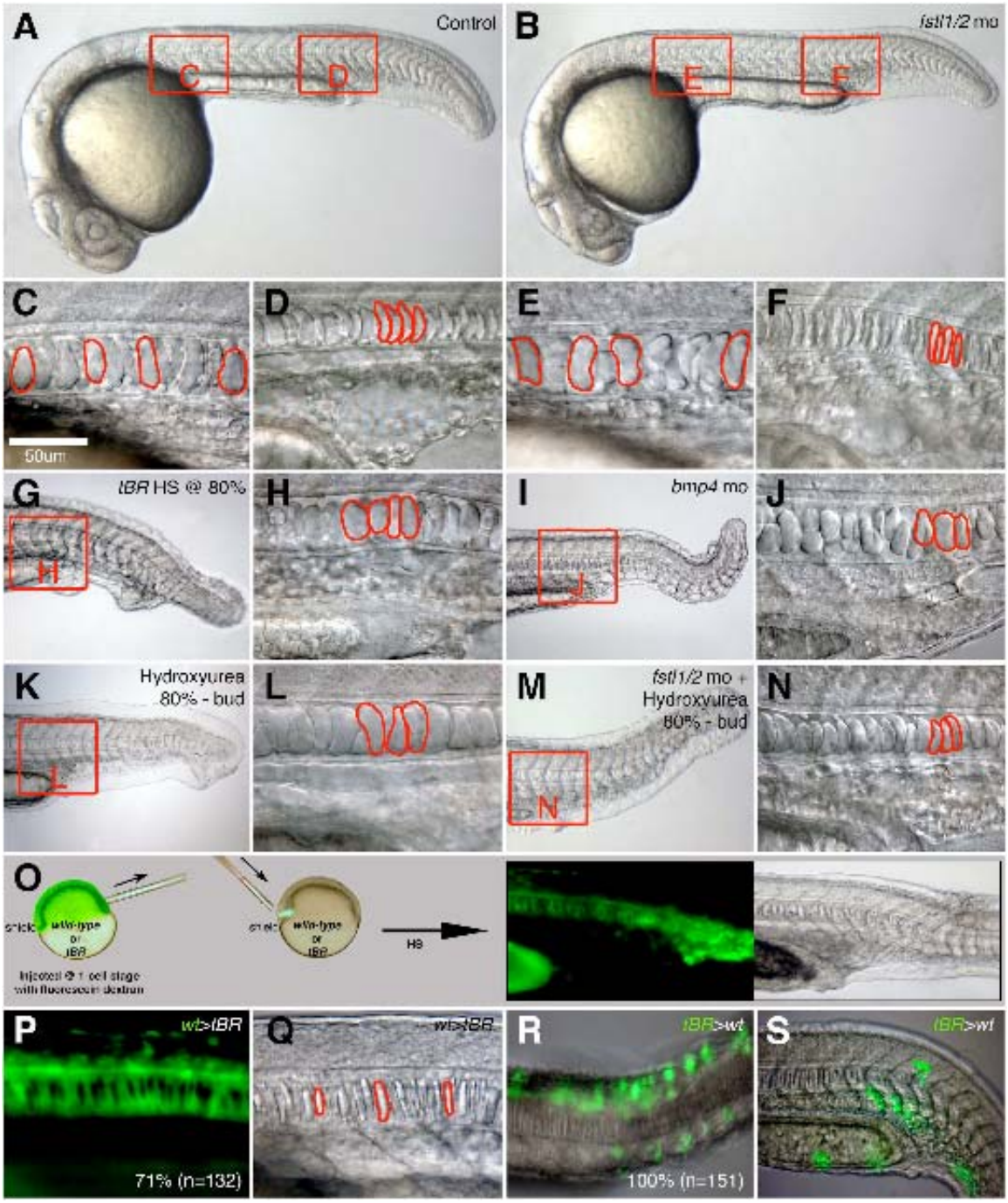
A
Control
B
fstl1/2 mo
C
D
E
F
50um
G
tBR HS @ 80%
H
I
bmp4 mo
J
K
Hydroxyurea
80% - bud
L
M
fstl1/2 mo +
Hydroxyurea
80% - bud
N
O
HS
P
wt>tBR
71% (n=132)
Q
wt>tBR
R
tBR>wt
100% (n=151)
S
tBR>wt

Figure 2.11: BrdU incorporation of embryos treated with the cell cycle inhibitors hydroxyurea and aphidicolin.

Embryos were treated from 80% epiboly to bud stage, then inhibitors were removed by washing. (A,B) BrdU incorporation of DMSO- (A) and hydroxyurea/aphidicolin-treated (B) bud stage embryos. (C-C'') Antibodies against PSMAD1/5/8 (red) and BrdU (green) in longitudinal sections of the tail of 14-somite hydroxyurea/aphidicolin treated embryos. (D,E) BrdU incorporation of DMSO- (D) and hydroxyurea/aphidicolin-treated (E) 24hpf embryos.

Figure 2.11

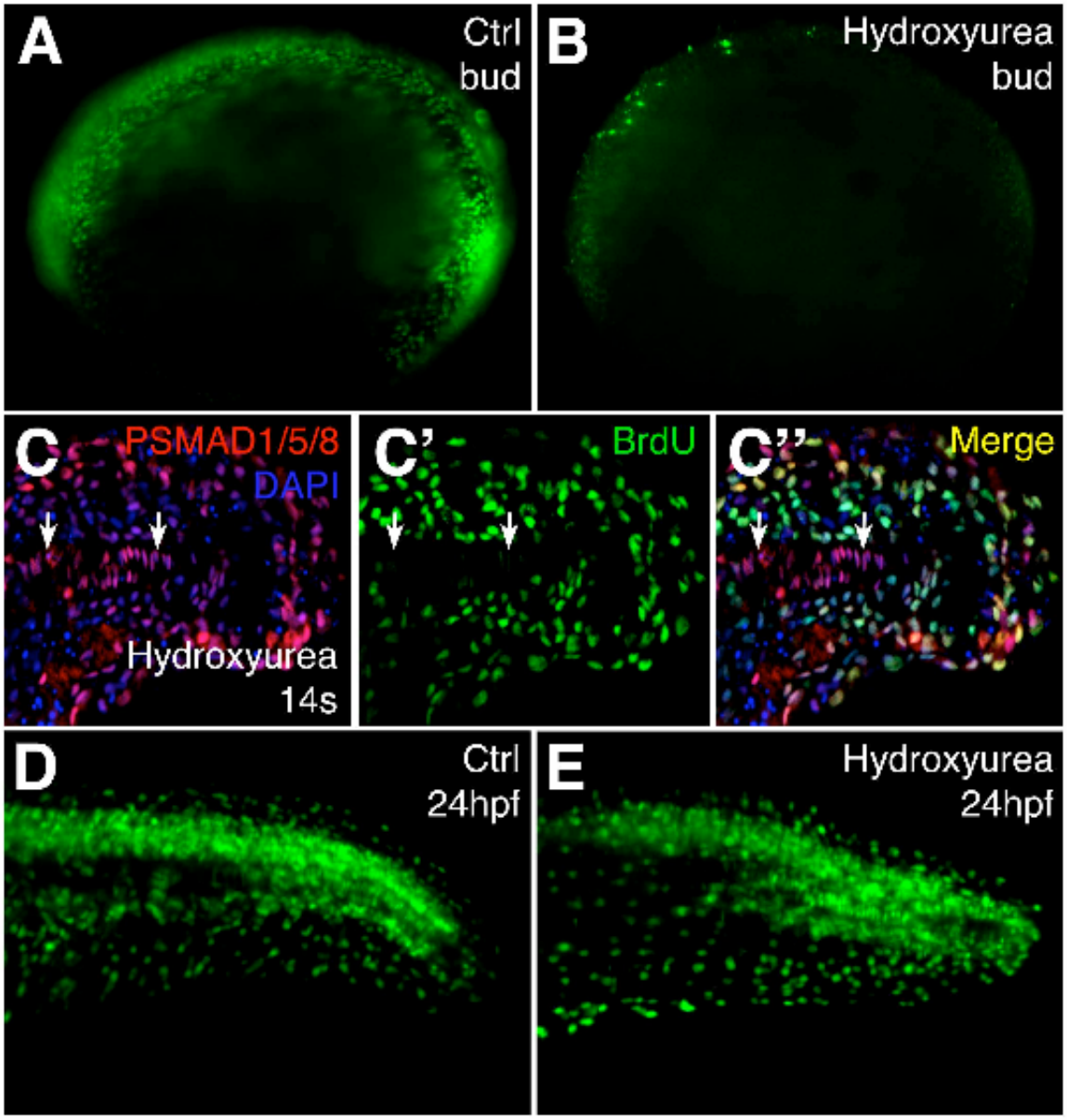
A
Ctrl
bud
B
Hydroxyurea
bud
C
PSMAD1/5/8
DAPI
Hydroxyurea
14s
C'
BrdU
C''
Merge
D
Ctrl
24hpf
E
Hydroxyurea
24hpf

Figure 2.12: A requirement for Bmp4 on the dorsal side of the gastrula.

(A) Bead implantation on the dorsal side of the gastrula. (B,C) *gsc* and *flh* expression in 90% epiboly embryos that have had BSA- (B) or Bmp4- (C) soaked beads implanted into axial tissue (C). (D,F) The notochord of 24 hpf embryos implanted with BSA- (D) or Bmp4- (F) soaked beads. (E) *tBR* embryos implanted with Bmp4-soaked beads and heat-shocked at 80% epiboly. (G-I) High magnification images of the notochord in (D-F). (J,K) *ntl* expression in 27hpf embryos implanted with BSA- (J) or Bmp4- (K) soaked beads. (L-N) High magnification images of the notochord at the level of the hind yolk extension of 48hpf embryos that were implanted with BSA- (L) or Bmp4- (M,N) soaked beads. Floor plate is out of the focal plane in (N). (B,C) Views are dorsal views, with anterior to the top. Bars in (B,C) denote the width of chordamesodermal domain at its widest point in the control embryo in (B). All other views are lateral views, with anterior to the left.

Figure 2.12

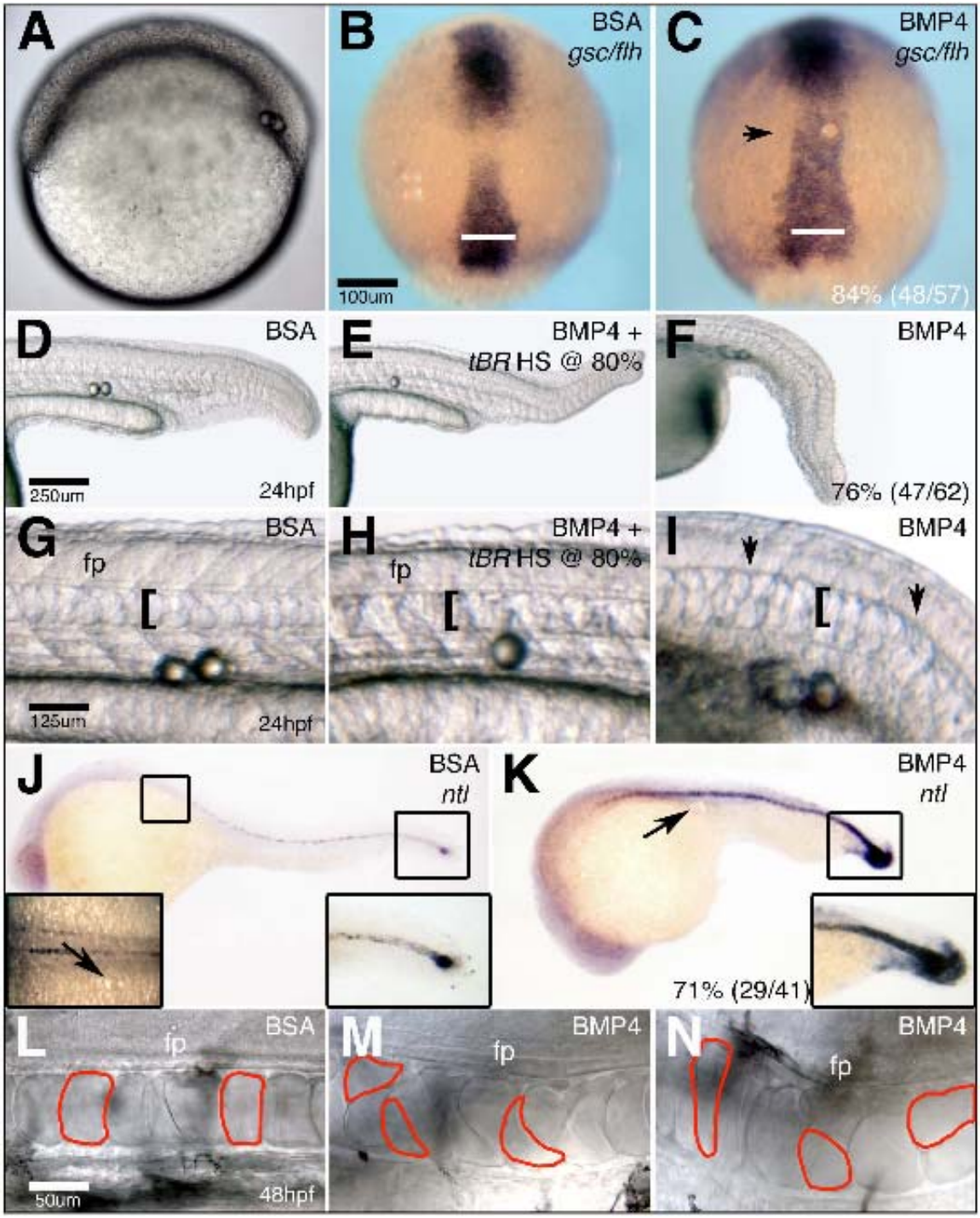
A
B
BSA
gsc/flh
100um
C
BMP4
gsc/flh
84% (48/57)
D
BSA
250um
24hpf
E
BMP4 +
tBR HS @ 80%
F
BMP4
76% (47/62)
G
BSA
fp
125um
24hpf
H
BMP4 +
tBR HS @ 80%
fp
I
BMP4
J
BSA
ntl
K
BMP4
ntl
71% (29/41)
L
BSA
fp
50um
48hpf
M
BMP4
fp
N
BMP4
fp

Figure 2.13: Bmp2/7 do not affect notochord morphology.

(A,B) *gsc* and *flh* expression in 90% epiboly embryos that have had BSA- (A) or Bmp2/7- (B) soaked beads implanted into axial tissue. (C,D) The notochord of 24 hpf embryos implanted with BSA- (C) or Bmp2/7- (D) soaked beads. Beads are located anterior to the region shown in (D). (E,F) *ntl* expression in 27hpf embryos implanted with BSA- (E) or Bmp2/7- (F) soaked beads. (G,H) High magnification images of the notochord at the level of the hind yolk extension of 48hpf embryos that were implanted with BSA- (G) or Bmp2/7- (H) soaked beads. fp, floorplate (A,B) Views are dorsal views, with anterior to the top. Bars in (A,B) denote the width of chordamesodermal domain at its widest point in the control embryo in (A). All other views are lateral views, with anterior to the left.

Figure 2.13

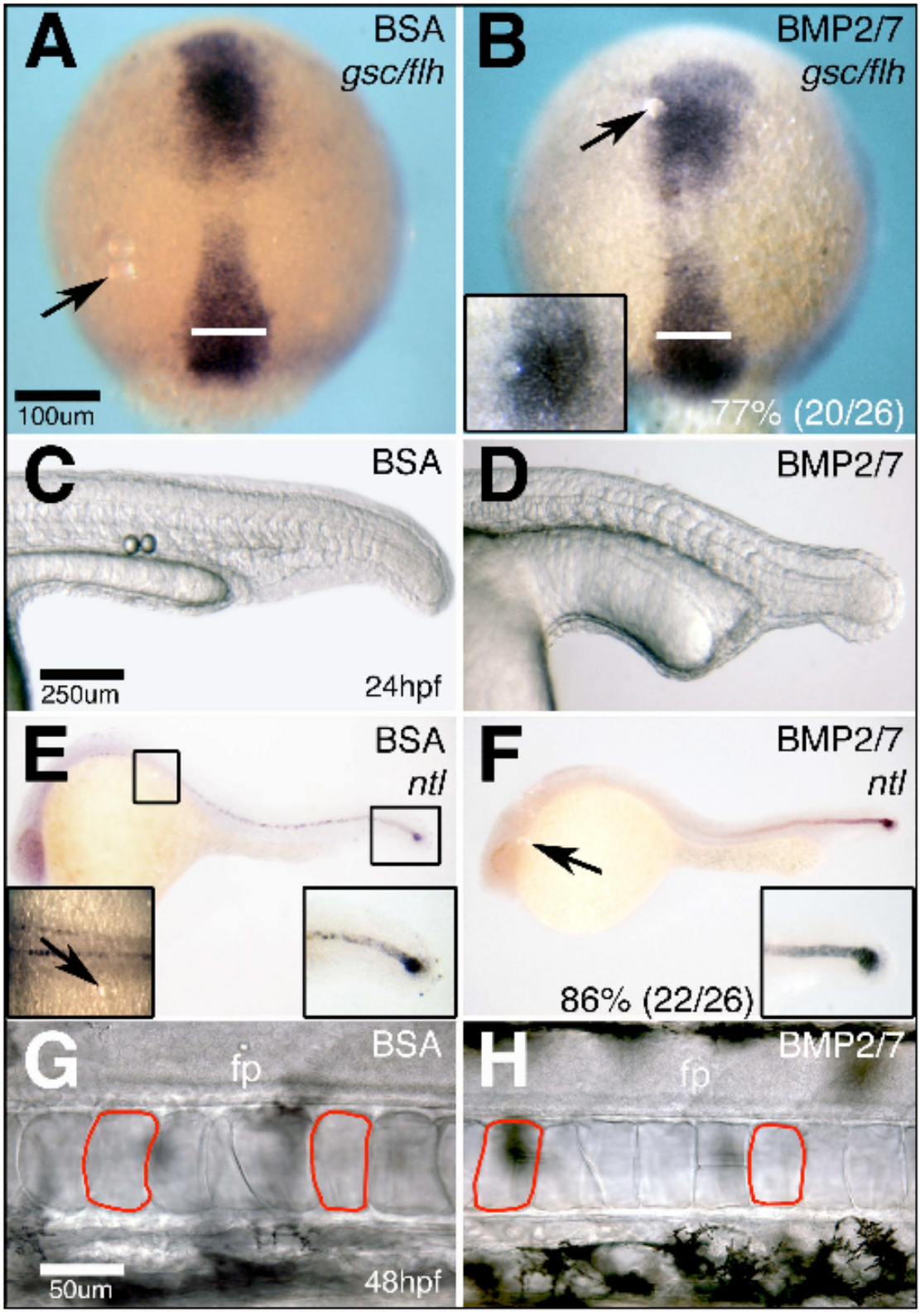
A
BSA
gsc/flh
100um
B
BMP2/7
gsc/flh
77% (20/26)
C
BSA
250um
24hpf
D
BMP2/7
E
BSA
ntl
F
BMP2/7
ntl
86% (22/26)
G
BSA
fp
50um
48hpf
H
BMP2/7
fp

Figure 2.14: Myotome patterning as a proxy of notochord maturity.

(A-C) *myoD* expression in 9-somite embryos is increased in adaxial and medial fast muscle cells of Fstl1/2 morphants (B), and is reduced in the medial fast muscle domain of *tBR* embryos heat-shocked at 80% epiboly (C). (D-F) Immunostaining against MyoD and F-actin reveals an increase in MyoD positive cells of the medial fast muscle domain of Fstl1/2 morphants (E), and a decrease in MyoD positive cells in *tBR* embryos (F). Images are of the anterior-most three somites. The mean number of MyoD-stained cells from 5 experimental embryos was subjected to one-way ANOVA, followed by a two-tailed, equal variance *t*-test. Asterisks denote significance ($p<0.001$). (G-I) Immunostaining with the F59 antibody, which recognizes mainly slow muscle, reveals that the horizontal myoseptum is increased in 24hpf Fstl1/2 morphant embryos (H). Muscle fibers are disorganized in *tBR* embryos (I). (J-L) Immunostaining with antibodies against 4D9, which labels Engrailed positive cells (red), and Prox1, which labels slow muscle cells (green), reveal an increase in medial fast muscle (red) and slow muscle pioneers (yellow) in 24hpf Fstl1/2 morphants (K), and a reduction of Engrailed positive cells in *tBR* embryos (L). (M-O) Sections through the trunk level of 24hpf embryos confirm the results in (J-L). Antibodies against PSMAD1/5/8 (red) and Engrailed (green) reveal an increase in PSMAD1/5/8-positive chondrocytes as well as medial fast muscle fibers and slow muscle pioneers (green) in Fstl1/2 morphants (N). Chondrocytes do not form in *tBR* embryos, and the domain of medial fast muscle fibers and slow muscle precursors is reduced (O).

Figure 2.14

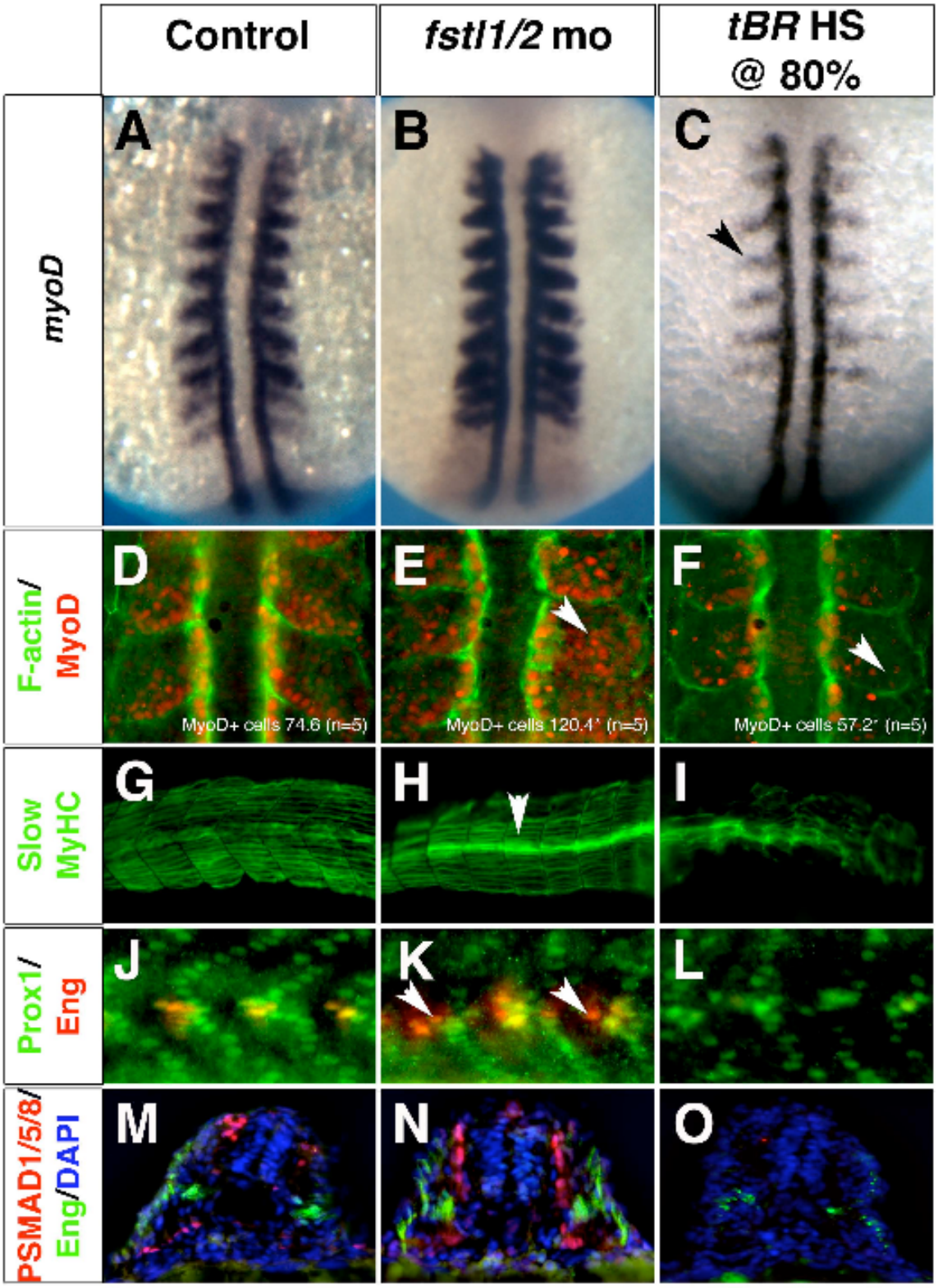
Control
fstl1/2 mo
tBR HS @ 80%
myoD
A
B
C
F-actin/ MyoD
D
E
F
MyoD+ cells 74.6 (n=5)
MyoD+ cells 120.4* (n=5)
MyoD+ cells 57.2* (n=5)
Slow MyHC
G
H
I
Prox1/ Eng
J
K
L
PSMAD1/5/8/ Eng/DAPI
M
N
O

CHAPTER 3

dlx3b/4b are required for the formation of the preplacodal region and otic placode through local modulation of BMP activity

(Esterberg and Fritz, *Developmental Biology*, in press)

Abstract

The vertebrate inner ear arises from the otic placode, a transient thickening of ectodermal epithelium adjacent to neural crest domains in the presumptive head. During late gastrulation, cells fated to comprise the inner ear are part of a domain in cranial ectoderm that contain precursors of all sensory placodes, termed the preplacodal region (PPR). The combination of low levels of BMP activity coupled with high levels of FGF signaling are required to establish the PPR through induction of members of the *six/eya/dach*, *iro*, and *dlx* families of transcription factors. The zebrafish *dlx3b/4b* transcription factors are expressed at the neural plate border where they play partially redundant roles in the specification of the PPR, otic and olfactory placodes. We demonstrate that *dlx3b/4b* assist in establishing the PPR through the transcriptional regulation of the BMP antagonist *cv2*. Morpholino-mediated knockdown of Dlx3b/4b results in loss of *cv2* expression in the PPR and a transient increase in Bmp4 activity that lasts throughout early somitogenesis. Through the *cv2*-mediated inhibition of BMP activity, *dlx3b/4b* create an environment where FGF activity is favorable for PPR and otic marker expression. Our results provide insight into the mechanisms of PPR specification as well as the role of *dlx3b/4b* function in PPR and otic placode induction.

The interface between neural and non-neural ectoderm gives rise to several cell types, including neural crest, paired placodes and, in anamniotes, Rohon-Beard sensory neurons (Baker and Bronner-Fraser, 1997; Gans and Northcutt, 1983; Holland and Holland, 2001; Meulemans and Bronner-Fraser, 2004; Northcutt and Gans, 1983; Schlosser, 2006). The paired placodes, transient thickenings of ectodermal epithelium, arise lateral and adjacent to neural crest and Rohon-Beard domains in the presumptive head. During late gastrulation and early segmentation stages, placodal cells comprise a domain of cranial ectoderm that contains precursors of all sensory placodes (termed the preplacodal region, or PPR) (reviewed in Bailey and Streit, 2006; Ohyama et al., 2007; Riley, 2003; Schlosser, 2006). Evidence from studies in *Xenopus,* zebrafish, and chick suggest that the convergence of multiple activities of signaling molecules are required for the establishment of the PPR. A balance of FGF activity and antagonism of both BMP and WNT signaling are required to induce expression of members of the *Eyes absent* (*Eya*)/*Sine oculis* (*Six*)/*Dachshund* (*Dach*), *Iroquois* (*Iro*), and *Distalless* (*Dlx*) families of transcription factors during late gastrulation, which are the earliest markers of PPR fate (Ahrens and Schlosser, 2005; Brugmann et al., 2004; Glavic et al., 2004; Litsiou et al., 2005; Nguyen et al., 1998). In particular, modulation of BMP activity at the neural plate border is instrumental in the establishment of the PPR and also patterns adjacent Rohon-Beard and neural crest domains (Nguyen et al., 1998; Nguyen et al., 2000; Rossi et al., 2008; Tribulo et al., 2003).

In *Xenopus* and zebrafish, a BMP gradient model has been proposed in which BMP activity is high in ventral/lateral regions and progressively lower in more dorsal/medial regions during gastrulation. High levels of BMP activity are required to

induce epidermis, low levels are required to specify neural plate, and intermediate levels are required to specify neural crest and Rohon-Beard domains (Aybar and Mayor, 2002; Nguyen et al., 1998; Nguyen et al., 2000; Tribulo et al., 2003). Although the PPR lies lateral to the domain of neural crest, evidence from *Xenopus*, zebrafish and chick suggests that BMP activity must be lower in the PPR than in adjacent neural crest and epidermal territories (Ahrens and Schlosser, 2005; Glavic et al., 2004; Litsiou et al., 2005). For example, implantation of Bmp4-containing beads near the PPR is sufficient to inhibit expression of the PPR marker *Six1* (Ahrens and Schlosser, 2005). Thus, it appears that establishment of the PPR requires lower levels of BMP activity than that required for neural crest and Rohon-Beard formation, contradictory to a simple gradient model.

While it is apparent that attenuation of BMP activity is critical in establishing the PPR, it is not yet clear how this attenuation is achieved. Tissue grafting experiments have revealed that potential BMP antagonists originate from tissues other than the PPR. Grafting of chicken head mesoderm onto extraembryonic ectoderm yields host tissue with PPR characteristics (Litsiou et al., 2005). Likewise, transplantation of neural ectoderm into domains of ventral ectoderm yields similar results in *Xenopus*, demonstrating the role these tissues have in creating an environment suitable for the formation of the PPR (Ahrens and Schlosser, 2005). However, the BMP antagonists involved in this process remain unidentified.

Members of the *Dlx* family of transcription factors are thought to play intrinsic roles in the formation of the PPR, although the mechanisms by which they do so are unclear. *Dlx* genes are required but not always sufficient for the expression of PPR markers from the *Eya*/*Six*/*Dach* families. For example, ectopic expression of *Six1* in

Xenopus and chick can only be achieved in the presence of functional Dlx3 and Dlx5, respectively (Woda et al., 2003). In zebrafish, *dlx3b/4b* are initially expressed along the entire neural plate border, which includes the PPR, at the end of gastrulation. Expression becomes restricted to the otic and olfactory placodes during somitogenesis (Ekker et al., 1992; Feledy et al., 1999; Pera et al., 1999). Only rudimentary otic and olfactory placodes form when *dlx3b/4b* function is lost, and the resulting size of these sensory organs is significantly reduced (reviewed in Ohyama et al., 2007; reviewed in Riley, 2003). Induction of early otic and olfactory markers, such as *pax2a* and *eya1*, is severely compromised, suggesting that *dlx3b/4b* function early in the process of otic and olfactory induction. Thus, it has been suggested that *Dlx* genes may act as competence factors for placode induction (Hans et al., 2007; Hans et al., 2004).

In amniotes, *Dlx5* and *Dlx6* are expressed in a similar pattern to *dlx3b/4b* in zebrafish (Acampora et al., 1999; Yang et al., 1998). However, inactivation of *Dlx5/6* in mouse does not appear to affect induction of the otic or olfactory placodes, but rather their subsequent development (Merlo et al., 2002; Robledo and Lufkin, 2006; Robledo et al., 2002). The reason for the discrepancy in phenotypes between zebrafish and mouse embryos lacking these *Dlx* paralogues is currently unclear.

To better understand the role of *dlx3b/4b* during the establishment of the PPR and otic placodes, we examined signaling activities involved in PPR and otic placode induction. We have identified that a BMP signaling modulator, Cv2, is critical for the formation of the PPR. The predominant function of this protein is as a BMP antagonist, although its proteolytic cleavage may allow Cv2 to act as an agonist of BMP activity (Rentzsch et al., 2006; Zhang et al., 2007; Zhang et al., 2008). We show that *cv2* lies

transcriptionally downstream of *dlx3b/4b*, and that the full-length protein is required to modulate BMP activity to levels conducive for PPR formation. Morpholino-mediated knockdown of Dlx3b/4b results in loss of *cv2* expression in the PPR and a transient increase in Bmp4 activity that is first observed at the end of gastrulation. This is followed by a transient decrease in FGF activity that can be rescued when *cv2* or *fgf-receptor 1* (*fgfr1*) mRNA is supplied in Dlx3b/4b morphants. Ectopic expression of either *dlx3b* or *cv2* is sufficient to drive PPR marker expression. Conversely, loss of *cv2* has similar effects on PPR development as loss of *dlx3b/4b*, indicating that a significant aspect of *dlx3b/4b* function at the end of gastrulation is mediated through *cv2*. Our results suggest a model in which *dlx3b/4b*-mediated modulation of BMP signaling through *cv2* lies upstream of *Six/Eya/Dach* genes and FGF responsiveness in the specification of the PPR and induction of the otic placode. Furthermore, our findings provide a possible explanation for the difference in function of the *Dlx* genes between mouse and zebrafish.

Materials and Methods

Animals

Wild-type (AB) mutant zebrafish were obtained from the Zebrafish International Resource Center (Eugene, OR). Embryos were maintained at 28.5°C and staged using standard criteria (Kimmel et al., 1995). *Tg(hsp70l:dnBmpr-GFP)*^{w30} (*tBR*) transgenic zebrafish were obtained from the Kimelman lab (University of Washington, Seattle). This transgenic line contains a truncated Type I Bmp receptor containing GFP in place of

the kinase domain under the control of a heat-shock promoter (Pyati et al., 2005). *tBR* embryos were heat shocked at 37°C for one hour at bud stage according to Pyati et al. (2005). They were then sorted according to GFP expression and raised at 28.5°C until fixation. Where appropriate, wild-type or control morpholino-injected embryos were heat-shocked at the same stage as controls.

In situ hybridization

The following probes were used: *bmp4 (Nikaido et al., 1997), chordin* (Miller-Bertoglio et al., 1997), *cv2* (Rentzsch et al., 2006), *dlx3b* (Ekker et al., 1992), *erm (Raible and Brand, 2001*), *eya1* (Sahly et al., 1999), *fgfr1* (Scholpp et al., 2004), *fgfr2* (Poss et al., 2000), *fgfr3* (Sleptsova-Friedrich et al., 2001), *fgfr4* (Thisse et al., 1995), *pax2a* (Krauss et al., 1991a), *six4.1* (Kobayashi et al., 2000), *spry4* (Fürthauer et al., 2001), and *tbx2b* (Dheen et al., 1999).

Real-time quantitative RT-PCR

RNA was isolated from three sets of 20 embryos of each experimental sample using the RNeasy kit (Qiagen). The SYBR Green I (Roche Applied Science) RNA amplification kit was used on the LightCycler according to the manufacturer's instructions and published protocols (Rajeevan et al., 2001). The primers used for each of the genes were: *bmp4* 5'- AGCCAACACCGTGAGAGGATTC -3' and 5'-TCTGCGGTGGATATGAGTTCGTC -3'; *fgfr1* 5'- GCGGCTCCCCAATGCTCTCAG -3' and 5'- ATCGCCTCGGCCATCATCACC -3'; *fgfr2* 5'-CACATCAACGGCGGCATAAAAACAT -3' and 5'-

TCGGGATCTGATTGGGAAGTAAC -3'; *fgfr3* 5'-GTGGCGGGAGTCGGGGATACAG -3' and 5'- ATTGATGATGCGGAGGGCTTTCT -3'; *fgfr4* 5'- CAATCAGGGTCATAAGGCAGTTCA -3' and 5'-GCAGCGCCAGAGGGAACGAAC -3'; *ef1α* 5'- GTACTACTCTTCTTATGCCC -3' and 5'- GTACAGTTCCAATACCTCCA -3'. The different samples were standardized using EF-1α transcript levels as a reference. Each experimental run was also performed in triplicate. Transcript levels were compared by one-way ANOVA, followed by a two-tailed, equal variance *t*-test.

Morpholino injection

Morpholino injections against *bmp4* (Chocron et al., 2007), *chordin* (Nasevicius and Ekker, 2000), *cv2* (mo1 sequence was used; Rentzsch et al., 2006) and *dlx3b/4b* (Solomon and Fritz, 2002) have been previously characterized. The control morpholino sequence was 5'-CCTCTTACCTCAGTTACAATTTATA -3'. For interaction analyses, *chd* mo concentration was chosen that elicited a V1 ventralization phenotype, approximately 2.5ng (Kishimoto et al., 1997; Mullins et al., 1996). *dlx3b/4b* mo concentration was chosen that elicited a mild otic phenotype, approximately 5ng each.

mRNA synthesis

Capped mRNAs were transcribed using T7 and SP6 RNA polymerase in vitro transcription kits (mMESSAGE mMACHINE; Ambion). *fgfr1* cDNA was amplified using the following primers: 5'- TTTGATAATAATAATGAAGATGATGATGATAAT -3' and 5'- ATGACGGATGTATTTGAGTTTTGAGA-3'. It was then cloned into

pCRII-TOPO, digested with *Spe*I and *Xho*I and ligated into pCS2+ digested with *Xba*I and *Xho*I. The vector was linearized with *Apa*I and mRNA was synthesized using SP6 polymerase. For rescue of the Dlx3b/4b morphant phenotype, approximately 15pg mRNA was co-injected into one- and two-cell embryos with *dlx3b/4b* MOs. *bmp2b*, *bmp4*, *dlx3b*, *cv2*, and *cv2-N* mRNA were synthesized and injected as previously described (Kishimoto et al., 1997; Rentzsch et al., 2006; Solomon and Fritz, 2002; Szeto and Kimelman, 2004).

Antibody staining

Labeling with PSMAD1/5/8 was as previously described (Rentzsch et al., 2006). The primary antibody was used at a dilution of 1:100 (anti-P SMAD1/5/8; Chemicon International). Secondary antibody was Alexa Fluor 594 goat anti-rabbit IgG at 1:500 (Molecular Probes).

Results

dlx3b/4b transiently regulate BMP activity

In *Xenopus* and chick, ectopic expression of BMP antagonists can induce ectopic PPR marker expression, while exposure to increased amounts of Bmp4 can ablate ectopic expression and reduce endogenous expression of the PPR markers *Six1/4* and *Eya2* (Ahrens and Schlosser, 2005; Brugmann et al., 2004; Litsiou et al., 2005). Furthermore, *Xenopus Dlx3* and chick *Dlx5* are both necessary and sufficient for *Six1* expression (McLarren et al., 2003; Woda et al., 2003), suggesting that *Dlx* genes lie upstream of *Eya*/*Six*/*Dach* members in the establishment of the PPR. Because of the inhibitory role of

Bmp4 in PPR marker expression, we examined BMP activity in Dlx3b/4b morphants. Although we did not observe changes in *bmp4* expression prior to late gastrulation, the domain of *bmp4* expression in prechordal mesoderm and tailbud was expanded in Dlx3b/4b morphants beginning at bud stage (Figure 3.1C,D). By mid-somitogenesis expression levels returned to those seen in embryos injected with control morpholino (Figure 3.1G,H). To quantify this increase in Bmp4 activity, we performed quantitative RT-PCR on mRNA extracted from bud stage Dlx3b/4b morphants. *bmp4* transcripts were detected to be elevated by approximately 40% in bud stage Dlx3b/4b morphants ($p<0.005$; Figure 3.2). We also examined the expression of *bmp2b*, which is expressed in a pattern similar to *bmp4* at the end of gastrulation, and which has been shown to be misregulated in *dlx3b/4b* morphant embryos (Kaji and Artinger, 2004). Consistent with previous observations (Kaji and Artinger, 2004), *bmp2b* transcript levels were reduced by approximately 15% in Dlx3b/4b morphants (data not shown).

To determine the effects of *bmp4* misregulation in Dlx3b/4b morphants, we labeled embryos with antibodies against phosphorylated (P)SMAD1/5/8, which is activated in response to BMP signaling (Yamamoto and Oelgeschlager, 2004). We observed an increase in PSMAD1/5/8 localization in the anterior neural plate of Dlx3b/4b morphants (Figure 3.1E,F), indicating that these cells have received and are responding to BMP signaling.

This transient misregulation of Bmp4 activity results in morphological dorsoventral (DV) patterning defects; Dlx3b/4b morphants exhibit an increase in intermediate cell mass of the tail similar to the mildest class of ventralization mutants (Figure 2B; Kishimoto et al., 1997; Mullins et al., 1996). Because the ventralization

phenotype of Dlx3b/4b morphants is mild, we wished to demonstrate that loss of Dlx3b/4b can increase the severity of ventralization in a sensitized background. We determined an amount of *chordin* (*chd*) morpholino that was sufficient to phenocopy the V1 ventralization phenotype and injected it in combination with *dlx3b/4b* morpholinos. In Chd/Dlx3b/4b triple morphants, the ventralization phenotype was compounded such that embryos resembled the V2 class of ventralization mutants, with a greater expanse in the tail than seen in Chd or Dlx3b/4b morphants alone (Figure 3.3B-D).

To further confirm that BMP activity is increased in Dlx3b/4b morphants we examined *chd* expression. BMP antagonists expressed on the dorsal side of the embryo, such as *chd*, are negatively regulated by BMP signaling (reviewed in Kimelman and Szeto, 2006; Yamamoto and Oelgeschlager, 2004). *chd* expression was reduced in the anterior neural plate and paraxial mesoderm of bud stage and 6-somite Dlx3b/4b morphants (Figure 3.4B,F,J), consistent with observed elevated BMP levels.

dlx3b/4b **mediate BMP signaling through** ***cv2***

Cv2 plays a role throughout embryogenesis predominantly as an antagonist of Bmp4 (Ambrosio et al., 2008; Rentzsch et al., 2006; Serpe et al., 2008; Zhang et al., 2008). During late gastrulation, *cv2* is expressed in a pattern around the neural plate (Figure 3C-F; Rentzsch et al., 2006) resembling that of *dlx3b/4b*. Our analysis suggests that this pattern of expression spatially overlaps with *dlx3b* in preplacodal ectoderm (Figure 3.5A,B), rather than being localized to the underlying mesendoderm as initially suggested (Rentzsch et al., 2006). Following early somitogenesis, *cv2* and *dlx3b/4b* are expressed in the otic placode and pharyngeal arches, raising the possibility that *cv2* lies

transcriptionally downstream of Dlx3b/4b (Figure 3G-J; Ekker et al., 1992; Rentzsch et al., 2006). Morpholino-mediated knockdown of Dlx3b/4b resulted in a loss of *cv2* expression from the PPR during late gastrulation, as well as in the otic placodes and pharyngeal arches during somitogenesis (Figure 3.5E-J). Importantly, *cv2* expression was not lost from ventral tissues before the onset of *dlx3b/4b* expression or tail mesoderm during somitogenesis, where its expression does not overlap with *dlx3b/4b* (data not shown; Figure 3C,D,G,H; Rentzsch et al., 2006).

Because loss of Dlx3b/4b increases BMP activity, we wished to determine the effects of overexpressing *dlx3b*. To do so, we injected *dlx3b* mRNA into one- and two-cell embryos. *bmp4* expression and PSMAD1/5/8 staining were reduced in embryos ectopically expressing *dlx3b* mRNA (Figure 3.6A-D). We also observed expansion of the hindbrain marker *krox20* in these embryos (Figure 3.6E,F), consistent with a dorsalization phenotype (Kishimoto et al., 1997; Mullins et al., 1996).

Because *cv2* expression is lost from *dlx3b/4b*-expressing tissues in Dlx3b/4b morphants, we wished to explore whether elevated BMP activity observed in these morphants was due to *cv2*. To demonstrate that *dlx3b* activates *cv2* expression cell-autonomously, the *dlx3b* ORF was cloned into pCS2+ and injected into 1-cell embryos. Typically, injection of plasmid DNA leads to mosaic distribution of the DNA in later stage embryos. In these embryos, *cv2* was co-expressed in the same cells ectopically expressing *dlx3b* (Figure 3.6G,H).

Furthermore, embryos ectopically expressing *dlx3b* or *cv2* mRNA were moderately (59%; 67/113 and 34; 49/146, respectively) or severely (41%; 46/113 and 24%; 35/146, respectively) dorsalized (Figure 3.6I-K,M,N), resembling C3 and C4

classes of dorsalization, respectively (Kishimoto et al., 1997; Mullins et al., 1996). Knockdown of Cv2 was able to rescue the dorsalization phenotype seen in embryos ectopically expressing *dlx3b* mRNA (Figure 3.6L).

Similarly, *chd* expression in embryos ectopically expressing a dominant negative form of *cv2* mRNA (*cv2-N*; Rentzsch et al., 2006) resembled that of Dlx3b/4b morphants (Figure 3.4D,H,L). Co-injection of *cv2* mRNA with *dlx3b/4b* morpholinos was sufficient to rescue *chd* expression (Figure 3.4C,G,K), demonstrating that the modulation of BMP activity by *dlx3b/4b* depends at least in part on *cv2*.

dlx3b/4b-mediated expression of *cv2* is necessary for PPR marker expression

Because we observed an increase in BMP activity and a loss of *cv2* expression from the PPR of Dlx3b/4b morphants, we wished to determine how disruption of Dlx3b/4b or Cv2 affects PPR formation. BMP activity, particularly Bmp4, inhibits the expression of PPR markers from the Six/Eya/Dach transcriptional network (reviewed in Bailey and Streit, 2006; Brugmann and Moody, 2005; Schlosser, 2006). Expression of the PPR markers *eya1* and *six4.1* is lost from the PPR of bud stage Dlx3b/4b and Cv2 morphant embryos (Figure 3.7A-C,F-H,). PPR marker expression was restored either when Bmp4 was knocked down or when *cv2* mRNA was ectopically expressed in Dlx3b/4b morphants (Figure 3.7D,E,I,J). Although the width of the PPR was not significantly altered in these embryos, we did observe ectopic expression of both *eya1* and *six4.1* within the neural plate.

Studies in *Xenopus* have demonstrated that *Dlx3* is required to position the PPR. Inhibition of endogenous Dlx activity expands the neural plate at the expense of the PPR

(Woda et al., 2003). To determine whether *dlx3b* was sufficient to induce ectopic PPR marker expression, we injected the pcs2::*dlx3b* DNA construct into one-cell embryos. Under these conditions ectopic *dlx3b* was sufficient to induce ectopic expression of both *eya1* and *six4.1* (Figure 3.7K, data not shown). Because we were able to rescue the PPR phenotype of Dlx3b/4b morphants by supplying *cv2* mRNA, we wished to determine the effects of ectopic *cv2* on PPR formation, independent of *dlx3b*. Injection of pcs2::*cv2* was sufficient to drive ectopic *eya1* or *six4.1* expression (Figure 3.7L, data not shown). Ectopic PPR marker expression was not observed when pcs2::*dlx3b* was co-injected with *cv2* morpholino (data not shown), suggesting that the PPR inducing properties of *dlx3b* require *cv2*.

A small number of cells that expressed either ectopic *dlx3b* or *cv2* did not co-express *eya1* or *six4.1*. Although full length Cv2 acts as a BMP antagonist, it is subject to proteolytic cleavage that renders it an agonist of BMP activity (Rentzsch et al., 2006; Zhang et al., 2008). We reasoned that the processing of Cv2 into a BMP agonist was responsible for the cells not expressing ectopic *eya1* or *six4.1*. As such, we injected a DNA construct containing an uncleavable form of the *cv2* ORF, in which the cleavage site of Cv2 is mutated (*cv2-CM*; Rentzsch et al., 2006), into one-cell embryos and assayed ectopic PPR marker expression (Rentzsch et al., 2006). In these embryos, all cells ectopically expressing *cv2-CM* co-expressed *eya1* and *six4.1* (Figure 3.7M, data not shown). These results suggest that Dlx3b/4b establish the PPR through transcriptional regulation of *cv2*. Furthermore, induction of PPR marker expression requires low levels of BMP activity, particularly Bmp4. This is mediated through the uncleaved form of Cv2, suggesting that in this context *cv2* acts as a BMP antagonist.

Cv2 antagonism of BMP activity promotes FGF activity

Establishment of the PPR requires not only the attenuation of BMP activity but FGF activity as well (Ahrens and Schlosser, 2005; Bailey and Streit, 2006; Brugmann and Moody, 2005; Litsiou et al., 2005; Schlosser, 2006). Since ectopic expression of either *dlx3b* or *cv2* induced expression of both *eya1* and *six4.1*, we wished to examine the effects of *dlx3b* and *cv2* on FGF activity. The expression of genes induced by FGF activity, including *erm* and *spry4* (Fürthauer et al., 2001; Raible and Brand, 2001), was observed in cells ectopically expressing *dlx3b* or *cv2* (Figure 3.8A,B,D,E). Ectopic *fgf receptor1* (*fgfr1*) expression was also detected in cells ectopically expressing *dlx3b* or *cv2* (Figure 3.8C,E). As with PPR marker expression, some cells expressing ectopic *cv2* did not express markers indicative of FGF responsiveness. We were able to drive all cells expressing the uncleavable form of *cv2* to express markers indicative of FGF competence (Figure 3.8G-I).

In addition to the role of FGF signaling in PPR formation, numerous studies have established that Fgf3/8 signaling from the mesendoderm and hindbrain are required for otic placode induction in zebrafish (Leger and Brand, 2002; Liu et al., 2003; Riley, 2003; Riley and Phillips, 2003; Solomon et al., 2004). The expression of these FGF ligands is unaffected by loss of Dlx3b/4b (Liu et al., 2003; Solomon et al., 2004). Nonetheless, Dlx3b/4b are required for the proper expression of the FGF target gene *pax2a* in otic placode induction (Leger and Brand, 2002; Phillips et al., 2001). Because our results suggested that Dlx3b/4b and Cv2 may affect competence to respond to FGF activity, we examined the expression of *erm* and the three *fgf receptors* (*fgfr1-3*) expressed in the otic placode (Poss et al., 2000; Scholpp et al., 2004; Sleptsova-Friedrich et al., 2001; Thisse et

al., 1995). *erm* expression was lost from the hindbrain and otic placode of Dlx3b/4b morphants at the 6-somite stage (Figure 3.9A,B). We observed decreases in *fgfr1-3* expression in the otic placode as well as in the hindbrain of Dlx3b/4b morphants (Figure 3.9E,H,K). *fgfr1* transcript, which is localized in rhombomere 3 of the hindbrain, otic placode, and MHB, was lost from both rhombomere 3 and the otic placodes of Dlx3b/4b morphants (Figure 3.9E). Similarly, *fgfr2* expression was lost from rhombomeres 4 and 6 as well as the otic placode in Dlx3b/4b morphants (Figure 3.9H). *fgfr3* expression was lost from the hindbrain and otic placode in Dlx3b/4b morphants (Figure 3.9K). Quantification of *fgfr* transcript levels in Dlx3b/4b morphants revealed that transcripts were reduced by approximately 30% compared to embryos injected with control morpholinos ($p<0.005$; Figure 3.2). The decrease in *fgfr* expression in Dlx3b/4b morphants is transient; we did not observe a change in *erm* or *fgfr* expression until early somitogenesis, after the increase in *bmp4* expression (Figure 3.10). Like the increase in *bmp4* expression, *erm* and *fgfr* expression returned to levels comparable to controls by mid-somitogenesis (Figure 3.11).

To determine whether the addition of *cv2* could rescue the decrease in FGF activity seen in Dlx3b/4b morphants, we co-injected *cv2* mRNA with *dlx3b/4b* morpholinos into one- and two-cell embryos. Ectopic *cv2* expression was sufficient to restore *erm* expression in the otic placode and hindbrain of Dlx3b/4b morphants (Figure 3.9C). Likewise, *fgfr1-3* expression returned to otic and hindbrain domains in Dlx3b/4b morphants (Figure 3.9F,I,L). Taken together, these results suggest that through their regulation of the BMP antagonist *cv2*, Dlx3b/4b indirectly promote competence to respond to FGF signaling.

Inhibition of BMP activity can rescue the otic phenotype of Dlx3b/4b morphants

Previous studies have shown that *pax2a* expression is delayed in the otic placode of Dlx3b/4b morphants until mid-somitogenesis stages (Liu et al., 2003; Solomon et al., 2004), which corresponds with the transient reduction in *fgfr* expression we observe in these morphants. As we observed rescue of *erm* expression when *cv2* mRNA was co-injected with *dlx3b/4b* morpholinos, we wished to determine if ectopic *cv2* mRNA was sufficient to rescue *pax2a* expression in Dlx3b/4b morphants. While we observed variability in the width of the midbrain-hindbrain boundary (MHB) and optic stalk of Cv2 morphants consistent with mild DV patterning defects (Rentzsch et al., 2006), *pax2a* expression was consistently absent from the otic placode (Figure 3.12B-D). Injection of *cv2* mRNA at levels that did not significantly affect DV patterning was sufficient to rescue *pax2a* expression in the otic placode (Figure 3.12E).

Despite its inhibition of PPR induction, the role of BMP activity in otic placode development has not been examined (reviewed in Ohyama et al., 2007; Riley, 2003). To examine the effects of elevated BMP activity levels on otic development, we inactivated Dlx3b/4b and Chd in concert. In Dlx3b/4b/Chd triple morphants the expression of *eya1*, *pax2a*, and *tbx2b* was lost from the otic vesicle yet maintained in surrounding tissues (Figure 3.3E-M). Therefore, we determined further how manipulation of Cv2 and BMP activity affects otic development in a Dlx3b/4b morphant background. Dlx3b/4b morphants develop an otic vesicle that is reduced in size and lacks otoliths (Figure 3.13A,B) (Liu et al., 2003; Solomon and Fritz, 2002). Although slightly larger, the otic vesicle of Cv2 morphants resembled that of Dlx3b/4b morphants (Figure 3.13C). The

otic phenotype of Cv2/Dlx3b/4b triple morphants was no more severe than Dlx3b/4b morphants (Figure 3.13D). Furthermore, the otic phenotype of Dlx3b/4b morphants was rescued when *cv2* mRNA was co-injected with *dlx3b/4b* morpholinos (Figure 3.13E,F).

To demonstrate that the otic phenotype of Dlx3b/4b morphants is due to the loss of BMP antagonizing activity of Cv2, we took advantage of a transgenic zebrafish line carrying a truncated form of a type I BMP receptor under the control of a heatshock promoter (abbreviated *tBR*; Pyati et al., 2005). In order to attenuate BMP signaling over the stages at which we observed increased BMP activity in Dlx3b/4b morphants, we heat-shocked *tBR* embryos at bud stage. Attenuating BMP activity in Dlx3b/4b morphants was sufficient to rescue the otic phenotype of Dlx3b/4b morphants Figure 3.13G,H). A similar rescue was observed when Bmp4 was knocked down in concert with Dlx3b/4b Figure 3.13I,J). This suggests that elevated BMP activity inhibits otic placode induction, and that a major role of Dlx3b/4b is to modulate BMP activity levels in the otic placode, primarily through regulation of *cv2* expression.

Because we observed a depression of FGF activity in Dlx3b/4b morphant embryos, we tested whether the Dlx3b/4b morphant phenotype could be rescued by supplying *fgfr* mRNA to Dlx3b/4b morphants. To do so, we overexpressed *fgfr1*, the Fgf receptor responsible for mediating Fgf8 signaling (Scholpp et al., 2004). Injection of *fgfr1* mRNA was also able to partially rescue the Dlx3b/4b morphant phenotype (81%; 104/129); the otic vesicle in these embryos was larger and contained one otolith (Figure 3.13K,L). Taken together, these results suggest that BMP activity in the otic placode inhibits the ability of preotic cells to respond to FGF signaling, and that this inhibition occurs at the level of *fgfr* expression.

Discussion

Numerous studies have shown that placodal precursor cells are derived from a molecularly and embryologically distinct domain, the PPR (Bhattacharyya et al., 2004; David et al., 2001; Ekker et al., 1992; Kobayashi et al., 2000; Kozlowski et al., 1997; Sahly et al., 1999; Streit, 2002; Whitlock and Westerfield, 2000). PPR formation is a complex process that requires the interplay of several signaling pathways, notably high levels of FGF and low levels of BMP activity (Ahrens and Schlosser, 2005; Brugmann et al., 2004; Glavic et al., 2004; Litsiou et al., 2005). To understand the development of sensory placodes, it is crucial to determine how the PPR is generated.

Members of the *Dlx* gene family are expressed in the PPR, raising the possibility that they mediate signaling events to levels conducive for further sensory placode development. In zebrafish *dlx3/4b* are required for at least otic and olfactory placode development, and in *Xenopus Dlx3* is required for the induction of *Six1* in the PPR (Solomon and Fritz, 2002; Woda et al., 2003), suggesting that *Dlx* genes play a central role in placodal competence (Hans et al., 2007; Hans et al., 2004). In this context, we have reexamined the role of *dlx3b/4b* in both the establishment of the PPR and otic placode induction.

Modulation of BMP activity by *dlx3b/4b* at the neural plate border

Here we show that *dlx3b/4b* are both necessary and sufficient for the expression of *cv2* in the PPR and developing otic placode. Loss of Dlx3b/4b function leads to a transient increase in Bmp4 activity at the end of gastrulation and early somite stages.

Introduction of *cv2* mRNA or inhibition of Bmp4 or total BMP activity can rescue the PPR and otic phenotypes observed in Dlx3b/4b morphants, demonstrating that Dlx3b/4b mediate BMP activity in the PPR. In the context of PPR specification and otic induction, Dlx3b/4b appear to act as permissive factors, allowing the expression of *Eya/Six/Dach* gene members in the PPR and *pax2a* in the otic placode without any direct transcriptional requirement.

In addition to their role in PPR formation, *dlx3b/4b* likely have other functions at the neural plate border. Our analysis shows that increased BMP signaling is not limited to *dlx3b/4b*-expressing cells as Dlx3b/4b morphant embryos are mildly ventralized in the tail region. Furthermore, studies by Artinger and colleagues have demonstrated that *Dlx*-expressing cells at the neural plate border in *Xenopus* and zebrafish affect neighboring cells in the lateral neural plate domain (Kaji and Artinger, 2004; Woda et al., 2003). The secretion of Cv2 from the PPR posits a likely mechanism of how *Dlx* genes can autonomously establish the PPR while exerting non-autonomous influence over the adjacent neural crest/Rohon-Beard domain. Recent studies in *Drosophila* and *Xenopus* have shown that Cv2 preferentially binds Bmp4 (and Dpp in *Drosohpila*), and that its pro- or anti- BMP effects occur in a dose-dependent manner (Ambrosio et al., 2008; Serpe et al., 2008), such that high Cv2 levels inhibit Bmp4 ligand-receptor interactions, while low Cv2 levels stabilize them. Furthermore, due to interactions of Cv2 with heparin sulfate proteoglycans, these activities occur over a very short distance from the secreted cell (Rentzsch et al., 2006; Serpe et al., 2008), potentially explaining why ectopic PPR marker expression is not observed at any distance from *cv2*-expressing cells. This evidence supports our model in which high levels of Cv2 secreted by *dlx3b/4b*-

expressing cells establishes the presumptive PPR by inhibiting Bmp4 signaling, and may explain how Cv2 enhances the Bmp4 requirements in neural crest and Rohon-Beard cells (Rossi et al., 2008). However, due to the recently revealed complexities that govern Cv2 function in BMP modulation (Ambrosio et al., 2008; Bier, 2008; Serpe et al., 2008; Zhang et al., 2008), this latter point remains to be investigated.

Integration of BMP and FGF signaling in PPR and placode formation

In both *Xenopus* and chick, FGF activity is required but not sufficient for the establishment of preplacodal territory (reviewed in Bailey and Streit, 2006; Schlosser, 2006). The combination of elevated levels of FGF activity and low levels of BMP activity, however, does appear to be able to induce the full range of PPR markers. *Six4*, which cannot be induced with ectopic Fgf8 activity alone, can be induced when BMP activity is inhibited in the presence of ectopic Fgf8 (Litsiou et al., 2005). Similarly in *Xenopus, Fgf8* can induce *Six1* expression only in the presence of the BMP antagonist *Noggin* (Ahrens and Schlosser, 2005). Together, these studies show that induction of the PPR requires a precise balance of high FGF activity and low BMP activity that is normally found at the border of the neural plate.

Despite these studies, it has remained unclear why PPR formation or otic placode induction require attenuation of BMP signaling. Although it is possible that BMP signaling is detrimental to the formation of these tissues per se, our evidence suggests that excessive BMP activity interferes with FGF signaling. Cells ectopically expressing *dlx3b* or *cv2* co-express markers indicative of PPR formation. Many of these cells also express *fgfr1* and the FGF feedback regulators *erm* and *spry4*, demonstrating Dlx3b/4b

and Cv2 confer competence to respond to FGF signaling. This appears to be through the BMP antagonizing activity of Cv2, as all cells ectopically expressing *cv2-CM* co-express *fgfr1*, *erm* and *spry4*. BMP signaling has similar effects in otic placode induction, where *fgfr1-3* expression is reduced in the otic placode and hindbrain of Dlx3b/4b morphants. Interestingly, we were able to significantly rescue both the PPR (data not shown) and otic vesicle defects seen in Dlx3b/4b morphants by overexpressing *fgfr1*. *fgfr1* has previously been shown to mediate Fgf8 signaling, a key component of otic placode induction (Leger and Brand, 2002; Phillips et al., 2001; Riley, 2003; Scholpp et al., 2004).

Interactions between BMP and FGF signaling pathways have been previously demonstrated. FGF signaling has been shown to interfere with BMP signaling by phosphorylation of the linker region of SMAD1 (Pera et al., 2003). Conversely, in murine limb bud development, BMP activity inhibits FGF signaling by downregulating *Fgf4* expression in the apical ectodermal ridge (Ganan et al., 1996; Pizette and Niswander, 1999; Zuniga et al., 1999). Our data suggest that in the context of PPR and otic placode induction, BMP activity leads to a downregulation of *fgfr* expression. This effect may be mediated by BMP targets such as the *vent/vox* transcriptional repressors (Imai et al., 2001; Melby et al., 2000; Shimizu et al., 2002); however, this remains to be elucidated. Thus, we propose that the balance of FGF and BMP activities at the neural plate border is established by in part by Dlx3b/4b through the transcriptional regulation of *cv2*. Our data suggest that Cv2 acts in its uncleaved, antagonistic form, and *dlx3/4b* acts to locally establish an environment of low BMP activity. Through the inhibition of BMP activity, Cv2 establishes a region favorable for FGF activity. While it has been suggested that BMP antagonists secreted from underlying mesendoderm act to regulate

PPR fate (Litsiou et al., 2005), Cv2 is the first identified BMP antagonist expressed in the PPR itself that is required for the establishment of this tissue.

Although low BMP activity levels are critical for PPR formation at the end of gastrulation, the initial establishment of *dlx3b/4b* expression requires BMP signaling. Fate-mapping studies have shown that cells that will become the PPR originate from regions of the gastrula that are initially exposed to higher levels of BMP activity than those cells that will give rise to neural plate (Kozlowski et al., 1997). These differences in BMP exposure of presumptive PPR and neural ectoderm are reflected by expression of *Dlx*, *Fox*, and *Msx* family members within presumptive PPR (Feledy et al., 1999; Luo et al., 2001; Matsuo-Takasaki et al., 2005; Nguyen et al., 1998; Pera et al., 1999; Phillips et al., 2006; Suzuki et al., 1997). BMP signaling directly regulates murine *Dlx3* expression through SMAD1 (Park and Morasso, 2002). Similarly, it has been demonstrated that *Dlx3/5/6* expression around chick and *Xenopus* neural plate are increased in response to elevated BMP activity levels (Feledy et al., 1999; Luo et al., 2001; Pera et al., 1999). In zebrafish *swirl* (*bmp2b*), *snailhouse* (*bmp7*), or *somitabun* (*smad5*) mutants, *dlx3b* is not expressed in the PPR or otic placode (data not shown; Nguyen et al., 1998). Thus, formation of the PPR first requires BMP signaling during early gastrulation to establish a domain of *Dlx* expression, which subsequently antagonizes BMP activity to levels favorable for induction of the PPR.

Dlx and Cv2: evolutionary implications for PPR establishment

In chick and mouse, *Cv2* is expressed in premigratory NC (Coffinier et al., 2002; Coles et al., 2004), a tissue that requires intermediate levels of BMP activity, while *cv2*

expression in zebrafish overlaps with *dlx3b* in preplacodal ectoderm, a tissue that requires low levels of BMP activity (reviewed in Aybar and Mayor, 2002; Bailey and Streit, 2006; Schlosser, 2006). Furthermore, *Cv2* appears to act as an agonist of BMP signaling in chick NC development (Coles et al., 2004). Although *Cv2* expression in chick has not been determined at the relevant stages, it is difficult to reconcile the known *Cv2* expression and function in chick with our results in PPR formation. In mouse, *Cv2* does not appear to be expressed in the PPR at the onset of somite stages (Coffinier et al., 2002). While *Cv2* expression needs to be more thoroughly examined in amniotes, it is clear that *Cv2* expression patterns have diverged between amniotes and zebrafish as there is no expression in zebrafish neural crest.

In amniotes, the *Dlx5/6* genes are expressed in a similar manner to zebrafish *dlx3b/4b* (Ekker et al., 1992; Pera et al., 1999; Yang et al., 1998). In chick, *Dlx5* misexpression leads to upregulation of *Six4* (McLarren et al., 2003), consistent with our observations in zebrafish. However, while the role of *Dlx5/6* in PPR formation has not been examined in detail in chick or mouse, knock-out of mouse *Dlx5/6* does not appear to affect the induction of the otic placode (Acampora et al., 1999; Merlo et al., 2002; Robledo and Lufkin, 2006; Robledo et al., 2002). Instead, mutant mice develop later defects in inner ear morphology. The role of the zebrafish *dlx3b/4b* genes in PPR establishment appears to remain conserved between *Xenopus* and zebrafish. While the *Xenopus Cv2* gene has been identified, its expression has not yet been analyzed (Coles et al., 2004; Moser et al., 2003). However, as discussed above, *Xenopus Dlx3* is required for expression of PPR markers in transplantation experiments, and Dlx3 in *Xenopus* appears to have similar effects on the lateral neural plate as seen in zebrafish (Kaji and

Artinger, 2004; Woda et al., 2003). Therefore, it is likely that at least in fish and amphibians the role of these genes is similar.

Based on our analysis, we suggest that the discrepancy in the early role of the *Dlx* genes between mouse and zebrafish in PPR establishment and placode induction might be due to differences in *Cv2* expression. Thus, the *Dlx5/6* genes are unlikely to play a role in modulation of BMP signaling and establishment of the PPR and seem to be principally involved in later aspects of placode development. Importantly, even though the precise molecular mechanism of PPR induction may show species specific differences, the overall requirements for high levels of FGF activity and attenuated BMP activity appear to be the same in chick, amphibians, and fish (Ahrens and Schlosser, 2005; Brugmann et al., 2004; Glavic et al., 2004; Litsiou et al., 2005). Evidence from tissue culture in chick supports a model whereby BMP antagonists secreted from mesoderm underlying the PPR are required to position the PPR (Litsiou et al., 2005), although specific signaling antagonists that act to position the PPR have not yet been identified *in vivo* in chick or mouse. While our data do not exclude a role of the underlying mesendoderm in fish, we show that a key component in the attenuation of BMP signaling, *cv2*, is indeed expressed in the PPR itself**.**

Acknowledgements

We would like to thank P. Chen for comments and criticisms on the manuscript, D. Kimelman and U. Pyati for the *Tg(hsp70l:dnBmpr-GFP)*^{w30} zebrafish line, M. Esterberg for assistance with statistics. This work was supported by an NIH grant to A.F. (DC004701).

Figure 3.1: BMP activity is transiently increased during early somitogenesis in Dlx3b/4b morphants.

(A,B) *bmp4* expression is unaffected in Dlx3b/4b morphants prior to the onset of *dlx3b/4b* expression in 70% epiboly embryos. (C,D) At bud stage, the domain of *bmp4* expression is expanded in the prechordal plate and tailbud of Dlx3b/4b morphants (D). Insets depict the increase of the prechordal domain. (E,F) Antibodies against PSMAD1/5/8 (red) reveal an increase in cells responding to BMP activity of Dlx3b/4b morphants (F). DAPI-stained nuclei are blue. Inset in (F) is a high magnification image depicting PSMAD1/5/8 co-localization with DAPI-stained nuclei. (G,H) *bmp4* expression in Dlx3b/4b morphants is comparable to controls at 18-somites. All views are lateral views, with ventral to the left in (A,B), anterior to the left in (C-F), and anterior to the bottom in (G,H). Insets in (C,D) are dorsal views, with anterior to the top.

Figure 3.1

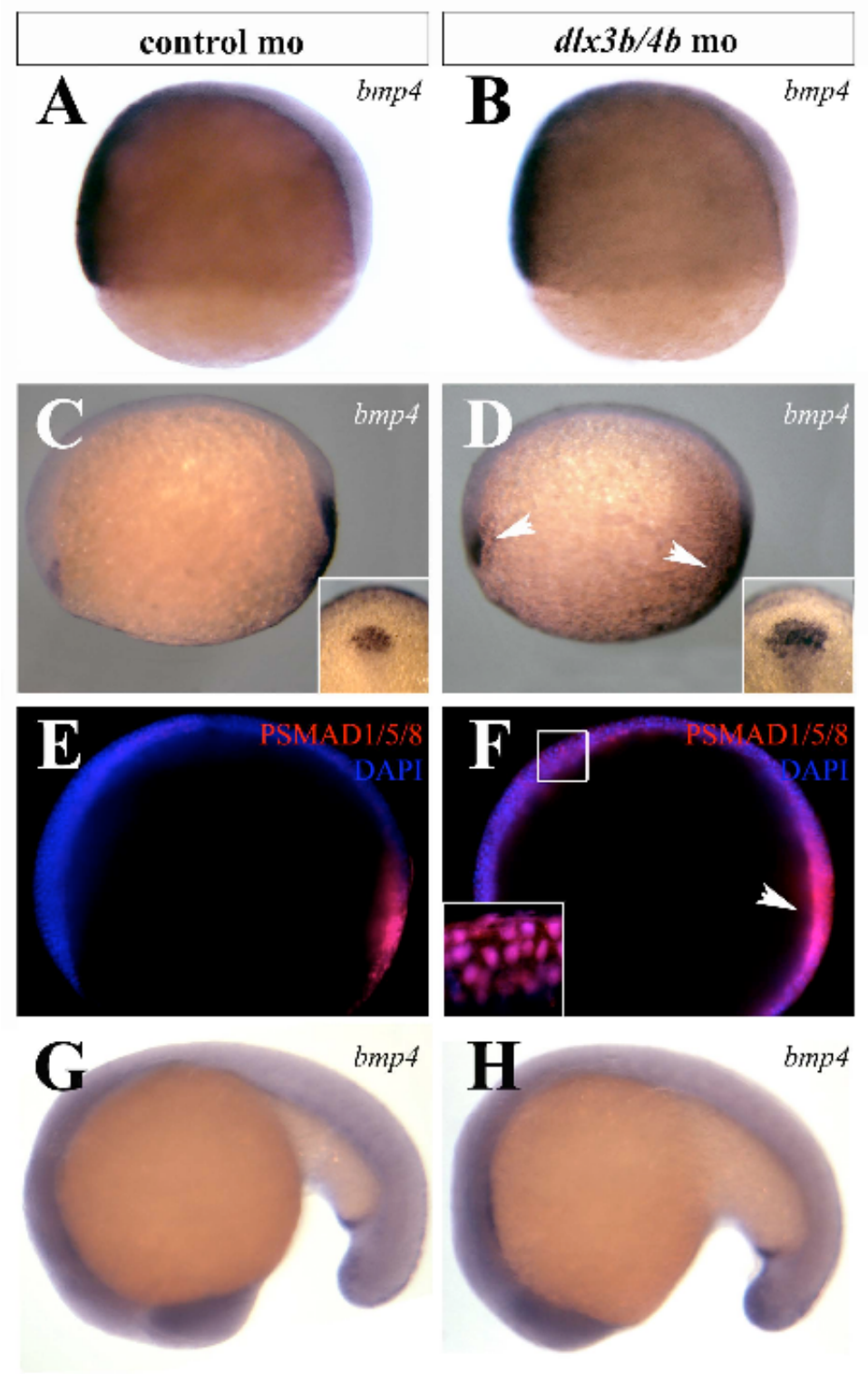
control mo
dlx3b/4b mo
A
bmp4
B
bmp4
C
bmp4
D
bmp4
E
PSMAD1/5/8
DAPI
F
PSMAD1/5/8
DAPI
G
bmp4
H
bmp4

Figure 3.2: Levels of *bmp4* and *fgfr1/2/3/4* transcript are a function of *dlx3b/4b* activity.

Real-time quantitative RT-PCR of *bmp4* and *fgfr1/2/3/4* transcript in Dlx3b/4b morphants as compared to embryos injected with a control morpholino. The mean transcript levels of three experimental runs performed in triplicate were subjected to one-way ANOVA, followed by a two-tailed, equal variance *t*-test. All means were significant ($p<0.005$).

Figure 3.2

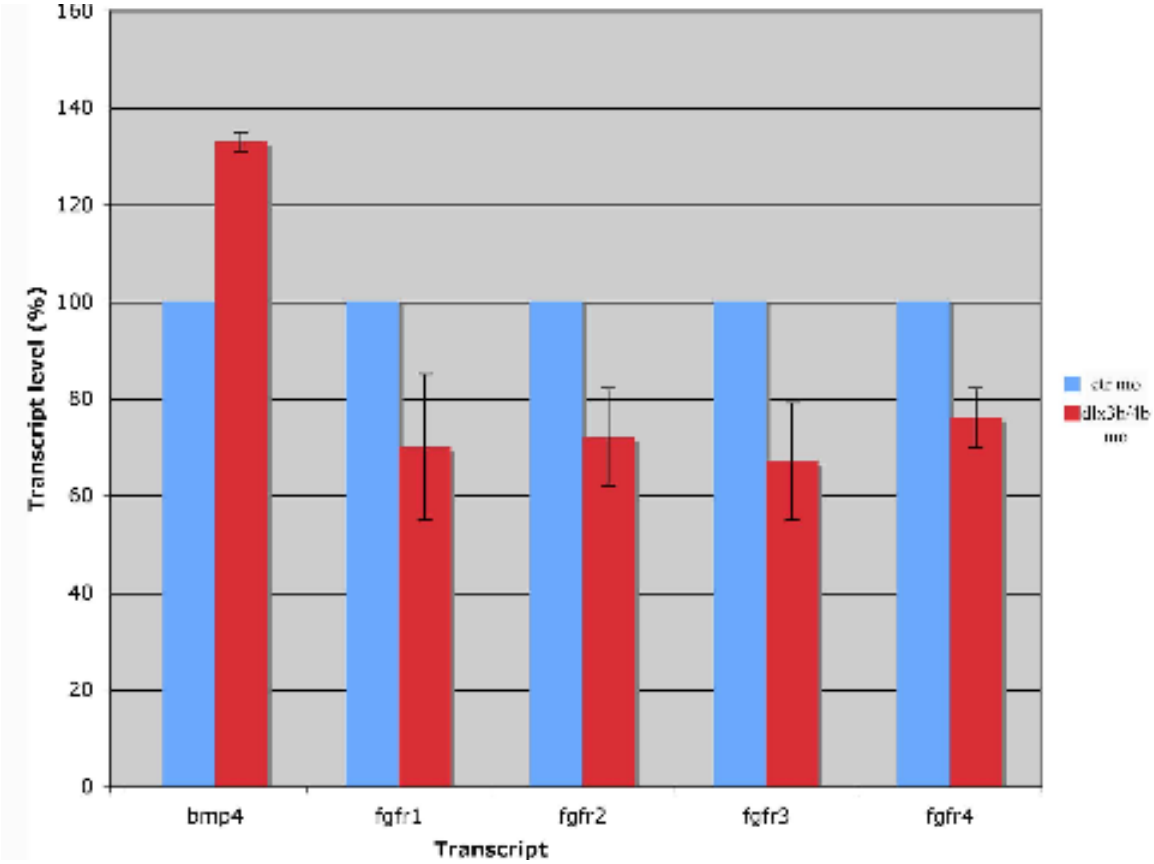
160
140
120
100
80
60
40
20
0
Transcript level (%)
bmp4
fgfr1
fgfr2
fgfr3
fgfr4
Transcript

Figure 3.3: Depletion of Chd reveals anti-BMP function of Dlx3b/4b.

(A-D) Intermediate cell mass of the tail is increased in Dlx3b/4b morphants (B), reminiscent of a ventralization phenotype. Injection of a low dose of *chd*-mo results in a mild V1 ventralization phenotype (C). Knockdown of Chd and Dlx3b/4b increases the severity of ventralization (D). (E-M) Heightened BMP activity in Chd/Dlx3b/4b triple morphant embryos severely reduces otic expression of *eya1* (E-G), *pax2a* (H-J), and *tbx2b* (K-M), while leaving expression in surrounding tissue intact. (A-D) are lateral views and (E-M) are dorsal views, with anterior to the left. All embryos are 24hpf.

Figure 3.3

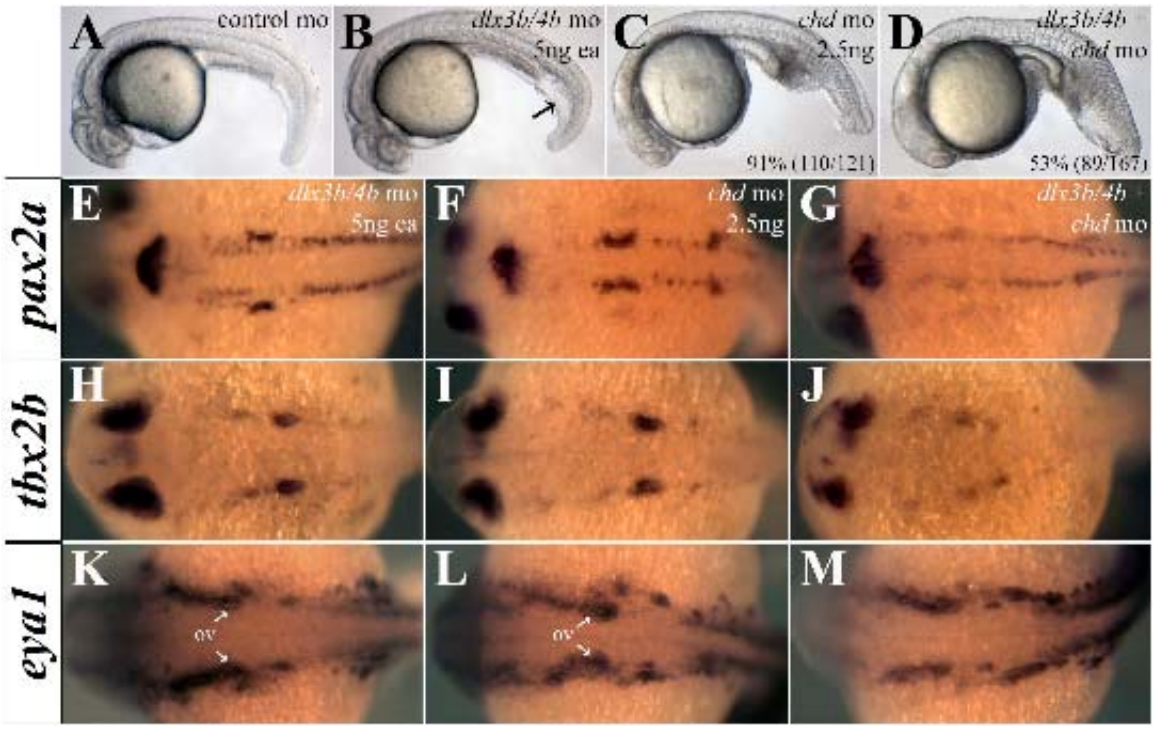
A
control mo
B
dlx3b/4b mo
5ng ea
C
chd mo
2.5ng
91% (110/121)
D
dlx3b/4b
chd mo
53% (89/167)
pax2a
E
dlx3b/4b mo
5ng ea
F
chd mo
2.5ng
G
dlx3b/4b
chd mo
tbx2b
H
I
J
eya1
K
ov
L
ov
M

Figure 3.4: *chd* expression is reduced in Dlx3b/4b morphants, but can be rescued when *cv2* is ectopically expressed.

(A,B,E,F,I,J) *chd* expression is reduced in Dlx3b/4b morphants (B,F,J). At bud stage, *chd* expression is reduced in the anterior neural plate (B). At 6 somites, *chd* expression is reduced in the paraxial mesoderm (F) as well as rhombomeres 3 and 5 (J). (C,G,K) *chd* expression can be rescued when *cv2* is ectopically expressed in Dlx3b/4b morphants. (D,H,L) Expression of the dominant negative form of *cv2*, *cv2-N*, causes a reduction of *chd* expression similar to Dlx3b/4b morphants. (A-D) Bud stage embryos. Dorsal views, with anterior to the top. (E-L) 6 somite stage embryos. (E-H) Caudal views, with dorsal to the top. (I-L) Lateral views, with anterior to the left.

Figure 3.4

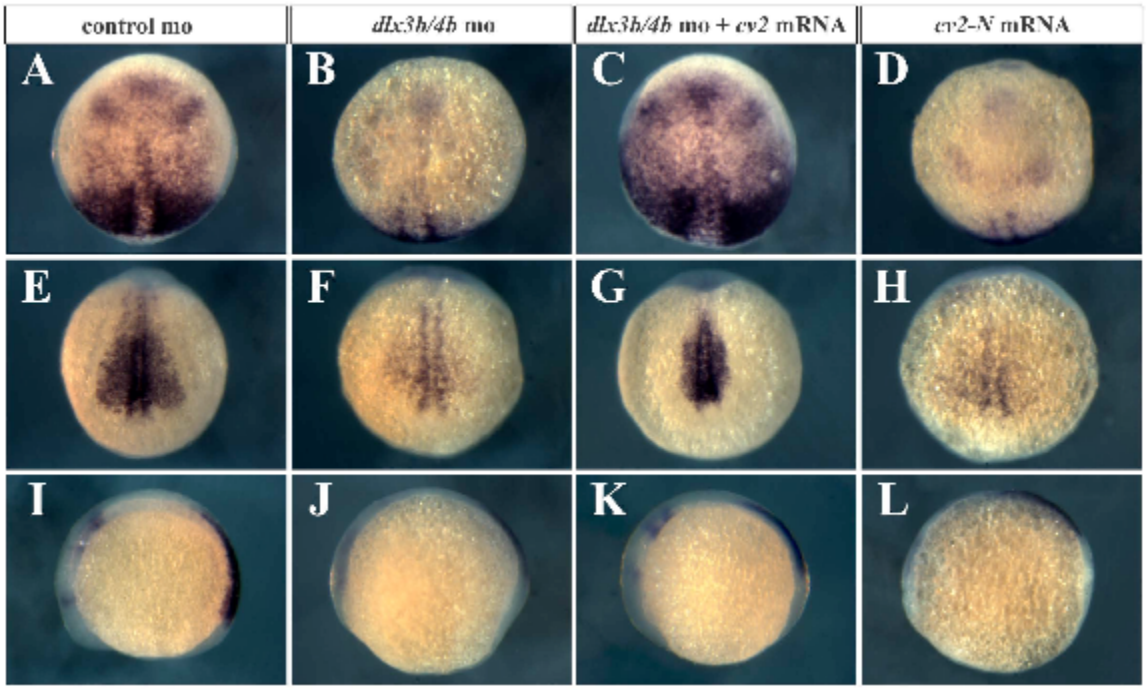
control mo
dlx3h/4b mo
dlx3h/4b mo + cv2 mRNA
cv2-N mRNA
A
B
C
D
E
F
G
H
I
J
K
L

Figure 3.5: *cv2* expression is lost from the PPR, otic placode, and pharyngeal arches in Dlx3b/4b morphants.

(A,B) *cv2* (purple) is co-expressed with *dlx3b* (red) in the ectoderm of the PPR. Transverse sections were taken through the neural plate of 3-somite embryos. (C,D) Prior to the onset of *dlx3b/4b* expression, *cv2* expression is unaffected on the ventral side of 60% epiboly embryos. (E,F) *cv2* expression is lost from the PPR in Dlx3b/4b morphants (F). (G,H) *cv2* expression is lost from the otic placode in 18 somite Dlx3b/4b morphants (H). (I,J) *cv2* expression is lost from the otic vesicle and pharyngeal arches in 30hpf (hours post fertilization) embryos (J). ov, otic vesicle; pa, pharyngeal arches. All views are lateral except (E,F), which are dorsal views.

Figure 3.5

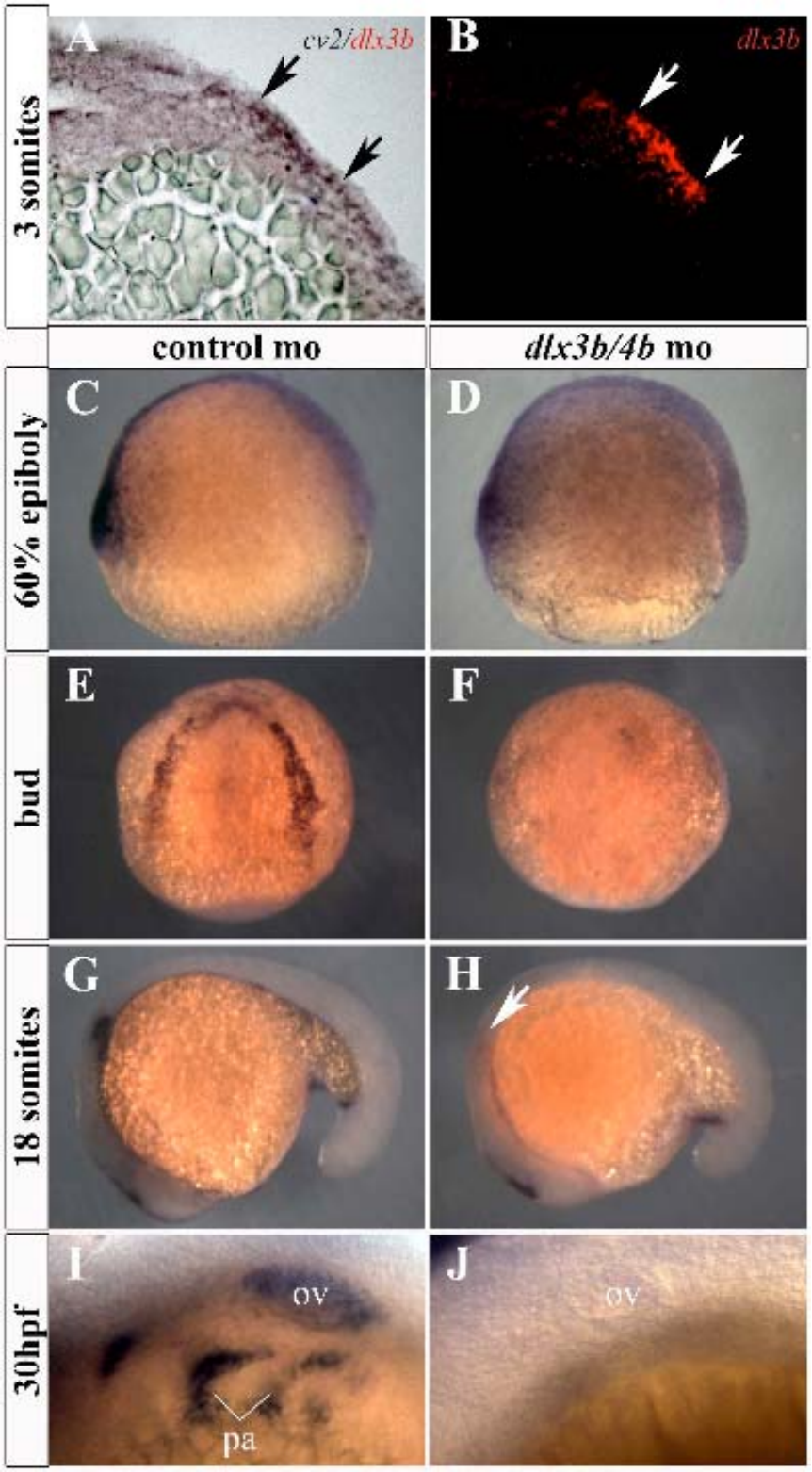
3 somites
A
cv2/dlx3b
B
dlx3b
control mo
dlx3b/4b mo
60% epiboly
C
D
bud
E
F
18 somites
G
H
30hpf
I
ov
pa
J
ov

Figure 3.6: *dlx3b* overexpression dorsalizes the zebrafish embryo.

(A-D) Embryos ectopically expressing *dlx3b* mRNA display molecular read-outs consistent with reduced BMP activity. (A,B) *bmp4* expression is reduced from the prechordal plate and tailbud of embryos ectopically expressing *dlx3b* (B). (C,D) Antibodies against PSMAD1/5/8 (red) reveal that BMP activity is reduced in embryos ectopically expressing *dlx3b* mRNA (D). (E,F) Riboprobes against *krox20* and *pax2a* reveal a widening of the hindbrain in embryos ectopically expressing *dlx3b* mRNA (F). (G,H) Ectopic *dlx3b* DNA (red) can induce ectopic *cv2* expression (purple). (I-N) Ectopic expression of *dlx3b* mRNA resembles the dorsalization seen in embryos ectopically expressing *cv2*. Knockdown of Cv2 can rescue the dorsalization seen in 81% (170/211) of embryos ectopically expressing *dlx3b* mRNA (L). (I-N) 30hpf embryos; lateral views, with anterior to the left. Embryos were grouped into dorsalization categories based on previous classifications (Kishimoto et al., 1997; Mullins et al., 1996). (A-F) Bud stage embryos. Lateral views, with anterior to the left. (G,H) 80% epiboly embryos; lateral views, with ventral to the left.

Figure 3.6

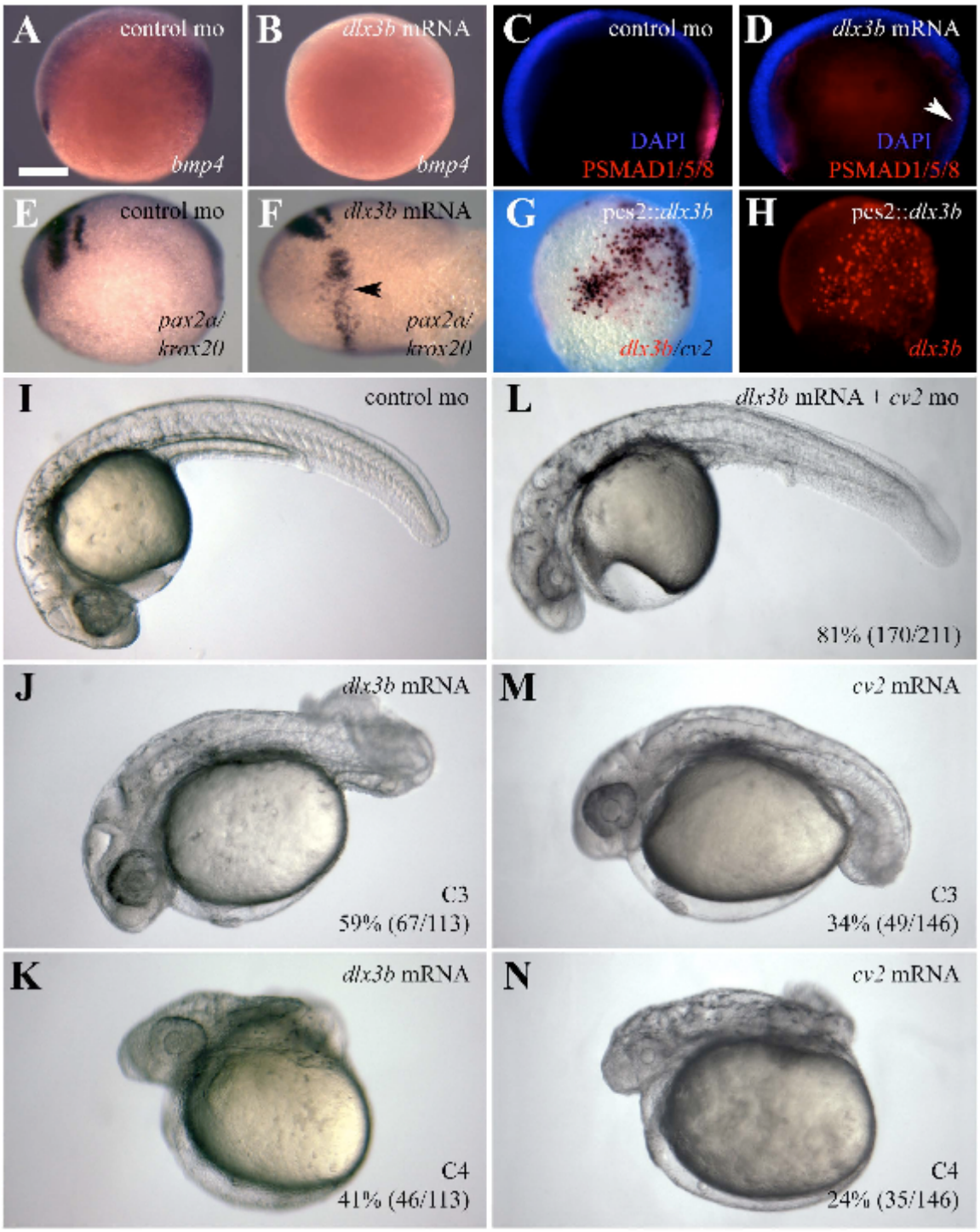
A
control mo
bmp4
B
dlx3b mRNA
bmp4
C
control mo
DAPI
PSMAD1/5/8
D
dlx3b mRNA
DAPI
PSMAD1/5/8
E
control mo
pax2a/
krox20
F
dlx3b mRNA
pax2a/
krox20
G
pes2::dlx3b
dlx3b/cv2
H
pes2::dlx3b
dlx3b
I
control mo
L
dlx3b mRNA + cv2 mo
81% (170/211)
J
dlx3b mRNA
C3
59% (67/113)
M
cv2 mRNA
C3
34% (49/146)
K
dlx3b mRNA
C4
41% (46/113)
N
cv2 mRNA
C4
24% (35/146)

Figure 3.7: *dlx3b/4b* and *cv2* are required for PPR marker expression.

(A-J) *eya1* (A-E) and *six4.1* (F-J) expression are reduced in the PPR of Dlx3b/4b (B,G) and Cv2 (C,H) morphants, but can be rescued when Bmp4 is knocked down (D,I) or when *cv2* mRNA is ectopically expressed (E,J). (K,L) Ectopic *dlx3b* or *cv2* (red) can induce ectopic *eya1* (purple). (M) All cells ectopically expressing the uncleavable form of Cv2, *cv2-CM* (red), ectopically express *eya1* (purple). (A-J) Bud stage embryos; dorsal views, with anterior to the top. (K-M) 80% epiboly embryos; lateral views, with ventral to the left.

Figure 3.7

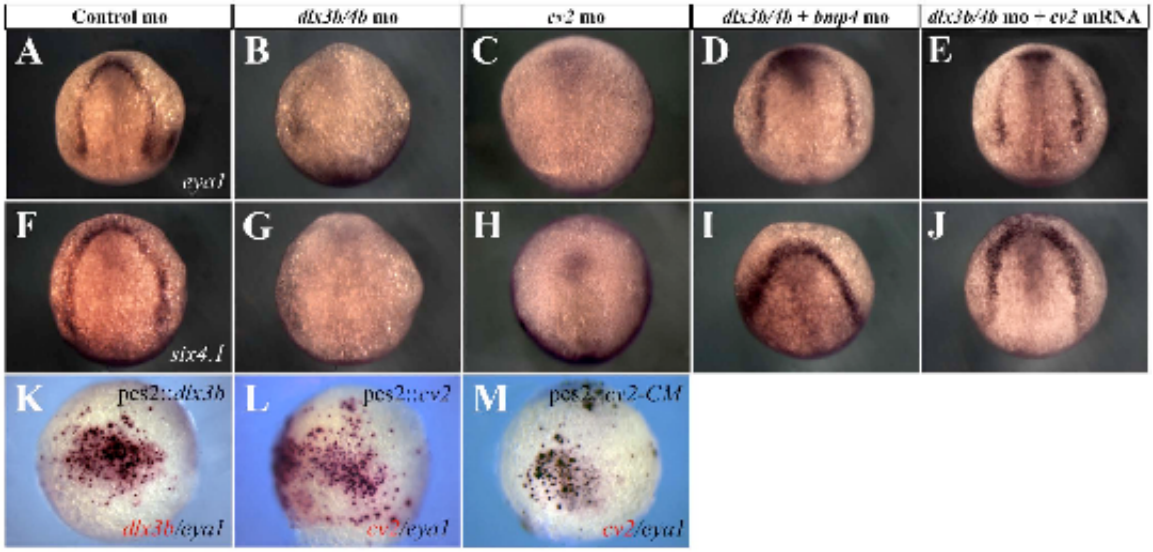
Control mo
dlx3b/4b mo
cv2 mo
dlx3b/4b + bmp4 mo
dlx3b/4b mo + cv2 mRNA
A
eya1
B
C
D
E
F
six4.1
G
H
I
J
K
pcs2::dlx3b
dlx3b/eya1
L
pcs2::cv2
cv2/eya1
M
pcs2::cv2-CΔ1
cv2/eya1

Figure 3.8: Ectopic *dlx3b* or *cv2* expression can induce ectopic FGF activity. (A-C) Ectopic *dlx3b* expression (red) can induce ectopic expression of *erm*, *spry4*, and *fgfr1* (purple). (D-F) Ectopic *cv2* expression (red) can induce ectopic expression of *erm*, *spry4*, and *fgfr1* (purple). (G-I) All cells ectopically expressing the uncleavable form of Cv2, *cv2-CM* (red), ectopically express *erm*, *spry4*, and *fgfr1* (purple). (A-I) 80% epiboly embryos; lateral views.

Figure 3.8

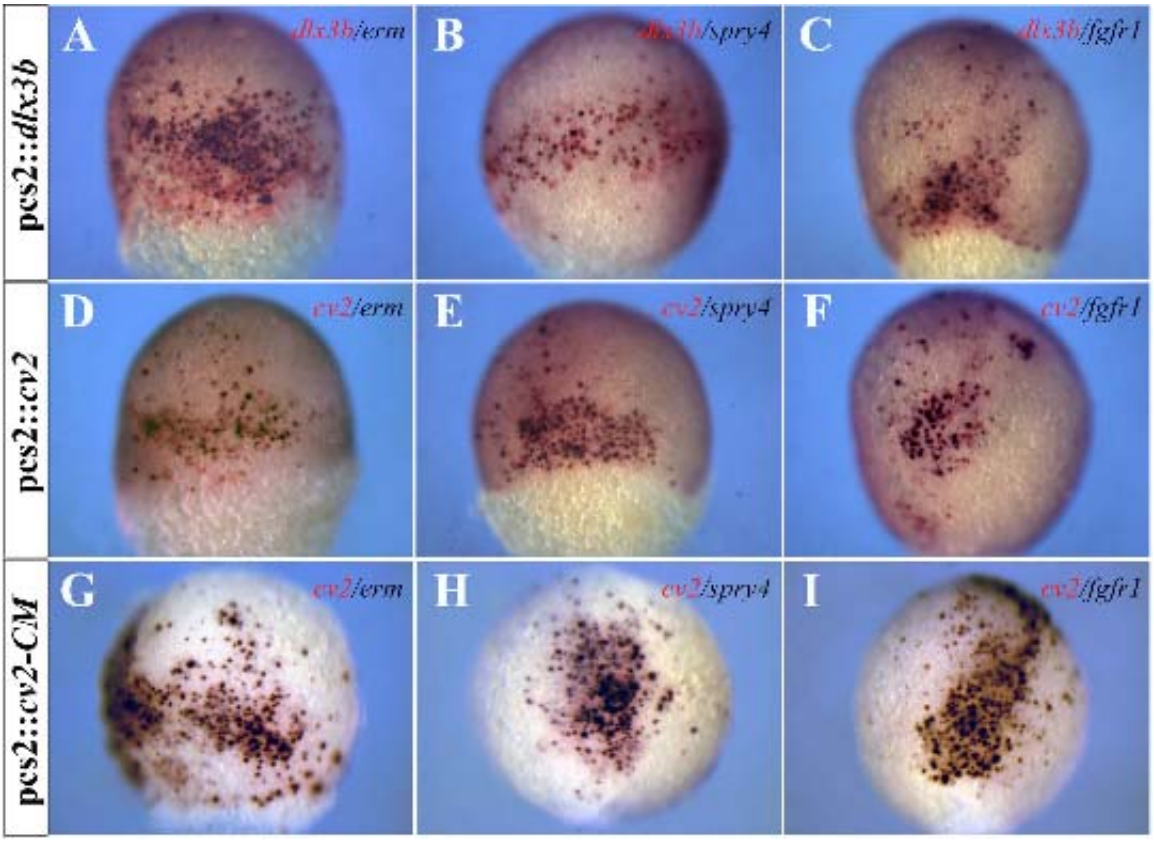
pcs2::dlx3b
pcs2::cv2
pcs2::cv2-CM
A
dlx3b/erm
B
dlx3b/spry4
C
dlx3b/fgfr1
D
cv2/erm
E
cv2/spry4
F
cv2/fgfr1
G
cv2/erm
H
cv2/spry4
I
cv2/fgfr1

Figure 3.9: *fgfr* expression is lost from the otic placode and hindbrain of Dlx3b/4b morphants.

erm and *fgfr1-3* expression are lost from the otic placode and hindbrain of Dlx3b/4b morphants (B,E,H,K). Brackets in (B,K) depict reduction of *erm* (B) and *fgfr3* (K) staining in the hindbrain. Arrows in (E,H) depict loss of *fgfr1* staining (E) from the otic placode and loss of *fgfr2* staining (H) from the hindbrain of Dlx3b/4b morphants. *erm* and *fgfr1-3* expression can be restored to the otic placode and hindbrain when *cv2* mRNA is ectopically expressed in Dlx3b/4b morphants (C,F,I,L). (A-P) 6 somite embryos; dorsal view with anterior to the top. MHB, midbrain-hindbrain boundary; r1, rhombomere 1; r2, rhombomere 2; r3, rhombomere 3; r4, rhombomere 4; r6, rhombomere 6; op, otic placode.

Figure 3.9

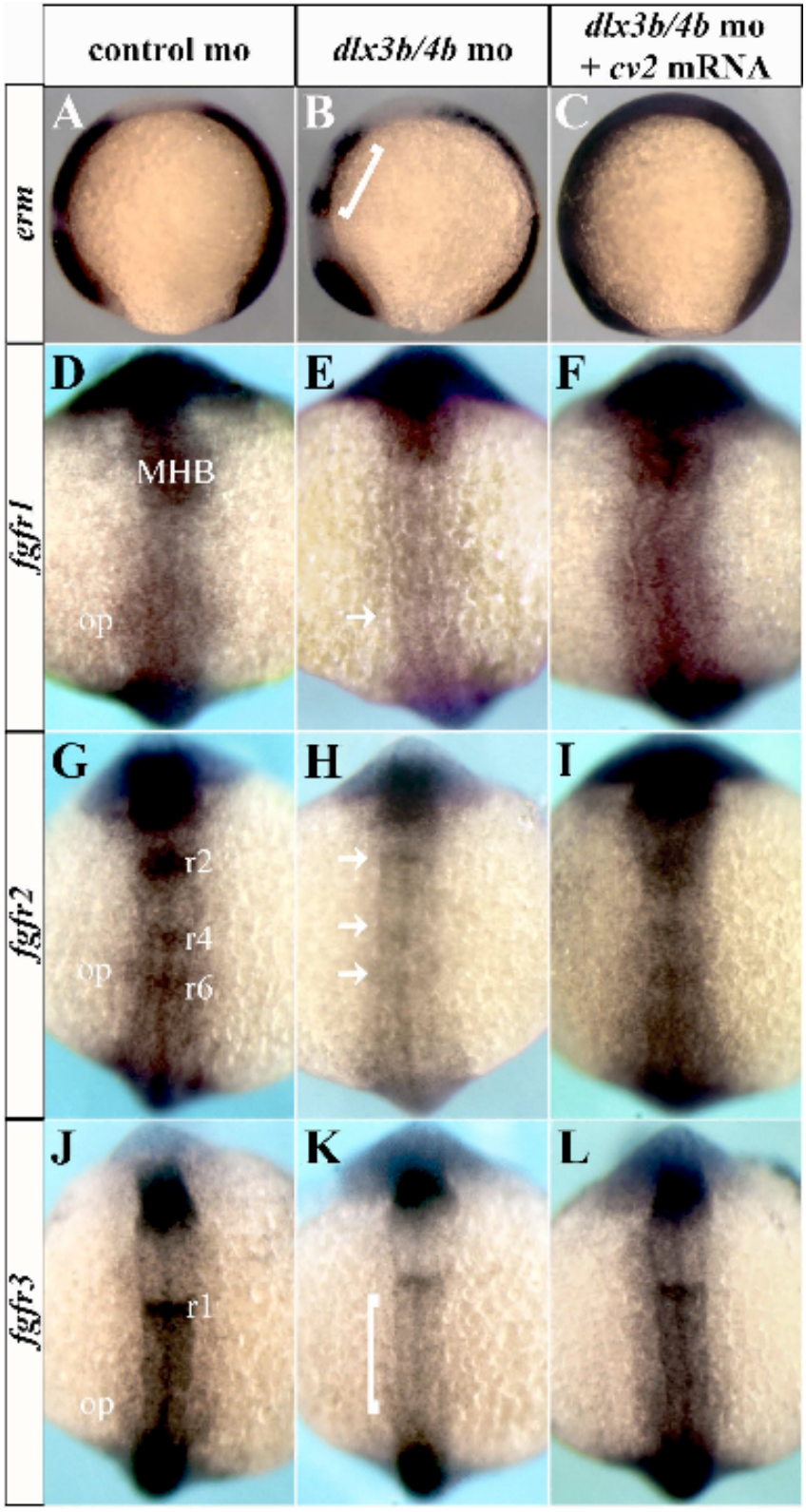
control mo
dlx3b/4b mo
dlx3b/4b mo + cv2 mRNA
erm
fgfr1
fgfr2
fgfr3
A
B
C
D
E
F
G
H
I
J
K
L
MHB
op
r2
r4
r6
r1

Figure 3.10: FGF activity is not compromised in Dlx3b/4b morphant embryos prior to the onset of somitogenesis.

Bud stage embryos stained with riboprobes against *erm, fgfr1, fgfr2, fgfr3,* or *fgfr4* show that expression is unchanged in Dlx3b/4b morphant embryos (B,D,F,H,J) when compared to controls (A,C,E,G,I). The arrow represents the otic placode. The arrowhead represents the notochord. The asterisk marks a region bordering the neural plate anterior to the otic placode. MHB, midbrain-hindbrain boundary; hb, hindbrain; r2, rhombomere 2; psm, presomitic mesoderm. (A-J) Bud stage embryos; dorsal views with anterior to the top.

Figure 3.10

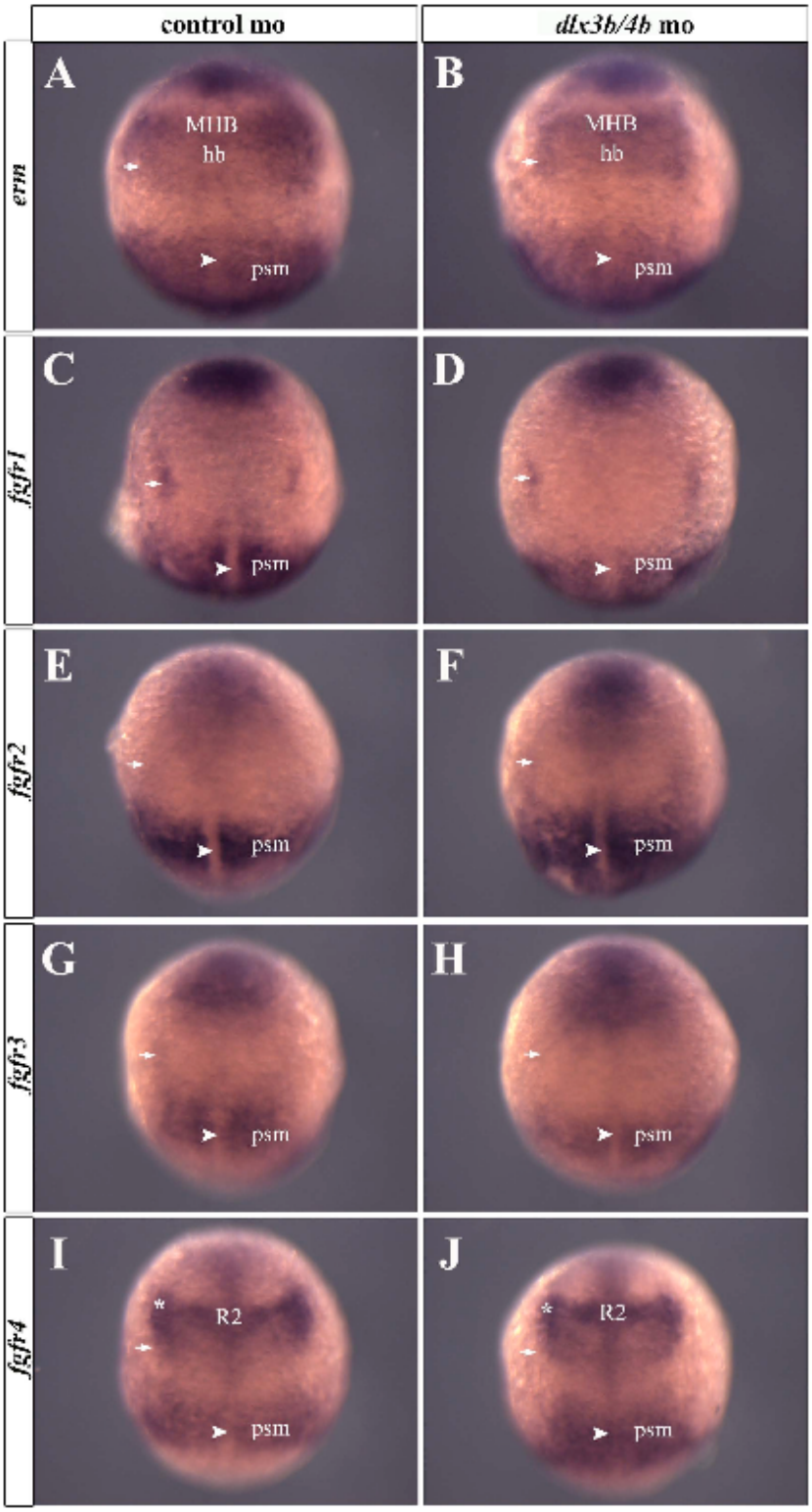
control mo
dlx3b/4b mo
erm
fgfr1
fgfr2
fgfr3
fgfr4
A
B
C
D
E
F
G
H
I
J
MHB
hb
psm
R2
*

Figure 3.11 The reduction of FGF activity in Dlx3b/4b morphant embryos is transient, and begins to return to control levels by mid-somitogenesis.

12-somite embryos stained with riboprobes against *erm, fgfr1, fgfr2, fgfr3,* or *fgfr4* show that expression is reduced in Dlx3b/4b morphant embryos (B,D,F,H,J) when compared to wild-type embryos (A,C,E,G,I). The asterisk marks the MHB. fb, forebrain; mb, midbrain; hb, hindbrain; r1, rhombomere 1; r2, rhombomere 2; r4, rhombomere 4; r6, rhombomere 6; som, somites; psm, presomitic mesoderm. (A-J) 12-somite embryos; lateral views with anterior to the top.

Figure 3.11

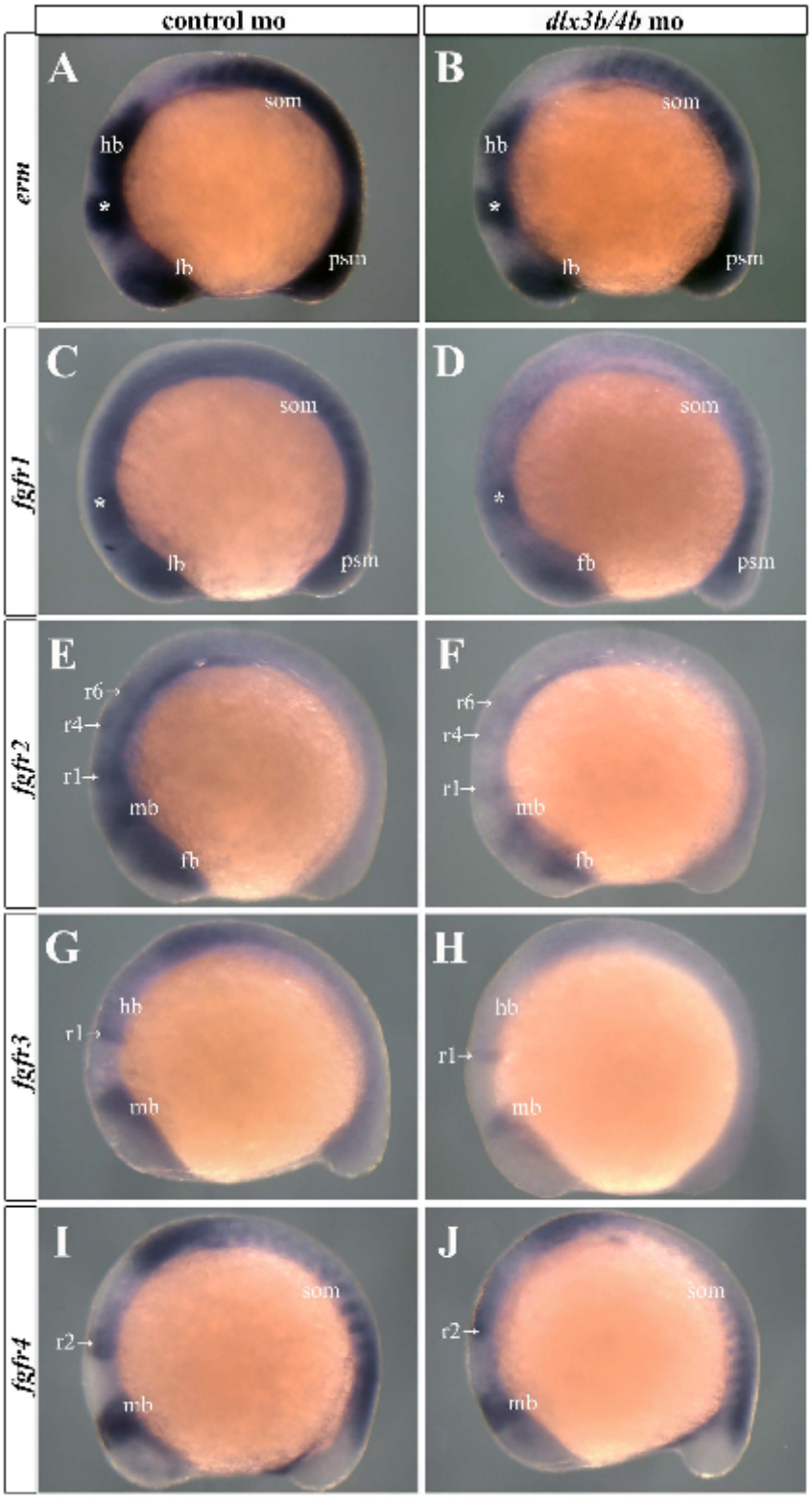
control mo
dlx3b/4b mo
erm
fgfr1
fgfr2
fgfr3
fgfr4
A
B
C
D
E
F
G
H
I
J
som
hb
fb
psm
mb
r6→
r4→
r1→
r2→
*

Figure 3.12: *pax2a* expression in the otic placode requires Cv2.

(A-E) *pax2a* expression is lost from the otic placode of Dlx3b/4b (B) and in 69% (27/39) of Cv2 (C,D) morphants. *pax2a* expression can be restored to the otic placode when *cv2* mRNA is ectopically expressed in Dlx3b/4b morphants (E). (A-E) 6-somite embryos; dorsal view, with anterior to the top.

Figure 3.12

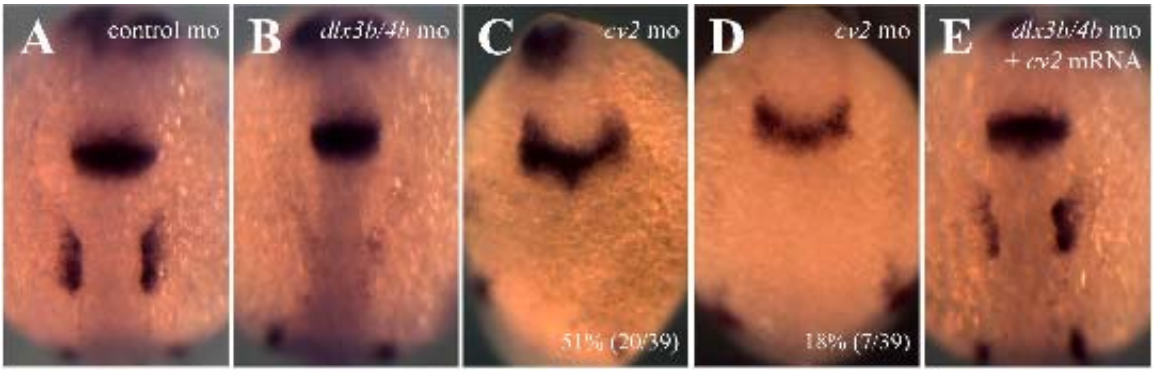
A
control mo
B
dlx3b/4b mo
C
cv2 mo
51% (20/39)
D
cv2 mo
18% (7/39)
E
dlx3b/4b mo
+ cv2 mRNA

Figure 3.13: Manipulation of PPR-inducing signals can rescue the otic phenotype of Dlx3b/4b morphants.

(B) Dlx3b/4b morphants display a small, circular otic vesicle that lacks otoliths. (C,D) The otic phenotype of Cv2 morphants resembles that of Dlx3b/4b morphants (B), and is not significantly affected by the additional loss of Dlx3b/4b (D). (E,F) Ectopic expression of *cv2* mRNA can rescue the Dlx3b/4b otic phenotype (F). (G-L) While heat shock of *tBR* embryos (G), knockdown of Bmp4 (I), or ectopic *fgfr1* expression (K) does not affect ear morphology, each is able to partially rescue the otic phenotype of Dlx3b/4b morphants (H,J,L). All embryos are 30hpf; lateral views, with anterior to the left.

Figure 3.13

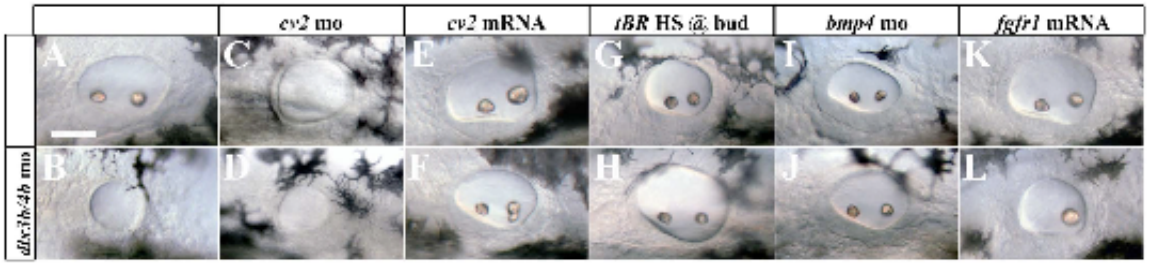
cv2 mo
cv2 mRNA
tBR HS @ bud
bmp4 mo
fgfr1 mRNA
dlx3b/4b mo
A
B
C
D
E
F
G
H
I
J
K
L

CHAPTER 4

The role of fgf receptors in otic development

(Esterberg and Fritz, in preparation)

Fibroblast growth factors (FGFs) are members of a large family of secreted molecules that activate signal transduction pathways involved in a wide range of biological processes. Database searches suggest that there are at least 26 members of the FGF family present in zebrafish (Itoh and Ornitz, 2004; Itoh and Ornitz, 2008; Thisse and Thisse, 2005). Similarly, 13, 23, and 22 FGF ligands have been identified in chick, mouse, and human, respectively. FGF ligands initiate a signaling cascade within a cell by first binding a transmembrane FGF receptor (FGFR), causing homodimerzation and transautophophorylation within it cytoplasmic domain, and ultimately activating the MAPK pathway in a Ras-specfic manner (Bottcher and Niehrs, 2005). These activating phosphorylations permit nuclear translocation of transcriptional complexes, allowing the transcription of target genes. Only four FGFRs have been identified in vertebrates that are thought to mediate all aspects of FGF signaling (Itoh and Ornitz, 2004; Itoh and Ornitz, 2008; Thisse and Thisse, 2005).

Evidence from *Xenopus*, zebrafish, chicken, and mouse strongly suggest that FGFs are the main inducers in otic placode development (Leger and Brand, 2002; Lombardo et al., 1998; Mansour et al., 1993; Maroon et al., 2002; Phillips et al., 2001; Represa et al., 1991; Wright and Mansour, 2003). Support from experiments performed in amphibian, zebrafish, and chick embryos suggest a two-signal model where FGF signals from the head mesoderm as well as the hindbrain act together for proper otic development. In all vertebrate species examined, Fgf3 signaling from the mesendoderm and hindbrain is required as an otic inducer. Targeted disruption of Fgf3 in zebrafish, chick, and mouse partially disrupt otic induction; loss of functional Fgf3 in zebrafish and mouse results in embryos with otic vesicles that are reduced in size and abnormally

patterned (Leger and Brand, 2002; Maroon et al., 2002; Phillips et al., 2001; Represa et al., 1991; Wright and Mansour, 2003). Unlike Fgf3, the requirement for FGF signaling from other family members varies among species. Zebrafish *fgf8* expression overlaps with *fgf3* in the hindbrain, and acts redundantly with Fgf3 in otic placode induction (Leger and Brand, 2002; Phillips et al., 2001; Reifers et al., 1998; Riley and Phillips, 2003; Whitfield et al., 2002). Loss of both Fgf3/8 ablates otic development. Conversely, ectopic expression of *fgf3* or *fgf8* can induce ectopic otic vesicles. In chick, *Fgf19* has been implicated to act redundantly with *Fgf3* in otic induction (Ladher et al., 2000). Blocking Fgf19 results in the formation of otic vesicles that are reduced in size. In mouse, *Fgf10* is expressed in mesendoderm underlying pre-otic cells and plays a partially redundant role with *Fgf3* in otic placode induction (Wright et al., 2003; Wright and Mansour, 2003). Although preotic cells are not exposed to *Fgf8* in chick or mouse, it does indirectly play a role in otic induction. In both species, *Fgf8* is expressed in endoderm subjacent to Fgf19 (in chick) and Fgf10 (in mouse) and is required for initiating their subsequent expression (Ladher et al., 2005).

Studies in otic induction support a model in which there are temporal requirements for FGF signaling (Martin and Groves, 2006; Riley and Phillips, 2003; Whitfield et al., 2002). The earliest requirement for FGF signaling in otic placode induction seems to be late gastrulation in the specification of otic cells from a domain of common precursors termed the pre-placodal region (PPR). This initial phase of induction is first observed through expression of the earliest otic marker, *pax8* (Krauss et al., 1991b). When gastrula stage embryos are treated with SU5402, a small molecule inhibitor of FGF signaling, otic placode induction does not occur and *pax8* is never

expressed (Leger and Brand, 2002; Maroon et al., 2002). If, however, SU5402 is applied after otic induction, expression of early otic markers is present, albeit expressed in slightly fewer cells depending on the stage of treatment. Finally, if SU5402 is applied over temporal windows following otic induction, otic markers disappear only to reappear a short time after inhibitor removal. Patterning of the ear is abnormal in these embryos. These results suggest that FGF signaling is required not only for otic induction, but throughout development for proper otic patterning.

Using recently identified null alleles of *fgf3* (*lia*; Herzog et al., 2004) and *fgf8* (*x15*; B. Riley, personal communication), we have attempted to identify zebrafish ligand-receptor relationships *in vivo*, particularly as their roles pertain to otic development. We have also attempted to identify this relationship on a global level in the embryo. We demonstrate that *fgfr1/2/3* play a necessary role in ear development. Knockdown of Fgfr1/3 phenocopies embryos null for *fgf8*. Knockdown of Fgfr1/3 in a *x15-/-* (*fgf8*) background does not increase the severity of the otic phenotype, suggesting that Fgfr1/3 mediate Fgf8 signals. Likewise, knockdown of Fgfr2 produces an otic phenotype similar to those seen in *lia-/-* (*fgf3*) embryos. Knockdown of Fgfr2 in a *lia-/-* background does not increase the severity of the otic phenotype, suggesting that Fgfr2 mediate Fgf3 signals. Furthermore, knockdown of Fgfr2, but not Fgfr1/3, ablates pituitary and epibranchial marker expression. Taken together, these results suggest a ligand-receptor relationship between of Fgf8 with Fgfr1/3, and Fgf3 with Fgfr2.

Materials and Methods

Animals

Wild-type (AB) zebrafish were obtained from the Zebrafish International Resource Center (Eugene, OR). Embryos were maintained at 28.5°C and staged using standard criteria (Westerfield, 1994). *lia* mutants were genotyped as previously described (Herzog et al., 2004). *x15* mutants were identified by the absence of a midbrain-hindbrain boundary, the development of which requires functional Fgf8 (Reifers et al., 1998).

In situ hybridization

In situ labeling was performed as previously described with probes against *dlx3b* (Ellies et al., 1997), *fgfr1* (Scholpp et al., 2004), *fgfr2* (Tonou-Fujimori et al., 2002), *fgfr3* (Sleptsova-Friedrich et al., 2001), *fgfr4* (Thisse et al., 1995), *neuroD* (Korzh et al., 1998), *pax8* (Pfeffer et al., 1998), and *pit1* (Nica et al., 2004).

Morpholino injection

Morpholino injections were performed as described (Nasevicius and Ekker, 2000). *fgfr1-4* translation-blocking MOs were as follows: *fgfr1* 5'-AAACCACAGCAATCCAAATGATCCA -3'; *fgfr2* 5'-CCAGAAGCCACCCTCGGGCGAACAT -3'; *fgfr3* 5'-CGACTGTCCTCACCACGGAGAGCAG -3'; *fgfr4* 5'-GAAAACCTTTAAGATGCTCAACATC -3'. For single morpholino injections, 8ng of MO were injected into one- and two-cell stage embryos. For double morpholino injections, approximately 6ng of each MO was injected. For triple morpholino injections,

approximately 4 ng of each morpholino was injected. The control morpholino sequence used was 5'-CCTCTTACCTCAGTTACAATTTATA -3'.

Results

fgfr expression in otic cells

As FGF signaling is essential for inducing the mesoderm as well as establishing the dorsovental axis (Bottcher and Niehrs, 2005; Fürthauer et al., 2004; Kimelman, 2006; Schier and Talbot, 2005; Thisse and Thisse, 2005), we reasoned that *fgfr* mRNA may be deposited into the egg maternally. RT-PCR revealed the presence of *fgfr1/2/4*, but not *fgfr3*, in 128-cell embryos (Figure 4.1M). Although the expression patterns of *fgfr1-4* during mid-to late- somitogenesis have been previously described, they have not been examined in the context of the PPR or the otic placode. Thus, we wished to determine the expression of *fgfr1-4* in the context of these tissues (Figure 4.1). To do so, we co-labelled embryos with riboprobes against each *fgfr* and *dlx3b*, a marker of the PPR and otic placode. *Dlx3b* is initially expressed in the PPR during late gastrulation, and following gastrulation its expression is gradually reduced there and upregulated in the otic placode (Ellies et al., 1997; Solomon and Fritz, 2002). In bud stage embryos, all four *fgfr*s overlap with *dlx3b* in the PPR. Of them, *fgfr1-3* were expressed strongly throughout the PPR and adjacent neural plate (Figure 4.1A-C), while *fgfr4* was expressed in a subset of cells in the PPR adjacent to its expression in the midbrain-hindbrain boundary (Figure 4.1D). In 6-somite stage embryos (early-mid somitogenesis), *fgfr1-3* expression was detected overlapping *dlx3b* in the otic placode (Figure 4.1E-G). While both *fgfr1/3* expression completely overlapped with *dlx3b*, *fgfr2* expression overlapped with *dlx3b*

only in the medial region of the otic placode. *fgfr4* expression was not detected in the otic placode (Figure 4.1H). In 18-somite embryos (late somitogenesis), only *fgfr1/2* were detected in the otic vesicle (Figure 4.1I,J). Similar patterns of expression were observed as late as 3dpf (not shown). Taken together, these results suggest that Fgfr1/2/3 may play essential roles in otic placode induction during late gastrulation/early somitogenesis, while Fgfr1/2 may mediate later requirements of FGF signaling in the otic vesicle of late somitogenesis stage embryos.

Fgfr1-3 are required for otic development

In order to determine the requirements of Fgfr1-4 in otic development, we knocked each Fgfr down and assayed otic induction by examining *pax8* expression (Figure 4.2). *pax8* expression was not observed when either Fgfr1 or Fgfr3 were knocked-down separately or in combination (Figure 4.2D,F,G,H). This resembled the expression pattern of embryos homozygous for the *x15* allele, which also did not express *pax8* (Figure 4.2B). Fgfr2 morphants displayed a milder reduction in *pax8* expression (Figure 4.2E), resembling that of embryos homozygous for the *lia* allele (Figure 4.2C). Knockdown of Fgfr4 had no noticeable defects on *pax8* expression (not shown).

Similar and consistent results were obtained when we assayed the size and shape of the otic vesicle (Figure 4.3). In control morphants, embryos form an oval-shaped otic vesicle with two otoliths spaced along the anteroposterior extent of the otic vesicle (Figure 4.3A). Morpholino-mediated knockdown of Fgfr1 or Fgfr3 resulted in circular-shaped otic vesicles that were reduced in size and lacked otoliths (Figure 4.3D,F). The otic phenotype of both Fgfr1 and Fgfr3 morphants resembled those of embryos

homozygous for the *x15* allele (Figure 4.3B), the otic vesicle of which was also circular and lacked otoliths. Fgfr2 morphants displayed a milder otic phenotype, resembling that of embryos homozygous for the *lia* allele (Figure 4.3C,E). In both Fgfr2 morphants and *lia* mutants, the otic vesicle was slightly smaller in shape and otoliths were spaced more closely together.

As the otic phenotype of Fgfr1 and Fgfr3 morphants resembled each other, we wished to determine if loss of Fgfr1/3 in combination increased the severity of otic defects. The otic phenotype observed in Fgfr1/3 morphants was not more severe than when Fgfr1 or Fgfr3 was knocked down alone (Figure 4.3H). A synergism was observed, however, when *fgfr2* morpholino was co-injected with *fgfr1/3* morpholinos (Figure 4.3I). Fgfr1/2/3 triple morphants failed to form an otic vesicle. These results suggest that Fgfr1-3 are essential in mediating FGF signaling in otic development.

Ligand-receptor interactions in otic development

As the otic phenotype of Fgfr1/3 morphants resembled that of *x15* mutants and Fgfr2 morphants resembled *lia* mutants, we wished to determine whether Fgfr1/3 were responsible for mediating Fgf8 signaling and Fgfr2 for mediating Fgf3 signaling. To do so, we performed an interaction analysis using *fgf* mutants and *fgfr* morpholinos. We reasoned that if an FGF ligand were primarily responsible for interacting with a particular receptor, then loss of that receptor in a mutant background would not significantly increase the severity of the otic phenotype.

To determine potential interactions with Fgf8, we knocked down both Fgfr1/3 and Fgfr2 in parallel in *x15* mutant embryos (Figure 4.4). The otic phenotype observed when

fgfr1/3 morpholino was injected into *x15* mutants did not differ significantly from either Fgfr1/3 morphants or *x15* mutants (Figure 4.4B,D). Conversely, when we knocked down Fgfr2 in an *x15* background, the otic vesicle was not detectable (Figure 4.4C). This suggests that at least in the context of otic development, Fgfr1/3 interact with Fgf8 ligands.

In *lia* mutants, knockdown of Fgfr2 did not increase the severity of the otic phenotype of Fgfr2 morphants or *lia* mutants alone (Figure 4.5B,D). Knockdown of Fgfr1/3 in a *lia* mutant background prevented otic vesicle formation (Figure 4.5C). Taken together, in the context of otic development, Fgfr1/3 transduce Fgf8-mediated signals and Fgfr2 transduces Fgf3-mediated signals.

Fgfr2 mediates Fgf3 signaling in pituitary and epibranchial development

Although most FGF signaling is partially redundant, there are some examples of the requirement of a unique FGF ligand in zebrafish organ system development. The epibranchial placodes, which form sensory neurons of the epibranchial ganglia, require Fgf3 for proper expression of neuronal markers (Nechiporuk et al., 2005). Similarly, Fgf3 signaling from the ventral diencephalon is also uniquely required for proper development of the adenohypophysis (Herzog et al., 2004).

To determine whether receptor-ligand interactions observed in the ear were present elsewhere in the embryo, we examined the effects of Fgfr knockdown on epibranchial (Figure 4.6) and pituitary development (Figure 4.7). In *lia* mutants, expression of *neuroD* in the epibranchial placodes is undetectable, consistent with previous reports (Figure 4.6C) (Nechiporuk et al., 2005). In Fgfr1, Fgfr3, and Fgfr4

morphants, *neuroD* expression was detectable in the epibranchial placodes (Figure 4.6D,F,G). *neuroD* expression could not be detected in the epibranchial placode region of Fgfr2 morphants (Figure 4.6E). Similarly, *pit1*, a marker of pituitary development, is not expressed in *lia* mutants (Figure 4.7B) (Herzog et al., 2004). Although *pit1* expression was observed in Fgfr1, Fgfr3, and Fgf4 morphants (Figure 4.7C,E), it could not be detected in Fgfr2 morphants (Figure 4.7D). Taken together, these results suggest that Fgfr2 transduces Fgf3-mediated signals in epibranchial placode and pituitary development.

Discussion

Although FGF family members have been ascribed many inductive roles throughout embryogenesis (Bottcher and Niehrs, 2005; Thisse and Thisse, 2005), their interactions with FGF receptors has not been established. Through loss of function analyses, we have attempted to elucidate FGF receptor-ligand interactions particularly as they pertain to otic development. We provide evidence that Fgfr1/2/3 are required for proper otic development. Knockdown of these three receptors prevents otic induction from occurring. Co-injection of *fgfr1/3* morpholino did not enhance the otic phenotype, suggesting that they act redundantly in transducing signals from the same ligand. Loss of Fgfr1/3 in an *fgf3* mutant background ablates otic formation, as does loss of Fgfr2 in an *fgf8* mutant background. Taken together, these results suggest that Fgfr2 transduces Fgf3-mediated signals, and that Fgfr1/3 transduces Fgf8-mediated signals. Our results are supported by the known requirements of Fgf3 in epibranchial placode and pituitary development (Herzog et al., 2004; Nechiporuk et al., 2005). As loss of Fgfr2 mimics the

phenotypes observed in *fgf3* mutants, our results suggest that our approach may be practical on a global level.

Making sense of multiple FGF signals

In most vertebrates, there are at least 20 identified members of the FGF signaling family, yet only four receptors with which to receive, transduce, and integrate these signals (Bottcher and Niehrs, 2005; Thisse and Thisse, 2005). Through work in mouse, it has become clear that multiple splice variants of each receptor exist, and these may be responsible for receiving different aspects of FGF signaling (Eswarakumar et al., 2005; Itoh and Ornitz, 2004; Itoh and Ornitz, 2008; Jiao et al., 2003; Kwiatkowski et al., 2008; Liu et al., 2007; Pirvola et al., 2000; Zhang et al., 2006). Although several FGFs have been demonstrated to bind with high affinity to a particular splice isoform (Pirvola et al., 2000), it is unclear to what extent these same ligands bind with other receptor-specific isoforms.

Our RT-PCR data also suggests that, like in mouse, zebrafish possess multiple splice isoforms of their FGF receptors. It will be interesting to determine the spatial distribution of the isoforms of each receptor. However, as most isoforms differ by less than 100 nucleotides (not shown), in situ hybridization using isoform-specific riboprobes will not be a trivial process.

Conservation of FGF Ligand-receptor interaction among vertebrates

Genome duplications that have given rise to the many members of the FGF family have also given rise to the four members of the FGFR family. It has been suggested that

the co-evolution of ligands and receptors has permitted an increase in ligand-receptor specificity between one receptor and a particular FGF subfamily (Itoh and Ornitz, 2004; Itoh and Ornitz, 2008). There are some data to suggest that ligand-receptor interactions have indeed remained conserved throughout the vertebrate species. Based on sequence homology, Fgf8/10/17/24 are grouped into the Fgf8 subfamily, so named for the founding family member (Bottcher and Niehrs, 2005; Itoh and Ornitz, 2004; Itoh and Ornitz, 2008; Thisse and Thisse, 2005). In mouse, the IIIb splice variant of Fgfr1 interacts with Fgf10 in the formation of otic epithelia (Pirvola et al., 2000). Furthermore, expression data also suggest that at least in the inner ear, FGF8 serves as a ligand for FGFR3 (Pirvola et al., 2000). Similarly in zebrafish, Fgfr1 has been implicated in transducing Fgf8-mediated signals in the development of the MHB. Knockdown of Fgfr1 mimics the MHB defects observed in embryos homozygous for a hypomorphic allele of *fgf8*.

Evidence in *Xenopus* and mouse also exist to suggest that Fgfr2-Fgf3 interactions are conserved amongst invertebrates. X*enopus* XFGF3 has been shown to have a high affinity for XFGFR2, but not XFGFR1/3/4 (Mathieu et al., 1995). Mice with null mutations in *fgfr2* form an ear that is slightly reduced in size. Although ligand-receptor interactions of mouse Fgfr2 have not been characterized, the mild otic phenotype observed is very similar to that observed in zebrafish lacking functional Fgfr2 or Fgf3, raising the possibility that mouse Fgfr2 interacts Fgf3 ligands.

Role of maternally loaded *fgfr*s in otic induction

Our analysis of *fgfr* expression have revealed that *fgfr1/2/4* are maternally loaded. It is unclear what, if any, role these maternally loaded *fgfr*s play in otic induction. By co-

culturing ectodermal tissues at successive stages with FGF ligands, embryological manipulations have demonstrated that all ectoderm is initially competent to initiate otogenesis (Noramly and Grainger, 2002). For example, in mid gastrula stage *Xenopus* embryos, all regions are equally competent to respond to FGF signals, and this competence continues through neurulation stages (Gallagher et al., 1996; Servetnick and Grainger, 1991). A possible explanation for this observation is the universal distribution of maternally-loaded *fgfr* mRNA.

Evidence from FGF signaling in chick has led to the proposal of a two-phase requirement for FGF signaling in otic placode induction. The first phase is required to establish a zone of tissue that is universally competent to respond to the second phase of signaling, which will actually specify the fate of otic cells (Martin and Groves, 2006). It is possible that maternally- and zygotically-transcribed *fgfr*s are responsible for mediating these two phases of induction. This is unlikely, however, for several reasons. First, zygotic transcription begins at the mid-blastula transition, which occurs at the 512-cell stage (Schier and Talbot, 2005). It is likely that by the stage at which FGF signaling is first required in otic induction a large proportion of transcripts present in the embryo would be zygotically-derived. Second, *fgfr3* is not maternally loaded. Yet, injection of *fgfr3* morpholino prevents expression of the earliest otic marker *pax8*, suggesting that zygotic *fgfr3* is required to mediate the earliest stages of otic induction. Together, this suggests that aspects of otic induction do not require transcripts deposited in the oocyte by the mother.

Direct and indirect roles of FGF signaling in otic induction

Recent evidence from studies examining signaling integration have revealed that FGF signaling can inhibit intracellular cascades initiated by BMP signaling. This occurs both through interference with BMP pathway members as well as transcriptional repression of BMP target genes. FGF-activated MAPK can phosphorylate intracellular proteins activated in response to BMP activity, thereby preventing their entry into the nucleus. Secondly, FGF target genes, such as *churchill,* act to repress transcription of BMP target genes.

Given the opposing relationship between FGF and BMP signaling, do the requirements of multiple phases of FGF signaling pose a requirement for BMP inhibition? There is some evidence to suggest that the initial phase of FGF signaling does act to repress BMP activity within the PPR. In the absence of FGF activity, PPR markers are not expressed. PPR induction can also be inhibited through elevation of BMP levels within the presumptive PPR, suggesting that PPR specification requires BMP activity levels to be low. Furthermore, expression of some PPR markers such as *six1* can be ectopically expressed either when Fgf8 or the BMP inhibitor Noggin is applied to the embryo. This suggests that low levels of BMP activity may be sufficient for PPR marker expression.

However, the second phase of FGF signaling is likely not required to alter BMP activity levels within pre-otic cells. Although SU5402 application during late gastrulation can block induction of the otic placode and expression of most otic markers, expression of *bmp4/7* in these cells is maintained. This raises the intriguing possibility that FGF signaling may function primarily to disrupt BMP signaling in the establishment

of the PPR, while being directly required to confer otic characteristics onto PPR cells during the second phase.

Future directions

As previously mentioned, several *fgfr*s are maternally loaded. To determine if the maternally loaded *fgfr* transcript is essential for any stage of otic development, we intend to inject splice-blocking morpholinos into embryos and assay otic induction through the expression of *pax8*. Splice-blocking morpholinos will permit the translation of maternally loaded transcript while inhibiting translation of zygotic *fgfr* transcript. If we observe normal *pax8* induction in embryos injected with *fgfr1/2/3* splice-blocking morpholinos, this may suggest that maternal transcript is sufficient for otic induction.

Second, generation of tagged FGF ligands and receptors will allow examination of physical interactions *in vivo*. Tagged ligand/receptor complexes can be purified through biochemical means to determine how these proteins interact on a global scale within the embryo.

Third, recent generation of a transgenic zebrafish line containing *fgf8* under the control of a heatshock promoter (Hans et al., 2007) will allow gain of function analyses of otic development without disrupting early roles for Fgf8 signaling in embryonic patterning. Misexpression of *fgf8* in this line of fish results in an abnormally large otic vesicle (Hans et al., 2007). Knockdown of either Fgfr1 or Fgfr3 should be able to ameliorate this phenotype; if Fgf8 interacts with either Fgfr1 or Fgfr3 we should observe a phenotype in these embryos that is similar to Fgfr1 or Fgfr3 morphants even when *fgf8* is overexpressed.

Finally, it will be interesting to determine whether a feedback loop exists between Fgf3 or Fgf8 and their potential receptors. These types of feedback loops are known to be present in *Drosophila* and mouse, where disruption of Hedgehog signaling result in an increase in the *patched* receptor. This relationship may exist in FGF signaling, and it will be interesting to determine if it is specific to receptor-ligand interactions. For example, if a similar relationship exists in FGF signaling as in Hedgehog signaling, one may expect *fgfr1/3* expression to be increased in *x15* mutants and *fgfr2* expression increased in *lia* mutants. This may provide more evidence to support the receptor-ligand interactions previously proposed.

Figure 4.1: *fgfr* expression during otic development

Expression patterns of *fgfr1* (A,E,I), *fgfr2* (B,F,J), *fgfr3* (C,G,K) and *fgfr4* (D,H,L) at bud stage (A-D), 6-somites (E-H), and 18-somites (I-L). (A-H) *dlx3b* expression (red) defines the PPR in (A-D) and otic placode in (E-H). (M) RT-PCR performed on total RNA extracted from 128-cell embryos using primers specific to *fgfr1-4* transcripts reveal the presence of *fgfr1/2/4* mRNA. *oep* served as a positive control. (A-L) All views are dorsal, with anterior to the top. Arrows in (E-H) and arrowheads in (I-L) indicate the position of otic cells. Insets in (E-H) are high magnification views of the otic placode.

Figure 4.1

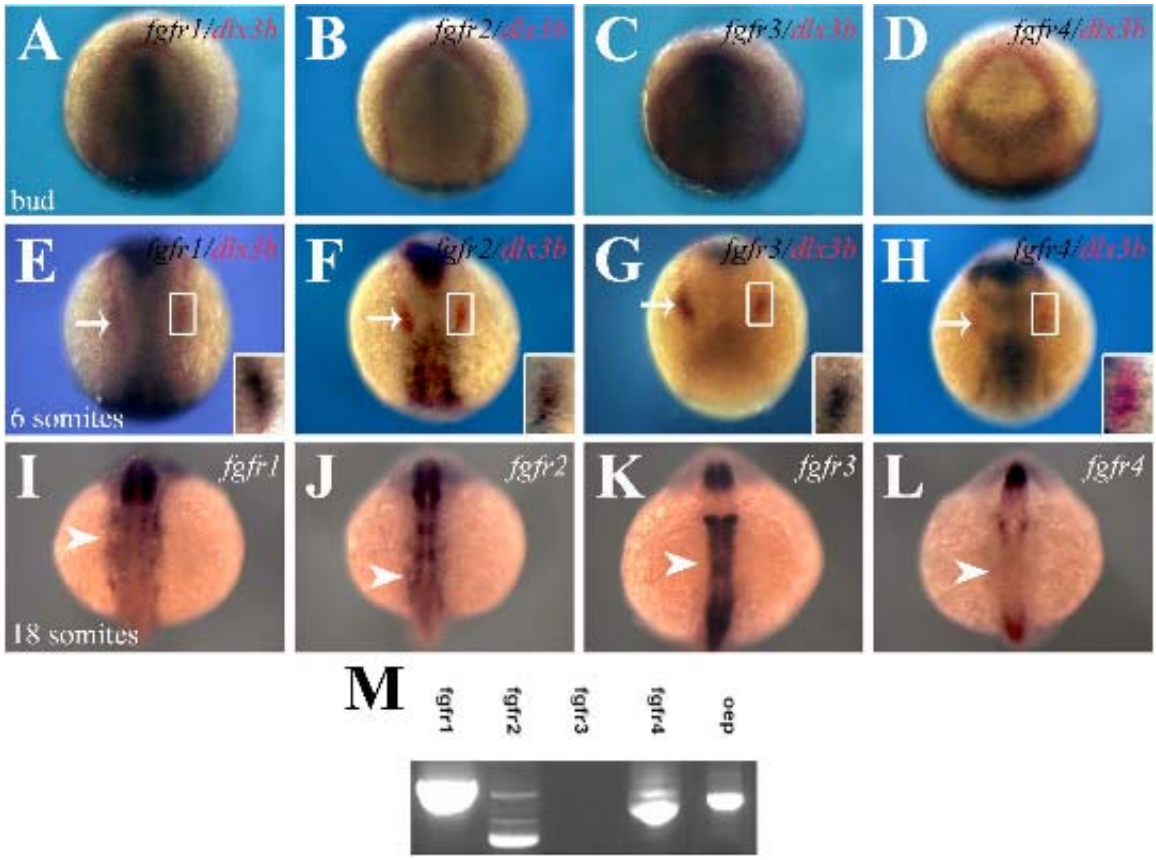
A
fgfr1/dlx3b
bud
B
fgfr2/dlx3b
C
fgfr3/dlx3b
D
fgfr4/dlx3b
E
fgfr1/dlx3b
6 somites
F
fgfr2/dlx3b
G
fgfr3/dlx3b
H
fgfr4/dlx3b
I
fgfr1
18 somites
J
fgfr2
K
fgfr3
L
fgfr4
M
fgfr1
fgfr2
fgfr3
fgfr4
oep

Figure 4.2: The requirements of *fgfr*s for *pax8* expression

pax8 expression in bud stage *x15* (B), *lia* (C), Fgfr1 morphants (D), Fgfr2 morphants (E), Fgfr3 morphants (F), Fgfr1/3 morphants (G), and Fgfr1/2/3 morphants (H). All views are dorsal, with anterior to the top.

Figure 4.2

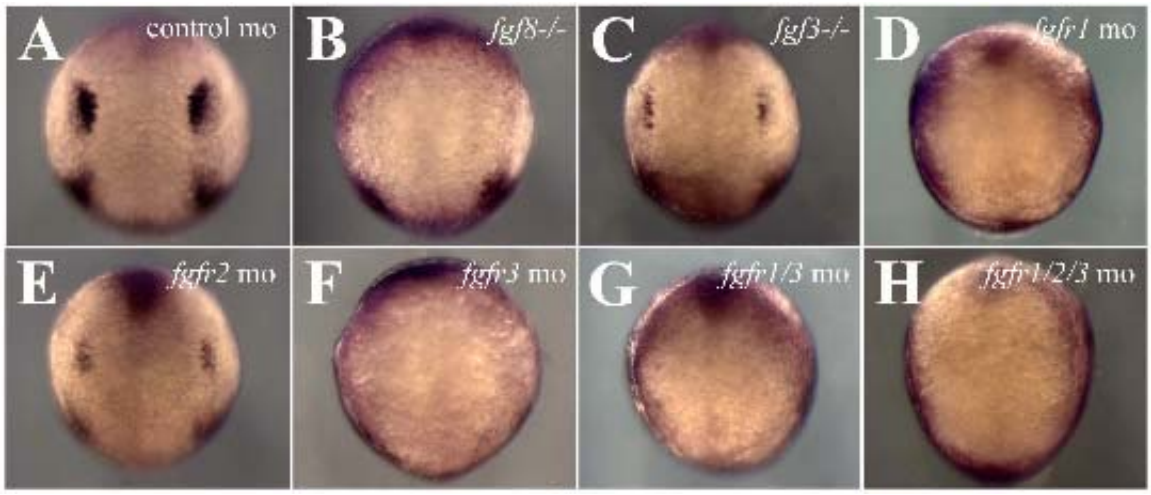
A
control mo
B
fgf8-/-
C
fgf3-/-
D
fgfr1 mo
E
fgfr2 mo
F
fgfr3 mo
G
fgfr1/3 mo
H
fgfr1/2/3 mo

Figure 4.3: Otic vesicle formation in Fgfr morphants

In 30hpf embryos (A), the ear can be visualized as an oval shaped otic vesicle containing two otoliths. (B,D,F,H) In *x15* mutants (B), Fgfr1 (D), Fgfr3 (F), and Fgfr1/3 (H) morphants, a circular otic vesicle forms that lacks otoliths. (C,E) In *lia* mutants (C) and Fgfr2 morphants (E), the otic vesicle is slightly smaller than in wild-type embryos. (G) Knockdown of Fgfr4 has no effect on otic morphology. (I) The otic vesicle is undetectable in Fgfr1/2/3 morphants. All views are lateral with anterior to the left.

Figure 4.3

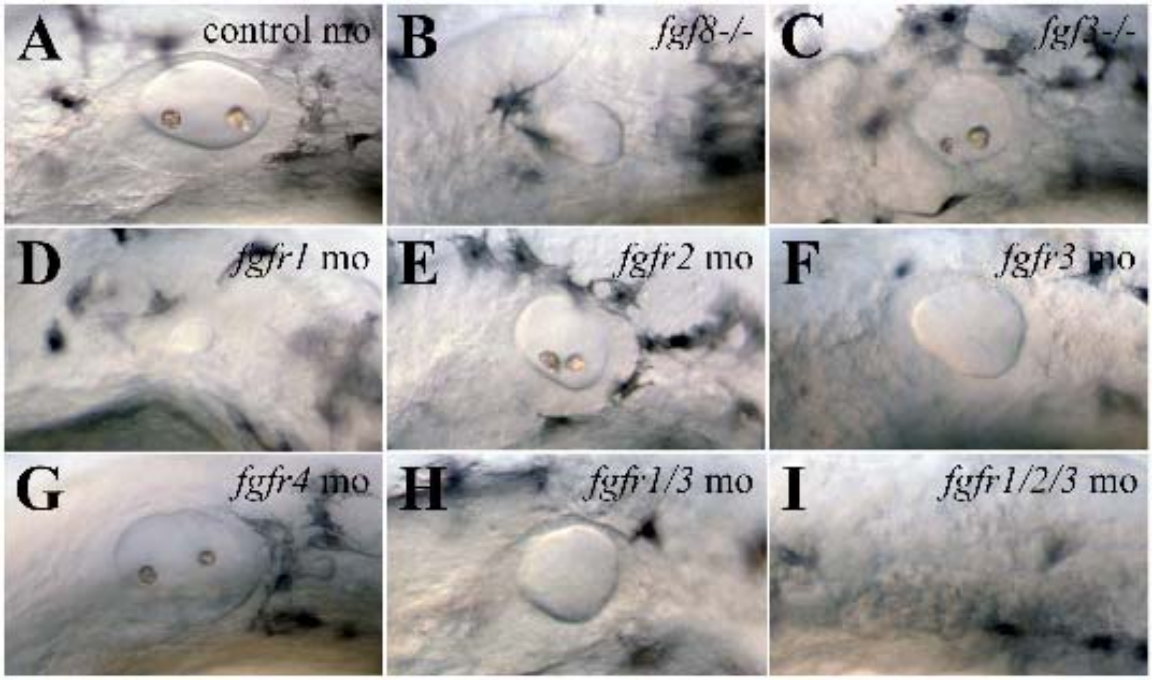
A
control mo
B
fgf8-/-
C
fgf3-/-
D
fgfr1 mo
E
fgfr2 mo
F
fgfr3 mo
G
fgfr4 mo
H
fgfr1/3 mo
I
fgfr1/2/3 mo

Figure 4.4: Interactions between Fgf8 and Fgfr1-3

(B,D) The otic phenotype observed when Fgfr1/3 are knocked down in an *x15* background (D) is not more severe than *x15* mutants (B) alone. (C) Knockdown of Fgfr2 in an *x15* mutant background ablates otic vesicle formation. All views are lateral, with anterior to the left.

Figure 4.4

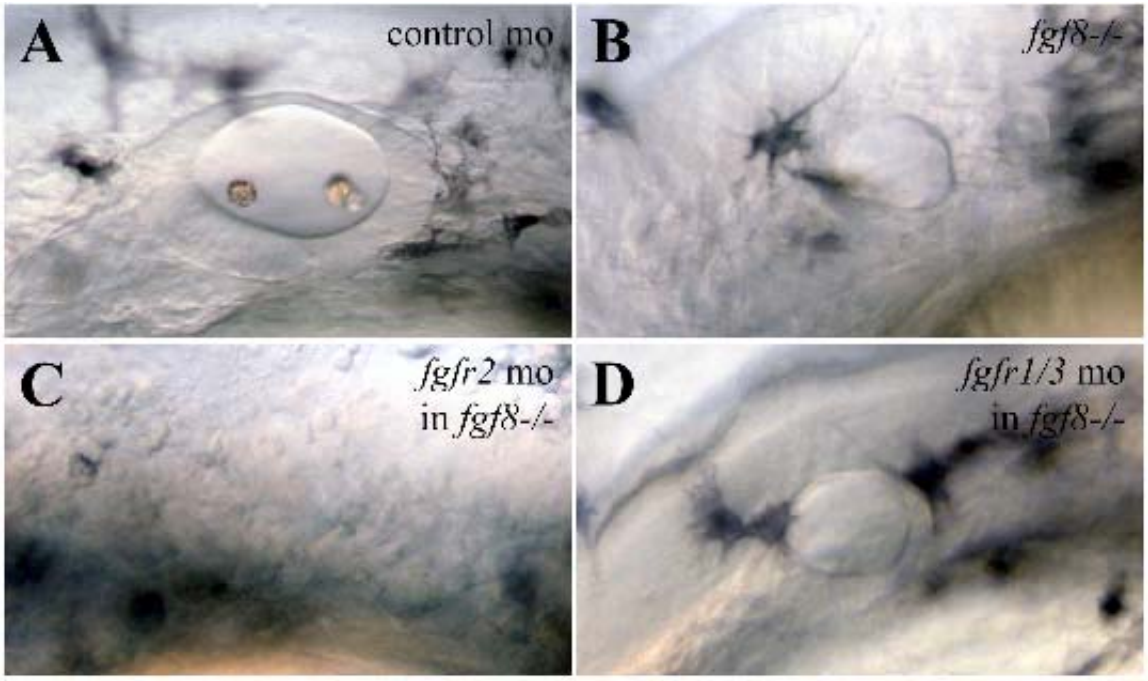

Figure 4.5: Interactions between Fgf3 and Fgfr1-3

(B,D) The otic phenotype observed when Fgfr2 is knocked down in an *lia* background (D) is not more severe than *lia* mutants (B) alone. (C) Knockdown of Fgfr1/3 in an *lia* mutant background ablates otic vesicle formation. All views are lateral, with anterior to the left.

Figure 4.5

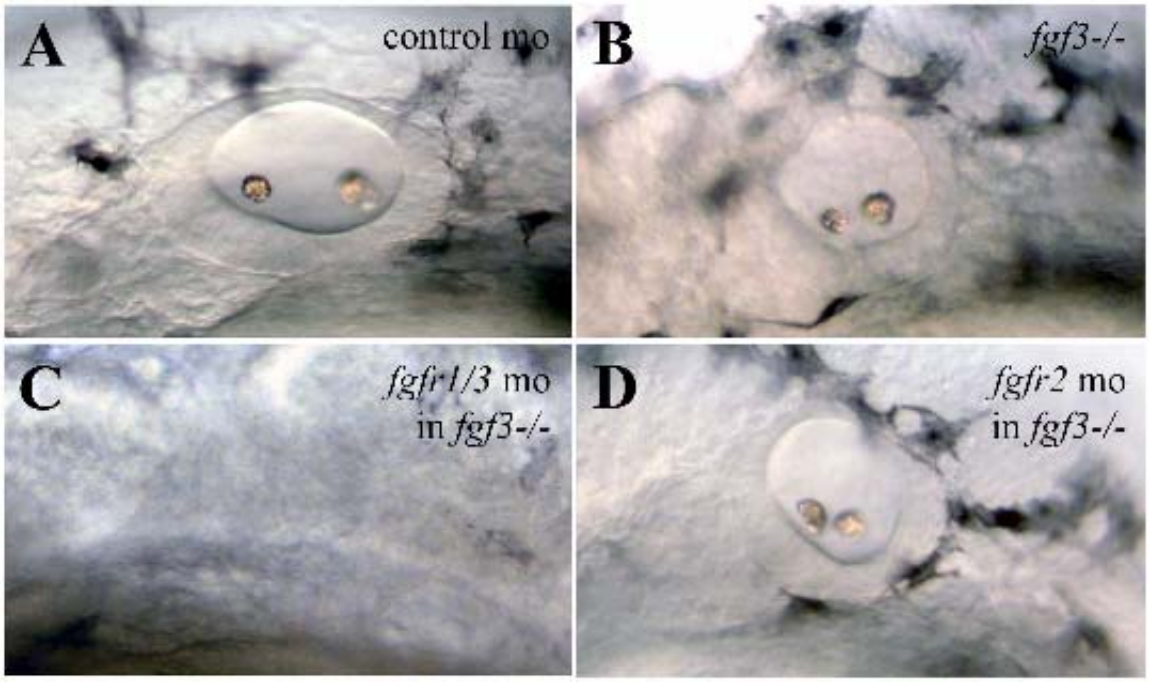

Figure 4.6: Fgfr2 mediates Fgf3 signaling in epibranchial placode development

(A,B,D,F,G) *neuroD* expression at 24hpf reveals that epibranchial placode development is unaffected in *x15* mutants (B) as well as Fgfr1, (D) Fgfr3 (F), and Fgfr4 (G) morphants. (C,E) *neuroD* expression is lost from the epibranchial placode of *lia* mutants (C) and in Fgfr2 morphants (E). All views are lateral views, with anterior to the left.

Figure 4.6

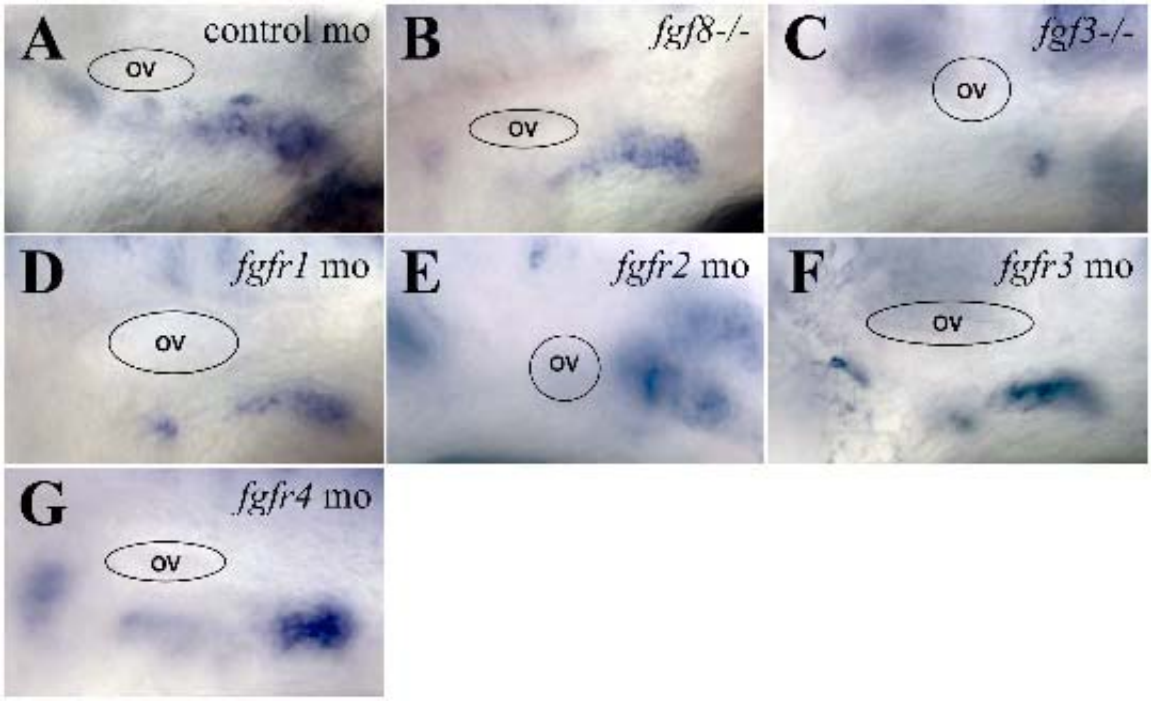
A
control mo
ov
B
fgf8-/-
ov
C
fgf3-/-
ov
D
fgfr1 mo
ov
E
fgfr2 mo
ov
F
fgfr3 mo
ov
G
fgfr4 mo
ov

Figure 4.7: Fgfr2 mediates Fgf3 signaling in pituitary development

(A,C,E) *pit1* expression at 30hpf reveals that pituitary development is unaffected in Fgfr1/3 (C) and Fgfr4 (E) morphants. (B,D) *pit1* expression is lost from the pituitary of *lia* mutants (B) and in Fgfr2 morphants (D). All views are lateral views, with anterior to the left.

Figure 4.7

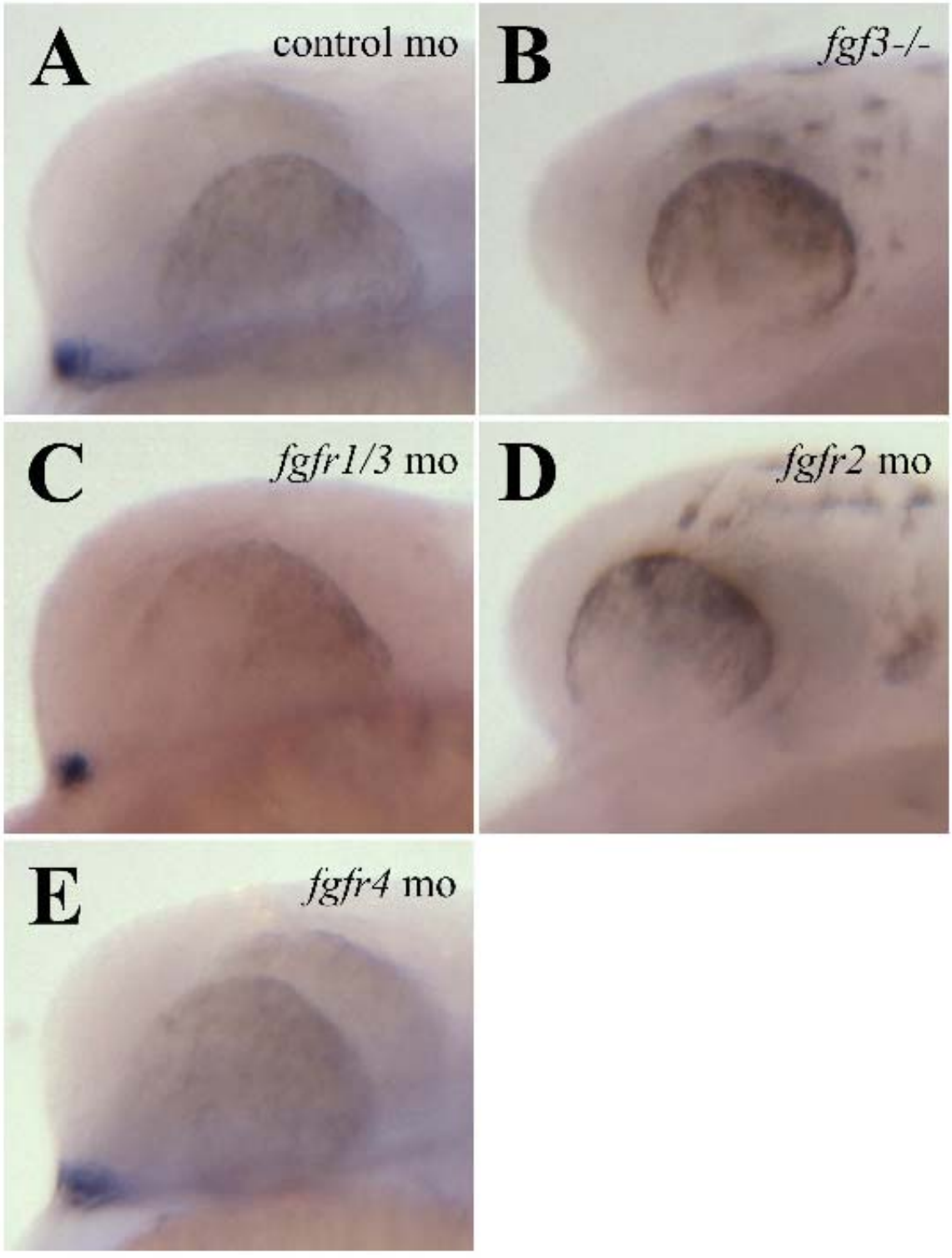

CHAPTER 5

Characterization of *tbx2a/b* reveals a novel pathway in otic induction

(Esterberg, R.[1], Setty, S.[1], Snelson, C.[2], Wuennenberg-Stapleton, K.[3], Ngai, J.[3], Gamse, J.[2], and Fritz, A.[1], in preparation)

[1]Department of Biology, Emory University, Atlanta, GA
[2] Department of Biological Sciences, Vanderbilt University, Nashville, TN
[3] Department of Molecular and Cell Biology, Helen Wills Neuroscience Institute, University of California, Berkeley, CA

The vertebrate inner ear is a complex sensory structure responsible for the detection of sound, gravity, and acceleration. Comprised of a series of communicating chambers and multiple cell types, it is complex in both structure and function. This complexity arises from a simple thickening of epithelium, the otic placode, which lies adjacent to the neural plate. The otic placode undergoes complex morphological rearrangements to form the otic vesicle, which will eventually give rise to the inner ear (Ohyama et al., 2007; Schneider-Maunoury and Pujades, 2007). Well before the otic placode is morphologically distinct, signaling events emanating from neural as well as non-neural ectoderm act to induce and pattern otic cell fate. These events act to make otic precursor cells distinct from other cells in the region.

Classical embryological manipulations as well as recent molecular techniques have provided evidence that otic induction requires multiple inductive events (Ohyama et al., 2007; Schlosser, 2006; Streit, 2007). Evidence from FGF signaling in chick has led to the proposal of a multi-stage model for FGF signaling in otic induction (Martin and Groves, 2006). The first phase establishes a zone of tissue that is common to all cranial sensory organs. Cells possessing this identity occupy the preplacodal region (PPR) and are initially capable of contributing to all cranial sensory organs (Ahrens and Schlosser, 2005; Bailey et al., 2006; Bhattacharyya et al., 2004; Jacobson, 1963; Kozlowski et al., 1997; Noramly and Grainger, 2002). Following PPR specification, inductive events gradually refine cell fate so that individual sensory placodes are specified. In response to these inductive events, expression of cell-intrinsic factors are initiated that act redundantly in a combinatorial manner to specify placodal fate. For example, members of the *Fox*, *Pax*, and *Sox* families share overlapping patterns of expression within the

presumptive otic domain (Chiang et al., 2001; Krauss et al., 1991b; Ohyama and Groves, 2004; Pohl et al., 2002; Solomon et al., 2003; Spokony et al., 2002). In zebrafish, inactivation of any of these genes does not inhibit otic induction although later otic development is abnormal (Hans et al., 2004; Mackereth et al., 2005; Nissen et al., 2003; Solomon et al., 2003; Yan et al., 2005).

foxi1 is one such gene in zebrafish that is critical in assigning otic fate to PPR cells (Nissen et al., 2003; Solomon et al., 2003). *foxi1* is first expressed during mid to late gastrulation within the PPR. Subsets of *foxi1*-expressing cells begin to express *pax8*, the earliest marker of otic induction, during late gastrulation. Foxi1 appears critical in integrating FGF signaling in this process; ectopic *foxi1* can induce ectopic *pax8* expression, but only when FGF signaling is not disrupted (Solomon et al., 2003; Solomon et al., 2004). In addition, loss of Foxi1 delays otic expression of FGF target genes *pax2a* and *sox9a*, and the resulting otic vesicle is reduced in size and often lacks otoliths (Solomon et al., 2003; Solomon et al., 2004). Although sufficient for *pax8* induction, Foxi1 cannot induce these other otic markers or the formation of ectopic otic vesicles. The mechanism by which Foxi1 mediates otic induction is currently unknown.

We have performed a microarray screen in an attempt to identify transcriptional targets of Foxi1. From this screen, we have identified two *tbx2* paralogues, *tbx2a/b*, that are differentially regulated by Foxi1. As little is known about the role of *Tbx* family members in otic placode induction (Schlosser, 2006), we have attempted to characterize the roles of *tbx2a/b* in this process. Through loss of function analyses, we find that *tbx2a/b* lie upstream of *pax8* and *fgf24* in pre-otic cells. Proper Tbx2a/b function is required in otic induction, as loss of either Tbx2a or Tbx2b results in an otic vesicle that

is reduced in size with misshapen otoliths. Loss of both Tbx2a/b results in otic tissue that expresses only rudimentary levels of otic markers, where otic vesicles do not form.

Materials and Methods

Animals

Wild-type (AB) mutant zebrafish were obtained from the Zebrafish International Resource Center (Eugene, OR). Embryos were maintained at 28.5°C and staged using standard criteria (Kimmel et al., 1995). *Tg(CM-isl1:GFP)*^{rw0} (Higashijima et al., 2000) and *Tg(foxd3:GFP)*^{fkg17}; *fby* (Snelson et al., 2008) zebrafish lines were obtained from the Gamse lab (Vanderbilt University, Nashville). The *from beyond* (*fby*) mutation is a putative null allele of *tbx2b* (Snelson et al., 2008). *fby* mutant embryos were identified as previously described (Snelson et al., 2008).

Microarray analysis

Embryos injected with control and *foxi1* morpholinos were homogenized at the 1-3 somite stage in Trizol (Invitrogen). Injections and RNA isolations were prepared in triplicate. One hundred embryos were used for each RNA preparation. RNA samples were used to prepare cDNA that was hybridized to a zebrafish gene chip, generated by Drs. K. Wuennenberg-Stapleton and J. Ngai (University of California, Berkeley). Three independent hybridizations were performed. Spot (CSIRO Mathematical and Information Sciences; North Ryde, Australia) was used for data extraction, and the data

were normalized with print tip and Lowess normalization. Gene expression data was analyzed on a $\log_2$ scale.

Real-time quantitative RT-PCR

RNA was isolated from three sets of 20 embryos of each experimental sample using the RNeasy kit (Qiagen). The SYBR Green I (Roche Applied Science) RNA amplification kit was used on the LightCycler according to the manufacturer's instructions and published protocols (Rajeevan et al., 2001). The primers used for each of the genes were: *tbx2a* 5'- GATGGCTTTTCTCCTCTGATGGTT -3' and 5'- TTGCCCGGGGTGAAATAAGAGTGA -3'; *tbx2b* 5'- GGCGAACAGGAATCCCCAAATC -3' and 5'- AAGGCGAGAGCAGACAGCGGTAGG -3'; *ef1α* 5'- GTACTACTCTTCTTATGCCC -3' and 5'- GTACAGTTCCAATACCTCCA -3'. The different samples were standardized using EF-1α transcript levels as a reference. Each experimental run was also performed in triplicate. Transcript levels were compared by one-way ANOVA, followed by a two-tailed, equal variance *t*-test.

In situ hybridization

The following probes were used: *dlx3b* (Ekker et al., 1992), *follistatin* (Mowbray et al., 2001), *foxi1* (Solomon et al., 2003), *hnf1b* (Lecaudey et al., 2004), *krox20* (Oxtoby and Jowett, 1993), *omp* (Murayama et al., 2005), *otolin* (Murayama et al., 2005), *pax2a* (Krauss et al., 1991a), *pax8* (Krauss et al., 1991a), *tbx2a* (Ribeiro et al., 2007), and *tbx2b* (Dheen et al., 1999).

Morpholino injection

Translation blocking morpholinos against *tbx2a/b* are as follows: *tbx2a* 5'-CGCTGTGAAAACTGGATCTCTCATC -3'; *tbx2b* 5'-GAGGTGTTCTCTGGCTAAAAAGGAG -3'.Morpholino injections against *dlx3b/4b* (Solomon and Fritz, 2002), *fgf24* (Fischer et al., 2003), *foxi1* (Solomon et al., 2003), and *mib* (Itoh et al., 2003) have been previously characterized. The control morpholino sequence was 5'-CCTCTTACCTCAGTTACAATTTATA -3'. For interaction analyses, *foxi1* and *dlx3b* mo concentration was chosen that elicited a mild otic phenotype, approximately 5ng.

Antibody staining

Labeling with 3A10, which detects the Mauthner neuron, was as previously described (Lorent et al., 2001).

Results

Identification of *tbx2a/b* as potential targets of Foxi1

We performed a microarray analysis to identify potential transcriptional targets of Foxi1, comparing total mRNA from 1-3 somite control embryos was compared to total mRNA isolated from embryos injected with *foxi1* morpholino. Our data suggested that the transcripts of two *tbx2* genes, *tbx2a/b*, were differentially regulated in the absence of Foxi1. In Foxi1 morphants, *tbx2a* transcript was found to be downregulated by approximately 30%, while *tbx2b* transcript was upregulated by approximately 50%

(Table 5.1). These results were confirmed by quantitative RT-PCR (not shown). We further attempted to verify our results through in situ hybridization (Figure 5.1). Consistent with our previous data, we observed fewer cells expressing *tbx2a* in the otic domain of embryos homozygous for a null allele of *foxi1* (*hearsay, hsy;* Solomon et al., 2003) although we were unable to detect upregulation of *tbx2b* expression in mutant embryos (Figure 5.1A-H). To determine whether a reciprocal interaction existed between *tbx2a/b* and *foxi1*, we injected embryos with translation-blocking morpholinos against *tbx2a/b*. Although loss of functional Tbx2a/b led to otic phenotypes that will be discussed in detail further, *foxi1* expression was unaffected in these embryos (Figure 5.1I-L). These results suggest that Foxi1 is required for proper expression of *tbx2a/b*, and that a reciprocal regulation of *foxi1* by Tbx2a/b does not exist.

tbx2a/b **expression**

Members of the *Tbx2* subfamily, including *tbx2*, are expressed in the otic placode of *Xenopus*, zebrafish, chick, and mouse during early somitogenesis (Dheen et al., 1999; Gibson-Brown et al., 1998; Harrelson and Papaioannou, 2006; Ribeiro et al., 2007; Takabatake et al., 2000), suggesting a role in mediating otic fate specification. Although *tbx2a/b* expression has been reported elsewhere, expression patterns in the context of sensory placode induction have not been examined. While both genes share largely overlapping expression patterns following gastrulation, *tbx2a* expression is initiated much earlier than *tbx2b*. *tbx2a* is first detectable during early gastrulation (Figure 5.2A,B). As gastrulation proceeds, expression is progressively restricted to the dorsal side of the embryo with enrichments observed in the otic placode and notochord (Figure 5.2C).

Unlike *tbx2a*, *tbx2b* expression is first detectable during mid to late gastrulation in the otic placode, midbrain-hindbrain boundary (MHB), and notochord (Figure 5.2I). During early somitogenesis, both *tbx2a/b* are expressed in the lens and otic placodes (Figure 5.2D,J). *tbx2a* expression was also detected in the MHB and cardiac precursors, while *tbx2b* expression was additionally detected in the pineal organ and olfactory placode. *tbx2a/b* expression was detected in the otic vesicle and retina through at least 3dpf (Figure 5.2E,F,K,L).

Tbx2a/b are required for proper otic development

To ascertain the role of *tbx2a/b* in otic development, we obtained translation-blocking morpholinos against *tbx2a* and *tbx2b*, as well as a zebrafish line carrying a putative null allele of *tbx2b* (*from beyond*; *fby*). Loss of either Tbx2a or Tbx2b resulted in visible otic defects (Figure 5.3). Instead of an oval-shaped otic vesicle containing two otoliths that was observed in 30hpf controls (Figure 5.3A), Tbx2a morphants developed a circular otic vesicle that contained one irregular-shaped otolith (Figure 5.3B). The otic phenotype observed in *fby* mutants was slightly less severe than Tbx2a morphants; both otoliths formed, but they were also irregular in shape (Figure 5.3C). By 3dpf, otolith defects observed in Tbx morphants were no longer apparent, although the otic vesicle remained improperly patterned. The semicircular canals of embryos lacking either Tbx2a or Tbx2b were fused and disorganized (Figure 5.3H,I). A synergism was observed when *tbx2a* morpholino was injected into *fby* mutants such that otic vesicles failed to form (Figure 5.3D). These results suggest that *tbx2a/b* play partially redundant roles in otic development.

Because we identified both *Tbx*2 genes in our screen as potential transcriptional targets of Foxi1, we wished to determine how the combined loss of either Tbx2a or Tbx2b and Foxi1 affected otic development. Loss of either Tbx2a or Tbx2b in a Foxi1-deficient background increased the severity of the otic defects observed in single Tbx2 loss of function embryos (Figure 5.3E,F). Taken together, t*bx2a/b* likely act in a pathway parallel to *foxi1* in otic development.

tbx2a/b* lie upstream of *pax8

As both *tbx2a/b* expression appear to precede that of the earliest known otic marker *pax8* (Krauss et al., 1991b), we wished to examine the effects of *tbx2a/b* inactivation on otic induction (Figure 5.4). Loss of either Tbx2a or Tbx2b was sufficient to inhibit *pax8* expression in the otic domain of bud stage (Figure 5.4A-C) or 6-somite (Figure 5.4D-F) embryos, while expression in the midbrain-hindbrain boundary remained intact (Figure 5.4D-F). Conversely, knockdown of Pax8 had no effect on *tbx2a/b* expression (Figure 5.4G-J). To explore the relationship between *tbx2a/b* and *pax8*, we co-injected *tbx2a* or *tbx2b* and *pax8* morpholinos and examined the resulting otic phenotype. Pax8 morphants develop an otic vesicle that is slightly smaller in size that contains two otoliths (Figure 5.4K). The otic phenotype observed in Tbx2a/Pax8 and Tbx2b/Pax8 double morphants resembled that of Tbx2a and Tbx2b single morphants, respectively (Figure 5.4L,M). Taken together, these results suggest that *tbx2a/b* lie upstream of *pax8*.

tbx2a/b* act in a pathway parallel to *dlx3b/4b

In addition to *foxi1*, members of the *Dlx* family of transcription factors have also been implicated in mediating early phases of otic induction (Ohyama et al., 2007; Schlosser, 2006; Streit, 2007). In zebrafish, *dlx3b/4b* play partially redundant roles in this process; knockdown of both proteins severely disrupts otic vesicle formation (Liu et al., 2003; Solomon and Fritz, 2002). In Dlx3b/4b morphants, we observed no change in *tbx2a/b* expression when compared to controls (Figure 5.5A-D). To determine whether *tbx2a/b* genetically interact with *dlx3b/4b*, we inactivated Dlx3b in concert with either Tbx2a or Tbx2b. Consistent with previous reports, knockdown of Dlx3b results in a slightly smaller otic vesicle that contains only one otolith (Figure 5.5E) (Solomon and Fritz, 2002). Knockdown of Tbx2a and Dlx3b severely enhanced the severity of the Dlx3b morphant phenotype, completely ablating otic formation (Figure 5.5F). Tbx2b/Dlx3b morphants formed an otic vesicle that was much smaller than Dlx3b morphants and lacked both otoliths (Figure 5.5G). These results suggest that *dlx3b/4b* and *tbx2a/b* act in parallel pathways during otic development.

The requirement of Tbx2a/b in otic gene regulation

As we observed a requirement of Tbx2a/b for *pax8* expression in pre-otic cells as well as proper otic vesicle morphology, we wished determine how loss of Tbx2a/b affect the expression of other genes involved in otic development (Figure 5.6). Some genes expressed in the otic placode, such as *claudin a* (*cldna*) and *fgf24*, were severely affected by the loss of Tbx2a/b. While fewer cells expressed *cldna* and *fgf24* when either Tbx2a or Tbx2b was knocked down, expression was completely lost from the otic domain when Tbx2a/b were knocked down in concert (Figure 5.6A-H). Other otic markers were not as

severely affected by loss of Tbx2a/b. For example, *pax2a* and *sox9a* were down-regulated in pre-otic cells to a greater extent in Tbx2a morphants than in Tbx2b morphants (Figure 5.6J,K,N,O). When Tbx2a/b were knocked down in concert, fewer cells expressed *pax2a* and *sox9a* in the otic domain than in single morphants (Figure 5.6L,P). These results suggest that *tbx2a/b* act redundantly to promote the expression of some otic markers, such as *cldna* and *fgf24*, but are not necessary for the expression of all otic genes.

Tbx2a/b specify anterior and lateral domains of the otic vesicle

Although the otic placode is initially comprised of cells possessing uniform identity, signals from adjacent tissues promote asymmetries along anteroposterior (AP), dorsoventral (DV), and mediolateral (ML) axes as development proceeds (Schneider-Maunoury and Pujades, 2007). These signaling events promote the sub-functionalization of sensory apparatuses within the ear. To determine whether Tbx2a/b are required for specification of any of these sub-domains, we analyzed expression of genes expressed in regional domains of the otic vesicle (Figure 5.7). Markers of the lateral otic vesicle, such as *omp* and *otolin* (Murayama et al., 2005), were reduced in both Tbx2a and Tbx2b morphants (Figure 5.7A-F). Similarly, expression of the anterior otic marker *pax5* (Krauss et al., 1991b) was reduced in both Tbx2a and Tbx2b morphants (Figure 5.7G-I). Expression of posterior markers such as *follistatin* (*fst*) (Mowbray et al., 2001) was unchanged in either Tbx2a or Tbx2b morphants when compared to controls (Figure 5.7J-L). Taken together, these results suggest that Tbx2a/b are required to promote anterior and lateral domains of the otic vesicle.

Tbx2a/b regulation of *fgf24* is critical in specification of some hindbrain neurons

Several FGF ligands, including *fgf24*, are expressed in the otic placode during early to mid somitogenesis (Draper et al., 2003; Schimmang, 2007), raising the possibility that the otic placode acts as a signaling center that exerts its effects on the hindbrain. In Tbx2a/b morphants, we observed that the domain of hindbrain interneurons labeled by *pax2a* was absent (Figure 5.8B). As *fgf24* expression requires Tbx2a/b, we wished to determine whether the neural defects observed in Tbx2a/b morphants was due to an absence of Fgf24 signaling from the otic placode. In Fgf24 morphants, the domain of hindbrain interneurons labeled by *pax2a* was absent, resembling the phenotype observed in Tbx2a/b morphants (Figure 5.8C). To ensure that loss of either Tbx2a/b or Fgf24 did not affect rhombomere identity, we labeled Tbx2a/b and Fgf24 morphants with riboprobes against *krox20* and *hnf1*. The expression of *krox20*, which labels rhombomeres 3 and 5 (Oxtoby and Jowett, 1993), and the expression of *hnf1*, which labels rhombomeres 5, 7, and 8 (Lecaudey et al., 2004), respectively, was comparable to controls (Figure 5.8A-C). In an attempt to further characterize the neuron defects observed in these embryos, we injected *tbx2a/b* and *fgf24* morpholinos into the *isl1*:GFP transgenic line of zebrafish, which express GFP in motor neurons (Higashijima et al., 2000). In both Tbx2a/b and Fgf24 morphants, the nucleus of the medial longitudinal fasiculus was disorganized, and motor neurons along the hindbrain did not extend to the posterior hindbrain as they did in controls (Figure 5.8G-I). Additionally, the Mauthner neuron, labeled by the 3A10 monoclonal antibody (Lorent et al., 2001), did not form in

36hpf Tbx2a/b or Fgf24 morphants (Figure 5.8J-L). To confirm that Tbx2a/b and Fgf24 are required for Mauthner cell specification, we co-injected the *mind bomb* (*mib*) morpholino with *tbx2a/b* or *fgf24* morpholinos. In embryos lacking Mib, a component of the E3 ubiquitin ligase, ectopic Mauthner neurons form (Figure 5.8M) (Chen and Casey Corliss, 2004; Itoh et al., 2003; Koo et al., 2005a; Koo et al., 2005b). When *tbx2a/b* or *fgf24* morpholinos were co-injected with the *mib* morpholino, no Mauthner neurons were observed (Figure 5.8N,O). Taken together, these results suggest that Tbx2a/b-mediated regulation of Fgf24 signaling from the otic placode is critical in neural development.

Discussion

Here we have begun to analyze the role of two *tbx2* paralogues in otic induction. Tbx2a/b act redundantly in otic development, and interaction analyses suggest that they occupy a novel third genetic pathway in otic induction. Through loss of function studies, we demonstrate that *tbx2a/b* lie upstream of *pax8* and *fgf24*. By examining neural patterning in embryos lacking Tbx2a/b and Fgf24, we have revealed a novel role of the otic placode as a signaling center in hindbrain neurogenesis.

Three parallel pathways in otic development

The zebrafish otic placode is known to require input from genetic pathways that exert their functions during different phases of otic development (Ohyama et al., 2007). The earliest known pathway acts during mid to late gastrulation, and is initiated by *foxi1* (Hans et al., 2007; Liu et al., 2003; Solomon et al., 2003; Solomon et al., 2004). The combination of FGF signaling and Foxi1 are required for the expression of the earliest

marker of otic induction, *pax8*. Ectopic *foxi1* can induce ectopic *pax8* expression, but only in the presence of FGF activity (Solomon et al., 2003; Solomon et al., 2004). In the absence of functional Foxi1, *pax8* is not expressed, and the expression of other otic markers is significantly delayed.

In addition to *foxi1*, *dlx3b/4b* also initiate a genetic cascade required for proper otic development. *dlx3b/4b* appear to act slightly later than *foxi1*, as loss of Dlx3b/4b does not affect *pax8*, but does disrupt expression of the FGF target gene *pax2a*, which is first expressed in the otic placode after the initiation of *pax8* expression (Liu et al., 2003; Solomon and Fritz, 2002; Solomon et al., 2004). As with Foxi1, loss of Dlx3b/4b delays otic gene expression. Inactivation of both pathways is capable of inhibiting otic formation, raising the possibility that these transcription factors may act as master regulators of otic fate. However, ectopic expression of either *foxi1* or *dlx3b* cannot induce ectopic otic vesicles or the full range of otic markers, suggesting that contribution of other unidentified intrinsic factors are required to act cooperatively with Foxi1 and Dlx3b/4b in the initiation of otic development.

Our preliminary results suggest that *tbx2a/b* may act in an otic determination pathway parallel to the ones specified by *foxi1* and *dlx3b/4b*. This pathway likely acts during a phase of otic induction similar to *foxi1*, as indicated by the requirement of Tbx2a/b in *pax8* expression. As the otic markers *pax2a* and *sox9a* are still expressed in Tbx2a/b morphants, *tbx2a/b* are unlikely to play roles as master regulators of otic fate. Further investigation is required to determine the extent of integration between the otic pathways specified by *foxi1* and *tbx2a/b*.

The positive regulation of otic development has largely been a function that has been assigned to FGF signaling. Recent evidence from chick and mouse has begun to suggest that other signaling molecules play a role in augmenting the size of the otic placode. For example, WNT signaling plays an important role in specifying the size of the otic placode following otic induction (Freter et al., 2008; Jayasena et al., 2008; Ohyama et al., 2006). Inactivation of WNT signaling in a subset of otic cells through the conditional deletion of ß-catenin leads to a reduction in the size of the otic placode and increase in cranial epidermis. Conversely, over activation of ß-catenin in the otic domain expands the otic placode at the expense of cranial epidermis (Ohyama et al., 2006). To date, it is unclear how competence to respond to WNT signaling is mediated within otic cells.

Mammary placode induction as a model for Tbx2a/b function

The role of Tbx3, a Tbx2 subfamily member, in mammary placode induction may provide valuable insights into the role of Tbx2a/b in WNT regulation during otic induction. Like in otic development, specification of the mammary domain initially requires FGF signaling and *Tbx* genes (Eblaghie et al., 2004; Howard and Ashworth, 2006). Application of ectopic Fgf8 in mouse can expand expression of both *Tbx3* and the WNT target gene *Lef1* (Eblaghie et al., 2004). In mammary development, integration of FGF signaling and Tbx3 appear to induce WNT activity in mammary cells. This is required for further mammary development; mammary placodes are induced in mice carrying null mutations of WNT target genes, but development stalls and differentiation of mammary tissue does not occur (Andl et al., 2002; Boras-Granic et al., 2006). These

data raises the possibility that Tbx2a/b act in a similar manner during otic development to integrate and balance the input of FGF signaling with the output of WNT signaling.

The otic phenotypes observed when Tbx2a/b are lost are consistent with the integration of FGF and WNT response mechanisms. For example, loss of Tbx2a/b ablates expression of the FGF target gene *pax8,* while also reducing the size of the otic vesicle as has been observed in WNT-deficient mice. Alternatively, the effects of Tbx2a/b inactivation may be due to inability of otic cells to respond to FGF signaling. Potential integration of FGF and WNT signaling by Tbx2a/b remain to be resolved.

The otic placode is a signaling center involved in hindbrain neurogenesis

Tissues surrounding the inner ear, such as the hindbrain, mesoderm, and endoderm, have been implicated as signaling sources required for otic development (Schneider-Maunoury and Pujades, 2007). The role of the hindbrain has been revealed by analyzing mutants that affect hindbrain segmentation, including *hnf1*, *hoxa1*, and *mafB* (Dolle et al., 1993; Eichmann et al., 1997; Giudicelli et al., 2003; Helmbacher et al., 1998; Lecaudey et al., 2007; McKay et al., 1994; Moens et al., 1998; Prince et al., 1998; Sadl et al., 2003; Sun and Hopkins, 2001). As these genes are not expressed in the otic vesicle, it is likely that their effects on hindbrain patterning influence secreted molecules that emanate from this tissue. For example, *fgf3* is expressed in rhombomere 4 of zebrafish, and the expansion of this domain in *mafB* (*valentino*) mutants results in an anterior expansion of the otic domain as well as the formation of ectopic sensory neurons (Moens et al., 1998; Prince et al., 1998).

A number of secreted molecules, including members of the FGF and BMP families, are expressed in otic cells during embryogenesis (Mowbray et al., 2001; Schimmang, 2007). In addition to their inferred roles in otic patterning, these molecules likely exert influences on surrounding tissue in the hindbrain. We have demonstrated a previously uncharacterized role of the otic placode as a signaling center that is required for proper specification of some hindbrain neurons. Our preliminary analysis of the hindbrain in Tbx2a/b and Fgf24 morphants has indicated that Fgf24 signaling from the otic placode is required for specification of Mauthner neurons. The Mauthner neuron is one of the earliest observed and most widely studied reticulospinal neurons (Eaton and Emberley, 1991; Eaton et al., 2001; Faber et al., 1989; Gahtan and Baier, 2004; Gahtan and O'Malley, 2003; Kimmel et al., 1982; Metcalfe et al., 1986). It is essential in integrating and executing escape mechanisms from external stimuli.

The role of other placodally-derived signaling molecules remains to be elucidated. It is likely that other members of the FGF and BMP families also function to specify hindbrain neurons in a manner similar to Fgf24. Unfortunately, ablation of otic formation likely exerts global consequences on the embryo, making it difficult to discern the complete role of otic-derived signaling in hindbrain neurogenesis. For example, sustained inhibition of FGF signaling following mid gastrulation is capable of preventing otic induction (Leger and Brand, 2002; Phillips et al., 2001), but this would also block local FGF activity within the hindbrain. Further study of these signaling molecules will require tissue specific inactivation of these signaling molecules.

Future directions

Elucidation of pathways mediating early phases of otic induction

While we demonstrate that Foxi1 differentially regulates *tbx2a/b*, the mechanism behind this regulation is unclear. Although our analysis suggests that *foxi1* and *tbx2a/b* act in parallel pathways during otic induction, differential regulation of *tbx2a/b* by Foxi1 as well as *pax8* regulation by both Tbx2a/b and Foxi1 suggest that there is interaction between these two pathways at some level. Promoter analysis of both *tbx2* genes is required to determine if Foxi1 directly promotes *tbx2a/b* expression, or whether the effects on *tbx2a/b* expression observed when Foxi1 is inactivated are indirect.

It is currently unclear what signaling molecules induce *tbx2a/b* expression. As otic induction requires FGF signaling, it is likely that *tbx2a/b* expression also requires FGF signaling. We will address the role of FGF activity in *tbx2a/b* expression through biochemical and genetic approaches. The application of SU5402, a small molecule inhibitor of FGF signaling (Mohammadi et al., 1997), will allow us to inactivate FGF signaling over several timepoints during mid to late gastrulation to determine what effect, if any, inactivation of FGF signaling has on *tbx2a/b* expression. Conversely, by using a transgenic line that drives *fgf8* expression under the control of a heatshock promoter (*Tg[hsp70:fgf8]*) (Hans et al., 2007), we will be able to address whether increased Fgf8 induces ectopic *tbx2a/b* expression.

Previous work demonstrated that the earliest phase of otic induction requires both FGF signaling and Foxi1 (Nissen et al., 2003; Solomon et al., 2003; Solomon et al., 2004). In the absence of either protein, *pax8* expression is not induced in pre-otic cells. Similarly, while misexpression of *foxi1* can induce ectopic *pax8* expression, the mechanism through which Foxi1 acts requires FGF signaling. When *foxi1* is ectopically

expressed and FGF activity is blocked, *pax8* is not expressed. Although it is clear that Tbx2a/b are required for otic *pax8* expression, it is unclear how Tbx2a/b and Foxi1 interact in this process. To further investigate the roles of *foxi1* and *tbx2a/b* in *pax8* regulation, we will induce Fgf8 in *Tg(hsp70:fgf8)* embryos that have been injected with *tbx2a/b* morpholinos. If Tbx2a/b mediate FGF signaling in *pax8* induction, loss of Tbx2a/b would be expected to block ectopic *pax8* expression.

There is evidence from studies examining *Tbx3* in mammary placode development to suggest that Tbx2a/b may act as a nexus in integrating FGF and WNT signaling (Howard and Ashworth, 2006). Several WNT signaling members, including the WNT receptors *fzd7a/b* and the secreted WNT antagonist *sfrp2,* are expressed in the otic placode beginning during early somitogenesis (Tendeng and Houart, 2006; Witzel et al., 2006). Examining the expression of these genes will be an initial step in determining how Tbx2a/b affect WNT activity in the otic placode. The use of a transgenic zebrafish line containing a dominant negative Tcf construct under the control of a heatshock promoter (*Tg[hsp70l:*Δ*tcf3-GFP]*$^{w26/+}$) (Lewis et al., 2004) will allow the further investigation of WNT requirements during otic development. Inactivation of WNT activity at various times after otic induction will allow us to attribute otic phenotypes seen in Tbx2a/b morphants to potential disruptions in WNT activity.

The requirements of the otic signaling center in hindbrain neurogenesis

We present evidence that the otic placode plays a previously uncharacterized role as an FGF signaling center during hindbrain neurogenesis. As multiple neuronal types exist within the hindbrain, it is necessary to fully characterize the role of signaling from

the otic placode in neuronal specification. Multiple pro-neural markers will be used to probe differences in hindbrain neurogenesis of control embryos versus Tbx2a/b and Fgf24 morphants.

Our preliminary analysis of the hindbrain in Tbx2a/b and Fgf24 morphants has indicated that Fgf24 signaling from the otic placode is required for specification of Mauthner neurons. In addition to the 3A10 monoclonal antibody, other markers also label the Mauthner neuron (Lowery et al., 2007). To confirm that this neuron requires Fgf24, we must label this neuron with additional markers. To demonstrate that Mauthner neuron specification requires Fgf24 signaling from the otic placode, we will attempt to generate a transgenic line that expresses *fgf24* under the control of an ear-specific promoter that is not affected by the loss of Tbx2a/b. Rescue of the Mauthner neuron phenotype in this transgenic line will demonstrate a non-cell autonomous requirement for Fgf24 in Mauthner neuron specification. To further confirm loss of the Mauthner neuron, we will attempt to analyze escape behavior in Tbx2a/b and Fgf24 morphants. If these morphant embryos do not form Mauthner neurons, we will expect a delay in timing of escape turns similar to that observed in the *space cadet* (*spc*) mutant, which is also Mauthner neuron deficient (Lorent et al., 2001). Although we demonstrate a requirement for Fgf24 in Mauthner cell specification, it is unclear whether Fgf24 is sufficient for its identity. Generation of recombinant Fgf24 will allow us to apply Fgf24 within the brain of zebrafish embryos after initial embryological patterning events to determine whether ectopic Fgf24 can induce supernumerary Mauthner neurons.

It is possible that hindbrain patterning defects represent an underlying cause of the neurogenic defects observed in Tbx2a/b and Fgf24 morphants. Although probes against

krox20 and *hnf1* have indicated that hindbrain patterning is unaffected in Tbx2a/b and Fgf24 morphants, it is still possible that identity of rhombomeres 1, 2, and 4, which are not labeled by these probes, are altered in Tbx2a/b and Fgf24 morphants. However, *fgf24* is not expressed in the otic placode until early somitogenesis, after rhombomere identity has been specified, making it unlikely that the regulation of *fgf24* by Tbx2a/b has any effect on rhombomere identity. Regardless, more detailed examination of hindbrain specification is necessary to exclude any roles in hindbrain patterning by Tbx2a/b or Fgf24.

Table 5.1: Microarray analysis of gene expression in Foxi1 morphants

The values compare gene expression levels in 3-somite Foxi1 morphant embryos to comparably staged embryos injected with a control morpholino. Analysis was performed in triplicate, and averaged values are shown on a log2 scale. Positive values indicate an increase in transcript levels while negative values indicate a decrease in transcript levels, relative to controls. The level of *tbx2b* transcript is significantly increased in Foxi1 morphants, while the level of *tbx2a* transcript is not.

Table 5.1

	Mean Foxi1 mo	*p* value
tbx2a	-0.00984	*p<0.92*
tbx2b	0.94118	*p<0.01*

Figure 5.1: Differential regulation of *tbx2a/b* by Foxi1

(A-H) Expression of *tbx2a* (A-D) and *tbx2b* (G-H) at 3-somites (A,B,E,F) and at 6-somites (C,D,G,H) in wild-type (A,C,E,G) and *hearsay* (B,D,F,H) backgrounds. (I-L) Expression of *foxi1* in Tbx2a (J), Tbx2b (K), and Tbx2a/b (L) morphant backgrounds. All views are dorsal, with anterior to the top.

Figure 5.1

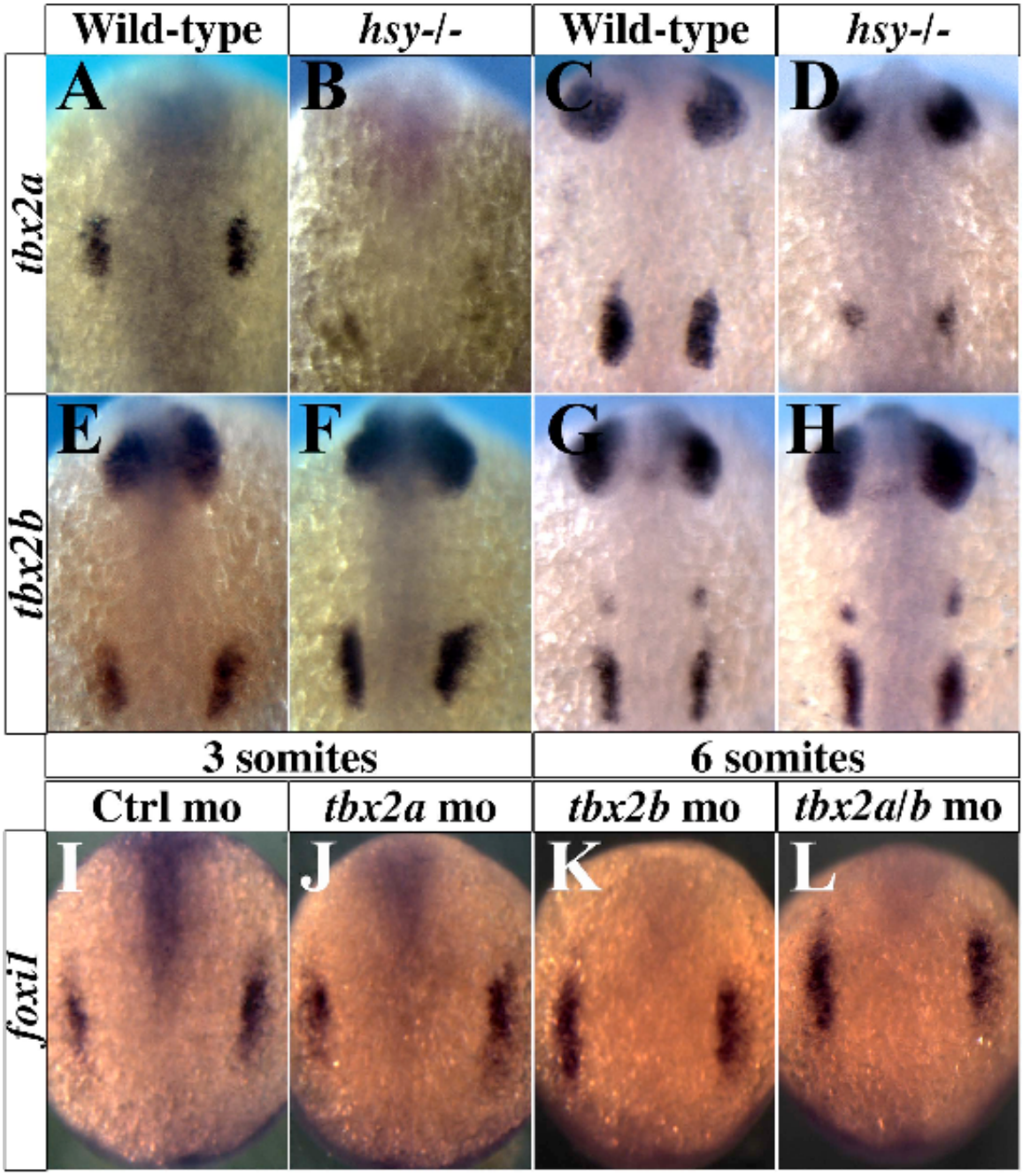
Wild-type
hsy-/-
Wild-type
hsy-/-
tbx2a
A
B
C
D
tbx2b
E
F
G
H
3 somites
6 somites
Ctrl mo
tbx2a mo
tbx2b mo
tbx2a/b mo
foxi1
I
J
K
L

Figure 5.2: *tbx2a/b* expression

tbx2a (A-F) and *tbx2b* (G-L) expression at 30% epiboly (A,G), shield stage (B,H), 80% epiboly (C,I), 6-somites (D,J), 24hpf (E,K), and 4dpf (F,L). (A,B,G,H) are lateral views with dorsal to the right, (C,D,I,J) are dorsal views with anterior to the top, and (E,F,K,L) are lateral views with anterior to the left. nc, notochord; lp, lens placode; op, otic placode; ov, otic vesicle; ret, retina.

Figure 5.2

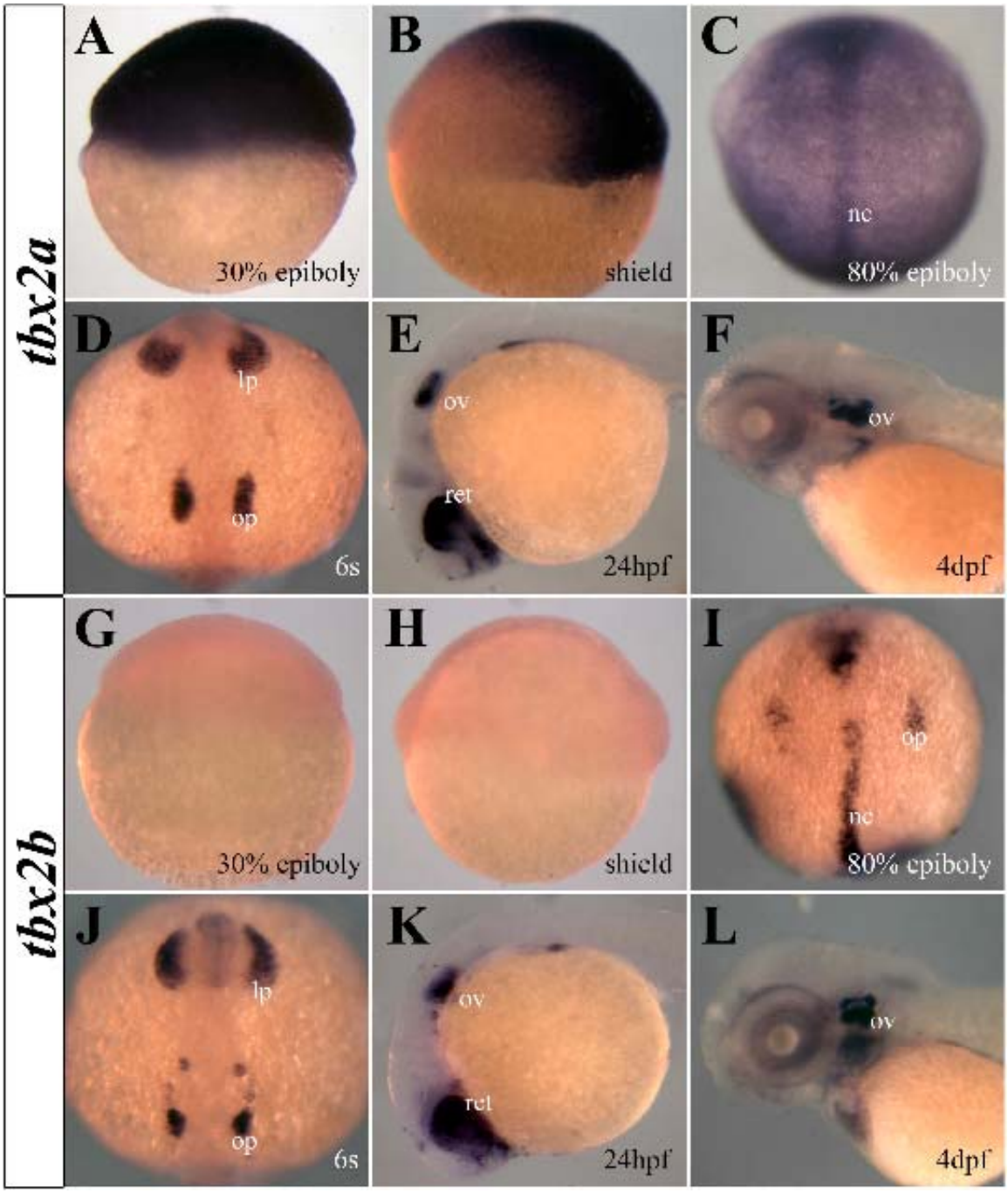
tbx2a
A
30% epiboly
B
shield
C
nc
80% epiboly
D
lp
op
6s
E
ov
ret
24hpf
F
ov
4dpf
tbx2b
G
30% epiboly
H
shield
I
op
nc
80% epiboly
J
lp
op
6s
K
ov
ret
24hpf
L
ov
4dpf

Figure 5.3: Tbx2a/b are required for proper otic formation

(A-E) In 30hpf controls (A), an otic vesicle forms that is oval in shape and contains to round otoliths. (B,C) Tbx2a morphants (B) and *fby* mutants (C) form smaller otic vesicles with irregular shaped otoliths. (E) Knockdown of Tbx2a in *fby* mutants ablates otic formation. (E,F) Combined loss of Tbx2a (E) or Tbx2b (F) and Foxi1 result in a more severe otic phenotype than single loss of Tbx2 function. (G-I) By 3dpf, the canal system within the inner ear is visible (G). In Tbx2a morphants (H) and *fby* mutants (I), these canals are disorganized. Insets in (A-C, G-I) are high magnification images of the posterior otolith. All views are lateral with anterior to the left.

Figure 5.3

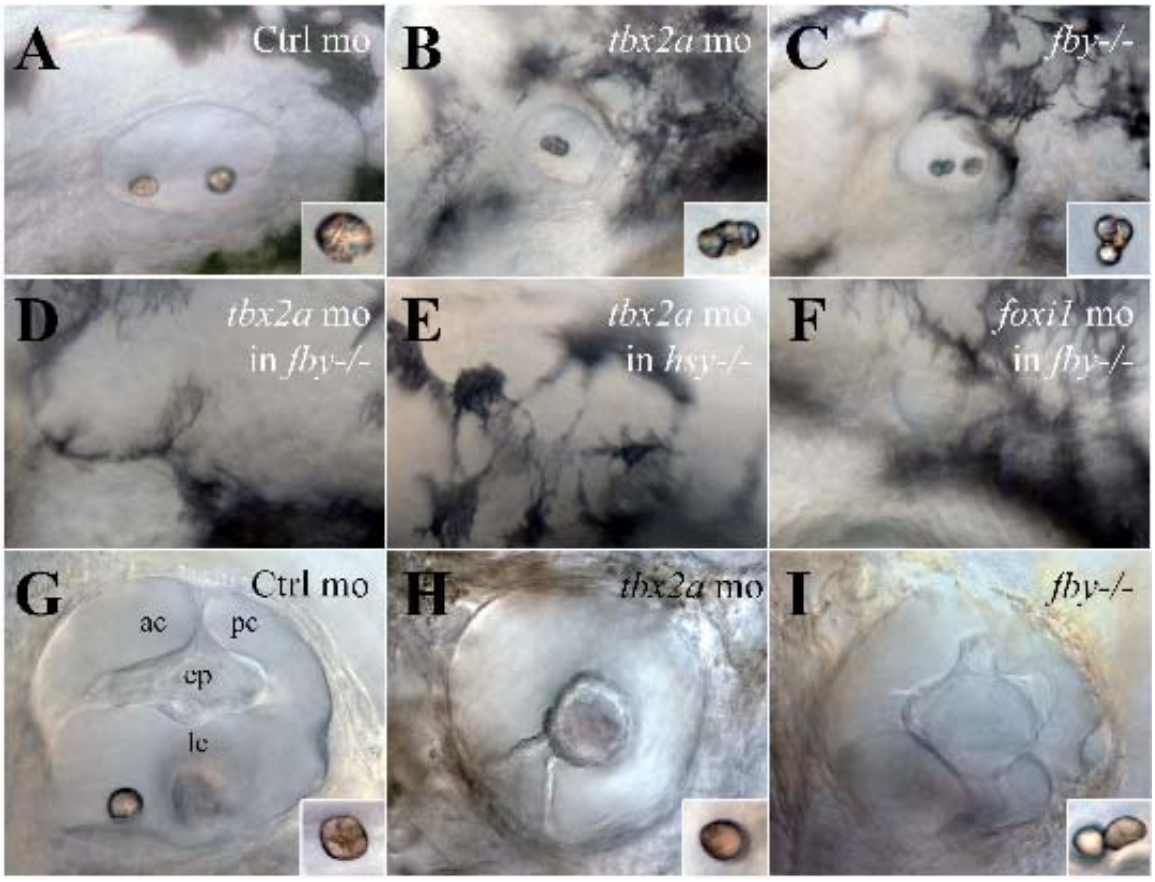
A
Ctrl mo
B
tbx2a mo
C
fby-/-
D
tbx2a mo
in fby-/-
E
tbx2a mo
in hsy-/-
F
foxi1 mo
in fby-/-
G
Ctrl mo
ac
pc
ep
lc
H
tbx2a mo
I
fby-/-

Figure 5.4: Tbx2a/b lie upstream of *pax8*

(A-F) Loss of either Tbx2a (B,E) or Tbx2b (C,F) is sufficient to prevent otic expression of *pax8*. (G-J) Loss of Pax8 has no effect on *tbx2a* (G,H) or *tbx2b* (I,J) expression. (K-M) The otic phenotype observed in combined loss of Pax8 and Tbx2a (L) or Tbx2b (M) is no more severe than loss of Tbx2a or Tbx2b alone. (A-C) Bud stage dorsal views with anterior to the top. (D-J) 6-somite dorsal views with anterior to the top. (K-M) 30hpf lateral views with anterior to the left. mhb, midbrain-hindbrain boundary; arrows denote loss of expression from the otic placode.

Figure 5.4

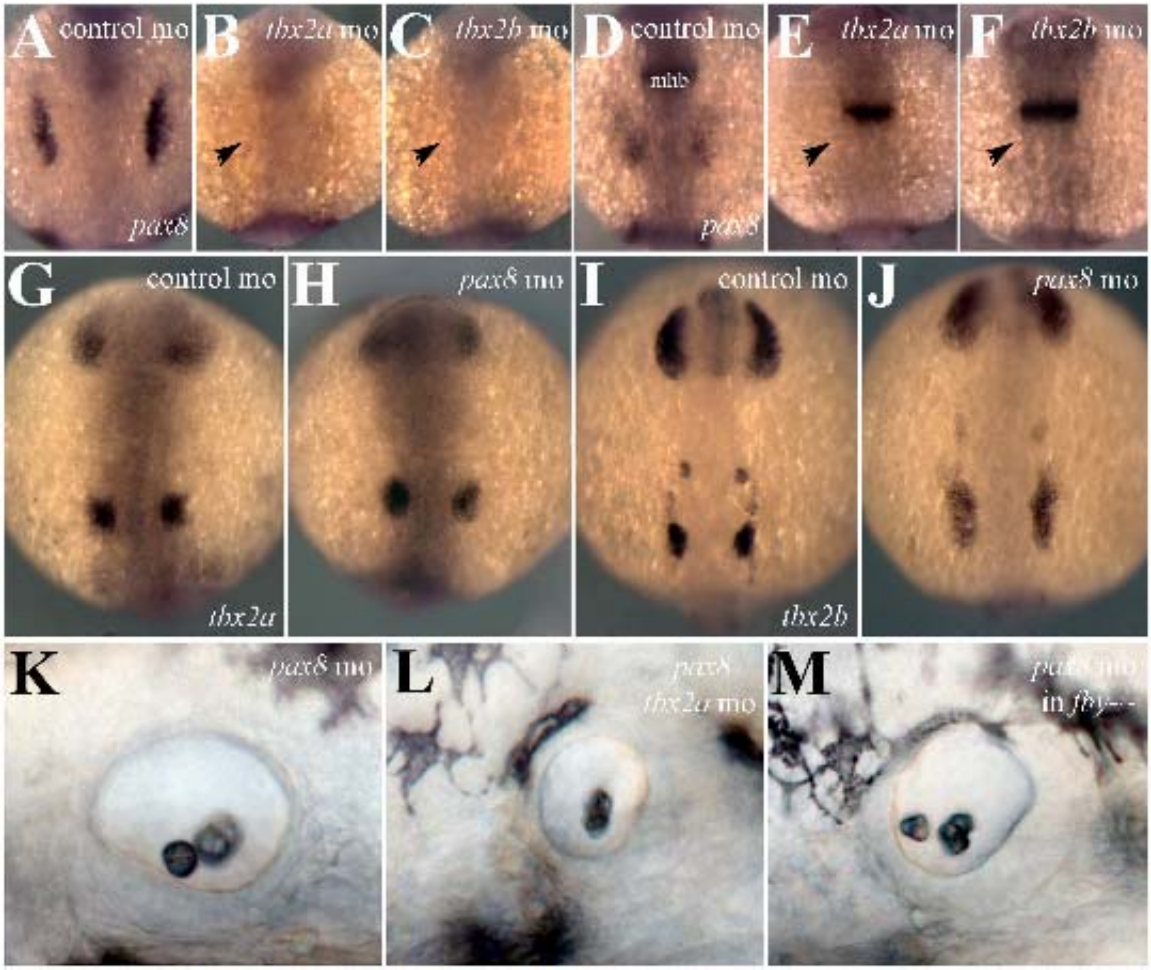
A control mo
pax8
B thx2a mo
C thx2b mo
D control mo
ntnb
pax8
E thx2a mo
F thx2b mo
G control mo
thx2a
H pax8 mo
I control mo
thx2b
J pax8 mo
K pax8 mo
L pax8
thx2a mo
M pax8 mo
in fbx--

Figure 5.5: *tbx2a/b* act in a pathway parallel to *dlx3b/4b*

(A-D) Loss of Dlx3b/4b has no effect on *tbx2a* (A,B) or *tbx2b* (C,D) expression. (E-G) Loss of either Tbx2a or Tbx2b increases the severity of the Dlx3b morphant phenotype. (E) Dlx3b morphants develop an otic vesicle that lacks an otolith. (F) Combined loss of Tbx2a and Dlx3b ablates otic vesicle formation. (G) Combined loss of Tbx2b and Dlx3b results in an otic vesicle that lacks otoliths. (A-D) 6-somite dorsal views with anterior to the top. (E-G) 30hpf lateral views with anterior to the left.

Figure 5.5

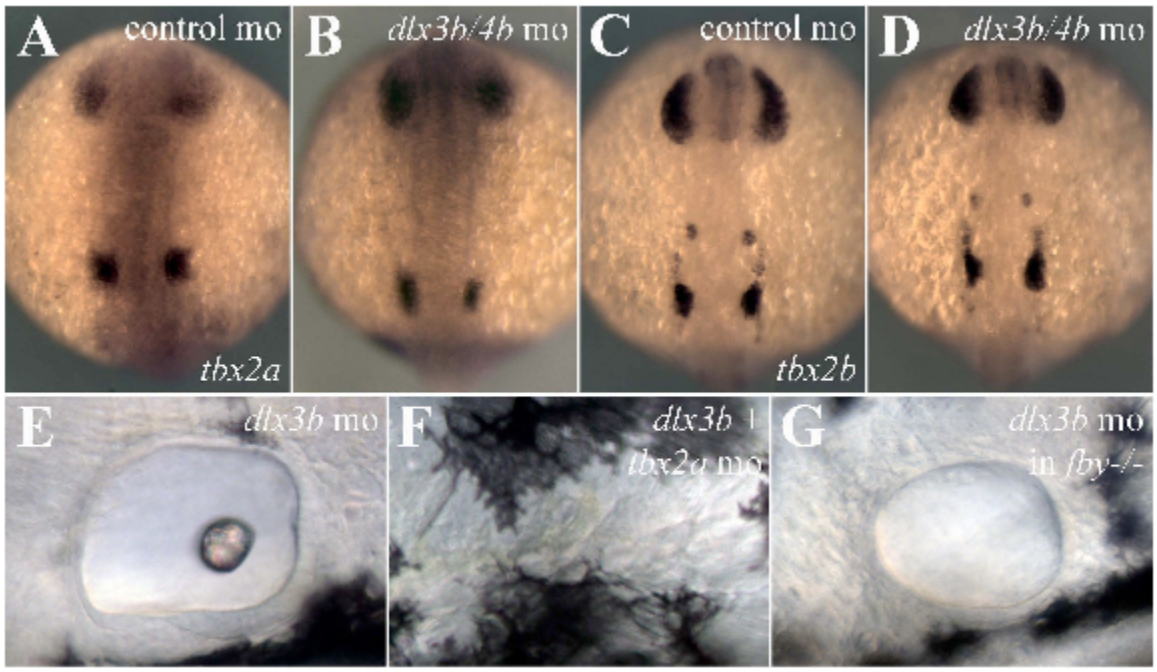
A
control mo
tbx2a
B
dlx3b/4b mo
C
control mo
tbx2b
D
dlx3b/4b mo
E
dlx3b mo
F
dlx3b +
tbx2a mo
G
dlx3b mo
in fby-/-

Figure 5.6: The role of Tbx2a/b in otic gene expression

Expression of *cldna* (A-D), *fgf24* (E-H), *pax2a* (I-L), and *sox9a* (M-P) in Tbx2a (B,F,J,N), Tbx2b (C,G,K,O) and Tbx2a/b (D,H,L,P) morphants. Dorsal views of 6-somite embryos with anterior to the left.

Figure 5.6

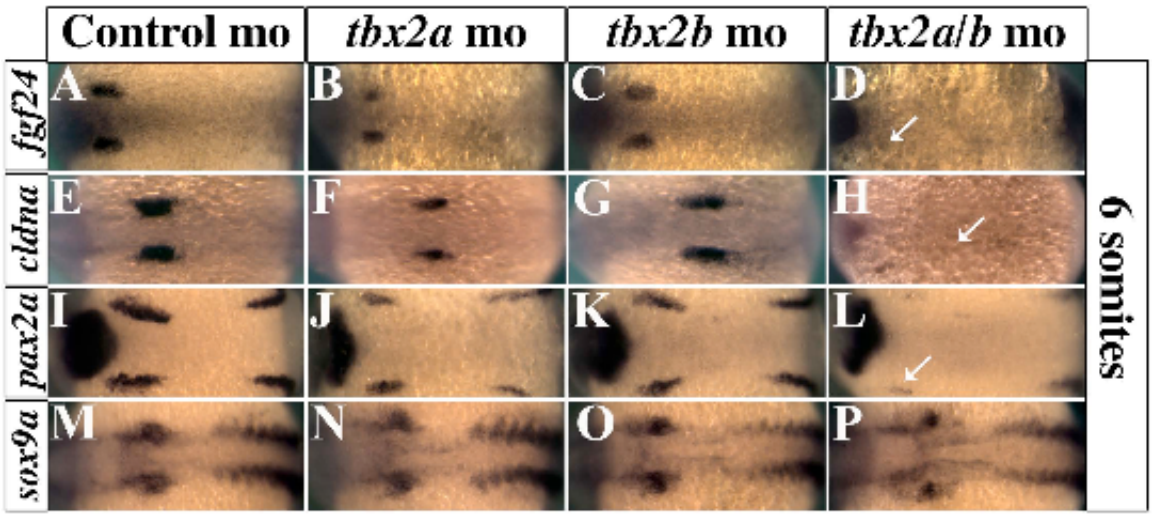
Control mo
tbx2a mo
tbx2b mo
tbx2a/b mo
fgf24
cldna
pax2a
sox9a
A
B
C
D
E
F
G
H
I
J
K
L
M
N
O
P
6 somites

Figure 5.7: Tbx2a/b specify the anterior and lateral domains of the otic vesicle

Expression of *otolin* (A-C), *omp* (D-F), *pax5* (G-I), and *fst* (J-L) in Tbx2a (B,E,H,K) and Tbx2b (C,F,I,L) morphants. (A-F) 24hpf embryos (G-L) 36hpf embryos. All views are lateral with anterior to the left.

Figure 5.7

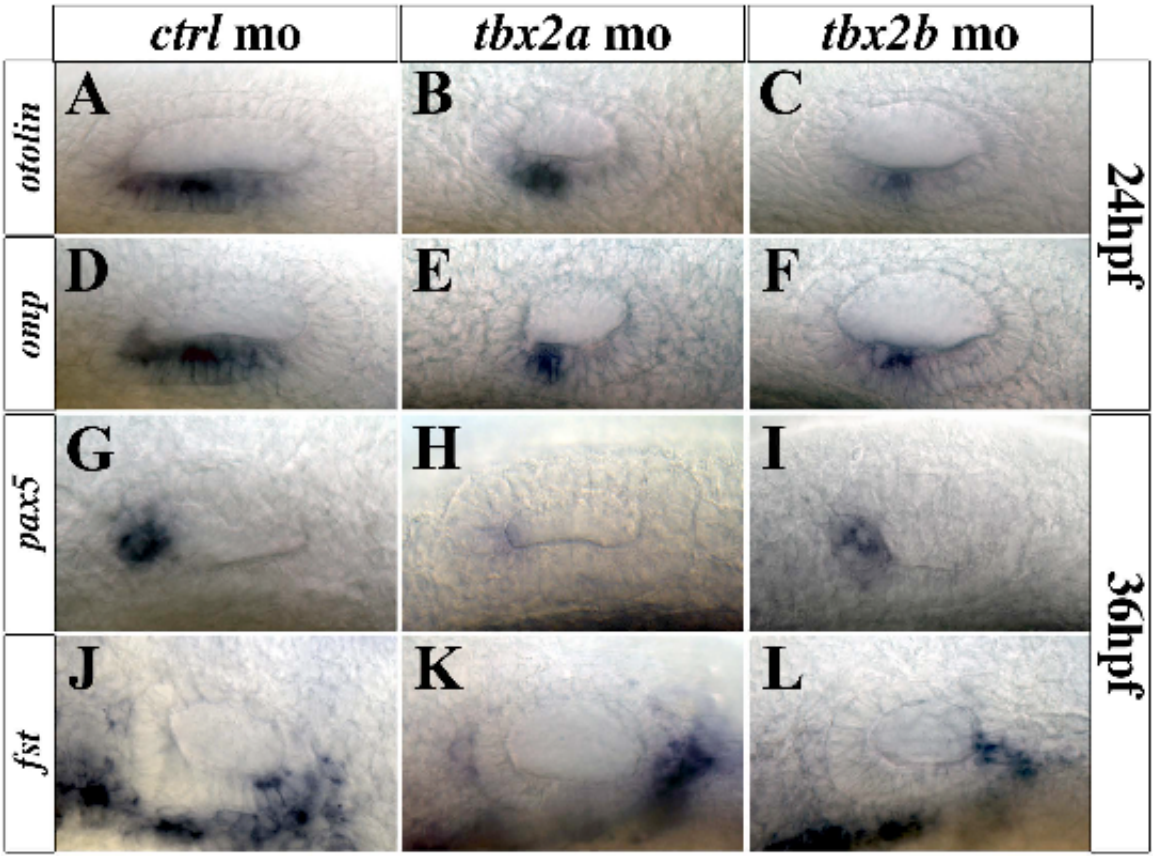
ctrl mo
tbx2a mo
tbx2b mo
otolin
omp
pax5
fst
A
B
C
D
E
F
G
H
I
J
K
L
24hpf
36hpf

Figure 5.8: Tbx2a/b and Fgf24 are required for hindbrain neurogenesis

(A-C) *krox20* (red) and *hnf1* (purple) expression reveal that hindbrain patterning is normal in 9-somite Tbx2a/b (B) and Fgf24 (C) morphants. (D-F) *pax2a* expression reveals that hindbrain interneurons are lost from 24hpf Tbx2a/b (E) and Fgf24 (F) morphants. (G-I) Motor neurons in 24hpf *Tg(isl:GFP)* zebrafish are disorganized in Tbx2a/b (H) and Fgf24 (I) morphants. (J-O) The Mauthner neuron cannot be detected in 36hpf Tbx2a/b (K,N) and Fgf24 (L,O) morphants. All views are dorsal with anterior to the left. mlf, medial longitudinal fasiculus; ov, otic vesicle; arrows denote defects in neurogenesis.

Figure 5.8

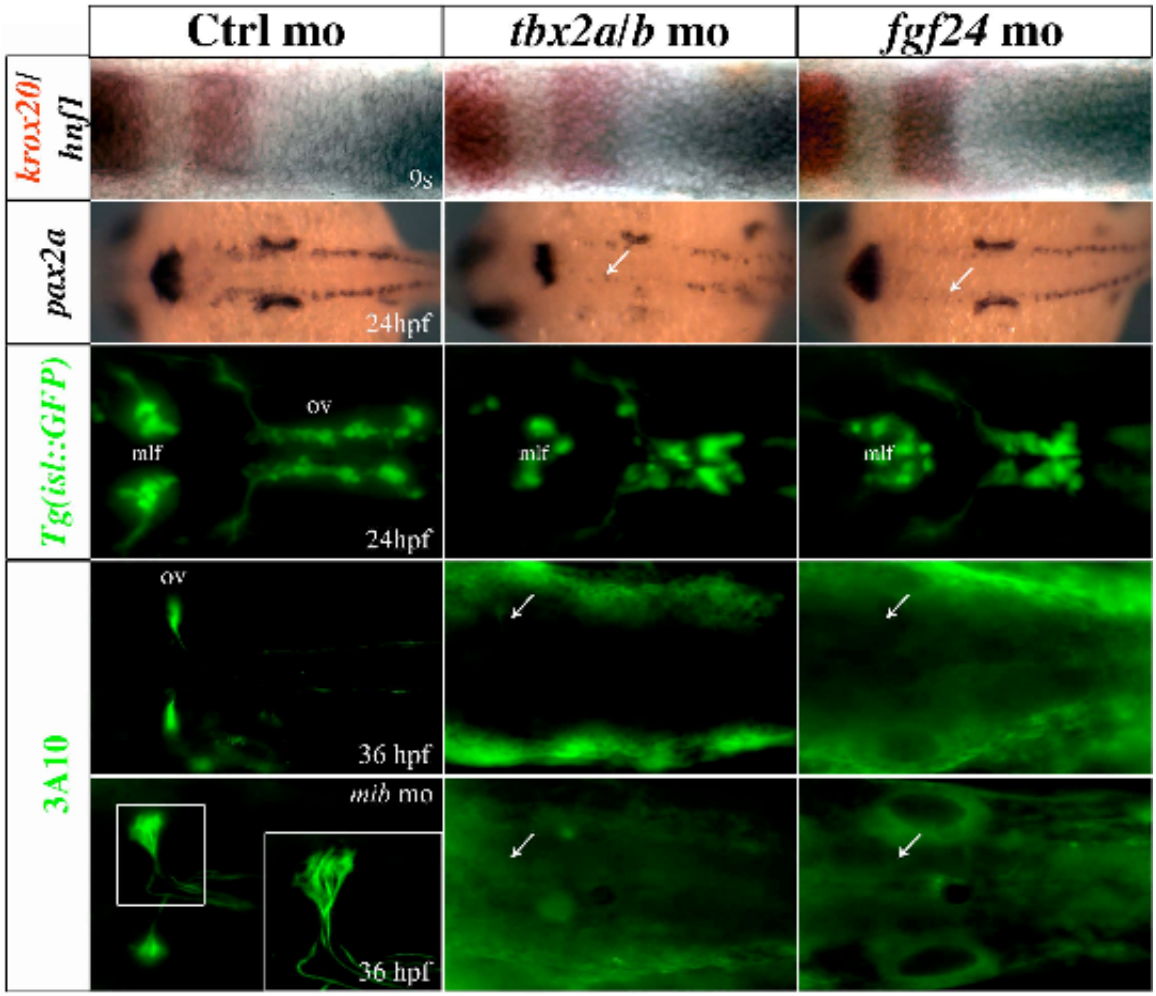
Ctrl mo
tbx2a/b mo
fgf24 mo
krox20/ hnf1
9s
pax2a
24hpf
Tg(isl::GFP)
ov
mlf
24hpf
3A10
ov
36 hpf
mib mo
36 hpf

CHAPTER 6

General conclusions

Most models of embryonic patterning posit that the passive diffusion of morphogens from their signaling centers create a gradient of signaling activity that decreases over distance (Kimelman, 2006; Neave et al., 1997; Nguyen et al., 1998; Schier and Talbot, 2005; Tribulo et al., 2003). While there is no doubt that simple morphogen gradients are essential in some aspects of embryonic patterning, recent interest in the self-regulative capabilities of the embryo has begun to suggest that signaling requirements during embryogenesis are far more complex than previously thought (Ambrosio et al., 2008; Hagos and Dougan, 2007; Rentzsch et al., 2006; Reversade and De Robertis, 2005; Serpe et al., 2008; Tucker et al., 2008). The identification that the ventral and dorsal organizers are capable of compensating for the loss of the other through complex positive and negative feedback mechanisms demonstrates that the establishment of morphogenetic gradients is not a passive process (Kimelman and Pyati, 2005; Reversade and De Robertis, 2005). The feedback mechanisms regulating this signaling, and the interaction of secreted morphogens with their antagonists, allows an embryo to convert a relatively simple diffusion gradient into one that varies depending on spatial-temporal contexts. Our work further illustrates the dynamic changes in signaling, as well as signaling requirements, that occur throughout the course of embryonic development.

In Chapter 2, we have shown that requirements for BMP signaling change throughout development. The patterning of mesoderm across the DV axis is primarily established by a gradient of BMP activity that is highest on the presumptive ventral side of the gastrula and lowest dorsally (Kishimoto et al., 1997; Lele et al., 2001; Melby et al., 2000; Mullins et al., 1996; Willot et al., 2002). Mesoderm positioned in the dorsal organizer receives little BMP activity, and is fated to become axial mesoderm. We

demonstrate that dorsal-most mesoderm possesses a requirement for Bmp4 that begins during late gastrulation. Contrary to static BMP gradient models, our results reflect the changing dynamic of BMP activity as gastrulation proceeds. Although mutagenesis screens for genes involved in DV patterning have yielded useful information about the role of the BMP pathway, they fail to encompass all requirements of BMP activity during embryogenesis. Requirements for BMP activity in tissue patterning can be masked by earlier roles in establishing embryonic polarity.

Previous work by Agathon and colleagues (2003) identified the presence of a ventral, or tail, organizer in zebrafish. This region of cells lies 180° from the dorsal organizer, and is the likely source of BMP ligands during gastrulation. As gastrulation proceeds, the two organizing centers migrate into proximity with one another. Following gastrulation, these two organizing centers contribute to the tailbud, a progenitor pool responsible for the coordinated outgrowth of ecto- and mesodermal derivatives that comprise the tail (Agathon et al., 2003; Kanki and Ho, 1997). Embryological manipulation and loss of function studies both demonstrated that although the two organizers share proximity, they contribute to distinct structures within the tail. For example, the ventral organizer is responsible for the outgrowth of non-axial mesoderm and non-neural ectoderm, while axial mesoderm and neural ectoderm depend upon the dorsal organizer. In *Xenopus* and zebrafish, the misexpression of ventral or dorsal organizer-derived morphogens is capable of inducing ectopic paraxial or lateral mesoderm and axial mesoderm, respectively (Agathon et al., 2003; Gont et al., 1993; Pyati et al., 2005; Tucker and Slack, 1995).

Formation of an ectopic tail containing both axial and non-axial mesoderm cannot occur without substantial contribution from both organizing centers. Thus, although dorsal and ventral organizers give rise to different structures within the tail, these derivatives likely must integrate signaling from both organizers to develop properly. Our results demonstrate that axial cells require ventrally-derived BMPs for both regulation of fate assignment as well as proliferation. When wild-type cells are transplanted into embryos that are not competent to respond to BMP signaling, the donor cells preferentially populate axial structures. Our results provide a likely mechanism of how ventral and dorsal organizer-derived cells communicate to promote outgrowth of a tail that contains the full complement of ecto- and mesodermal derivatives.

Unlike the initial roles of BMP signaling in DV patterning, little is known about signaling events that occur during tail specification and outgrowth. This is because selection parameters in early mutagenesis screens for embryonic patterning defects were focused on easily definable, gross morphological defects. For example, the DV patterning defects observed in BMP pathway mutants mask potential later, milder, roles of BMP signaling in embryonic development (Hammerschmidt et al., 1996a; Mullins et al., 1996). Furthermore, the same screens have been used to identify genes involved chordamesoderm specification and tail outgrowth, with similar consequences to the elucidation of later, more subtle roles. For example, although *flh* is expressed in chordamesoderm from mid gastrulation through 24hpf, chordamesoderm is not present in this mutant (Talbot et al., 1995). Similarly, the severe tail outgrowth defects observed in *ntl* mutants preclude any examination of tailbud fate specification or tissue interaction in these embryos (Halpern et al., 1993).

In addition to its contributions to the notochord, cells from the CNH give rise to floor plate and tailbud mesoderm (Cambray and Wilson, 2002; Charrier et al., 1999; Davis and Kirschner, 2000). Although elevated BMP activity leads to an overall increase in the size of the CNH, CNH-derived tissues are not equally affected by the increase in precursor cells. While the expression domains of tailbud ecto- and mesoderm genes are increased in Fstl1/2 morphants, these embryos display no appreciable defects in tail morphology. It is likely that BMP ligands confer differential fate assignment upon tailbud precursors. Bmp4 may uniquely affect axial development, while other BMPs such as Bmp2b/7 affect development of other tailbud tissues. The combined influence of these signals may be required to promote the development of the full range of CNH derivatives within the tailbud.

Several techniques will prove invaluable in the future examination of these interactions. Fate-mapping of cells within the tailbud would reveal the origin of each tissue, and potentially provide evidence for a niche population of stem cells that contribute to each tissue type. Additionally, these cells could be labeled and traced under conditions of varying BMP activity, either through Bmp4 knockdown or *tBR* inactivation, to determine the exact requirements of BMP signaling on fate assignment within the CNH.

It is clear that, in addition to BMP signaling, other signaling molecules are also essential for posterior mesoderm formation. Signaling from FGF, Nodal, and WNT family members promote axial and paraxial development, notably through the regulation of the T-box transcription factors *ntl*, *spt*, and *tbx16* (Amacher et al., 2002; Amacher and Kimmel, 1998; Griffin et al., 1995; Griffin et al., 1998; Griffin and Kimelman, 2002;

Griffin and Kimelman, 2003; Martin and Kimelman, 2008; Schulte-Merker and Smith, 1995; Yamamoto et al., 1998). Although the specification of these mesodermal territories occurs during gastrulation, members of all three signaling pathways are expressed in the CNH during somitogenesis (Komoike et al., 2005; Marlow et al., 2004; Munchberg et al., 1999; Scholpp et al., 2004; Thisse et al., 1995; Zhang et al., 1998), suggesting that they also play critical roles in assigning fate to the CNH. The use of small molecule inhibitors of FGF and Nodal signaling, as well as the transgenic *hsp70l:fgf8* and *hsp70l:*Δ*tcf3-GFP* zebrafish lines, will allow us to determine the effects of manipulating signaling within the CNH on fate assignment.

The recent generation of photocleavable morpholinos will allow the better understanding of a gene's role in the context of tail outgrowth (Shestopalov et al., 2007). Although processed like a traditional morpholino, photocleavable morpholinos remain inactive until uncaged with light from a 380nm laser. In this way, only cells exposed to the laser beam inhibit translation of the target gene. This will overcome morphological defects outside the area of interest when determining the role of genes such as *ntl* and *flh.* Systematic inactivation of a gene in a small population of axial cells throughout the tail can be performed to determine what spatial roles these genes play in tail outgrowth. Similarly, cells within the CNH could be targeted, and the subsequent effects on tissue contribution could be assayed.

As several BMP receptors are expressed throughout the tailbud, cells in this region are likely competent to respond to BMP signaling (Bauer et al., 2001; Monteiro et al., 2008; Nikaido et al., 1999a; Nikaido et al., 1999b). What, then, drives cell fate choice within this domain? The answer likely lies with the interaction of PSMAD1/5/8

and tissue-promoting transcription factors that have begun to be expressed earlier in gastrulation. Evidence from *Xenopus* has revealed that the orthologue of Ntl, Xbra, interacts with the C-terminus of PSMAD1 (Messenger et al., 2005). This interaction allows transcriptional activation of the BMP target gene *vox*. Through the transcriptional repression of *gsc*, Vox prevents axial mesoderm from becoming prechordal plate (Messenger et al., 2005). As the prechordal plate is not expanded in *ntl* mutants (Halpern et al., 1997; Halpern et al., 1993; Schulte-Merker et al., 1994), it is likely that PSMAD1/5/8 interact with other chordamesodermal transcription factors to repress the development of chordamesoderm.

In the future, it will be interesting to determine how cells in the tailbud become fated to contribute to axial versus non-axial mesoderm. Although promoter analysis of axial genes may reveal if they require BMP activity, it will not elucidate how these proteins interact with PSMAD1/5/8. To determine the full range of BMP interactions that occur within the tailbud, it will be necessary to immunoprecipitate PSMAD1/5/8 and probe with antibodies against known axial regulators.

In Chapter 3, we demonstrate that BMP requirements change within border ectoderm to subdivide neural crest and PPR domains. This is interesting, as the initial establishment of the border region appears to require BMP signaling. Fate mapping studies have demonstrated that cells lateral to the neural plate arise from a region of ectoderm that is positioned slightly more ventral than that of presumptive neural plate (Kozlowski et al., 1997). Furthermore, the expression of all known border genes, including members of the *Dlx*, *Fox*, and *Msx* gene families, require BMP signaling to be

expressed. Direct requirements for BMP signaling have been demonstrated in cell culture with mouse *Dlx3* (Park and Morasso, 2002), while *in vivo* requirements have been demonstrated in *Xenopus* and zebrafish (Feledy et al., 1999; Luo et al., 2001; Pera et al., 1999). For example, the zebrafish *bmp2b* (*swirl*) mutant does not express *dlx3b* within border ectoderm or in subsequent PPR (Nguyen et al., 1998).

The observation that the border region lies between the neural plate and epidermis, regions that require low and high levels of BMP activity, respectively, has led to a passive diffusion model of BMP activity in the establishment of ectodermal domains (Nguyen et al., 1998; Tribulo et al., 2003). In this model, cells on the ventral side of the gastrula receiving the highest levels of BMP activity become epidermis, cells more lateral to epidermal precursors receive less BMP activity and become border tissue, while cells most dorsal receive the least BMP activity and become neural plate. This passive diffusion model has been strengthened by the observation that in both loss and gain of function analyses involving BMP signaling components, the neural crest is lost (Nguyen et al., 1998; Tribulo et al., 2003). However, this does not take into account how PPR is specified from the same tissue that also gives rise to neural crest. The PPR lies in between neural crest and epidermis, and numerous studies have demonstrated the requirement of low BMP activity in PPR specification (Bailey and Streit, 2006; Schlosser, 2006; Streit, 2007). Thus, a model in which BMP activity patterns all ectodermal cell types as it passively diffuses from the ventral organizer cannot account for PPR specification.

Our results provide evidence for a complex, active model of BMP regulation in the subdivision of border ectoderm. This is brought about through the transcriptional

regulation of *cv2* by Dlx3b/4b. Although numerous biochemical studies have demonstrated both pro- and anti-BMP roles of Cv2, the *in vivo* mechanism of this BMP modulator is still poorly understood (Ambrosio et al., 2008; Bier, 2008; Heinke et al., 2008; Moser et al., 2003; Moser et al., 2007; Rentzsch et al., 2006; Serpe et al., 2008; Zhang et al., 2008). In areas of high concentration, Cv2 binds BMP receptors, preventing interactions with Bmp4. When lower amounts of Cv2 are present the protein acts to stabilize Bmp4-receptor interactions, thus promoting BMP signaling. Furthermore, Cv2 is capable of interacting with the BMP antagonist Chordin, forming a ternary complex that also contains Bmp4 (Ambrosio et al., 2008; Bier, 2008; Serpe et al., 2008). This affinity is increased 10-fold when Chordin has been cleaved by the Tolloid family of proteases. These data paint a complex picture of BMP regulation within the embryo, and likely represent only a small fraction of the actual mechanisms by which BMP activity is regulated.

Although Cv2 is a secreted molecule, it does not travel over a distance of more than a few cell diameters. This is due to a von Willebrand Factor D (vWFd) domain in the C-terminus of the protein that interacts with heparin sulfate proteoglycans, raising the possibility that Cv2 can act as a dual function BMP modulator at the resolution of one cell diameter (Bier, 2008; Rentzsch et al., 2006; Serpe et al., 2008). Thus, it is possible that in addition to lowering BMP activity within the PPR, Cv2 may promote BMP activity in adjacent border ectoderm to levels necessary for neural crest specification. In support of this interpretation, Cv2 has been implicated in neural crest development in chick (Coles et al., 2004). As *tolloid* is expressed in the neural crest domain of *Xenopus* and zebrafish (Connors et al., 1999; Goodman et al., 1998), Cv2 is an attractive candidate

as a BMP modulator that plays multifunctional roles, including inhibiting Bmp4 within the PPR and also in promoting Bmp4 signaling in adjacent neural crest.

All studies that examine the anti-BMP role of vertebrate Cv2 have been *in vitro* or performed in a way that potentially disrupt embryonic patterning and exaggerate the anti-BMP role of Cv2 (Ambrosio et al., 2008; Coles et al., 2004; Moser et al., 2003; Rentzsch et al., 2006). It would be therefore interesting to generate transgenic zebrafish where *cv2* expression is driven in specific tissues. This would be followed by generation of Cv2 truncations that are unable to interact with Chordin-Bmp4 complexes, and the resulting effects on border ectoderm subdivision could be examined. Alternatively, the role of the vWFd domain could be removed in some truncations to determine whether diffusion of Cv2 away from the PPR expands or shrinks this domain. A major caveat of these ideas is that, in order to examine the effects of Cv2 on PPR and neural crest specification, the promoter of a gene expressed universally throughout border ectoderm must first be characterized. Although extensive effort has been expended to define such a promoter element, these sequences are not currently known (A. Fritz, unpublished observations). However, the promoters of genes expressed slightly later in specified PPR and neural crest have been identified. These include the *pks1* and *foxd3* promoters (A. Fritz, unpublished observations; Gilmour et al., 2002). Although these promoters drive expression at a time at which PPR and neural crest domains are likely determined, alteration of BMP activity levels by misexpression of *cv2* may cause subtle defects in PPR or neural crest domains.

Evidence from our loss of function and interaction analyses as well as the prolonged expression of *cv2* within pre-otic cells suggests that in addition to inhibitory

effects on PPR establishment, BMP activity is also detrimental to early phases of otic induction. As *dlx3b/4b* and *cv2* expression are gradually restricted to the otic placode, is there a gradation of increased BMP activity as distance from the otic placode increases? Although this seems likely, it is unclear what effect altering this gradient has on the induction of surrounding placodes. Markers of other placodal identities, such as *six3* in the lens placode, have been shown to play active roles in BMP inhibition (Cvekl and Duncan, 2007; Gestri et al., 2005), raising the possibility that each placode utilizes a mechanism to inhibit BMP signaling during the earliest stages of induction. It would be interesting to locally apply BMP inhibitors in interspersed regions along the PPR to determine whether this inhibition alters placodal fate.

In our gain of function experiments, ectopic expression of *dlx3b* or *cv2* induced competence to respond to FGF signaling, as observed through the expression of FGF feedback molecules. As high FGF and low BMP activity levels are critical in PPR establishment (Bailey and Streit, 2006; Schlosser, 2006; Streit, 2007), it is no surprise that we also observe expression of PPR markers in cells ectopically expressing *dlx3b* or *cv2*. It is unclear, however, why we do not also observe otic marker expression in these cells. There are several possible explanations for this observation.

Studies from a variety of vertebrates have illustrated that FGF signals emanating from the hindbrain and underlying mesoderm are essential for otic induction. Zebrafish Fgf3/8 are required in this process (Leger and Brand, 2002; Phillips et al., 2001; Solomon et al., 2004), and to our knowledge, otic induction cannot occur through other FGF molecules. As cells ectopically expressing *dlx3b* or *cv2* are not within the proximity of these tissues, otic induction may not occur even though PPR fate is specified.

It is also possible that these cells do acquire a placodal identity although it is not otic. Evidence from placodal specification in chick suggests that all PPR cells possess a default "ground" state, where in a neutral environment these cells adopt a common identity (Bailey et al., 2006). Culture of chick PPR explants in such a neutral environment causes them all to express markers consistent with the acquisition of lens identity. Although cells ectopically expressing *dlx3b* or *cv2* are not in a neutral environment, it is possible that the location of these cells significantly alters the signaling inputs received, which ultimately causes them to adopt an alternate placodal fate. It may prove useful to examine other placodal markers in embryos ectopically expressing *dlx3b* or *cv2*.

In Chapter 4, we have begun to analyze FGF ligand-receptor interactions in otic development. Although the role of FGF signaling in otic induction is well characterized (Ohyama et al., 2007; Schimmang, 2007; Schneider-Maunoury and Pujades, 2007), the function of FGFRs in this process is largely unknown. Through epistasis analyses, it is possible to dissect ligand-receptor interactions *in vivo*. Although these interactions should be confirmed *in vitro*, sequence homology between the large family of FGF ligands and small family of FGFRs present the possibility that promiscuous interactions occur *in vitro* that would not be observed *in vivo*. Our data suggest that null mutations in FGF ligands can be useful tools in identifying their complementary receptors. Null mutations must be identified for at least one member of the interactive ligand-receptor pair. Morpholino injection can be only used for one member of the pair, as it is difficult to assess knockdown efficacy. Functional protein may still be produced in morphant

embryos even though it is below detectable levels. The combined effects of two strong hypomorphic backgrounds may generate false positives that would not be detected with a null allele.

The expression of FGFRs during embryogenesis is dynamic. Although *fgfr1/2/3* are expressed in pre-otic cells during late gastrulation through mid-somitogenesis, only *fgfr1/2* are expressed in the otic vesicle during late somitogenesis. It is unclear how competence to respond to otic inducing signals is regulated. Like in the Hedgehog signaling pathway (Denef et al., 2000; Lum et al., 2003; Nakano et al., 2004; Ruel et al., 2003), it is possible that the expression of a particular FGFR is maintained through a positive feedback loop initiated by the interacting ligand. This may not be the only mechanism governing competence however, as *fgfr3* expression is no longer detectable in the otic vesicle after mid-somitogenesis. Thus, competence to respond to otic inducing signals likely originates from within pre-otic cells in response to another signaling pathway.

The role of genes responsible for conferring competence onto pre-otic cells has gone largely unaddressed in previous works. Competence factors are generally though to be unaffected by the signaling pathway that they promote. As most genes identified in otic induction are targets of FGF signaling, this leaves very few possible candidates. Those that have emerged include Dlx3b/4b. The expression of these genes is unaffected in the complete absence of FGF signaling (Leger and Brand, 2002; Phillips et al., 2001), and are activated by BMP signaling as previously mentioned. Furthermore, disruption of these genes inhibits the expression of the FGF target genes *pax2a* and *sox9a* (Liu et al., 2003; Solomon and Fritz, 2002; Solomon et al., 2004). Loss of functional Dlx3b/4b does

not affect *fgf3/8* expression (Liu et al., 2003; Solomon and Fritz, 2002; Solomon et al., 2004), suggesting that if Dlx3b/4b do confer otic competence, they do it through another means.

In Chapter 3, we demonstrated that Dlx3b/4b play an indirect role in mediating FGF competence during early somitogenesis through inhibition of BMP activity. The mechanisms behind this inhibition are still unclear. It is likely that BMP signaling activates transcriptional repressors that block *fgfr* expression. Mechanisms of BMP-mediated opposition of FGF activity have been observed at the level of ligand expression, where BMP activity represses *Fgf4* expression in the apical ectodermal ridge of mouse (Ganan et al., 1996; Pizette and Niswander, 1999; Zuniga et al., 1999). The presence of ectopic FGF feedback markers in cells ectopically expressing *dlx3b/4b* and *cv2* strengthens our model that low levels of BMP activity are required to promote FGF competence. As BMP and FGF signaling play opposing roles in specification of neural versus non-neural ectoderm (De Robertis et al., 2000; Massague, 2003; Sakai, 2008; Weinstein and Hemmati-Brivanlou, 1999), it would be interesting to examine the expression of epidermal markers in Dlx3b/4b morphants to determine if the hindbrain has transfated into epidermis as the result of dampened FGF activity. Although FGF activity returns to normal during mid-somitogenesis in Dlx3b/4b morphants, hindbrain patterning and neuronal specification should be more closely examined to determine whether the transient loss of FGF activity results in severe patterning defects.

fgf3/8, *dlx3b/4b* and *foxi1* have been independently described as three of the earliest molecular components required for otic placode formation in zebrafish (Leger

and Brand, 2002; Liu et al., 2003; Phillips et al., 2001; Solomon and Fritz, 2002; Solomon et al., 2003; Solomon et al., 2004). Combined loss of function of Dlx3b/4b and Foxi1 produces a strong synergistic effect on otic development (Solomon et al., 2004), suggesting that these components function in independent pathways. The loss of *pax8* expression when *foxi1* is compromised suggests that Foxi1 acts during the earliest stages of otic development (Solomon et al., 2003).

In Chapter 5, we have begun to analyze two novel factors, *tbx2a/b*, that are also required for proper otic induction. Interaction analyses between Tbx2a/b and both Foxi1 and Dlx3b/4b suggest that Tbx2a/b act in a novel third pathway of otic placode formation. As observed by the loss of *pax8*, Tbx2a/b likely function during a stage of otic development similar to that of Foxi1. However, unlike Foxi1 (Solomon et al., 2003; Solomon et al., 2004), otic markers at later stages are also disrupted in Tbx2a/b morphants, suggesting that Tbx2a/b are required over multiple stages of otic development.

To address the respective roles of Tbx2a/b and Foxi1 during *pax8* induction, the interactions between *foxi1* and *tbx2a/b* in pre-otic cells must be defined. Loss of Foxi1 does not ablate *tbx2a/b* expression from otic cells, indicating that Foxi1 does not act directly on *tbx2a/b*. Rather, Foxi1 may remodel chromatin to permit transcription of *tbx2a/b* as well as *pax8* because all Fox proteins contain a highly conserved DNA binding domain whose structure is remarkably similar to the winged helix structures of histones H1 and H5 (Burley et al., 1997; Cirillo et al., 1998; Clark et al., 1993; el-Deiry et al., 1992). The chromatin of cell lines transfected with zebrafish *foxi1* become more susceptible to treatment with DNaseI, suggesting that Foxi1 stably remodels chromatin

structure (Yan et al., 2006). Furthermore, when mapping 134 putative Foxi1 consensus sites to the zebrafish genome, less than 20 were found to be located within 10 kb of a putative transcriptional start site (Zeng et al., 2008). As a Foxi1 consensus is not found upstream of the *pax8* or *tbx2a/b* transcriptional start sites (not shown), Foxi1 likely acts through chromatin remodeling.

To determine how Foxi1 and Tbx2a/b interact to regulate *pax8*, it will first be necessary to determine whether Tbx2a/b are sufficient for *pax8* expression. If ectopic *tbx2a/b* can drive ectopic *pax8* expression, then it will be necessary to determine ectopic *pax8* can be induced even in the absence of Foxi1. The role of Foxi1 as a general chromatin remodeling factor may offer an explanation as to why ectopic Foxi1 cannot induce ectopic otic vesicles, as it may only permit the transcription of some otic genes through the remodeling of chromatin.

Recent evidence has begun to suggest that proper development of the ear requires integration of multiple signaling families. In addition to the inductive and maintenance phases of FGF signaling, studies in chick and mouse have demonstrated that WNT signaling is also critical in specifying the size of the otic placode (Freter et al., 2008; Jayasena et al., 2008; Ladher et al., 2000; Ohyama et al., 2007). In the absence of WNT activity, the otic placode is induced, but the resulting otic vesicle is reduced in size while cranial epidermis is expanded. Conversely, hyperactivation of WNT signaling increases the size of the otic vesicle at the expense of cranial epidermis (Ohyama et al., 2007). The *Tbx2* genes are attractive candidates for the regulation of WNT competence within the otic placode for several reasons. First, Tbx2b appears to regulate WNT activity during neural tube closure. Tbx2b morphant phenotypes can be mimicked by knocking down

the WNT receptor Fzd7a. Furthermore, overexpression of *fzd7a* mRNA in a Tbx2b-deficient background can rescue cell migration defects, suggesting that Tbx2b mediates competence to respond to WNT signaling through the regulation of *fzd7a* (Fong et al., 2005). Second, *fzd7a/b* are expressed in the otic placode during early to mid-somitogenesis (overlapping with *tbx2a/b*) (Witzel et al., 2006), suggesting that WNT activity is required during zebrafish otic development at stages analogous to the requirements observed in chick and mouse. Finally, in the context of other epithelial placodes, notably the mammary placode, FGF signaling has been demonstrated to be critical in the initiation of *Tbx* gene expression, which then acts to mediate WNT signaling (Andl et al., 2002; Boras-Granic et al., 2006; Davenport et al., 2003; Eblaghie et al., 2004; Howard and Ashworth, 2006). We are beginning to address the role of *tbx2a/b* in *pax8* induction as well as WNT signaling.

In this work, we have demonstrated tissue-specific mechanisms for regulating signaling activity. In particular, we demonstrate the strategies that two tissues, chordamesoderm and PPR, utilize to modulate BMP activity to appropriate levels for further development. Although there are direct consequence of inappropriate BMP activity on these tissues, we demonstrate that BMP misregulation can further disrupt subsequent signaling events. In chordamesoderm, increased BMP activity levels during late gastrulation elevate Hedgehog signaling from a major midline signaling center, the notochord. In the PPR, BMP activity must be attenuated to maintain competence to respond to FGF signals within the otic placode as well as the hindbrain. Our work adds to the increasing numbers of studies that demonstrate that signaling events within a

particular pathway do not occur in isolation. As transcription factors within the responding cell possess the ability to respond to multiple signaling cues and further mediate developmental events, it is critical to further characterize their roles in integrating inputs from multiple signaling centers.

References

Aberle, H., Bauer, A., Stappert, J., Kispert, A., Kemler, R., 1997. beta-catenin is a target for the ubiquitin-proteasome pathway. EMBO J. 16**,** 3797-804.

Acampora, D., Merlo, G. R., Paleari, L., Zerega, B., Postiglione, M. P., Mantero, S., Bober, E., Barbieri, O., Simeone, A., Levi, G., 1999. Craniofacial, vestibular and bone defects in mice lacking the Distal-less-related gene Dlx5. Development. 126**,** 3795-809.

Adamska, M., Herbrand, H., Adamski, M., Kruger, M., Braun, T., Bober, E., 2001. FGFs control the patterning of the inner ear but are not able to induce the full ear program. Mech Dev. 109**,** 303-13.

Adamson, E. D., Minchiotti, G., Salomon, D. S., 2002. Cripto: a tumor growth factor and more. J Cell Physiol. 190**,** 267-78.

Agathon, A., Thisse, C., Thisse, B., 2003. The molecular nature of the zebrafish tail organizer. Nature. 424**,** 448-52.

Ahrens, K., Schlosser, G., 2005. Tissues and signals involved in the induction of placodal Six1 expression in Xenopus laevis. Dev Biol. 288**,** 40-59.

Akimenko, M. A., Ekker, M., Wegner, J., Lin, W., Westerfield, M., 1994. Combinatorial expression of three zebrafish genes related to distal-less: part of a homeobox gene code for the head. J Neurosci. 14**,** 3475-86.

Alvarez, Y., Alonso, M. T., Vendrell, V., Zelarayan, L. C., Chamero, P., Theil, T., Bosl, M. R., Kato, S., Maconochie, M., Riethmacher, D., Schimmang, T., 2003. Requirements for FGF3 and FGF10 during inner ear formation. Development. 130**,** 6329-38.

Amacher, S. L., Draper, B. W., Summers, B. R., Kimmel, C. B., 2002. The zebrafish T-box genes no tail and spadetail are required for development of trunk and tail mesoderm and medial floor plate. Development. 129**,** 3311-23.

Amacher, S. L., Kimmel, C. B., 1998. Promoting notochord fate and repressing muscle development in zebrafish axial mesoderm. Development. 125**,** 1397-406.

Ambrosio, A. L., Taelman, V. F., Lee, H. X., Metzinger, C. A., Coffinier, C., De Robertis, E. M., 2008. Crossveinless-2 Is a BMP feedback inhibitor that binds Chordin/BMP to regulate Xenopus embryonic patterning. Dev Cell. 15**,** 248-60.

Amit, S., Hatzubai, A., Birman, Y., Andersen, J. S., Ben-Shushan, E., Mann, M., Ben-Neriah, Y., Alkalay, I., 2002. Axin-mediated CKI phosphorylation of beta-catenin at Ser 45: a molecular switch for the Wnt pathway. Genes Dev. 16**,** 1066-76.

Andl, T., Reddy, S. T., Gaddapara, T., Millar, S. E., 2002. WNT signals are required for the initiation of hair follicle development. Dev Cell. 2**,** 643-53.

Aubert, J., Dunstan, H., Chambers, I., Smith, A., 2002. Functional gene screening in embryonic stem cells implicates Wnt antagonism in neural differentiation. Nat Biotechnol. 20**,** 1240-5.

Aybar, M. J., Mayor, R., 2002. Early induction of neural crest cells: lessons learned from frog, fish and chick. Curr Opin Genet Dev. 12**,** 452-8.

Bailey, A. P., Bhattacharyya, S., Bronner-Fraser, M., Streit, A., 2006. Lens specification is the ground state of all sensory placodes, from which FGF promotes olfactory identity. Dev Cell. 11**,** 505-17.

Bailey, A. P., Streit, A., 2006. Sensory organs: making and breaking the pre-placodal region. Curr Top Dev Biol. 72**,** 167-204.

Baker, C. V., Bronner-Fraser, M., 1997. The origins of the neural crest. Part I: embryonic induction. Mech Dev. 69**,** 3-11.

Bamford, R. N., Roessler, E., Burdine, R. D., Saplakoglu, U., dela Cruz, J., Splitt, M., Goodship, J. A., Towbin, J., Bowers, P., Ferrero, G. B., Marino, B., Schier, A. F., Shen, M. M., Muenke, M., Casey, B., 2000. Loss-of-function mutations in the EGF-CFC gene CFC1 are associated with human left-right laterality defects. Nat Genet. 26**,** 365-9.

Barresi, M. J., Stickney, H. L., Devoto, S. H., 2000. The zebrafish slow-muscle-omitted gene product is required for Hedgehog signal transduction and the development of slow muscle identity. Development. 127**,** 2189-99.

Bauer, H., Lele, Z., Rauch, G. J., Geisler, R., Hammerschmidt, M., 2001. The type I serine/threonine kinase receptor Alk8/Lost-a-fin is required for Bmp2b/7 signal transduction during dorsoventral patterning of the zebrafish embryo. Development. 128**,** 849-58.

Bauer, H., Meier, A., Hild, M., Stachel, S., Economides, A., Hazelett, D., Harland, R. M., Hammerschmidt, M., 1998. Follistatin and noggin are excluded from the zebrafish organizer. Dev Biol. 204**,** 488-507.

Beck, C. W., Whitman, M., Slack, J. M., 2001. The role of BMP signaling in outgrowth and patterning of the Xenopus tail bud. Dev Biol. 238**,** 303-14.

Beer, J. S. H. a. G. R. d., 1934. The Elements of Experimental Embryology. Cambridge.

Beetschen, J. C., 2001. Amphibian gastrulation: history and evolution of a 125 year-old concept. Int J Dev Biol. 45**,** 771-95.

Behrens, J., von Kries, J. P., Kuhl, M., Bruhn, L., Wedlich, D., Grosschedl, R., Birchmeier, W., 1996. Functional interaction of beta-catenin with the transcription factor LEF-1. Nature. 382**,** 638-42.

Ben-Zvi, D., Shilo, B. Z., Fainsod, A., Barkai, N., 2008. Scaling of the BMP activation gradient in Xenopus embryos. Nature. 453**,** 1205-11.

Bessarab, D. A., Chong, S. W., Korzh, V., 2004. Expression of zebrafish six1 during sensory organ development and myogenesis. Dev Dyn. 230**,** 781-6.

Bhatia, M., Bonnet, D., Wu, D., Murdoch, B., Wrana, J., Gallacher, L., Dick, J. E., 1999. Bone morphogenetic proteins regulate the developmental program of human hematopoietic stem cells. J Exp Med. 189**,** 1139-48.

Bhattacharyya, S., Bailey, A. P., Bronner-Fraser, M., Streit, A., 2004. Segregation of lens and olfactory precursors from a common territory: cell sorting and reciprocity of Dlx5 and Pax6 expression. Dev Biol. 271**,** 403-14.

Bier, E., 2008. Intriguing extracellular regulation of BMP signaling. Dev Cell. 15**,** 176-7.

Birsoy, B., Kofron, M., Schaible, K., Wylie, C., Heasman, J., 2006. Vg 1 is an essential signaling molecule in Xenopus development. Development. 133**,** 15-20.

Blader, P., Rastegar, S., Fischer, N., Strahle, U., 1997. Cleavage of the BMP-4 antagonist chordin by zebrafish tolloid. Science. 278**,** 1937-40.

Boras-Granic, K., Chang, H., Grosschedl, R., Hamel, P. A., 2006. Lef1 is required for the transition of Wnt signaling from mesenchymal to epithelial cells in the mouse embryonic mammary gland. Dev Biol. 295**,** 219-31.

Bottcher, R. T., Niehrs, C., 2005. Fibroblast growth factor signaling during early vertebrate development. Endocr Rev. 26**,** 63-77.

Brannon, M., Gomperts, M., Sumoy, L., Moon, R. T., Kimelman, D., 1997. A beta-catenin/XTcf-3 complex binds to the siamois promoter to regulate dorsal axis specification in Xenopus. Genes Dev. 11**,** 2359-70.

Brugmann, S. A., Moody, S. A., 2005. Induction and specification of the vertebrate ectodermal placodes: precursors of the cranial sensory organs. Biol Cell. 97**,** 303-19.

Brugmann, S. A., Pandur, P. D., Kenyon, K. L., Pignoni, F., Moody, S. A., 2004. Six1 promotes a placodal fate within the lateral neurogenic ectoderm by functioning as both a transcriptional activator and repressor. Development. 131**,** 5871-81.

Burley, S. K., Xie, X., Clark, K. L., Shu, F., 1997. Histone-like transcription factors in eukaryotes. Curr Opin Struct Biol. 7**,** 94-102.

Cambray, N., Wilson, V., 2002. Axial progenitors with extensive potency are localised to the mouse chordoneural hinge. Development. 129**,** 4855-66.

Cambray, N., Wilson, V., 2007. Two distinct sources for a population of maturing axial progenitors. Development. 134**,** 2829-40.

Carroll, S. B., Grenier, J.K., Weathebee, S.D., 2001. From DNA to Diversity: Molecular Genetics and the Evolution of Animal Design. Blackwell Sciences, Malden.

Cavallo, R. A., Cox, R. T., Moline, M. M., Roose, J., Polevoy, G. A., Clevers, H., Peifer, M., Bejsovec, A., 1998. Drosophila Tcf and Groucho interact to repress Wingless signalling activity. Nature. 395**,** 604-8.

Charrier, J. B., Teillet, M. A., Lapointe, F., Le Douarin, N. M., 1999. Defining subregions of Hensen's node essential for caudalward movement, midline development and cell survival. Development. 126**,** 4771-83.

Chen, W., Casey Corliss, D., 2004. Three modules of zebrafish Mind bomb work cooperatively to promote Delta ubiquitination and endocytosis. Dev Biol. 267**,** 361-73.

Chiang, E. F., Pai, C. I., Wyatt, M., Yan, Y. L., Postlethwait, J., Chung, B., 2001. Two sox9 genes on duplicated zebrafish chromosomes: expression of similar transcription activators in distinct sites. Dev Biol. 231**,** 149-63.

Chocron, S., Verhoeven, M. C., Rentzsch, F., Hammerschmidt, M., Bakkers, J., 2007. Zebrafish Bmp4 regulates left-right asymmetry at two distinct developmental time points. Dev Biol. 305**,** 577-88.

Christ, B., Huang, R., Scaal, M., 2004. Formation and differentiation of the avian sclerotome. Anat Embryol (Berl). 208**,** 333-50.

Cirillo, L. A., McPherson, C. E., Bossard, P., Stevens, K., Cherian, S., Shim, E. Y., Clark, K. L., Burley, S. K., Zaret, K. S., 1998. Binding of the winged-helix transcription factor HNF3 to a linker histone site on the nucleosome. EMBO J. 17**,** 244-54.

Clark, K. L., Halay, E. D., Lai, E., Burley, S. K., 1993. Co-crystal structure of the HNF-3/fork head DNA-recognition motif resembles histone H5. Nature. 364**,** 412-20.

Coffinier, C., Ketpura, N., Tran, U., Geissert, D., De Robertis, E. M., 2002. Mouse Crossveinless-2 is the vertebrate homolog of a Drosophila extracellular regulator of BMP signaling. Mech Dev. 119 Suppl 1**,** S179-84.

Coles, E., Christiansen, J., Economou, A., Bronner-Fraser, M., Wilkinson, D. G., 2004. A vertebrate crossveinless 2 homologue modulates BMP activity and neural crest cell migration. Development. 131**,** 5309-17.

Connors, S. A., Trout, J., Ekker, M., Mullins, M. C., 1999. The role of tolloid/mini fin in dorsoventral pattern formation of the zebrafish embryo. Development. 126**,** 3119-30.

Connors, S. A., Tucker, J. A., Mullins, M. C., 2006. Temporal and spatial action of tolloid (mini fin) and chordin to pattern tail tissues. Dev Biol. 293**,** 191-202.

Cox, R. T., Pai, L. M., Miller, J. R., Orsulic, S., Stein, J., McCormick, C. A., Audeh, Y., Wang, W., Moon, R. T., Peifer, M., 1999. Membrane-tethered Drosophila Armadillo cannot transduce Wingless signal on its own. Development. 126**,** 1327-35.

Currie, P. D., Ingham, P. W., 1996. Induction of a specific muscle cell type by a hedgehog-like protein in zebrafish. Nature. 382**,** 452-5.

Cvekl, A., Duncan, M. K., 2007. Genetic and epigenetic mechanisms of gene regulation during lens development. Prog Retin Eye Res. 26**,** 555-97.

Dal-Pra, S., Furthauer, M., Van-Celst, J., Thisse, B., Thisse, C., 2006. Noggin1 and Follistatin-like2 function redundantly to Chordin to antagonize BMP activity. Dev Biol. 298**,** 514-26.

Dale, L., Howes, G., Price, B. M., Smith, J. C., 1992. Bone morphogenetic protein 4: a ventralizing factor in early Xenopus development. Development. 115**,** 573-85.

Danos, M. C., Yost, H. J., 1995. Linkage of cardiac left-right asymmetry and dorsal-anterior development in Xenopus. Development. 121**,** 1467-74.

Davenport, T. G., Jerome-Majewska, L. A., Papaioannou, V. E., 2003. Mammary gland, limb and yolk sac defects in mice lacking Tbx3, the gene mutated in human ulnar mammary syndrome. Development. 130**,** 2263-73.

David, R., Ahrens, K., Wedlich, D., Schlosser, G., 2001. Xenopus Eya1 demarcates all neurogenic placodes as well as migrating hypaxial muscle precursors. Mech Dev. 103**,** 189-92.

Davis, R. L., Kirschner, M. W., 2000. The fate of cells in the tailbud of Xenopus laevis. Development. 127**,** 255-67.

De Robertis, E. M., 2006. Spemann's organizer and self-regulation in amphibian embryos. Nat Rev Mol Cell Biol. 7**,** 296-302.

De Robertis, E. M., Kuroda, H., 2004. Dorsal-ventral patterning and neural induction in Xenopus embryos. Annu Rev Cell Dev Biol. 20**,** 285-308.

De Robertis, E. M., Larrain, J., Oelgeschlager, M., Wessely, O., 2000. The establishment of Spemann's organizer and patterning of the vertebrate embryo. Nat Rev Genet. 1**,** 171-81.

De Robertis, E. M., Morita, E. A., Cho, K. W., 1991. Gradient fields and homeobox genes. Development. 112**,** 669-78.

Denef, N., Neubuser, D., Perez, L., Cohen, S. M., 2000. Hedgehog induces opposite changes in turnover and subcellular localization of patched and smoothened. Cell. 102**,** 521-31.

Devoto, S. H., Melancon, E., Eisen, J. S., Westerfield, M., 1996. Identification of separate slow and fast muscle precursor cells in vivo, prior to somite formation. Development. 122**,** 3371-80.

Dheen, T., Sleptsova-Friedrich, I., Xu, Y., Clark, M., Lehrach, H., Gong, Z., Korzh, V., 1999. Zebrafish tbx-c functions during formation of midline structures. Development. 126**,** 2703-13.

Dickmeis, T., Rastegar, S., Aanstad, P., Clark, M., Fischer, N., Korzh, V., Strahle, U., 2001. Expression of the anti-dorsalizing morphogenetic protein gene in the zebrafish embryo. Dev Genes Evol. 211**,** 568-72.

Dolle, P., Lufkin, T., Krumlauf, R., Mark, M., Duboule, D., Chambon, P., 1993. Local alterations of Krox-20 and Hox gene expression in the hindbrain suggest lack of rhombomeres 4 and 5 in homozygote null Hoxa-1 (Hox-1.6) mutant embryos. Proc Natl Acad Sci U S A. 90**,** 7666-70.

Dorsky, R. I., Itoh, M., Moon, R. T., Chitnis, A., 2003. Two tcf3 genes cooperate to pattern the zebrafish brain. Development. 130**,** 1937-47.

Dosch, R., Niehrs, C., 2000. Requirement for anti-dorsalizing morphogenetic protein in organizer patterning. Mech Dev. 90**,** 195-203.

Dougan, S. T., Warga, R. M., Kane, D. A., Schier, A. F., Talbot, W. S., 2003. The role of the zebrafish nodal-related genes squint and cyclops in patterning of mesendoderm. Development. 130**,** 1837-51.

Draper, B. W., Stock, D. W., Kimmel, C. B., 2003. Zebrafish fgf24 functions with fgf8 to promote posterior mesodermal development. Development. 130**,** 4639-54.

Driesch, H., 1892. The potency of the first two cleavage cells in echinoderm development: Experimental production of partial and double formations. Hafner, New York.

Driesch, H., 1893. Zur Verlagerung der Blastomeren des Echinideneies. Anat. Anz. 8**,** 348-357.

Eaton, R. C., Emberley, D. S., 1991. How stimulus direction determines the trajectory of the Mauthner-initiated escape response in a teleost fish. J Exp Biol. 161**,** 469-87.

Eaton, R. C., Lee, R. K., Foreman, M. B., 2001. The Mauthner cell and other identified neurons of the brainstem escape network of fish. Prog Neurobiol. 63**,** 467-85.

Eblaghie, M. C., Song, S. J., Kim, J. Y., Akita, K., Tickle, C., Jung, H. S., 2004. Interactions between FGF and Wnt signals and Tbx3 gene expression in mammary gland initiation in mouse embryos. J Anat. 205**,** 1-13.

Eichmann, A., Grapin-Botton, A., Kelly, L., Graf, T., Le Douarin, N. M., Sieweke, M., 1997. The expression pattern of the mafB/kr gene in birds and mice reveals that the kreisler phenotype does not represent a null mutant. Mech Dev. 65**,** 111-22.

Eivers, E., Fuentealba, L. C., De Robertis, E., 2008. Integrating positional information at the level of Smad1/5/8. Curr Opin Genet Dev.

Ekker, M., Akimenko, M. A., Bremiller, R., Westerfield, M., 1992. Regional expression of three homeobox transcripts in the inner ear of zebrafish embryos. Neuron. 9**,** 27-35.

el-Deiry, W. S., Kern, S. E., Pietenpol, J. A., Kinzler, K. W., Vogelstein, B., 1992. Definition of a consensus binding site for p53. Nat Genet. 1**,** 45-9.

Ellies, D. L., Stock, D. W., Hatch, G., Giroux, G., Weiss, K. M., Ekker, M., 1997. Relationship between the genomic organization and the overlapping embryonic expression patterns of the zebrafish dlx genes. Genomics. 45**,** 580-90.

Erter, C. E., Solnica-Krezel, L., Wright, C. V., 1998. Zebrafish nodal-related 2 encodes an early mesendodermal inducer signaling from the extraembryonic yolk syncytial layer. Dev Biol. 204**,** 361-72.

Erter, C. E., Wilm, T. P., Basler, N., Wright, C. V., Solnica-Krezel, L., 2001. Wnt8 is required in lateral mesendodermal precursors for neural posteriorization in vivo. Development. 128**,** 3571-83.

Eswarakumar, V. P., Lax, I., Schlessinger, J., 2005. Cellular signaling by fibroblast growth factor receptors. Cytokine Growth Factor Rev. 16**,** 139-49.

Faber, D. S., Fetcho, J. R., Korn, H., 1989. Neuronal networks underlying the escape response in goldfish. General implications for motor control. Ann N Y Acad Sci. 563**,** 11-33.

Fainsod, A., Deissler, K., Yelin, R., Marom, K., Epstein, M., Pillemer, G., Steinbeisser, H., Blum, M., 1997. The dorsalizing and neural inducing gene follistatin is an antagonist of BMP-4. Mech Dev. 63**,** 39-50.

Fekany, K., Yamanaka, Y., Leung, T., Sirotkin, H. I., Topczewski, J., Gates, M. A., Hibi, M., Renucci, A., Stemple, D., Radbill, A., Schier, A. F., Driever, W., Hirano, T., Talbot, W. S., Solnica-Krezel, L., 1999. The zebrafish bozozok locus encodes Dharma, a homeodomain protein essential for induction of gastrula organizer and dorsoanterior embryonic structures. Development. 126**,** 1427-38.

Feledy, J. A., Morasso, M. I., Jang, S. I., Sargent, T. D., 1999. Transcriptional activation by the homeodomain protein distal-less 3. Nucleic Acids Res. 27**,** 764-70.

Fischer, S., Draper, B. W., Neumann, C. J., 2003. The zebrafish fgf24 mutant identifies an additional level of Fgf signaling involved in vertebrate forelimb initiation. Development. 130**,** 3515-24.

Fong, S. H., Emelyanov, A., Teh, C., Korzh, V., 2005. Wnt signalling mediated by Tbx2b regulates cell migration during formation of the neural plate. Development. 132**,** 3587-96.

Freter, S., Muta, Y., Mak, S. S., Rinkwitz, S., Ladher, R. K., 2008. Progressive restriction of otic fate: the role of FGF and Wnt in resolving inner ear potential. Development. 135**,** 3415-24.

Fuentealba, L. C., Eivers, E., Ikeda, A., Hurtado, C., Kuroda, H., Pera, E. M., De Robertis, E. M., 2007. Integrating patterning signals: Wnt/GSK3 regulates the duration of the BMP/Smad1 signal. Cell. 131**,** 980-93.

Fürthauer, M., Lin, W., Ang, S. L., Thisse, B., Thisse, C., 2002. Sef is a feedback-induced antagonist of Ras/MAPK-mediated FGF signalling. Nat Cell Biol. 4**,** 170-4.

Fürthauer, M., Reifers, F., Brand, M., Thisse, B., Thisse, C., 2001. sprouty4 acts in vivo as a feedback-induced antagonist of FGF signaling in zebrafish. Development. 128**,** 2175-86.

Fürthauer, M., Thisse, B., Thisse, C., 1999. Three different noggin genes antagonize the activity of bone morphogenetic proteins in the zebrafish embryo. Dev Biol. 214**,** 181-96.

Fürthauer, M., Thisse, C., Thisse, B., 1997. A role for FGF-8 in the dorsoventral patterning of the zebrafish gastrula. Development. 124**,** 4253-64.

Fürthauer, M., Van Celst, J., Thisse, C., Thisse, B., 2004. Fgf signalling controls the dorsoventral patterning of the zebrafish embryo. Development. 131**,** 2853-64.

Gahtan, E., Baier, H., 2004. Of lasers, mutants, and see-through brains: functional neuroanatomy in zebrafish. J Neurobiol. 59**,** 147-61.

Gahtan, E., O'Malley, D. M., 2003. Visually guided injection of identified reticulospinal neurons in zebrafish: a survey of spinal arborization patterns. J Comp Neurol. 459**,** 186-200.

Gallagher, B. C., Henry, J. J., Grainger, R. M., 1996. Inductive processes leading to inner ear formation during Xenopus development. Dev Biol. 175**,** 95-107.

Ganan, Y., Macias, D., Duterque-Coquillaud, M., Ros, M. A., Hurle, J. M., 1996. Role of TGF beta s and BMPs as signals controlling the position of the digits and the areas of interdigital cell death in the developing chick limb autopod. Development. 122**,** 2349-57.

Gans, C., Northcutt, R. G., 1983. Neural Crest and the Origin of Vertebrates: A New Head. Science. 220**,** 268-273.

Gestri, G., Carl, M., Appolloni, I., Wilson, S. W., Barsacchi, G., Andreazzoli, M., 2005. Six3 functions in anterior neural plate specification by promoting cell proliferation and inhibiting Bmp4 expression. Development. 132**,** 2401-13.

Gibson-Brown, J. J., S, I. A., Silver, L. M., Papaioannou, V. E., 1998. Expression of T-box genes Tbx2-Tbx5 during chick organogenesis. Mech Dev. 74**,** 165-9.

Gilmour, D. T., Maischein, H. M., Nusslein-Volhard, C., 2002. Migration and function of a glial subtype in the vertebrate peripheral nervous system. Neuron. 34**,** 577-88.

Giudicelli, F., Gilardi-Hebenstreit, P., Mechta-Grigoriou, F., Poquet, C., Charnay, P., 2003. Novel activities of Mafb underlie its dual role in hindbrain segmentation and regional specification. Dev Biol. 253**,** 150-62.

Glavic, A., Maris Honore, S., Gloria Feijoo, C., Bastidas, F., Allende, M. L., Mayor, R., 2004. Role of BMP signaling and the homeoprotein Iroquois in the specification of the cranial placodal field. Dev Biol. 272**,** 89-103.

Glinka, A., Wu, W., Onichtchouk, D., Blumenstock, C., Niehrs, C., 1997. Head induction by simultaneous repression of Bmp and Wnt signalling in Xenopus. Nature. 389**,** 517-9.

Gont, L. K., Steinbeisser, H., Blumberg, B., de Robertis, E. M., 1993. Tail formation as a continuation of gastrulation: the multiple cell populations of the Xenopus tailbud derive from the late blastopore lip. Development. 119**,** 991-1004.

Goodman, S. A., Albano, R., Wardle, F. C., Matthews, G., Tannahill, D., Dale, L., 1998. BMP1-related metalloproteinases promote the development of ventral mesoderm in early Xenopus embryos. Dev Biol. 195**,** 144-57.

Griffin, K., Patient, R., Holder, N., 1995. Analysis of FGF function in normal and no tail zebrafish embryos reveals separate mechanisms for formation of the trunk and the tail. Development. 121**,** 2983-94.

Griffin, K. J., Amacher, S. L., Kimmel, C. B., Kimelman, D., 1998. Molecular identification of spadetail: regulation of zebrafish trunk and tail mesoderm formation by T-box genes. Development. 125**,** 3379-88.

Griffin, K. J., Kimelman, D., 2002. One-Eyed Pinhead and Spadetail are essential for heart and somite formation. Nat Cell Biol. 4**,** 821-5.

Griffin, K. J., Kimelman, D., 2003. Interplay between FGF, one-eyed pinhead, and T-box transcription factors during zebrafish posterior development. Dev Biol. 264**,** 456-66.

Gritsman, K., Talbot, W. S., Schier, A. F., 2000. Nodal signaling patterns the organizer. Development. 127**,** 921-32.

Groves, A. K., Bronner-Fraser, M., 2000. Competence, specification and commitment in otic placode induction. Development. 127**,** 3489-99.

Hagos, E. G., Dougan, S. T., 2007. Time-dependent patterning of the mesoderm and endoderm by Nodal signals in zebrafish. BMC Dev Biol. 7**,** 22.

Halpern, M. E., Hatta, K., Amacher, S. L., Talbot, W. S., Yan, Y. L., Thisse, B., Thisse, C., Postlethwait, J. H., Kimmel, C. B., 1997. Genetic interactions in zebrafish midline development. Dev Biol. 187**,** 154-70.

Halpern, M. E., Ho, R. K., Walker, C., Kimmel, C. B., 1993. Induction of muscle pioneers and floor plate is distinguished by the zebrafish no tail mutation. Cell. 75**,** 99-111.

Halpern, M. E., Thisse, C., Ho, R. K., Thisse, B., Riggleman, B., Trevarrow, B., Weinberg, E. S., Postlethwait, J. H., Kimmel, C. B., 1995. Cell-autonomous shift from axial to paraxial mesodermal development in zebrafish floating head mutants. Development. 121**,** 4257-64.

Hammerschmidt, M., Pelegri, F., Mullins, M. C., Kane, D. A., van Eeden, F. J., Granato, M., Brand, M., Furutani-Seiki, M., Haffter, P., Heisenberg, C. P., Jiang, Y. J., Kelsh, R. N., Odenthal, J., Warga, R. M., Nusslein-Volhard, C., 1996a. dino and mercedes, two genes regulating dorsal development in the zebrafish embryo. Development. 123**,** 95-102.

Hammerschmidt, M., Serbedzija, G. N., McMahon, A. P., 1996b. Genetic analysis of dorsoventral pattern formation in the zebrafish: requirement of a BMP-like ventralizing activity and its dorsal repressor. Genes Dev. 10**,** 2452-61.

Hammond, C. L., Hinits, Y., Osborn, D. P., Minchin, J. E., Tettamanti, G., Hughes, S. M., 2007. Signals and myogenic regulatory factors restrict pax3 and pax7 expression to dermomyotome-like tissue in zebrafish. Dev Biol. 302**,** 504-21.

Hans, S., Christison, J., Liu, D., Westerfield, M., 2007. Fgf-dependent otic induction requires competence provided by Foxi1 and Dlx3b. BMC Dev Biol. 7**,** 5.

Hans, S., Liu, D., Westerfield, M., 2004. Pax8 and Pax2a function synergistically in otic specification, downstream of the Foxi1 and Dlx3b transcription factors. Development. 131**,** 5091-102.

Harland, R. M., 1994. Neural induction in Xenopus. Curr Opin Genet Dev. 4**,** 543-9.

Harrelson, Z., Papaioannou, V. E., 2006. Segmental expression of the T-box transcription factor, Tbx2, during early somitogenesis. Dev Dyn. 235**,** 3080-4.

Harrington, A. E., Morris-Triggs, S. A., Ruotolo, B. T., Robinson, C. V., Ohnuma, S., Hyvonen, M., 2006. Structural basis for the inhibition of activin signalling by follistatin. EMBO J. 25**,** 1035-45.

Harrison, R. G., 1918. Experiments on the development of the fore-limb of Amblystoma, a self-differentiating equipotential system. J. Exp. Zool. 25**,** 413-461.

Hart, M. J., de los Santos, R., Albert, I. N., Rubinfeld, B., Polakis, P., 1998. Downregulation of beta-catenin by human Axin and its association with the APC tumor suppressor, beta-catenin and GSK3 beta. Curr Biol. 8**,** 573-81.

Heinke, J., Wehofsits, L., Zhou, Q., Zoeller, C., Baar, K. M., Helbing, T., Laib, A., Augustin, H., Bode, C., Patterson, C., Moser, M., 2008. BMPER Is an Endothelial

Cell Regulator and Controls Bone Morphogenetic Protein-4-Dependent Angiogenesis. Circ Res.

Heisenberg, C. P., Houart, C., Take-Uchi, M., Rauch, G. J., Young, N., Coutinho, P., Masai, I., Caneparo, L., Concha, M. L., Geisler, R., Dale, T. C., Wilson, S. W., Stemple, D. L., 2001. A mutation in the Gsk3-binding domain of zebrafish Masterblind/Axin1 leads to a fate transformation of telencephalon and eyes to diencephalon. Genes Dev. 15**,** 1427-34.

Heisenberg, C. P., Tada, M., 2002. Zebrafish gastrulation movements: bridging cell and developmental biology. Semin Cell Dev Biol. 13**,** 471-9.

Helmbacher, F., Pujades, C., Desmarquet, C., Frain, M., Rijli, F. M., Chambon, P., Charnay, P., 1998. Hoxa1 and Krox-20 synergize to control the development of rhombomere 3. Development. 125**,** 4739-48.

Herzog, W., Sonntag, C., von der Hardt, S., Roehl, H. H., Varga, Z. M., Hammerschmidt, M., 2004. Fgf3 signaling from the ventral diencephalon is required for early specification and subsequent survival of the zebrafish adenohypophysis. Development. 131**,** 3681-92.

Higashijima, S., Hotta, Y., Okamoto, H., 2000. Visualization of cranial motor neurons in live transgenic zebrafish expressing green fluorescent protein under the control of the islet-1 promoter/enhancer. J Neurosci. 20**,** 206-18.

Holland, L. Z., Holland, N. D., 2001. Evolution of neural crest and placodes: amphioxus as a model for the ancestral vertebrate? J Anat. 199**,** 85-98.

Holley, S. A., 2006. Anterior-posterior differences in vertebrate segments: specification of trunk and tail somites in the zebrafish blastula. Genes Dev. 20**,** 1831-7.

Hopkins, D. R., Keles, S., Greenspan, D. S., 2007. The bone morphogenetic protein 1/Tolloid-like metalloproteinases. Matrix Biol. 26**,** 508-23.

Howard, B., Ashworth, A., 2006. Signalling pathways implicated in early mammary gland morphogenesis and breast cancer. PLoS Genet. 2**,** e112.

Hurtado, C., De Robertis, E. M., 2007. Neural induction in the absence of organizer in salamanders is mediated by MAPK. Dev Biol. 307**,** 282-9.

Iemura, S., Yamamoto, T. S., Takagi, C., Uchiyama, H., Natsume, T., Shimasaki, S., Sugino, H., Ueno, N., 1998. Direct binding of follistatin to a complex of bone-morphogenetic protein and its receptor inhibits ventral and epidermal cell fates in early Xenopus embryo. Proc Natl Acad Sci U S A. 95**,** 9337-42.

Imai, Y., Gates, M. A., Melby, A. E., Kimelman, D., Schier, A. F., Talbot, W. S., 2001. The homeobox genes vox and vent are redundant repressors of dorsal fates in zebrafish. Development. 128**,** 2407-20.

Itoh, M., Kim, C. H., Palardy, G., Oda, T., Jiang, Y. J., Maust, D., Yeo, S. Y., Lorick, K., Wright, G. J., Ariza-McNaughton, L., Weissman, A. M., Lewis, J., Chandrasekharappa, S. C., Chitnis, A. B., 2003. Mind bomb is a ubiquitin ligase that is essential for efficient activation of Notch signaling by Delta. Dev Cell. 4**,** 67-82.

Itoh, N., Ornitz, D. M., 2004. Evolution of the Fgf and Fgfr gene families. Trends Genet. 20**,** 563-9.

Itoh, N., Ornitz, D. M., 2008. Functional evolutionary history of the mouse Fgf gene family. Dev Dyn. 237**,** 18-27.

Jacobson, A. G., 1963. The Determination and Positioning of the Nose, Lens and Ear. Iii. Effects of Reversing the Antero-Posterior Axis of Epidermis, Neural Plate and Neural Fold. J Exp Zool. 154**,** 293-303.

Jayasena, C. S., Ohyama, T., Segil, N., Groves, A. K., 2008. Notch signaling augments the canonical Wnt pathway to specify the size of the otic placode. Development. 135**,** 2251-61.

Jiao, J., Greendorfer, J. S., Zhang, P., Zinn, K. R., Diglio, C. A., Thompson, J. A., 2003. Alternatively spliced FGFR-1 isoform signaling differentially modulates endothelial cell responses to peroxynitrite. Arch Biochem Biophys. 410**,** 187-200.

Joly, J. S., Joly, C., Schulte-Merker, S., Boulekbache, H., Condamine, H., 1993. The ventral and posterior expression of the zebrafish homeobox gene eve1 is perturbed in dorsalized and mutant embryos. Development. 119**,** 1261-75.

Kaji, T., Artinger, K. B., 2004. dlx3b and dlx4b function in the development of Rohon-Beard sensory neurons and trigeminal placode in the zebrafish neurula. Dev Biol. 276**,** 523-40.

Kanki, J. P., Ho, R. K., 1997. The development of the posterior body in zebrafish. Development. 124**,** 881-93.

Kawahara, A., Wilm, T., Solnica-Krezel, L., Dawid, I. B., 2000. Antagonistic role of vega1 and bozozok/dharma homeobox genes in organizer formation. Proc Natl Acad Sci U S A. 97**,** 12121-6.

Kelly, C., Chin, A. J., Leatherman, J. L., Kozlowski, D. J., Weinberg, E. S., 2000. Maternally controlled (beta)-catenin-mediated signaling is required for organizer formation in the zebrafish. Development. 127**,** 3899-911.

Kelly, G. M., Greenstein, P., Erezyilmaz, D. F., Moon, R. T., 1995. Zebrafish wnt8 and wnt8b share a common activity but are involved in distinct developmental pathways. Development. 121**,** 1787-99.

Khokha, M. K., Yeh, J., Grammer, T. C., Harland, R. M., 2005. Depletion of three BMP antagonists from Spemann's organizer leads to a catastrophic loss of dorsal structures. Dev Cell. 8**,** 401-11.

Kicheva, A., Gonzalez-Gaitan, M., 2008. The Decapentaplegic morphogen gradient: a precise definition. Curr Opin Cell Biol. 20**,** 137-43.

Kil, S. H., Streit, A., Brown, S. T., Agrawal, N., Collazo, A., Zile, M. H., Groves, A. K., 2005. Distinct roles for hindbrain and paraxial mesoderm in the induction and patterning of the inner ear revealed by a study of vitamin-A-deficient quail. Dev Biol. 285**,** 252-71.

Kim, C. H., Oda, T., Itoh, M., Jiang, D., Artinger, K. B., Chandrasekharappa, S. C., Driever, W., Chitnis, A. B., 2000. Repressor activity of Headless/Tcf3 is essential for vertebrate head formation. Nature. 407**,** 913-6.

Kimelman, D., 2006. Mesoderm induction: from caps to chips. Nat Rev Genet. 7**,** 360-72.

Kimelman, D., Kirschner, M., 1987. Synergistic induction of mesoderm by FGF and TGF-beta and the identification of an mRNA coding for FGF in the early Xenopus embryo. Cell. 51**,** 869-77.

Kimelman, D., Pyati, U. J., 2005. Bmp signaling: turning a half into a whole. Cell. 123**,** 982-4.

Kimelman, D., Szeto, D. P., 2006. Chordin cleavage is sizzling. Nat Cell Biol. 8**,** 305-7.

Kimmel, C. B., Ballard, W. W., Kimmel, S. R., Ullmann, B., Schilling, T. F., 1995. Stages of embryonic development of the zebrafish. Dev Dyn. 203**,** 253-310.

Kimmel, C. B., Powell, S. L., Metcalfe, W. K., 1982. Brain neurons which project to the spinal cord in young larvae of the zebrafish. J Comp Neurol. 205**,** 112-27.

Kimmel, C. B., Warga, R. M., Schilling, T. F., 1990. Origin and organization of the zebrafish fate map. Development. 108**,** 581-94.

Kinoshita, N., Minshull, J., Kirschner, M. W., 1995. The identification of two novel ligands of the FGF receptor by a yeast screening method and their activity in Xenopus development. Cell. 83**,** 621-30.

Kishida, S., Yamamoto, H., Ikeda, S., Kishida, M., Sakamoto, I., Koyama, S., Kikuchi, A., 1998. Axin, a negative regulator of the wnt signaling pathway, directly interacts with adenomatous polyposis coli and regulates the stabilization of beta-catenin. J Biol Chem. 273**,** 10823-6.

Kishimoto, Y., Lee, K. H., Zon, L., Hammerschmidt, M., Schulte-Merker, S., 1997. The molecular nature of zebrafish swirl: BMP2 function is essential during early dorsoventral patterning. Development. 124**,** 4457-66.

Kitisin, K., Saha, T., Blake, T., Golestaneh, N., Deng, M., Kim, C., Tang, Y., Shetty, K., Mishra, B., Mishra, L., 2007. Tgf-Beta signaling in development. Sci STKE. 2007**,** cm1.

Knockaert, M., Sapkota, G., Alarcon, C., Massague, J., Brivanlou, A. H., 2006. Unique players in the BMP pathway: small C-terminal domain phosphatases dephosphorylate Smad1 to attenuate BMP signaling. Proc Natl Acad Sci U S A. 103**,** 11940-5.

Kobayashi, M., Osanai, H., Kawakami, K., Yamamoto, M., 2000. Expression of three zebrafish Six4 genes in the cranial sensory placodes and the developing somites. Mech Dev. 98**,** 151-5.

Komoike, Y., Kawamura, A., Shindo, N., Sato, C., Satoh, J., Shiurba, R., Higashinakagawa, T., 2005. Zebrafish Polycomb group gene ph2alpha is required for epiboly and tailbud formation acting downstream of FGF signaling. Biochem Biophys Res Commun. 328**,** 858-66.

Koo, B. K., Lim, H. S., Song, R., Yoon, M. J., Yoon, K. J., Moon, J. S., Kim, Y. W., Kwon, M. C., Yoo, K. W., Kong, M. P., Lee, J., Chitnis, A. B., Kim, C. H., Kong, Y. Y., 2005a. Mind bomb 1 is essential for generating functional Notch ligands to activate Notch. Development. 132**,** 3459-70.

Koo, B. K., Yoon, K. J., Yoo, K. W., Lim, H. S., Song, R., So, J. H., Kim, C. H., Kong, Y. Y., 2005b. Mind bomb-2 is an E3 ligase for Notch ligand. J Biol Chem. 280**,** 22335-42.

Kornberg, T. B., Guha, A., 2007. Understanding morphogen gradients: a problem of dispersion and containment. Curr Opin Genet Dev. 17**,** 264-71.

Korzh, V., Sleptsova, I., Liao, J., He, J., Gong, Z., 1998. Expression of zebrafish bHLH genes ngn1 and nrd defines distinct stages of neural differentiation. Dev Dyn. 213**,** 92-104.

Koster, M., Plessow, S., Clement, J. H., Lorenz, A., Tiedemann, H., Knochel, W., 1991. Bone morphogenetic protein 4 (BMP-4), a member of the TGF-beta family, in early embryos of Xenopus laevis: analysis of mesoderm inducing activity. Mech Dev. 33**,** 191-9.

Kozlowski, D. J., Murakami, T., Ho, R. K., Weinberg, E. S., 1997. Regional cell movement and tissue patterning in the zebrafish embryo revealed by fate mapping with caged fluorescein. Biochem Cell Biol. 75**,** 551-62.

Krauss, S., Concordet, J. P., Ingham, P. W., 1993. A functionally conserved homolog of the Drosophila segment polarity gene hh is expressed in tissues with polarizing activity in zebrafish embryos. Cell. 75**,** 1431-44.

Krauss, S., Johansen, T., Korzh, V., Fjose, A., 1991a. Expression of the zebrafish paired box gene pax[zf-b] during early neurogenesis. Development. 113**,** 1193-206.

Krauss, S., Johansen, T., Korzh, V., Moens, U., Ericson, J. U., Fjose, A., 1991b. Zebrafish pax[zf-a]: a paired box-containing gene expressed in the neural tube. EMBO J. 10**,** 3609-19.

Kretzschmar, M., Doody, J., Massague, J., 1997. Opposing BMP and EGF signalling pathways converge on the TGF-beta family mediator Smad1. Nature. 389**,** 618-22.

Kumar, A., Novoselov, V., Celeste, A. J., Wolfman, N. M., ten Dijke, P., Kuehn, M. R., 2001. Nodal signaling uses activin and transforming growth factor-beta receptor-regulated Smads. J Biol Chem. 276**,** 656-61.

Kuroda, H., Fuentealba, L., Ikeda, A., Reversade, B., De Robertis, E. M., 2005. Default neural induction: neuralization of dissociated Xenopus cells is mediated by Ras/MAPK activation. Genes Dev. 19**,** 1022-7.

Kwak, S. J., Phillips, B. T., Heck, R., Riley, B. B., 2002. An expanded domain of fgf3 expression in the hindbrain of zebrafish valentino mutants results in mis-patterning of the otic vesicle. Development. 129**,** 5279-87.

Kwiatkowski, B. A., Kirillova, I., Richard, R. E., Israeli, D., Yablonka-Reuveni, Z., 2008. FGFR4 and its novel splice form in myogenic cells: Interplay of glycosylation and tyrosine phosphorylation. J Cell Physiol. 215**,** 803-17.

Ladher, R. K., Anakwe, K. U., Gurney, A. L., Schoenwolf, G. C., Francis-West, P. H., 2000. Identification of synergistic signals initiating inner ear development. Science. 290**,** 1965-7.

Ladher, R. K., Wright, T. J., Moon, A. M., Mansour, S. L., Schoenwolf, G. C., 2005. FGF8 initiates inner ear induction in chick and mouse. Genes Dev. 19**,** 603-13.

Latres, E., Chiaur, D. S., Pagano, M., 1999. The human F box protein beta-Trcp associates with the Cul1/Skp1 complex and regulates the stability of beta-catenin. Oncogene. 18**,** 849-54.

Lecaudey, V., Anselme, I., Rosa, F., Schneider-Maunoury, S., 2004. The zebrafish Iroquois gene iro7 positions the r4/r5 boundary and controls neurogenesis in the rostral hindbrain. Development. 131**,** 3121-31.

Lecaudey, V., Ulloa, E., Anselme, I., Stedman, A., Schneider-Maunoury, S., Pujades, C., 2007. Role of the hindbrain in patterning the otic vesicle: a study of the zebrafish vhnf1 mutant. Dev Biol. 303**,** 134-43.

Lee, H. X., Ambrosio, A. L., Reversade, B., De Robertis, E. M., 2006. Embryonic dorsal-ventral signaling: secreted frizzled-related proteins as inhibitors of tolloid proteinases. Cell. 124**,** 147-59.

Lee, M. A., Heasman, J., Whitman, M., 2001. Timing of endogenous activin-like signals and regional specification of the Xenopus embryo. Development. 128**,** 2939-52.

Leger, S., Brand, M., 2002. Fgf8 and Fgf3 are required for zebrafish ear placode induction, maintenance and inner ear patterning. Mech Dev. 119**,** 91-108.

Lekven, A. C., Thorpe, C. J., Waxman, J. S., Moon, R. T., 2001. Zebrafish wnt8 encodes two wnt8 proteins on a bicistronic transcript and is required for mesoderm and neurectoderm patterning. Dev Cell. 1**,** 103-14.

Lele, Z., Nowak, M., Hammerschmidt, M., 2001. Zebrafish admp is required to restrict the size of the organizer and to promote posterior and ventral development. Dev Dyn. 222**,** 681-7.

Lemaire, P., Bertrand, V., Hudson, C., 2002. Early steps in the formation of neural tissue in ascidian embryos. Dev Biol. 252**,** 151-69.

Lewis, J. L., Bonner, J., Modrell, M., Ragland, J. W., Moon, R. T., Dorsky, R. I., Raible, D. W., 2004. Reiterated Wnt signaling during zebrafish neural crest development. Development. 131**,** 1299-308.

Linker, C., Lesbros, C., Stark, M. R., Marcelle, C., 2003. Intrinsic signals regulate the initial steps of myogenesis in vertebrates. Development. 130**,** 4797-807.

Linsenmayer, T. F., Gibney, E., Schmid, T. M., 1986. Intracellular avian type X collagen in situ and determination of its thermal stability using a conformation-dependent monoclonal antibody. Exp Cell Res. 166**,** 15-22.

Litsiou, A., Hanson, S., Streit, A., 2005. A balance of FGF, BMP and WNT signalling positions the future placode territory in the head. Development. 132**,** 4051-62.

Liu, C., Kato, Y., Zhang, Z., Do, V. M., Yankner, B. A., He, X., 1999. beta-Trcp couples beta-catenin phosphorylation-degradation and regulates Xenopus axis formation. Proc Natl Acad Sci U S A. 96**,** 6273-8.

Liu, C., Li, Y., Semenov, M., Han, C., Baeg, G. H., Tan, Y., Zhang, Z., Lin, X., He, X., 2002. Control of beta-catenin phosphorylation/degradation by a dual-kinase mechanism. Cell. 108**,** 837-47.

Liu, D., Chu, H., Maves, L., Yan, Y. L., Morcos, P. A., Postlethwait, J. H., Westerfield, M., 2003. Fgf3 and Fgf8 dependent and independent transcription factors are required for otic placode specification. Development. 130**,** 2213-24.

Liu, Z., Neiss, N., Zhou, S., Henne-Bruns, D., Korc, M., Bachem, M., Kornmann, M., 2007. Identification of a fibroblast growth factor receptor 1 splice variant that inhibits pancreatic cancer cell growth. Cancer Res. 67**,** 2712-9.

Logan, C. Y., Nusse, R., 2004. The Wnt signaling pathway in development and disease. Annu Rev Cell Dev Biol. 20**,** 781-810.

Lohr, J. L., Danos, M. C., Yost, H. J., 1997. Left-right asymmetry of a nodal-related gene is regulated by dorsoanterior midline structures during Xenopus development. Development. 124**,** 1465-72.

Lombardo, A., Isaacs, H. V., Slack, J. M., 1998. Expression and functions of FGF-3 in Xenopus development. Int J Dev Biol. 42**,** 1101-7.

Lombardo, A., Slack, J. M., 1998. Postgastrulation effects of fibroblast growth factor on Xenopus development. Dev Dyn. 212**,** 75-85.

Lorent, K., Liu, K. S., Fetcho, J. R., Granato, M., 2001. The zebrafish space cadet gene controls axonal pathfinding of neurons that modulate fast turning movements. Development. 128**,** 2131-42.

Lowery, L. A., Rubin, J., Sive, H., 2007. Whitesnake/sfpq is required for cell survival and neuronal development in the zebrafish. Dev Dyn. 236**,** 1347-57.

Lum, L., Zhang, C., Oh, S., Mann, R. K., von Kessler, D. P., Taipale, J., Weis-Garcia, F., Gong, R., Wang, B., Beachy, P. A., 2003. Hedgehog signal transduction via Smoothened association with a cytoplasmic complex scaffolded by the atypical kinesin, Costal-2. Mol Cell. 12**,** 1261-74.

Luo, T., Matsuo-Takasaki, M., Lim, J. H., Sargent, T. D., 2001. Differential regulation of Dlx gene expression by a BMP morphogenetic gradient. Int J Dev Biol. 45**,** 681-4.

Mackereth, M. D., Kwak, S. J., Fritz, A., Riley, B. B., 2005. Zebrafish pax8 is required for otic placode induction and plays a redundant role with Pax2 genes in the maintenance of the otic placode. Development. 132**,** 371-82.

Mansour, S. L., Goddard, J. M., Capecchi, M. R., 1993. Mice homozygous for a targeted disruption of the proto-oncogene int-2 have developmental defects in the tail and inner ear. Development. 117**,** 13-28.

Marlow, F., Gonzalez, E. M., Yin, C., Rojo, C., Solnica-Krezel, L., 2004. No tail co-operates with non-canonical Wnt signaling to regulate posterior body morphogenesis in zebrafish. Development. 131**,** 203-16.

Maroon, H., Walshe, J., Mahmood, R., Kiefer, P., Dickson, C., Mason, I., 2002. Fgf3 and Fgf8 are required together for formation of the otic placode and vesicle. Development. 129**,** 2099-108.

Martin, B. L., Kimelman, D., 2008. Regulation of canonical Wnt signaling by Brachyury is essential for posterior mesoderm formation. Dev Cell. 15**,** 121-33.

Martin, K., Groves, A. K., 2006. Competence of cranial ectoderm to respond to Fgf signaling suggests a two-step model of otic placode induction. Development. 133**,** 877-87.

Massague, J., 2003. Integration of Smad and MAPK pathways: a link and a linker revisited. Genes Dev. 17**,** 2993-7.

Mathieu, M., Kiefer, P., Mason, I., Dickson, C., 1995. Fibroblast growth factor (FGF) 3 from Xenopus laevis (XFGF3) binds with high affinity to FGF receptor 2. J Biol Chem. 270**,** 6779-87.

Matsuo-Takasaki, M., Matsumura, M., Sasai, Y., 2005. An essential role of Xenopus Foxi1a for ventral specification of the cephalic ectoderm during gastrulation. Development. 132**,** 3885-94.

McKay, I. J., Muchamore, I., Krumlauf, R., Maden, M., Lumsden, A., Lewis, J., 1994. The kreisler mouse: a hindbrain segmentation mutant that lacks two rhombomeres. Development. 120**,** 2199-211.

McLarren, K. W., Litsiou, A., Streit, A., 2003. DLX5 positions the neural crest and preplacode region at the border of the neural plate. Dev Biol. 259**,** 34-47.

Melby, A. E., Beach, C., Mullins, M., Kimelman, D., 2000. Patterning the early zebrafish by the opposing actions of bozozok and vox/vent. Dev Biol. 224**,** 275-85.

Merlo, G. R., Paleari, L., Mantero, S., Zerega, B., Adamska, M., Rinkwitz, S., Bober, E., Levi, G., 2002. The Dlx5 homeobox gene is essential for vestibular morphogenesis in the mouse embryo through a BMP4-mediated pathway. Dev Biol. 248**,** 157-69.

Messenger, N. J., Kabitschke, C., Andrews, R., Grimmer, D., Nunez Miguel, R., Blundell, T. L., Smith, J. C., Wardle, F. C., 2005. Functional specificity of the Xenopus T-domain protein Brachyury is conferred by its ability to interact with Smad1. Dev Cell. 8**,** 599-610.

Metcalfe, W. K., Mendelson, B., Kimmel, C. B., 1986. Segmental homologies among reticulospinal neurons in the hindbrain of the zebrafish larva. J Comp Neurol. 251**,** 147-59.

Meulemans, D., Bronner-Fraser, M., 2004. Gene-regulatory interactions in neural crest evolution and development. Dev Cell. 7**,** 291-9.

Miller, J. R., Moon, R. T., 1997. Analysis of the signaling activities of localization mutants of beta-catenin during axis specification in Xenopus. J Cell Biol. 139**,** 229-43.

Miller-Bertoglio, V. E., Fisher, S., Sanchez, A., Mullins, M. C., Halpern, M. E., 1997. Differential regulation of chordin expression domains in mutant zebrafish. Dev Biol. 192**,** 537-50.

Moens, C. B., Cordes, S. P., Giorgianni, M. W., Barsh, G. S., Kimmel, C. B., 1998. Equivalence in the genetic control of hindbrain segmentation in fish and mouse. Development. 125**,** 381-91.

Mohammadi, M., McMahon, G., Sun, L., Tang, C., Hirth, P., Yeh, B. K., Hubbard, S. R., Schlessinger, J., 1997. Structures of the tyrosine kinase domain of fibroblast growth factor receptor in complex with inhibitors. Science. 276**,** 955-60.

Molenaar, M., van de Wetering, M., Oosterwegel, M., Peterson-Maduro, J., Godsave, S., Korinek, V., Roose, J., Destree, O., Clevers, H., 1996. XTcf-3 transcription factor mediates beta-catenin-induced axis formation in Xenopus embryos. Cell. 86**,** 391-9.

Monteiro, R., van Dinther, M., Bakkers, J., Wilkinson, R., Patient, R., ten Dijke, P., Mummery, C., 2008. Two novel type II receptors mediate BMP signalling and are required to establish left-right asymmetry in zebrafish. Dev Biol. 315**,** 55-71.

Moser, M., Binder, O., Wu, Y., Aitsebaomo, J., Ren, R., Bode, C., Bautch, V. L., Conlon, F. L., Patterson, C., 2003. BMPER, a novel endothelial cell precursor-derived protein, antagonizes bone morphogenetic protein signaling and endothelial cell differentiation. Mol Cell Biol. 23**,** 5664-79.

Moser, M., Yu, Q., Bode, C., Xiong, J. W., Patterson, C., 2007. BMPER is a conserved regulator of hematopoietic and vascular development in zebrafish. J Mol Cell Cardiol. 43**,** 243-53.

Mowbray, C., Hammerschmidt, M., Whitfield, T. T., 2001. Expression of BMP signalling pathway members in the developing zebrafish inner ear and lateral line. Mech Dev. 108**,** 179-84.

Mullins, M. C., Hammerschmidt, M., Kane, D. A., Odenthal, J., Brand, M., van Eeden, F. J., Furutani-Seiki, M., Granato, M., Haffter, P., Heisenberg, C. P., Jiang, Y. J., Kelsh, R. N., Nusslein-Volhard, C., 1996. Genes establishing dorsoventral pattern formation in the zebrafish embryo: the ventral specifying genes. Development. 123**,** 81-93.

Munchberg, S. R., Ober, E. A., Steinbeisser, H., 1999. Expression of the Ets transcription factors erm and pea3 in early zebrafish development. Mech Dev. 88**,** 233-6.

Munemitsu, S., Albert, I., Rubinfeld, B., Polakis, P., 1996. Deletion of an amino-terminal sequence beta-catenin in vivo and promotes hyperphosporylation of the adenomatous polyposis coli tumor suppressor protein. Mol Cell Biol. 16**,** 4088-94.

Murayama, E., Herbomel, P., Kawakami, A., Takeda, H., Nagasawa, H., 2005. Otolith matrix proteins OMP-1 and Otolin-1 are necessary for normal otolith growth and their correct anchoring onto the sensory maculae. Mech Dev. 122**,** 791-803.

Nakamura, T., Sugino, K., Titani, K., Sugino, H., 1991. Follistatin, an activin-binding protein, associates with heparan sulfate chains of proteoglycans on follicular granulosa cells. J Biol Chem. 266**,** 19432-7.

Nakano, Y., Nystedt, S., Shivdasani, A. A., Strutt, H., Thomas, C., Ingham, P. W., 2004. Functional domains and sub-cellular distribution of the Hedgehog transducing protein Smoothened in Drosophila. Mech Dev. 121**,** 507-18.

Nasevicius, A., Ekker, S. C., 2000. Effective targeted gene 'knockdown' in zebrafish. Nat Genet. 26**,** 216-20.

Neave, B., Holder, N., Patient, R., 1997. A graded response to BMP-4 spatially coordinates patterning of the mesoderm and ectoderm in the zebrafish. Mech Dev. 62**,** 183-95.

Nechiporuk, A., Linbo, T., Raible, D. W., 2005. Endoderm-derived Fgf3 is necessary and sufficient for inducing neurogenesis in the epibranchial placodes in zebrafish. Development. 132**,** 3717-30.

Nguyen, V. H., Schmid, B., Trout, J., Connors, S. A., Ekker, M., Mullins, M. C., 1998. Ventral and lateral regions of the zebrafish gastrula, including the neural crest progenitors, are established by a bmp2b/swirl pathway of genes. Dev Biol. 199**,** 93-110.

Nguyen, V. H., Trout, J., Connors, S. A., Andermann, P., Weinberg, E., Mullins, M. C., 2000. Dorsal and intermediate neuronal cell types of the spinal cord are established by a BMP signaling pathway. Development. 127**,** 1209-20.

Nica, G., Herzog, W., Sonntag, C., Hammerschmidt, M., 2004. Zebrafish pit1 mutants lack three pituitary cell types and develop severe dwarfism. Mol Endocrinol. 18**,** 1196-209.

Niehrs, C., Steinbeisser, H., De Robertis, E. M., 1994. Mesodermal patterning by a gradient of the vertebrate homeobox gene goosecoid. Science. 263**,** 817-20.

Nikaido, M., Tada, M., Saji, T., Ueno, N., 1997. Conservation of BMP signaling in zebrafish mesoderm patterning. Mech Dev. 61**,** 75-88.

Nikaido, M., Tada, M., Takeda, H., Kuroiwa, A., Ueno, N., 1999a. In vivo analysis using variants of zebrafish BMPR-IA: range of action and involvement of BMP in ectoderm patterning. Development. 126**,** 181-90.

Nikaido, M., Tada, M., Ueno, N., 1999b. Restricted expression of the receptor serine/threonine kinase BMPR-IB in zebrafish. Mech Dev. 82**,** 219-22.

Nissen, R. M., Yan, J., Amsterdam, A., Hopkins, N., Burgess, S. M., 2003. Zebrafish foxi one modulates cellular responses to Fgf signaling required for the integrity of ear and jaw patterning. Development. 130**,** 2543-54.

Nojima, H., Shimizu, T., Kim, C. H., Yabe, T., Bae, Y. K., Muraoka, O., Hirata, T., Chitnis, A., Hirano, T., Hibi, M., 2004. Genetic evidence for involvement of maternally derived Wnt canonical signaling in dorsal determination in zebrafish. Mech Dev. 121**,** 371-86.

Noramly, S., Grainger, R. M., 2002. Determination of the embryonic inner ear. J Neurobiol. 53**,** 100-28.

Northcutt, R. G., Gans, C., 1983. The genesis of neural crest and epidermal placodes: a reinterpretation of vertebrate origins. Q Rev Biol. 58**,** 1-28.

Oelgeschlager, M., Larrain, J., Geissert, D., De Robertis, E. M., 2000. The evolutionarily conserved BMP-binding protein Twisted gastrulation promotes BMP signalling. Nature. 405**,** 757-63.

Ohyama, T., Groves, A. K., 2004. Expression of mouse Foxi class genes in early craniofacial development. Dev Dyn. 231**,** 640-6.

Ohyama, T., Groves, A. K., Martin, K., 2007. The first steps towards hearing: mechanisms of otic placode induction. Int J Dev Biol. 51**,** 463-72.

Ohyama, T., Mohamed, O. A., Taketo, M. M., Dufort, D., Groves, A. K., 2006. Wnt signals mediate a fate decision between otic placode and epidermis. Development. 133**,** 865-75.

Oxtoby, E., Jowett, T., 1993. Cloning of the zebrafish krox-20 gene (krx-20) and its expression during hindbrain development. Nucleic Acids Res. 21**,** 1087-95.

Pagnon-Minot, A., Malbouyres, M., Haftek-Terreau, Z., Kim, H. R., Sasaki, T., Thisse, C., Thisse, B., Ingham, P. W., Ruggiero, F., Le Guellec, D., 2008. Collagen XV, a novel factor in zebrafish notochord differentiation and muscle development. Dev Biol. 316**,** 21-35.

Pandur, P. D., Moody, S. A., 2000. Xenopus Six1 gene is expressed in neurogenic cranial placodes and maintained in the differentiating lateral lines. Mech Dev. 96**,** 253-7.

Papalopulu, N., Kintner, C., 1993. Xenopus Distal-less related homeobox genes are expressed in the developing forebrain and are induced by planar signals. Development. 117**,** 961-75.

Park, G. T., Morasso, M. I., 2002. Bone morphogenetic protein-2 (BMP-2) transactivates Dlx3 through Smad1 and Smad4: alternative mode for Dlx3 induction in mouse keratinocytes. Nucleic Acids Res. 30**,** 515-22.

Parsons, M. J., Pollard, S. M., Saude, L., Feldman, B., Coutinho, P., Hirst, E. M., Stemple, D. L., 2002. Zebrafish mutants identify an essential role for laminins in notochord formation. Development. 129**,** 3137-46.

Pera, E., Stein, S., Kessel, M., 1999. Ectodermal patterning in the avian embryo: epidermis versus neural plate. Development. 126**,** 63-73.

Pera, E. M., Ikeda, A., Eivers, E., De Robertis, E. M., 2003. Integration of IGF, FGF, and anti-BMP signals via Smad1 phosphorylation in neural induction. Genes Dev. 17**,** 3023-8.

Pfeffer, P. L., Gerster, T., Lun, K., Brand, M., Busslinger, M., 1998. Characterization of three novel members of the zebrafish Pax2/5/8 family: dependency of Pax5 and Pax8 expression on the Pax2.1 (noi) function. Development. 125**,** 3063-74.

Phillips, B. T., Bolding, K., Riley, B. B., 2001. Zebrafish fgf3 and fgf8 encode redundant functions required for otic placode induction. Dev Biol. 235**,** 351-65.

Phillips, B. T., Kwon, H. J., Melton, C., Houghtaling, P., Fritz, A., Riley, B. B., 2006. Zebrafish msxB, msxC and msxE function together to refine the neural-nonneural border and regulate cranial placodes and neural crest development. Dev Biol. 294**,** 376-90.

Piccolo, S., Agius, E., Leyns, L., Bhattacharyya, S., Grunz, H., Bouwmeester, T., De Robertis, E. M., 1999. The head inducer Cerberus is a multifunctional antagonist of Nodal, BMP and Wnt signals. Nature. 397**,** 707-10.

Piccolo, S., Agius, E., Lu, B., Goodman, S., Dale, L., De Robertis, E. M., 1997. Cleavage of Chordin by Xolloid metalloprotease suggests a role for proteolytic processing in the regulation of Spemann organizer activity. Cell. 91**,** 407-16.

Pirvola, U., Spencer-Dene, B., Xing-Qun, L., Kettunen, P., Thesleff, I., Fritzsch, B., Dickson, C., Ylikoski, J., 2000. FGF/FGFR-2(IIIb) signaling is essential for inner ear morphogenesis. J Neurosci. 20**,** 6125-34.

Pizette, S., Niswander, L., 1999. BMPs negatively regulate structure and function of the limb apical ectodermal ridge. Development. 126**,** 883-94.

Plouhinec, J. L., De Robertis, E. M., 2007. Systems biology of embryonic morphogens. Mol Biosyst. 3**,** 454-7.

Pohl, B. S., Knochel, S., Dillinger, K., Knochel, W., 2002. Sequence and expression of FoxB2 (XFD-5) and FoxI1c (XFD-10) in Xenopus embryogenesis. Mech Dev. 117**,** 283-7.

Pollard, S. M., Parsons, M. J., Kamei, M., Kettleborough, R. N., Thomas, K. A., Pham, V. N., Bae, M. K., Scott, A., Weinstein, B. M., Stemple, D. L., 2006. Essential and overlapping roles for laminin alpha chains in notochord and blood vessel formation. Dev Biol. 289**,** 64-76.

Poss, K. D., Shen, J., Nechiporuk, A., McMahon, G., Thisse, B., Thisse, C., Keating, M. T., 2000. Roles for Fgf signaling during zebrafish fin regeneration. Dev Biol. 222**,** 347-58.

Pourquie, O., Coltey, M., Teillet, M. A., Ordahl, C., Le Douarin, N. M., 1993. Control of dorsoventral patterning of somitic derivatives by notochord and floor plate. Proc Natl Acad Sci U S A. 90**,** 5242-6.

Prince, V. E., Moens, C. B., Kimmel, C. B., Ho, R. K., 1998. Zebrafish hox genes: expression in the hindbrain region of wild-type and mutants of the segmentation gene, valentino. Development. 125**,** 393-406.

Pyati, U. J., Webb, A. E., Kimelman, D., 2005. Transgenic zebrafish reveal stage-specific roles for Bmp signaling in ventral and posterior mesoderm development. Development. 132**,** 2333-43.

Raible, F., Brand, M., 2001. Tight transcriptional control of the ETS domain factors Erm and Pea3 by Fgf signaling during early zebrafish development. Mech Dev. 107**,** 105-17.

Rajeevan, M. S., Ranamukhaarachchi, D. G., Vernon, S. D., Unger, E. R., 2001. Use of real-time quantitative PCR to validate the results of cDNA array and differential display PCR technologies. Methods. 25**,** 443-51.

Ramel, M. C., Buckles, G. R., Baker, K. D., Lekven, A. C., 2005. WNT8 and BMP2B co-regulate non-axial mesoderm patterning during zebrafish gastrulation. Dev Biol. 287**,** 237-48.

Reifers, F., Bohli, H., Walsh, E. C., Crossley, P. H., Stainier, D. Y., Brand, M., 1998. Fgf8 is mutated in zebrafish acerebellar (ace) mutants and is required for maintenance of midbrain-hindbrain boundary development and somitogenesis. Development. 125**,** 2381-95.

Rentzsch, F., Zhang, J., Kramer, C., Sebald, W., Hammerschmidt, M., 2006. Crossveinless 2 is an essential positive feedback regulator of Bmp signaling during zebrafish gastrulation. Development. 133**,** 801-11.

Represa, J., Leon, Y., Miner, C., Giraldez, F., 1991. The int-2 proto-oncogene is responsible for induction of the inner ear. Nature. 353**,** 561-3.

Reversade, B., De Robertis, E. M., 2005. Regulation of ADMP and BMP2/4/7 at opposite embryonic poles generates a self-regulating morphogenetic field. Cell. 123**,** 1147-60.

Reversade, B., Kuroda, H., Lee, H., Mays, A., De Robertis, E. M., 2005. Depletion of Bmp2, Bmp4, Bmp7 and Spemann organizer signals induces massive brain formation in Xenopus embryos. Development. 132**,** 3381-92.

Ribeiro, I., Kawakami, Y., Buscher, D., Raya, A., Rodriguez-Leon, J., Morita, M., Rodriguez Esteban, C., Izpisua Belmonte, J. C., 2007. Tbx2 and Tbx3 regulate the dynamics of cell proliferation during heart remodeling. PLoS ONE. 2**,** e398.

Riley, B. B., 2003. Genes controlling the development of the zebrafish inner ear and hair cells. Curr Top Dev Biol. 57**,** 357-88.

Riley, B. B., Phillips, B. T., 2003. Ringing in the new ear: resolution of cell interactions in otic development. Dev Biol. 261**,** 289-312.

Robledo, R. F., Lufkin, T., 2006. Dlx5 and Dlx6 homeobox genes are required for specification of the mammalian vestibular apparatus. Genesis. 44**,** 425-37.

Robledo, R. F., Rajan, L., Li, X., Lufkin, T., 2002. The Dlx5 and Dlx6 homeobox genes are essential for craniofacial, axial, and appendicular skeletal development. Genes Dev. 16**,** 1089-101.

Rossi, C. C., Hernandez-Lagunas, L., Zhang, C., Choi, I. F., Kwok, L., Klymkowsky, M., Artinger, K. B., 2008. Rohon-Beard sensory neurons are induced by BMP4 expressing non-neural ectoderm in Xenopus laevis. Dev Biol. 314**,** 351-61.

Roux, W., 1888. Contributions to the developmental mechanics of the embryo. On the artificial production of half-embryos by destruction of one of the first two blastomeres and the later development (postgeneration) of the missing half of the body. Hafner, New York.

Ruel, L., Rodriguez, R., Gallet, A., Lavenant-Staccini, L., Therond, P. P., 2003. Stability and association of Smoothened, Costal2 and Fused with Cubitus interruptus are regulated by Hedgehog. Nat Cell Biol. 5**,** 907-13.

Sadl, V. S., Sing, A., Mar, L., Jin, F., Cordes, S. P., 2003. Analysis of hindbrain patterning defects caused by the kreisler(enu) mutation reveals multiple roles of Kreisler in hindbrain segmentation. Dev Dyn. 227**,** 134-42.

Sahly, I., Andermann, P., Petit, C., 1999. The zebrafish eya1 gene and its expression pattern during embryogenesis. Dev Genes Evol. 209**,** 399-410.

Sakai, M., 2008. Cell-autonomous and inductive processes among three embryonic domains control dorsal-ventral and anterior-posterior development of Xenopus laevis. Dev Growth Differ. 50**,** 49-62.

Sakamoto, I., Kishida, S., Fukui, A., Kishida, M., Yamamoto, H., Hino, S., Michiue, T., Takada, S., Asashima, M., Kikuchi, A., 2000. A novel beta-catenin-binding protein inhibits beta-catenin-dependent Tcf activation and axis formation. J Biol Chem. 275**,** 32871-8.

Sander, V., Reversade, B., De Robertis, E. M., 2007. The opposing homeobox genes Goosecoid and Vent1/2 self-regulate Xenopus patterning. EMBO J. 26**,** 2955-65.

Sapkota, G., Alarcon, C., Spagnoli, F. M., Brivanlou, A. H., Massague, J., 2007. Balancing BMP signaling through integrated inputs into the Smad1 linker. Mol Cell. 25**,** 441-54.

Sapkota, G., Knockaert, M., Alarcon, C., Montalvo, E., Brivanlou, A. H., Massague, J., 2006. Dephosphorylation of the linker regions of Smad1 and Smad2/3 by small C-terminal domain phosphatases has distinct outcomes for bone morphogenetic protein and transforming growth factor-beta pathways. J Biol Chem. 281**,** 40412-9.

Saude, L., Woolley, K., Martin, P., Driever, W., Stemple, D. L., 2000. Axis-inducing activities and cell fates of the zebrafish organizer. Development. 127**,** 3407-17.

Scaal, M., Christ, B., 2004. Formation and differentiation of the avian dermomyotome. Anat Embryol (Berl). 208**,** 411-24.

Schier, A. F., 2003. Nodal signaling in vertebrate development. Annu Rev Cell Dev Biol. 19**,** 589-621.

Schier, A. F., Talbot, W. S., 2005. Molecular genetics of axis formation in zebrafish. Annu Rev Genet. 39**,** 561-613.

Schimmang, T., 2007. Expression and functions of FGF ligands during early otic development. Int J Dev Biol. 51**,** 473-81.

Schlosser, G., 2006. Induction and specification of cranial placodes. Dev Biol. 294**,** 303-51.

Schlosser, G., Ahrens, K., 2004. Molecular anatomy of placode development in Xenopus laevis. Dev Biol. 271**,** 439-66.

Schneider, S., Steinbeisser, H., Warga, R. M., Hausen, P., 1996. Beta-catenin translocation into nuclei demarcates the dorsalizing centers in frog and fish embryos. Mech Dev. 57**,** 191-8.

Schneider-Maunoury, S., Pujades, C., 2007. Hindbrain signals in otic regionalization: walk on the wild side. Int J Dev Biol. 51**,** 495-506.

Scholpp, S., Groth, C., Lohs, C., Lardelli, M., Brand, M., 2004. Zebrafish fgfr1 is a member of the fgf8 synexpression group and is required for fgf8 signalling at the midbrain-hindbrain boundary. Dev Genes Evol. 214**,** 285-95.

Schulte-Merker, S., Hammerschmidt, M., Beuchle, D., Cho, K. W., De Robertis, E. M., Nusslein-Volhard, C., 1994. Expression of zebrafish goosecoid and no tail gene products in wild-type and mutant no tail embryos. Development. 120**,** 843-52.

Schulte-Merker, S., Ho, R. K., Herrmann, B. G., Nusslein-Volhard, C., 1992. The protein product of the zebrafish homologue of the mouse T gene is expressed in nuclei of the germ ring and the notochord of the early embryo. Development. 116**,** 1021-32.

Schulte-Merker, S., Lee, K. J., McMahon, A. P., Hammerschmidt, M., 1997. The zebrafish organizer requires chordino. Nature. 387**,** 862-3.

Schulte-Merker, S., Smith, J. C., 1995. Mesoderm formation in response to Brachyury requires FGF signalling. Curr Biol. 5**,** 62-7.

Seoane, J., Le, H. V., Shen, L., Anderson, S. A., Massague, J., 2004. Integration of Smad and forkhead pathways in the control of neuroepithelial and glioblastoma cell proliferation. Cell. 117**,** 211-23.

Serpe, M., Umulis, D., Ralston, A., Chen, J., Olson, D. J., Avanesov, A., Othmer, H., O'Connor, M. B., Blair, S. S., 2008. The BMP-binding protein Crossveinless 2 is

a short-range, concentration-dependent, biphasic modulator of BMP signaling in Drosophila. Dev Cell. 14**,** 940-53.
Servetnick, M., Grainger, R. M., 1991. Changes in neural and lens competence in Xenopus ectoderm: evidence for an autonomous developmental timer. Development. 112**,** 177-88.
Shen, M. M., 2007. Nodal signaling: developmental roles and regulation. Development. 134**,** 1023-34.
Shen, M. M., Schier, A. F., 2000. The EGF-CFC gene family in vertebrate development. Trends Genet. 16**,** 303-9.
Shestopalov, I. A., Sinha, S., Chen, J. K., 2007. Light-controlled gene silencing in zebrafish embryos. Nat Chem Biol. 3**,** 650-1.
Shih, J., Fraser, S. E., 1996. Characterizing the zebrafish organizer: microsurgical analysis at the early-shield stage. Development. 122**,** 1313-22.
Shimizu, T., Bae, Y. K., Muraoka, O., Hibi, M., 2005. Interaction of Wnt and caudal-related genes in zebrafish posterior body formation. Dev Biol. 279**,** 125-41.
Shimizu, T., Yamanaka, Y., Nojima, H., Yabe, T., Hibi, M., Hirano, T., 2002. A novel repressor-type homeobox gene, ved, is involved in dharma/bozozok-mediated dorsal organizer formation in zebrafish. Mech Dev. 118**,** 125-38.
Slack, J. M., Darlington, B. G., Heath, J. K., Godsave, S. F., 1987. Mesoderm induction in early Xenopus embryos by heparin-binding growth factors. Nature. 326**,** 197-200.
Sleptsova-Friedrich, I., Li, Y., Emelyanov, A., Ekker, M., Korzh, V., Ge, R., 2001. fgfr3 and regionalization of anterior neural tube in zebrafish. Mech Dev. 102**,** 213-7.
Smith, J. C., 1987. A mesoderm-inducing factor is produced by Xenopus cell line. Development. 99**,** 3-14.
Smith, M., 1997. Considerations on a possible viral etiology for B-precursor acute lymphoblastic leukemia of childhood. J Immunother. 20**,** 89-100.
Smits, P., Lefebvre, V., 2003. Sox5 and Sox6 are required for notochord extracellular matrix sheath formation, notochord cell survival and development of the nucleus pulposus of intervertebral discs. Development. 130**,** 1135-48.
Snelson, C. D., Santhakumar, K., Halpern, M. E., Gamse, J. T., 2008. Tbx2b is required for the development of the parapineal organ. Development. 135**,** 1693-702.
Solomon, K. S., Fritz, A., 2002. Concerted action of two dlx paralogs in sensory placode formation. Development. 129**,** 3127-36.
Solomon, K. S., Kudoh, T., Dawid, I. B., Fritz, A., 2003. Zebrafish foxi1 mediates otic placode formation and jaw development. Development. 130**,** 929-40.
Solomon, K. S., Kwak, S. J., Fritz, A., 2004. Genetic interactions underlying otic placode induction and formation. Dev Dyn. 230**,** 419-33.
Spemann, H., 1903. Entwicklungsphysiologische Studien am Tritonei III. Arch. f. Entw. Mech. 16**,** 551-631.
Spemann, H., 1938. Embryonic Development and Induction. Yale University Press, New Haven, CT.
Spemann, H., Mangold, H., 1924. Über Induktion von Embryonalanlagen durch Implantation artfremder
Organisatoren. Archiv fü r Mikroskopische Anatomie und Entwicklungsmechanik. 100**,** 599-638.

Spemann, H., Mangold, H., 1964. Archiv fü r Mikroskopische Anatomie und Entwicklungsmechanik. Englewood Cliffs.

Spokony, R. F., Aoki, Y., Saint-Germain, N., Magner-Fink, E., Saint-Jeannet, J. P., 2002. The transcription factor Sox9 is required for cranial neural crest development in Xenopus. Development. 129**,** 421-32.

Stemple, D. L., 2005. Structure and function of the notochord: an essential organ for chordate development. Development. 132**,** 2503-12.

Stemple, D. L., Solnica-Krezel, L., Zwartkruis, F., Neuhauss, S. C., Schier, A. F., Malicki, J., Stainier, D. Y., Abdelilah, S., Rangini, Z., Mountcastle-Shah, E., Driever, W., 1996. Mutations affecting development of the notochord in zebrafish. Development. 123**,** 117-28.

Stern, H. M., Murphey, R. D., Shepard, J. L., Amatruda, J. F., Straub, C. T., Pfaff, K. L., Weber, G., Tallarico, J. A., King, R. W., Zon, L. I., 2005. Small molecules that delay S phase suppress a zebrafish bmyb mutant. Nat Chem Biol. 1**,** 366-70.

Stickney, H. L., Imai, Y., Draper, B., Moens, C., Talbot, W. S., 2007. Zebrafish bmp4 functions during late gastrulation to specify ventroposterior cell fates. Dev Biol. 310**,** 71-84.

Streit, A., 2002. Extensive cell movements accompany formation of the otic placode. Dev Biol. 249**,** 237-54.

Streit, A., 2007. The preplacodal region: an ectodermal domain with multipotential progenitors that contribute to sense organs and cranial sensory ganglia. Int J Dev Biol. 51**,** 447-61.

Sun, Z., Hopkins, N., 2001. vhnf1, the MODY5 and familial GCKD-associated gene, regulates regional specification of the zebrafish gut, pronephros, and hindbrain. Genes Dev. 15**,** 3217-29.

Suzuki, A., Ueno, N., Hemmati-Brivanlou, A., 1997. Xenopus msx1 mediates epidermal induction and neural inhibition by BMP4. Development. 124**,** 3037-44.

Swiderski, R. E., Solursh, M., 1992. Localization of type II collagen, long form alpha 1(IX) collagen, and short form alpha 1(IX) collagen transcripts in the developing chick notochord and axial skeleton. Dev Dyn. 194**,** 118-27.

Szeto, D. P., Kimelman, D., 2004. Combinatorial gene regulation by Bmp and Wnt in zebrafish posterior mesoderm formation. Development. 131**,** 3751-60.

Szeto, D. P., Kimelman, D., 2006. The regulation of mesodermal progenitor cell commitment to somitogenesis subdivides the zebrafish body musculature into distinct domains. Genes Dev. 20**,** 1923-32.

Takabatake, Y., Takabatake, T., Takeshima, K., 2000. Conserved and divergent expression of T-box genes Tbx2-Tbx5 in Xenopus. Mech Dev. 91**,** 433-7.

Talbot, W. S., Trevarrow, B., Halpern, M. E., Melby, A. E., Farr, G., Postlethwait, J. H., Jowett, T., Kimmel, C. B., Kimelman, D., 1995. A homeobox gene essential for zebrafish notochord development. Nature. 378**,** 150-7.

Tendeng, C., Houart, C., 2006. Cloning and embryonic expression of five distinct sfrp genes in the zebrafish Danio rerio. Gene Expr Patterns. 6**,** 761-71.

Thisse, B., Thisse, C., 2005. Functions and regulations of fibroblast growth factor signaling during embryonic development. Dev Biol. 287**,** 390-402.

Thisse, B., Thisse, C., Weston, J. A., 1995. Novel FGF receptor (Z-FGFR4) is dynamically expressed in mesoderm and neurectoderm during early zebrafish embryogenesis. Dev Dyn. 203**,** 377-91.

Tian, T., Meng, A. M., 2006. Nodal signals pattern vertebrate embryos. Cell Mol Life Sci. 63**,** 672-85.

Tolwinski, N. S., Wieschaus, E., 2004. A nuclear function for armadillo/beta-catenin. PLoS Biol. 2**,** E95.

Tonou-Fujimori, N., Takahashi, M., Onodera, H., Kikuta, H., Koshida, S., Takeda, H., Yamasu, K., 2002. Expression of the FGF receptor 2 gene (fgfr2) during embryogenesis in the zebrafish Danio rerio. Gene Expr Patterns. 2**,** 183-8.

Topczewska, J. M., Topczewski, J., Shostak, A., Kume, T., Solnica-Krezel, L., Hogan, B. L., 2001. The winged helix transcription factor Foxc1a is essential for somitogenesis in zebrafish. Genes Dev. 15**,** 2483-93.

Tribulo, C., Aybar, M. J., Nguyen, V. H., Mullins, M. C., Mayor, R., 2003. Regulation of Msx genes by a Bmp gradient is essential for neural crest specification. Development. 130**,** 6441-52.

Tucker, A. S., Slack, J. M., 1995. Tail bud determination in the vertebrate embryo. Curr Biol. 5**,** 807-13.

Tucker, J. A., Mintzer, K. A., Mullins, M. C., 2008. The BMP signaling gradient patterns dorsoventral tissues in a temporally progressive manner along the anteroposterior axis. Dev Cell. 14**,** 108-19.

van de Wetering, M., Cavallo, R., Dooijes, D., van Beest, M., van Es, J., Loureiro, J., Ypma, A., Hursh, D., Jones, T., Bejsovec, A., Peifer, M., Mortin, M., Clevers, H., 1997. Armadillo coactivates transcription driven by the product of the Drosophila segment polarity gene dTCF. Cell. 88**,** 789-99.

Wardle, F. C., Angerer, L. M., Angerer, R. C., Dale, L., 1999. Regulation of BMP signaling by the BMP1/TLD-related metalloprotease, SpAN. Dev Biol. 206**,** 63-72.

Wardle, F. C., Smith, J. C., 2004. Refinement of gene expression patterns in the early Xenopus embryo. Development. 131**,** 4687-96.

Warga, R. M., Nusslein-Volhard, C., 1999. Origin and development of the zebrafish endoderm. Development. 126**,** 827-38.

Weinstein, D. C., Hemmati-Brivanlou, A., 1999. Neural induction. Annu Rev Cell Dev Biol. 15**,** 411-33.

Weng, W., Stemple, D. L., 2003. Nodal signaling and vertebrate germ layer formation. Birth Defects Res C Embryo Today. 69**,** 325-32.

Wessely, O., Agius, E., Oelgeschlager, M., Pera, E. M., De Robertis, E. M., 2001. Neural induction in the absence of mesoderm: beta-catenin-dependent expression of secreted BMP antagonists at the blastula stage in Xenopus. Dev Biol. 234**,** 161-73.

Wessely, O., De Robertis, E. M., 2002. Neural plate patterning by secreted signals. Neuron. 33**,** 489-91.

Westerfield, M., 1994. The Zebrafish Book: A Guide for the Laboratory Use of Zebrafish. University of Oregon Press, Eugene (OR).

Whitfield, T. T., Riley, B. B., Chiang, M. Y., Phillips, B., 2002. Development of the zebrafish inner ear. Dev Dyn. 223**,** 427-58.

Whitlock, K. E., Westerfield, M., 2000. The olfactory placodes of the zebrafish form by convergence of cellular fields at the edge of the neural plate. Development. 127**,** 3645-53.

Wiellette, E. L., Sive, H., 2003. vhnf1 and Fgf signals synergize to specify rhombomere identity in the zebrafish hindbrain. Development. 130**,** 3821-9.

Willot, V., Mathieu, J., Lu, Y., Schmid, B., Sidi, S., Yan, Y. L., Postlethwait, J. H., Mullins, M., Rosa, F., Peyrieras, N., 2002. Cooperative action of ADMP- and BMP-mediated pathways in regulating cell fates in the zebrafish gastrula. Dev Biol. 241**,** 59-78.

Wilson, P. A., Hemmati-Brivanlou, A., 1995. Induction of epidermis and inhibition of neural fate by Bmp-4. Nature. 376**,** 331-3.

Witzel, S., Zimyanin, V., Carreira-Barbosa, F., Tada, M., Heisenberg, C. P., 2006. Wnt11 controls cell contact persistence by local accumulation of Frizzled 7 at the plasma membrane. J Cell Biol. 175**,** 791-802.

Woda, J. M., Pastagia, J., Mercola, M., Artinger, K. B., 2003. Dlx proteins position the neural plate border and determine adjacent cell fates. Development. 130**,** 331-42.

Wolff, C., Roy, S., Ingham, P. W., 2003. Multiple muscle cell identities induced by distinct levels and timing of hedgehog activity in the zebrafish embryo. Curr Biol. 13**,** 1169-81.

Woo, K., Fraser, S. E., 1997. Specification of the zebrafish nervous system by nonaxial signals. Science. 277**,** 254-7.

Wright, T. J., Hatch, E. P., Karabagli, H., Karabagli, P., Schoenwolf, G. C., Mansour, S. L., 2003. Expression of mouse fibroblast growth factor and fibroblast growth factor receptor genes during early inner ear development. Dev Dyn. 228**,** 267-72.

Wright, T. J., Mansour, S. L., 2003. Fgf3 and Fgf10 are required for mouse otic placode induction. Development. 130**,** 3379-90.

Yabe, S., Tanegashima, K., Haramoto, Y., Takahashi, S., Fujii, T., Kozuma, S., Taketani, Y., Asashima, M., 2003. FRL-1, a member of the EGF-CFC family, is essential for neural differentiation in Xenopus early development. Development. 130**,** 2071-81.

Yamada, T., Pfaff, S. L., Edlund, T., Jessell, T. M., 1993. Control of cell pattern in the neural tube: motor neuron induction by diffusible factors from notochord and floor plate. Cell. 73**,** 673-86.

Yamamoto, A., Amacher, S. L., Kim, S. H., Geissert, D., Kimmel, C. B., De Robertis, E. M., 1998. Zebrafish paraxial protocadherin is a downstream target of spadetail involved in morphogenesis of gastrula mesoderm. Development. 125**,** 3389-97.

Yamamoto, Y., Oelgeschlager, M., 2004. Regulation of bone morphogenetic proteins in early embryonic development. Naturwissenschaften. 91**,** 519-34.

Yan, J., Xu, L., Crawford, G., Wang, Z., Burgess, S. M., 2006. The forkhead transcription factor FoxI1 remains bound to condensed mitotic chromosomes and stably remodels chromatin structure. Mol Cell Biol. 26**,** 155-68.

Yan, Y. L., Hatta, K., Riggleman, B., Postlethwait, J. H., 1995. Expression of a type II collagen gene in the zebrafish embryonic axis. Dev Dyn. 203**,** 363-76.

Yan, Y. L., Willoughby, J., Liu, D., Crump, J. G., Wilson, C., Miller, C. T., Singer, A., Kimmel, C., Westerfield, M., Postlethwait, J. H., 2005. A pair of Sox: distinct and

overlapping functions of zebrafish sox9 co-orthologs in craniofacial and pectoral fin development. Development. 132**,** 1069-83.

Yanagawa, S., Matsuda, Y., Lee, J. S., Matsubayashi, H., Sese, S., Kadowaki, T., Ishimoto, A., 2002. Casein kinase I phosphorylates the Armadillo protein and induces its degradation in Drosophila. EMBO J. 21**,** 1733-42.

Yang, L., Zhang, H., Hu, G., Wang, H., Abate-Shen, C., Shen, M. M., 1998. An early phase of embryonic Dlx5 expression defines the rostral boundary of the neural plate. J Neurosci. 18**,** 8322-30.

Yeo, C., Whitman, M., 2001. Nodal signals to Smads through Cripto-dependent and Cripto-independent mechanisms. Mol Cell. 7**,** 949-57.

Yost, C., Torres, M., Miller, J. R., Huang, E., Kimelman, D., Moon, R. T., 1996. The axis-inducing activity, stability, and subcellular distribution of beta-catenin is regulated in Xenopus embryos by glycogen synthase kinase 3. Genes Dev. 10**,** 1443-54.

Zeng, J., Yan, J., Wang, T., Mosbrook-Davis, D., Dolan, K. T., Christensen, R., Stormo, G. D., Haussler, D., Lathrop, R. H., Brachmann, R. K., Burgess, S. M., 2008. Genome wide screens in yeast to identify potential binding sites and target genes of DNA-binding proteins. Nucleic Acids Res. 36**,** e8.

Zernicka-Goetz, M., 2002. Patterning of the embryo: the first spatial decisions in the life of a mouse. Development. 129**,** 815-29.

Zhang, J., Li, L., 2005. BMP signaling and stem cell regulation. Dev Biol. 284**,** 1-11.

Zhang, J., Niu, C., Ye, L., Huang, H., He, X., Tong, W. G., Ross, J., Haug, J., Johnson, T., Feng, J. Q., Harris, S., Wiedemann, L. M., Mishina, Y., Li, L., 2003. Identification of the haematopoietic stem cell niche and control of the niche size. Nature. 425**,** 836-41.

Zhang, J., Talbot, W. S., Schier, A. F., 1998. Positional cloning identifies zebrafish one-eyed pinhead as a permissive EGF-related ligand required during gastrulation. Cell. 92**,** 241-51.

Zhang, J. L., Huang, Y., Qiu, L. Y., Nickel, J., Sebald, W., 2007. von Willebrand factor type C domain-containing proteins regulate bone morphogenetic protein signaling through different recognition mechanisms. J Biol Chem. 282**,** 20002-14.

Zhang, J. L., Qiu, L. Y., Kotzsch, A., Weidauer, S., Patterson, L., Hammerschmidt, M., Sebald, W., Mueller, T. D., 2008. Crystal structure analysis reveals how the Chordin family member crossveinless 2 blocks BMP-2 receptor binding. Dev Cell. 14**,** 739-50.

Zhang, P., Greendorfer, J. S., Jiao, J., Kelpke, S. C., Thompson, J. A., 2006. Alternatively spliced FGFR-1 isoforms differentially modulate endothelial cell activation of c-YES. Arch Biochem Biophys. 450**,** 50-62.

Zuniga, A., Haramis, A. P., McMahon, A. P., Zeller, R., 1999. Signal relay by BMP antagonism controls the SHH/FGF4 feedback loop in vertebrate limb buds. Nature. 401**,** 598-602.